

Identifying the intracellular survival strategies of chlamydiae

Hayley Louise Clissold

PhD

University of York

Biology

December 2017

Abstract

Chlamydia is the most commonly diagnosed sexually transmitted infection in the UK. The etiological agent, *Chlamydia trachomatis* (*Ct*), is an obligate intracellular bacterium that resides within an intracellular niche, termed the inclusion, following entry into host cells. Chlamydiae avoid lysosomal destruction by diverging away from the normal endocytic trafficking pathway. *Ct* expresses a type-III secretion system (T3SS) that enables the translocation of *Ct* effector proteins into the host cytoplasm and these proteins are essential for virulence. Relatively little is understood regarding the pathogenesis of chlamydiae and the mechanisms they use to manipulate host defences because, until recently, they have been intractable to genetic manipulation.

In this thesis, we describe both a targeted and random screening approach for the identification of *Ct* T3SS effector proteins in the yeast *Saccharomyces cerevisiae*. We firstly use an *in silico* prediction program to identify *Ct* proteins that are likely to be secreted by the bacterium's T3SS. The predicted proteins were then screened for their ability to disrupt membrane trafficking using an established pathogen effector protein screening in yeast (PEPSY) screening method. In parallel, we also generated a *Ct* genomic library in order to PEPSY screen the entire chlamydial genome for proteins involved in disrupting membrane trafficking.

We identified two chlamydial deubiquitinases (DUB), ChlaDUB1 and ChlaDUB2, which disrupt intracellular membrane trafficking in a yeast model system. These chlamydial DUBs were expressed in mammalian cells and their effects on endosomal compartments, EGFR internalisation and degradation, I κ B α levels and global ubiquitin levels were examined. Our findings suggest that ChlaDUB1 and ChlaDUB2 are likely to demonstrate broad substrate specificity towards host substrates and this research paves the way for future research to investigate the role of chlamydial DUBs in the manipulation of host membrane trafficking during infection.

Table of Contents

Abstract	2
Table of Contents	3
List of Tables	8
List of Figures	9
List of Accompanying Material	12
Acknowledgements	13
Author's Declaration	14
Chapter 1: Introduction	15
1.1.1. The endocytic pathway.....	15
1.1.2. Phagocytosis	20
1.1.3. Pathogen manipulation of intracellular membrane trafficking.....	23
1.1.4. <i>Chlamydia trachomatis</i>	24
1.1.4.1. Chlamydial infections	24
1.1.4.2. Pathobiology	25
1.1.4.3. Avoidance of host immune and signalling responses	30
1.1.5. Research aims	31
Chapter 2: Materials and Methods	33
2.1. Antibiotics	33
2.2. Microbiological culture and media	33
2.2.1. Bacterial media and culture	33
2.2.2. Yeast media and culture.....	34
2.3. <i>Chlamydia trachomatis</i> culture	35
2.3.1. Ct propagation in McCoy cells.....	35
2.3.2. Harvesting Ct EBs	35
2.3.3. Density gradient purification of EBs	35
2.4. DNA extraction	37
2.4.1. Plasmid DNA extraction from bacteria by Miniprep	37
2.4.2. Plasmid DNA extraction from bacteria by Midiprep	37
2.4.3. Plasmid DNA extraction from yeast.....	37
2.4.4. Genomic DNA extraction from chlamydial elementary bodies	38

2.4.4.1. Commercial Promega kit.....	38
2.4.4.2. Phenol-chloroform extraction	38
2.5. DNA electrophoresis	39
2.6. Purification of PCR products	39
2.7. Restriction enzyme digests	39
2.8. Polymerase Chain Reaction (PCR)	40
2.8.1. Generation of PCR products for cloning.....	40
2.8.2. Colony PCR screen of transformed bacteria	40
2.9. Sequencing	40
2.10. DNA cloning	41
2.10.1. In-Fusion homologous end recombination	41
2.10.2. Ligation-based cloning	41
2.10.3. Bacterial transformation	41
2.10.3.1. Transformation of chemically competent cells	41
2.10.3.2. Transformation of electrocompetent cells	41
2.11. Generating detergent soluble lysates	42
2.11.1. NP-40 lysis buffer	42
2.11.2. HEPES lysis buffer	42
2.11.3. Urea lysis buffer	42
2.12. BCA protein assay	43
2.13. SDS-PAGE.....	43
2.14. Western blotting	43
2.15. CPY-invertase secretion assay	44
2.15.1. Qualitative assessment of CPY-inv secretion	44
2.15.2. Quantitative assessment of CPY-inv secretion	44
2.16. Visualisation of yeast vacuoles	45
2.17. Mammalian cell culture.....	46
2.18. Long-term cell storage.....	46
2.19. Contaminant removal by dialysis	47
2.20. Antibody coupling.....	47
2.21. Immunoprecipitation.....	48
2.22. Deubiquitinase activity assay	48
2.23. Immunofluorescence	49
2.24. Image acquisition	49
2.25. EGFR recycling.....	49
2.26. Protein production	50
2.27. Immobilised metal ion chromatography	50

2.28. Mass spectroscopy	51
2.28.1. Sample preparation	51
2.28.2. LC-MS/MS	51
2.28.3. Immunoaffinity purification.....	52
2.29. Antibodies	53
Chapter 3: Identification of <i>Ct</i> virulence proteins by <i>in silico</i> predictions	55
3.1. Introduction	55
3.1.1. The type III secretion system	55
3.1.2. The targeting of effectors for secretion via a T3SS	58
3.1.3. Mechanism of secretion by the T3SS.....	59
3.1.4. The use of bioinformatics as a tool to predict T3SS effectors	61
3.1.4.1. Opportunities offered by computational approaches	61
3.1.4.2. EffectiveT3	62
3.1.5. Yeast as a tool to study bacterial pathogenicity	64
3.1.6. Conservation of membrane trafficking in eukaryotes	65
3.1.7. Yeast as a tool to study chlamydial virulence.....	65
3.1.8. Pathogen effector protein screening in yeast (PEPSY).....	66
3.1.9. Objectives.....	67
3.2. Results	69
3.2.1. Selection of EffectiveT3 as a tool to predict T3SS substrates.....	69
3.2.2. Prediction of <i>Ct</i> T3S effectors using EffectiveT3	70
3.2.3. Isolation of <i>Ct</i> DNA.....	73
3.2.4. Expression of predicted <i>Ct</i> T3S effectors in a yeast model system	73
3.2.4.1. The use of yeast as a model organism	73
3.2.4.2. Linearisation of plasmid vector	73
3.2.4.3. Cloning <i>Ct</i> T3S effectors into yeast	74
3.2.5. Assessment of intracellular membrane trafficking defects	75
3.3. Discussion	79
3.3.1. The use of <i>in silico</i> approaches to predict <i>Ct</i> T3S effectors	79
3.3.2. Analysis of predicted <i>Ct</i> T3S effectors	80
3.3.3. Screening for T3S <i>Ct</i> virulence proteins.....	82
3.3.4. Study progression	85
Chapter 4: Generation and screening of a <i>Chlamydia trachomatis</i> library to identify virulence proteins	86
4.1. Introduction	86
4.1.1. Objectives.....	86

4.2. Results	87
4.2.1. Chlamydia trachomatis infections.....	87
4.2.2. Isolation of Ct DNA.....	88
4.2.3. Generation of a Ct genomic library.....	90
4.2.3.1. Digestion of Ct genomic DNA	90
4.2.3.2. Linearisation of plasmid vector	92
4.2.3.3. Plasmid ligation and the transformation of competent bacteria	92
4.2.3.4. Estimation of genome coverage	94
4.2.3.5. Scaling up the gene library	96
4.2.4. Ct genomic library screen.....	96
4.2.4.1. Optimisation of yeast transformations.....	96
4.2.4.2. Assessment of CPY-inv secretion.....	97
4.2.5. Initial characterisation of PSCs	100
4.2.5.1. PSC48.....	100
4.2.5.2. PSC50.....	102
4.2.5.3. PSC66.....	104
4.2.5.4. PSC54.....	106
4.2.5.5. PSC72.....	108
4.2.6. Investigation of the genes responsible for trafficking disruption.....	111
4.2.6.1. BOUR_00931-3 (PSC50).....	111
4.2.6.2. BOUR_00925-9 (PSC54).....	115
4.2.7. Visualisation of yeast vacuoles	117
4.2.8. Examination of CPY precursors	121
4.3. Discussion	123
4.3.1. Generation of a Ct genomic library.....	123
4.3.2. Screening the Ct genomic library	123
4.3.3. Characterisation of PSCs	126
4.3.3.1. PSC48.....	126
4.3.3.2. PSC50 and PSC66	126
4.3.3.3. PSC54.....	129
4.3.4. Study progression	130
Chapter 5: Analysis of ChlaDUB1 and ChlaDUB2.....	132
5.1. Introduction	132
5.1.1. Ubiquitin signalling	132
5.1.2. Deubiquitinases	134
5.1.2.1. DUB families	134
5.1.2.2. Layers of DUB complexity.....	134
5.1.2.3. Bacterial deubiquitinases	135

5.1.3. ChlaDUB1 and ChlaDUB2	136
5.1.4. Objectives.....	137
5.2. Results	138
5.2.1. Bioinformatic analysis of ChlaDUB1 and ChlaDUB2.....	138
5.2.2. Expression of ChlaDUB1 and ChlaDUB2 in mammalian cells	141
5.2.2.1. Cloning of myc-ChlaDUB1 and myc-ChlaDUB2	141
5.2.3. Effect of ChlaDUB1 or ChlaDUB2 on intracellular compartments	150
5.2.4. Effect of ChlaDUB1 and ChlaDUB2 on global ubiquitin levels	155
5.2.5. Identification of substrates for ChlaDUB1 and ChlaDUB2	156
5.2.5.1. Optimisation of mass spectroscopy experiments.....	156
5.2.5.2. Expression of ChlaDUB1 or ChlaDUB2 in protein production vectors	160
5.2.5.3. Protein production of ChlaDUB1 or ChlaDUB2.....	161
5.3. Discussion	170
5.3.1. Bioinformatic analysis of ChlaDUB1 and ChlaDUB2.....	170
5.3.2. Expression of ChlaDUB1 and ChlaDUB2 in mammalian cells	171
5.3.3. Effect of ChlaDUB1 or ChlaDUB2 on intracellular compartments	174
5.3.4. Effect of ChlaDUB1 and ChlaDUB2 on global ubiquitin levels	177
5.3.5. Identification of substrates for ChlaDUB1 and ChlaDUB2	178
5.3.5.1. Optimisation of mass spectroscopy experiments.....	179
5.3.5.2. Production of recombinant ChlaDUB1 and ChlaDUB2	181
5.3.6. Study progression	184
Chapter 6: General discussion	185
6.1.1. The host-pathogen interface	185
6.1.2. Identification of Ct virulence factors	186
6.1.3. The role of ChlaDUB1 and ChlaDUB2 during Ct infection	187
6.1.4. Future directions.....	189
6.1.5. Concluding remarks	191
Appendix.....	192
Oligomer sequences	192
Abbreviations	198
References.....	203

List of Tables

Table 2.1 The genotypes of the yeast strains used in this study.	34
Table 2.2 Primary antibodies used in this study.	53
Table 2.3 Secondary antibodies used in this study.....	54
Table 3.1 <i>Ct</i> proteins predicted by EffectiveT3 to be T3S.	72
Table 4.1 <i>Ct</i> DNA extraction yields.	90
Table 4.2 Optimisation of ligations and bacterial transformations.	93
Table 4.3 Optimisation of BHY10 yeast transformations.	97
Table 4.4 Assessment of CPY- <i>inv</i> secretion in library-transformed BHY10 or BHY12. PSCs were examined for plasmid-dependent CPY- <i>inv</i> secretion.	99
Table 4.5 Vacuolar morphologies induced by <i>vps</i> mutants.	118
Table 5.1 The location of catalytic active site residues of bacterial DUBs.	140

List of Figures

Figure 1.1 Schematic representation of endocytosis.	19
Figure 1.2 Schematic representation of phagocytosis.	22
Figure 1.3 The development cycle of <i>Chlamydia trachomatis</i>	29
Figure 3.1 The chlamydial Type III Secretion System.	58
Figure 3.2 The generation of a machine-learning algorithm.	63
Figure 3.3 Linearisation of pVT100-U by BamHI.	74
Figure 3.4 Cloning predicted <i>Ct</i> T3S effectors into pVT100-U.	75
Figure 3.5 Assessing CPY-inv secretion in predicted <i>Ct</i> T3S effectors.	76
Figure 3.6 Assessing plasmid-dependent effects of chlamydial clones.	78
Figure 4.1 Digestion of <i>Ct</i> genomic DNA with <i>Sau3AI</i>	91
Figure 4.2 Linearisation of pVT100-U by <i>BamHI</i>	92
Figure 4.3 Estimation of <i>Ct</i> DNA insert size.	95
Figure 4.4 CPY-inv secretion by PSCs encoding putative <i>Ct</i> virulence proteins in the presence and absence of plasmid.	100
Figure 4.5 CPY-inv secretion by PSC48.	102
Figure 4.6 CPY-inv secretion by PSC50.	104
Figure 4.7 CPY-inv secretion by PSC66.	106
Figure 4.8 CPY-inv secretion by PSC54.	108
Figure 4.9 CPY-inv secretion in PSC72.	109

Figure 4.10 CPY-inv secretion by BHY12 encoding <i>BOUR_00932</i> or <i>BOUR_00933</i>	112
Figure 4.11 CPY-inv secretion by BHY12 encoding <i>BOUR_00932</i> and <i>BOUR_00933</i>	113
Figure 4.12 CPY-inv secretion by BHY12 encoding <i>BOUR_00932</i> or <i>BOUR_00933</i> with their intragenic regions.....	114
Figure 4.13 CPY-inv secretion by BHY12 encoding the catalytic DUB domain of <i>BOUR_00932</i> or the PSC50-encoded gene fragment of <i>BOUR_00933</i> fragment.....	115
Figure 4.14 CPY-inv secretion by BHY12 encoding each of the individual full- length PSC54 genes.....	116
Figure 4.15 CPY-inv secretion of BHY12 encoding gene combinations of PSC54 genes.....	117
Figure 4.16 Vacuolar phenotypes induced by BY4741 <i>vps</i> mutants.	120
Figure 4.17 Vacuolar phenotypes induced by PSC50 or PSC54.....	121
Figure 4.18 Assessment of CPY precursors in BHY12 expressing <i>BOUR_00932</i> or <i>BOUR_00933</i>	122
Figure 5.1 Full length protein alignment of bacterial DUBs.....	139
Figure 5.2 Protein alignment of the catalytic domain of bacterial DUBs.	141
Figure 5.3 Expression of myc-ChlaDUB1 or myc-ChlaDUB2 in a HeLa cell line.	143
Figure 5.4 Enhanced DUB activity detected in HeLa lysates expressing ChlaDUB1.....	144
Figure 5.5 Optimisation of conditions required for immunoprecipitating myc- ChlaDUB1 or myc-ChlaDUB2.....	145

Figure 5.6 K63-linked deubiquitinase activity of ChlaDUB1 or ChlaDUB2.	147
Figure 5.7 K48-linked deubiquitinase activity of ChlaDUB2.....	149
Figure 5.8 The effect of ChlaDUB1 expression on endocytic compartments.	151
Figure 5.9 The effect of ChlaDUB2 expression on endocytic compartments.	152
Figure 5.10 The effect of ChlaDUB1 or ChlaDUB2 expression on autophagosomes.	153
Figure 5.11 The effect of ChlaDUB1 or ChlaDUB2 expression on actin.....	154
Figure 5.12 The effect of ChlaDUB1 or ChlaDUB2 on global ubiquitin levels.	156
Figure 5.13 The formation of the signature ubiquitin K-ε-GG motif remnant following trypsin digestion.	158
Figure 5.14 Cloning ChlaDUB1 or ChlaDUB2 into pETFPP_21.....	161
Figure 5.15 Bacterial expression of recombinant ChlaDUB1 or ChlaDUB2. ..	163
Figure 5.16 Purification of ChlaDUB1 or ChlaDUB2.....	166
Figure 5.17 Expression and enzymatic activity of recombinant ChlaDUB1 and ChlaDUB2.....	168

List of Accompanying Material

USB (attached with this thesis)

./ LC-MS/MS data

Raw data obtained from the final optimisation trial run.

./ Thesis

An electronic version of this thesis.

Acknowledgements

First and foremost, I would like to extend my thanks to my primary supervisor, Dr Paul Pryor, for his continuous support and guidance throughout the course of my PhD. Thank you for your encouragement and advice and for always being so friendly and approachable whenever I have had a query. I am grateful for all of the time you have taken out of your busy schedule to help me develop my technical skills and to introduce me to new experimental techniques. I am also extremely grateful for your timely and constructive feedback on TAP reports, presentations and ultimately this thesis. You have taught me so much over the past few years, motivated me through the tough times and have been patient when I have had ditzy moments. I am extremely thankful.

I would also like to thank my secondary supervisor, Prof Tony Wilkinson. Although the project did not take the direction we had originally planned, I would like to thank you for all of your help and constructive feedback provided throughout my PhD.

Thank you to my thesis advisory panel, Prof Nia Bryant and Prof Marek Brzozowski, for insightful comments and feedback throughout this project. Thanks to Dr Becky Wiggins and Dr Wayne Paes for teaching me how to culture *Chlamydia*; Dr James Chong for help with sequencing PSC72; and Dr Adam Dowle for proteomics expertise.

Thank you to the Wellcome Trust for funding my PhD and for providing me with the opportunity to broaden my horizons and skills through the provision of an initial rotation year and the chance to undertake a policy internship.

I would also like to thank my friends in the Biology department, particularly those in the Cell Biology Lab and the Centre of Immunology and Infection, who have made my time in York so enjoyable.

Finally, thank you to my family who have been there for me every step of the way. I am eternally grateful for your continuous support, encouragement and motivational talks. I would not be where I am today without you.

Author's Declaration

All data presented in this thesis are original work and have not previously been presented for an award at this, or any other, university. All sources are acknowledged as references.

Hayley Clissold performed all work, with the exception of the mass spectroscopy experiments presented in Chapter 5, which was performed by Adam Dowle from the Technology Facility at the University of York Biology department.

Chapter 1: Introduction

1.1.1. The endocytic pathway

Endocytosis is the process by which cells internalise extracellular or membrane-bound material less than 200nm in size by the invagination of the plasma membrane and the formation of *de novo* membrane-bound vesicles.

Endocytosed cargo includes nutrients, receptor-ligand complexes, lipids, membrane proteins and cell debris. Furthermore, fluid and solutes can also be engulfed by this process where it is instead termed pinocytosis. Endocytosis enables the interaction between cells and their extracellular environment and this process is therefore highly regulated to ensure that cellular processes such as antigen presentation and intracellular signalling cascades are activated or inhibited according to the requirements of the cell.

Endocytic trafficking consists of a dynamic network of organelles that includes the early endosome, late endosome and endolysosome and each of these have a distinctive composition and function (Figure 1.1). A central feature of this network is the regulation of endocytic trafficking by the Rab family of guanosine triphosphate (GTP)ases that preferentially associate with distinct endocytic organelles and regulate the trafficking of materials through the system (Zerial and McBride, 2001). Rab GTPases function as 'molecular switches' that alternate between an active GTP-bound state and an inactive guanosine diphosphate (GDP)-bound state and this transition governs their interactions with other endocytic proteins to mediate trafficking events. GDP-bound Rabs require a guanine nucleotide exchange factor (GEF) for its conversion into the active GTP form.

The internalisation of extracellular components requires the invagination of the plasma membrane. Although this invagination and the subsequent fission of the membrane-bound vesicle during the formation of an early endosome is not an energetically favourable process, the presence of specialised fission machinery facilitates the process to enable the formation of early endosomes (Frolov and Zimmerberg, 2010, Chernomordik and Kozlov, 2003). Typically, early

endosomes can be formed in a clathrin-mediated, caveolae-mediated or raft-mediated (clathrin-independent) manner (Parkar et al., 2009).

The first organelle of the endocytic pathway is the early endosome, which is characterised by the presence of early endosome antigen 1 (EEA1) and Rab5 (Christoforidis et al., 1999, Jovic et al., 2010). Early endosomes first receive internalised cargo and function as the main sorting station in the endocytic pathway. These sorting endosomes are peripherally located and have a luminal pH 6.8 – 5.9 (Maxfield and Yamashiro, 1987). Within 10 min of arrival in the early endosome, cargo is directed for delivery back to the plasma membrane, delivered to the endocytic recycling compartment (ERC) or detained for progression along the endocytic pathway (Maxfield and McGraw, 2004). This sorting and recycling process is required for proteins such as receptor-ligand complexes that dissociate upon delivery to the mildly acidic early endosome lumen. Typically, receptors, such as the transferrin receptor, are recycled back to the plasma membrane, while their ligands are destined for progression along the endocytic pathway (Dautry-Varsat et al., 1983). Receptors can be rapidly recycled directly back to the plasma membrane or trafficked to the plasma membrane via the ERC. The ERC is composed of tubular organelles that are associated with microtubules (Hopkins, 1983, Yamashiro et al., 1984) and although the ERC functions to sort molecules to several different cellular destinations, most molecules sorted by the ERC are returned to the plasma membrane (Maxfield and McGraw, 2004).

Early endosomes undergo a maturation process to form late endosomes. During this maturation, the early endosome membrane buds inwards to form intraluminal vesicles (ILV) that specifically sequester ubiquitinated cargo that is destined for lysosomal degradation (Sachse et al., 2002). ILV formation is controlled by various phosphoinositides and components of the endosomal sorting complex required for transport (ESCRT) machinery. The lumen of early endosomes typically contains several ILVs (van Meel and Klumperman, 2008). ILVs are transported with their ubiquitinated cargo to lysosomes for degradation. Thus, ILVs play a key role in the down-regulation of receptors and

are hence fundamental in the regulation of signalling cascades (Scott et al., 2014).

Early endosomal maturation into late endosomes is mediated by Rab conversions. Late endosomes characteristically express Rab7 and harbour a decreased intraluminal pH of 6.0 – 4.9 (Maxfield and Yamashiro, 1987). During early endosomal maturation, the protein complex Mon1B-Ccz1 is recruited at early endosomal sites to remove the Rab5 GEF, RABGEF1, in order to reduce Rab5 activity. Furthermore, in yeast, Mon1B-Ccz1 functions as a GEF for Rab7, thus is likely to contribute to Rab7 recruitment to endosomes (Nordmann et al., 2010). This Rab switch is essential for maturation in the endocytic pathway as Rab5 effectors are removed and Rab7 effectors are acquired for the trafficking of endocytosed cargo through the late endosomal stage.

The final step in endosomal maturation is the fusion between late endosomes and lysosomes to form the endolysosome. Upon the formation of the endolysosome, lysosomes are reformed by budding off of the endolysosome in a process referred to as lysosome reformation (Bright et al., 1997). The reformation of lysosomes is fundamental to ensure further fusions with late endosomes, given that the hydrolysis of endocytosed cargo takes place within the endolysosome (Huotari and Helenius, 2011).

Mature late endosomes can be up to 1µm in diameter and can contain several ILVs of 50-100nm in diameter (Huotari and Helenius, 2011). Lysosomes maintain a luminal pH of 4.6 - 5.0 (Mellman et al., 1986) and are comprised of approximately 60 different lysosomal enzymes that can degrade molecules upon fusion with late endosomes (Repnik et al., 2013). These hydrolases include sulphatases, glycosidases, peptidases, phosphatases, lipases and nucleases, all of which are active at an acidic pH and allow the lysosome to hydrolyse a huge repertoire of biological substrates (Settembre et al., 2013).

Lysosomes are characterised by the presence of specific proteins such as lysosomal-associated membrane protein (LAMP) 1 and LAMP2. There are a multitude of different lysosomal membrane proteins and the most abundant are the LAMPs, CD63 and lysosomal integral membrane protein (LIMP) 2

(Eskelinen et al., 2003). The luminal domain of lysosomal membrane proteins is commonly highly glycosylated and this feature forms a continuous glycoprotein layer at the luminal side of the lysosomal membrane that is believed to protect the lysosomal membrane from the action of luminal hydrolases (Fukuda, 1991).

As well as extracellular cargo, intracellular material such as cytoplasmic contents destined for degradation and recycling, can also enter the lysosome by autophagy. Autophagy is activated by a plethora of stress-inducing conditions and mediates the degradation of protein aggregates, oxidised lipids, damaged organelles and intracellular pathogens. The lysosome functions to degrade these components and, in doing so, generates energy and breakdown products that can be used as nutrient and energy sources for the cell.

The correct functioning of lysosomes is fundamental for cell maintenance and deregulation of lysosomal functionality is linked to several lysosomal storage disorders. The deficiency of a single hydrolase can lead to the inability of the lysosome to degrade a particular macromolecule. Alternatively, some lysosomal hydrolases require activator proteins to become active, thus any mutations affecting activator proteins can also mimic the deficiency of a hydrolase (Ferreira and Gahl, 2017). The subsequent accumulation of a macromolecule or the perturbation in a related biochemical pathway disrupts normal lysosomal function and can result in a variety of clinical manifestations including swollen joints, heart failure, mental and motor dysfunction and blindness (Ferreira and Gahl, 2017). For example, Danon disease is a rare lysosomal disorder caused by a mutation in LAMP2 that results in a LAMP2 deficiency in the lysosome. This deficiency mediates the disruption of autophagy and causes clinical manifestations such as skeletal myopathy, cognitive defects and visual problems (Rowland et al., 2016).

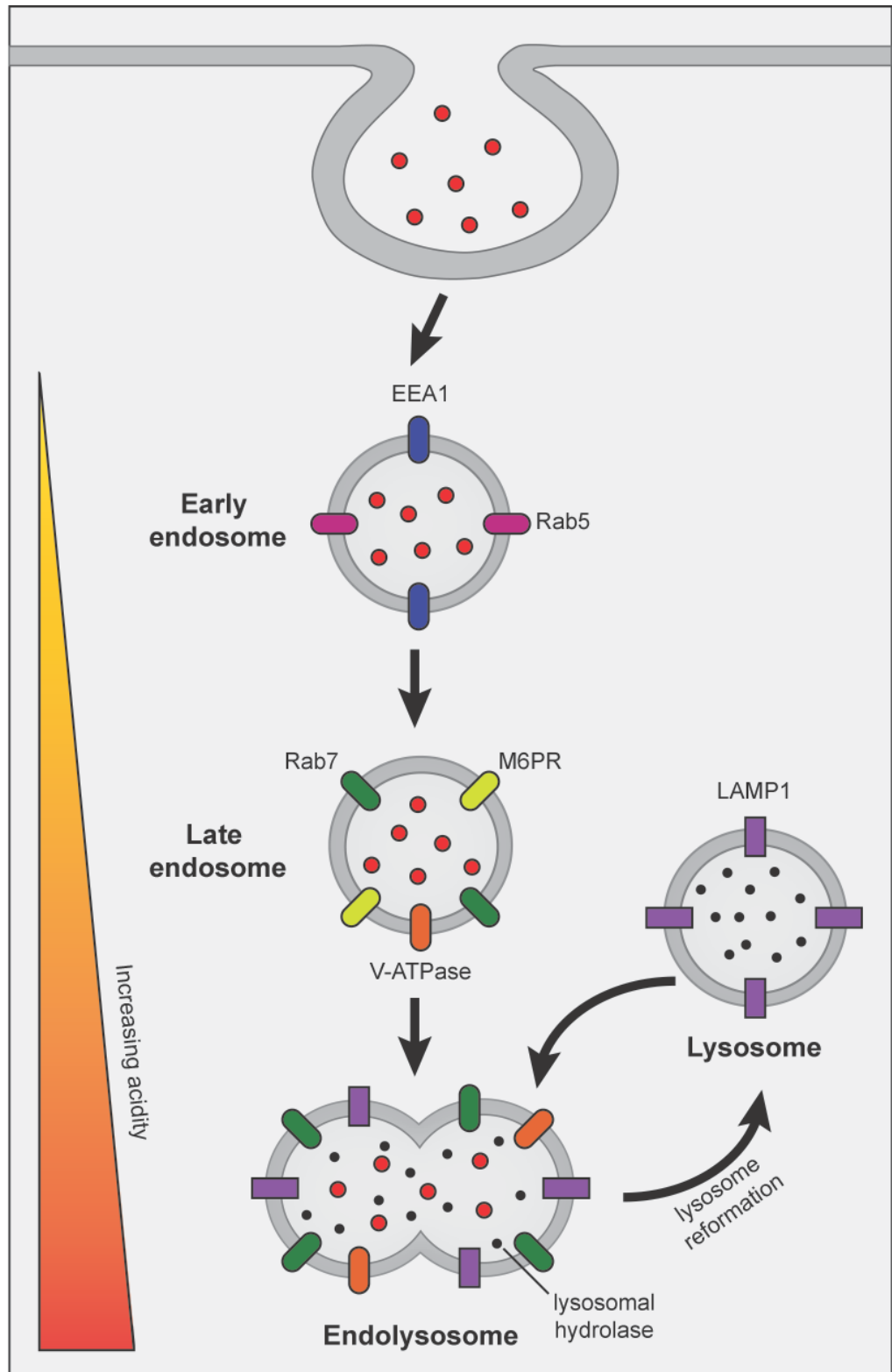


Figure 1.1 Schematic representation of endocytosis. Extracellular components are engulfed by invaginations of the plasma membrane into early endosomes. Early endosomes undergo maturation steps involving the loss of EEA1 and Rab5 and the acquisition of Rab7 and M6PR to form the late endosome. The late endosome fuses with lysosomes to form the endolysosome where internalised cargo is degraded by hydrolytic enzymes.

The luminal pH of endocytic compartments becomes increasingly acidic as the endocytic pathway progresses. This increasing acidity is essential for membrane trafficking and the sorting and degradation of cargo (Huotari and Helenius, 2011). The pH gradient throughout the endocytic pathway enables receptors to bind ligands in one compartment and release them in another. Furthermore, lysosomal hydrolytic enzymes, such as sulphatases, lipases and peptidases, which function optimally at a low pH, are able to degrade cargo in these acidic compartments. The acidification of endosomes and lysosomes is performed by the vacuolar ATPase (V-ATPase). The V-ATPase is widely expressed in eukaryotic cells and is composed of two multimeric subunits: the cytoplasmic V_1 domain and vacuolar membrane V_0 domain. Activity of the V-ATPase depends upon the correct assembly of these two domains in order to regulate vesicular trafficking and proteostasis (Hu et al., 2015).

Membrane fusion events require the cooperation of several different proteins in multi-protein complexes to enable effective and efficient vesicle tethering, docking and fusion. The tethering of membranes requires ATP and the interaction of Rab GTPases and soluble NSF attachment protein receptors (SNAREs) with multi-protein complexes. In early endosome maturation, Rab5 interacts with the core Class C vacuole/endosome tethering (CORVET) complex, while Rab7 interacts with the homotypic fusion and vacuole protein sorting (HOPS) complex during the fusion of late endosomes and lysosomes (Balderhaar and Ungermann, 2013). The interaction between Rab GTPases, SNAREs and the HOPS/CORVET complexes enables the tethering and docking of membranes for membrane fusion and maturation to take place.

1.1.2. Phagocytosis

Phagocytosis describes the cellular process whereby particulates of size $0.2\mu\text{m}$ or larger are engulfed into a plasma membrane-bound organelle termed the phagosome (Gordon, 2016). The phagosome undergoes a sequence of membrane fission and fusion events during its maturation until its eventual fusion with the lysosome for the degradation of the phagocytosed material (Figure 1.2). Phagocytosis is closely related to endocytosis and these two

cellular processes share several regulatory and effector proteins. Phagocytosis is commonly attributed to the clearance of microbial pathogens and thus contributes to the first line of defence against infections (Flannagan et al., 2012).

Phagocytic cells, such as macrophages, neutrophils and dendritic cells, are highly specialised in their ability to engulf and destroy invading microorganisms. Phagocytic cells are able to initiate the engulfment of macromolecules and microorganisms by phagocytosis through the attachment of conserved pathogen-associated molecular patterns (PAMP) or damage-associated molecular patterns (DAMP) to a myriad of receptors displayed on the plasma membrane of phagocytic cells. Given the multitude of different pathogens and particles that phagocytic cells could encounter, they display multiple types of receptors including pattern recognition receptors (PRR) for the recognition of PAMPs, Fc receptors (FcR) that bind to antibodies attached to infected cells or pathogens, and complement receptors such as CR3 involved in the onset of the complement pathway (Gordon, 2016). Each of these receptors are capable of recognising distinctive molecular patterns and, upon activation, can initiate a variety of signalling cascades that can lead to an appropriate and effective immunological response. Thus, the diverse receptor types collaborate to detect and ingest particles and pathogens for effective clearance (Freeman and Grinstein, 2014). In addition to specialised phagocytic receptors whose primary role is to recognise molecular pathogen antigens, phagocytes also present non-phagocytic receptors, such as toll-like receptors (TLR) and G-protein coupled receptors (GPCR), which modulate the phagocytic process (Freeman and Grinstein, 2014).

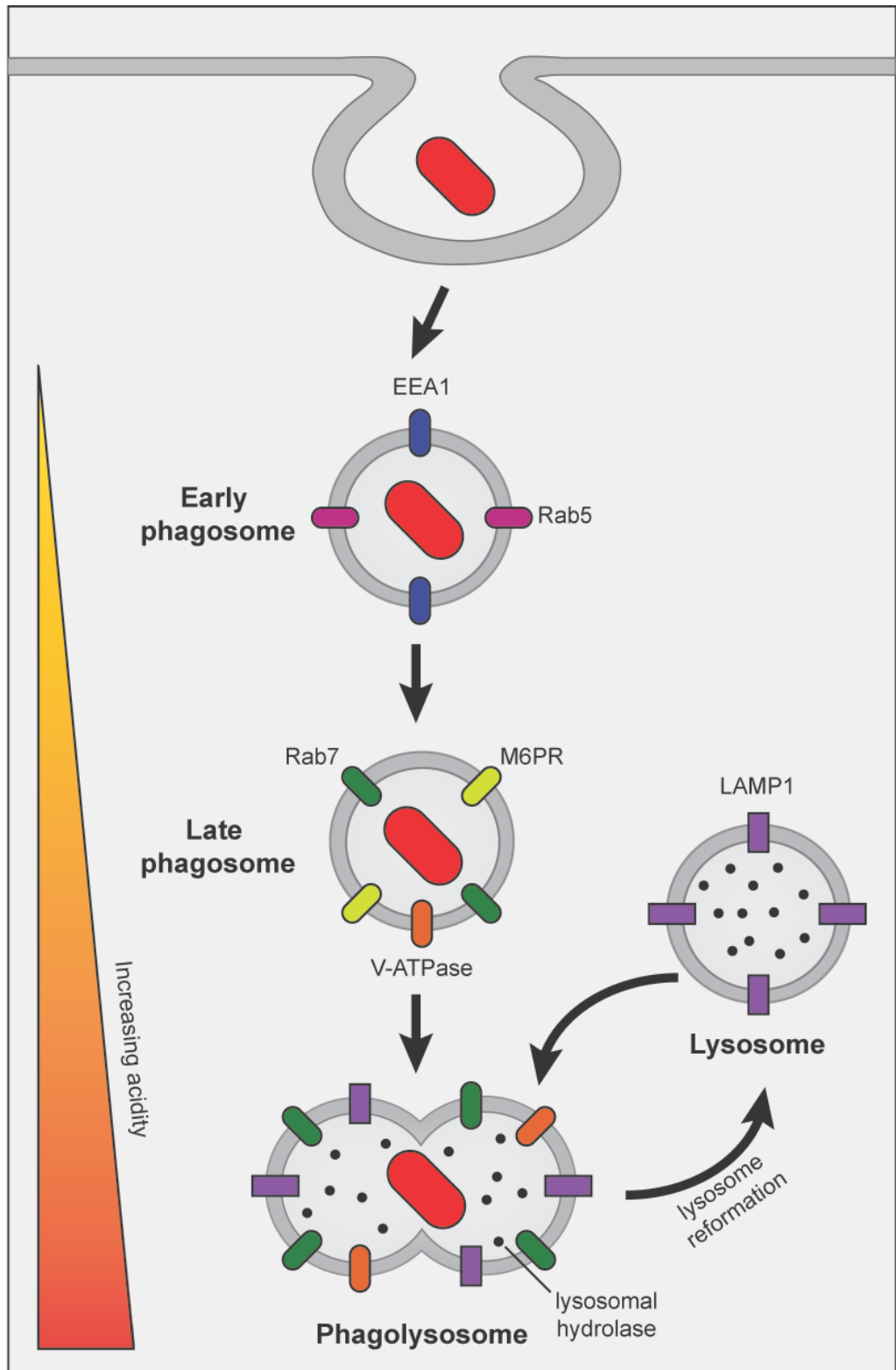


Figure 1.2 Schematic representation of phagocytosis. The process of phagocytosis and endocytosis are very similar. Phagocytic cells internalise microbes into membrane-bound phagosomes, which undergo a series of maturation steps and ultimately fuse with the lysosome to form the phagolysosome where lysosomal hydrolases can destroy phagocytosed microbes.

Comparable to the endosomal maturation process during endocytosis, phagosomes undergo sequential rounds of fission and fusion with intracellular organelles while acquiring and removing characteristic membrane proteins and luminal contents. This maturation of nascent phagosomes to phagolysosomes results in the destruction of invading microorganisms. However, several intracellular pathogens have evolved diverse and intricate mechanisms to evade these host defences.

1.1.3. Pathogen manipulation of intracellular membrane trafficking

By definition, intracellular pathogens are able to modulate host cell defences in order to survive intracellularly. These pathogens are able to either diverge away from normal phagocytic trafficking that would otherwise target the pathogen for destruction or the pathogen is able to mediate host defences in such a way that allows for the survival of the pathogen within the phagolysosome. Many pathogenic Gram-negative bacteria express type III secretion systems (T3SS) or type IV secretion systems (T4SS) that translocate a myriad of effector proteins into the host cell which manipulate various host signalling pathways, such as cytoskeletal dynamics and vesicle trafficking (Ham et al., 2011). Notably, some pathogens actively seek phagocytes, because the pathogen can make use of its arsenal of secreted bacterial effectors to survive within a compartment that protects the intracellular bacterium from circulating antibodies and components of the complement system, while also receiving a consistent supply of nutrients from endocytic cargo.

Intracellular pathogens that escape the phagosome tend to survive within the host cell cytoplasm or they establish a protected replicative niche. For example, *Shigella* avoids the endolysosomal system by secreting the T3SS effectors IpaB and IpaC that rapidly lyse the phagosomal membrane (Blocker et al., 1999). IpaB forms membrane-disrupting pores that forms an escape route for the bacterium to enter the host cell cytoplasm (High et al., 1992). To enable cytoplasmic survival, the *Shigella* protein, IcsB, effectively camouflages another *Shigella* protein, VirG, which would otherwise induce autophagy (Ogawa et al.,

2005). Thus, the host cell does not undergo autophagy and hence the bacterium is able to survive intracellularly.

Furthermore, some viruses and bacteria exploit the characteristic increase in acidity along the endosomal pathway as some pathogen toxins become activated in acidic conditions. For example, *Bacillus anthracis* produces the anthrax toxin that depends upon a low pH to induce activity (Batra et al., 2001).

Effector proteins secreted by intracellular bacteria demonstrate a multitude of evasion tactics. For example, several bacterial effectors modulate host membrane trafficking through interactions with Rab GTPases, phosphoinositide lipids, vesicle tethering proteins and the actin cytoskeleton (Ham et al., 2011).

1.1.4. Chlamydia trachomatis

1.1.4.1. Chlamydial infections

Chlamydiae are Gram-negative obligate intracellular bacteria that can infect a broad spectrum of organisms, from humans to free-living amoebae. Of this family, *Chlamydia trachomatis* (*Ct*) and *Chlamydia pneumoniae* (*Cpn*) are the main species that infect humans, although *Chlamydia psittaci* (*Cps*) can be transmitted to humans via avian hosts.

Ct is classified into three biovars that are individually further divided into serovars. The trachoma biovars consists of serovars A-C and is the leading cause of preventable blindness in the developing world. The genital tract biovar includes serovars D-K and is the causative agent of the most common sexually transmitted infection (STI) in the UK. Finally, the lymphogranuloma venereum (LGV) biovar is comprised of L1-L3 serovars and causes invasive urogenital or anorectal infection. This study focuses on the *Ct* genital tract biovar and thus the terms 'chlamydia' and '*Ct*' will hereafter refer to the genital tract biovar unless otherwise stated.

Genital tract chlamydial infections are typically asymptomatic and 70-80% of women with chlamydia do not show any visible signs of the disease (Malhotra et al., 2013). However, between 15-40% of chlamydial infections ascend to the

upper genital tract and subsequently lead to more serious health conditions such as pelvic inflammatory disease, ectopic pregnancies, tubal obstruction and infertility.

In 2016, there were approximately 420,000 diagnoses of chlamydia in England and 128,098 of these cases were diagnosed among young people aged 15-24 years old (Public Health England, 2017). Comparatively, chlamydia dominates STI diagnoses and accounted for 49% of all new STI diagnoses in England in 2016 (Public Health England, 2017). Cases of other STIs were relatively low by comparison with 36,244 diagnoses of gonorrhoea and 5,920 diagnoses of syphilis (Public Health England, 2017).

An effective vaccine for the prevention of chlamydial infections is not yet available and although infections can currently be treated using antibiotics, such as azithromycin or doxycycline, there is a continuing threat of the development of antibiotic resistance. Given its prevalence and asymptomatic nature, the National Chlamydia Screening Programme (NCSP) was implemented in England in 2003 to control the spread of the disease through early detection and treatment of asymptomatic infection, thus reducing onward transmissions and the consequences of untreated infections.

1.1.4.2. Pathobiology

Chlamydiae undergo a biphasic developmental cycle in which they alternate between two morphologically and functionally distinct entities: the extracellular, infectious elementary body (EB) and the intracellular, non-infectious reticulate body (RB) (Figure 1.3). The EB has long been understood to be metabolically inactive, but recent evidence suggests that EBs are capable of metabolism and biosynthetic activities in the presence of D-glucose-6-phosphate as a source of energy (Omsland et al., 2014). Furthermore, quantitative proteomics have indicated that EBs encompass several proteins involved in metabolism, which are likely to drive metabolic activity immediately upon entry into host cells (Saka et al., 2011).

The infectious EB binds to host cells by forming a tri-molecular bridge that connects bacterial adhesins, host cell receptors and host heparin sulphate proteoglycans (HSPG) (Mehlitz and Rudel, 2013). Adhesion of EBs to the host cell is a two-step process consisting of an initial low affinity interaction of the EB with host HSPG followed by high affinity binding to host cell receptors. A main chlamydial adhesin involved in host cell attachment is the glycosylated major outer membrane protein (MOMP) (Swanson and Kuo, 1994). The glycan moiety of MOMP shares similarities with mannose-6-phosphate (M6P) and thus MOMP is believed to bind to the host M6P receptor (M6PR). Furthermore, the blocking of M6PR prevents *Cpn* attachment and invasion (Puolakkainen et al., 2005). Other chlamydial adhesins include OmcB that mediates the attachment of EBs to HSPG, and lipopolysaccharide (LPS) that is believed to bind to the cystic fibrosis transmembrane conductance regulator (CFTR) (Ajonuma et al., 2010). Furthermore, the polymorphic membrane protein (Pmp) family plays a key role in bacterial adhesion, particularly Pmp21, which binds to the epidermal growth factor receptor (EGFR) and functions as both an adhesin and an invasin (Becker and Hegemann, 2014, Molleken et al., 2013). These various bacterial adhesins can bind to a multitude of different host cell receptors, including EGFR, fibroblast growth factor (FGF) receptor (FGFR) (Kim et al., 2011), platelet derived growth factor receptor (PDGFR) (Elwell et al., 2008) and ephrin receptor A2 (EPHA2) (Subbarayal et al., 2015). Given the diversity in bacterial adhesins and host cell receptors, it is likely that chlamydial invasion varies depending upon the host cell type and the chlamydial species (Bastidas et al., 2013).

Following attachment to host cells, the EB secretes pre-synthesised effector proteins into the host via its type III secretion system (T3SS). These effectors function to induce host cytoskeletal rearrangements that subsequently promote bacterial invasion and activate host signalling. Well-studied effectors that are immediately secreted into host cells are the translocated actin recruiting phosphoprotein (Tarp) and CT694. Tarp is a multi-domain protein that nucleates and bundles actin to enhance its oligomerisation and facilitate chlamydial internalisation. The N-terminus of Tarp is phosphorylated on several tyrosine residues and the C-terminus harbours actin binding domains (ABD).

These structural features enable Tarp to nucleate actin via ABD and enhance its oligomerisation to facilitate cytoskeletal rearrangements for chlamydial invasion (Jewett et al., 2010). This Tarp-mediated actin binding is believed to be required for chlamydial invasion given that internalisation is blocked in the presence of anti-ABD sera (Jewett et al., 2010). Furthermore, CT694 contains a membrane localisation domain and an actin-binding AHNAK domain. AHNAK is a large human protein involved in cytoskeletal maintenance and cell signalling. Thus, when CT694 interacts with AHNAK, actin dynamics become disrupted and this facilitates the internalisation of chlamydial EBs (Hower et al., 2009).

EBs are soon endocytosed into a membrane-bound compartment known as the inclusion by either caveolin (Stuart et al., 2003), membrane rafts (Jutras et al., 2003) or clathrin-mediated endocytosis. Unlike during normal phagocytic trafficking, the chlamydial inclusion rapidly dissociates away from the canonical phagolysosomal pathway and migrates along microtubules towards the microtubule organising centre (MTOC). It has been suggested that chlamydial effectors tether the inclusion to dynein in order to migrate towards the MTOC. Inclusion membrane proteins (Inc) are thought to play a role in the migration of the inclusion. For example, the *Ct* Inc, CT850, directly binds dynein light chain I to promote the positioning of the inclusion at the MTOC (Mital et al., 2015). Similarly, *Cps* IncB binds to the Snapin protein that associates with host SNARE proteins. Snapin also binds to dynein and thus its interaction with IncB is likely to connect the inclusion to the dynein motor complex (Bocker et al., 2014).

Early chlamydial effectors remodel the inclusion membrane and redirect exocytic vesicles to facilitate host-pathogen interactions. At around 6-8 h post-infection, EBs differentiate into the metabolically active and replicative RB and effectors that function to acquire host nutrients and maintain the viability of the cell host are expressed. Chlamydiae do not encode the necessary biosynthetic enzymes to synthesise lipids for survival (Stephens et al., 1998). Thus, they have evolved sophisticated mechanisms to acquire lipids from the host cell. For example, inclusion membrane proteins (Inc) are secreted via the chlamydial T3SS and are inserted into the inclusion membrane to promote nutrient

acquisition by redirecting exocytic vesicles that are transiting between the Golgi and the plasma membrane. Notably, the host ceramide endoplasmic reticulum transport protein (CERT) that normally transports ceramide from the ER to the *trans*-Golgi is recruited to the chlamydial inclusion membrane where it interacts with the inclusion membrane protein, IncD. This interaction enables the chemical conversion of ceramide into sphingomyelin as a nutrient source for chlamydiae (Derre et al., 2011). Furthermore, the chlamydial inclusion also interacts with other host organelles for nutrient acquisition. For example, multivesicular bodies (MVB) serve as a source of sphingolipids and cholesterol (Beatty, 2008); lipid droplets and peroxisomes serve as a possible source of triacylglycerides and metabolic enzymes following their translocation into the inclusion lumen (Cocchiaro et al., 2008, Kumar et al., 2006, Boncompain et al., 2014); and mitochondria and lysosomes are also believed to be a source of essential amino acids derived from the degradation of host proteins (Matsumoto et al., 1991, Ouellette et al., 2011).

Chlamydial RBs are replicative and thus at 8-16 h post infection the bacteria divide by binary fission subsequently causing the inclusion to expand considerably in order to accommodate the increasing volume. Moreover, if a single cell is infected with multiple EBs that have been engulfed into multiple individual inclusions, these inclusions can undergo homotypic fusion mediated by IncA (Hackstadt et al., 1999).

During the late stages of infection, at around 24-72 h post infection, RBs asynchronously differentiate back into EBs pre-packaged with early cycle effectors. The precise signal for EB-to-RB and RB-to-EB differentiation is not well understood, but the transition from RB to EB is believed to be linked to the detachment of RBs from the inclusion membrane (Elwell et al., 2016). In preparation for the transition into a metabolically inactive EB, late cycle gene expression includes DNA-binding histone proteins, Hc1 and Hc2, which condense chlamydial DNA in order to switch off the transcription of several genes (Brickman et al., 1993, Hackstadt et al., 1993).

EBs are released from the host cell by either host cell lysis or the extrusion of the chlamydial inclusion. Firstly, for lytic release of EBs, the type II secretion system (T2SS) effector, chlamydia protease-like activity factor (CPAF), is believed to disassemble the host cell membranes and prepare for the exit of EBs (Snaveley et al., 2014). During host cell lysis, the inclusion membrane is firstly permeabilised, followed by the permeabilisation of the nuclear membrane and finally calcium-dependent lysis of the plasma membrane (Hybiske and Stephens, 2007, Elwell et al., 2016). The exit of chlamydiae by this method results in the death of the host cell. Alternatively, the extrusion of the inclusion resembles exocytosis and thus leaves the host cell intact. The *Ct* Inc, CT228, is involved in extrusion, together with the polymerisation of actin and the coordination of several proteins such as RHOA GTPase, myosin II and components of the myosin phosphatase pathway (Hybiske and Stephens, 2007). Extrusion of the chlamydial inclusion prevents the onset of pro-inflammatory host responses and protects the EBs from host immunological factors.

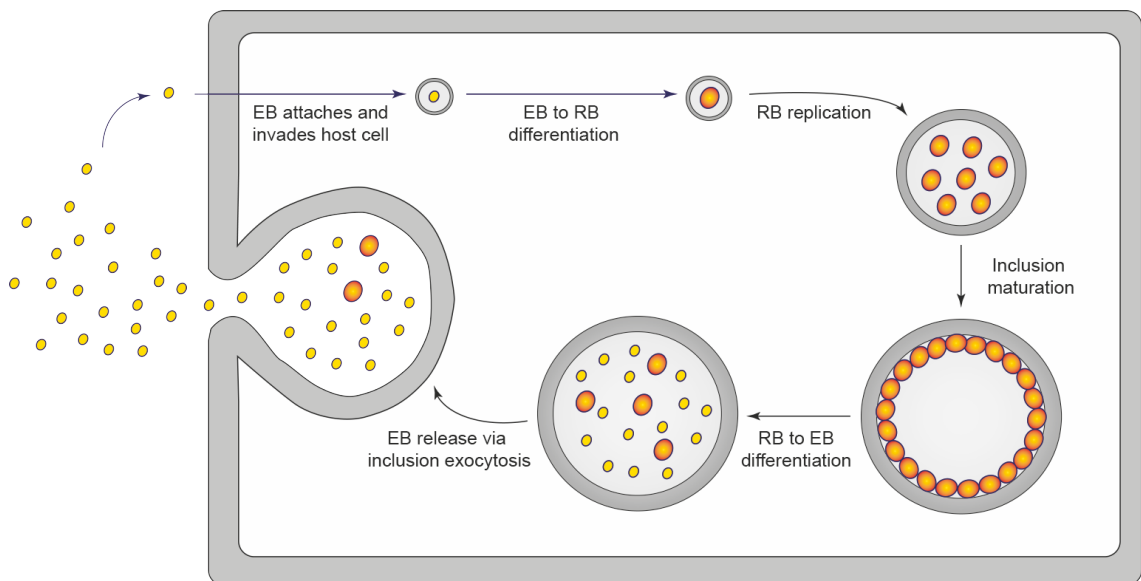


Figure 1.3 The development cycle of *Chlamydia trachomatis*. Infectious EBs are endocytosed into a membrane-bound compartment known as the inclusion, which rapidly dissociates from the endolysosomal system. EBs differentiate into the metabolically active RBs that replicate exponentially. During the late stages of infection, RBs differentiate back into EBs. EBs exit the host by cell lysis or extrusion of the inclusion.

1.1.4.3. Avoidance of host immune and signalling responses

The intricate survival mechanisms by which chlamydiae are able to survive intracellularly depend upon the ability of the chlamydial inclusion to selectively fuse with certain intracellular compartments (e.g. nutrient-rich exocytic vesicles) and avoid fusion with others (e.g. lysosomes). Several protein families including the Rab GTPases, phosphoinositide lipid kinases and SNARE proteins regulate the fusion of endocytic vesicles and thus these proteins are targeted for manipulation by intracellular pathogens. Rabs can be recruited to the chlamydial inclusion in a species-dependent or independent manner. For example, Rab4 and Rab11, which are usually associated with recycling endosomes and control the transferrin recycling pathways that are intercepted by the chlamydial inclusion, are recruited to the inclusion during infection of all chlamydia species (Damiani et al., 2014, Bastidas et al., 2013). The *Ct* Inc, CT229, has been identified as a Rab4-interacting protein and is the only *Ct* Inc proven to be a Rab binding partner (Damiani et al., 2014), but this is not conserved among other strains or serovars (Rzomp et al., 2006). Moreover, Rab6, which is typically associated with ER-Golgi trafficking and facilitates the chlamydial acquisition of lipids from the Golgi, is also recruited to the *Ct* inclusion, but not in other species, thus demonstrating species-dependency.

Phosphoinositides are key determinants of host vesicle fusion and during chlamydial infections, several proteins associated with phosphoinositol-4-phosphate (PI4P) metabolism, such as Arf1, are recruited to the chlamydial inclusion. Arf1 is a GTPase that associates with Golgi membranes in its active form and recruits phosphatidylinositol 4-kinases (PI4K) and PI4P-binding proteins to the Golgi. Inclusion formation and the generation of infectious progeny are disrupted when levels of Arf1 are depleted, thus suggesting that PI4P generation at the inclusion plays a key role during infection (Moorhead et al., 2010).

Chlamydiae can also modulate host cell vesicle fusion and trafficking through interactions with SNARE proteins. The *trans*-Golgi SNARE proteins, syntaxin 6 (STX6) and STX10, are recruited to the inclusion (Moore et al., 2011, Lucas et

al., 2015). The utilisation of host STX10 has recently been demonstrated as a requirement for the maturation of the inclusion and the differentiation of RB to EB (Lucas et al., 2015). Furthermore, some chlamydial Incs contain SNARE-like motifs and thus mimic host SNAREs to modulate vesicle fusion. For example, IncA has reported functionality in protecting the chlamydial inclusion from fusing with the lysosome and also in the homotypic fusion of inclusions (Hackstadt et al., 1999) and contains two structural regions homologous to the eukaryotic SNARE domains, SNARE-like domain 1 (SLD1) and SLD2 (Ronzone et al., 2014). IncA binds to the host SNAREs, vesicle-associated membrane protein (Vamp) 3, Vamp7 and Vamp8, and has been reported to act in concert with host SNAREs to regulate membrane fusion (Delevoye et al., 2004), but also act as an inhibitory SNARE to limit fusion with endocytic compartments (Paumet et al., 2009). This careful interplay between chlamydial effectors and host proteins enables the fusion of the inclusion with certain intracellular compartments (e.g. exocytic vesicles), but inhibits fusion with others (e.g. lysosomes).

1.1.5. Research aims

Chlamydiae have evolved to be able to diverge away from normal endocytic trafficking to reside and replicate within an intracellular niche, termed the inclusion, following uptake into cells. *Ct* harbours a very small genome, which is only approximately 1Mb in size and encodes 314 *Chlamydia*-specific open reading frames (ORFs) (Stephens et al., 1998). Furthermore, *Ct* possesses a T3SS to translocate a myriad of effector proteins into the host cell to form the inclusion, evade host defences and acquire host nutrients. Given the ability to translocate effector proteins into the host cytoplasm and inclusion membranes, the T3SS is an attractive target for the identification of *Ct* effectors. However, few virulence proteins secreted by this mechanism have been well characterised in the present literature. Moreover, much remains to be understood regarding the ability of the chlamydial inclusion to divert away from host endocytic trafficking and evade fusion with the lysosome.

Therefore, we sought to:

- I. Make use of an *in silico* prediction program to predict *Ct* effector proteins likely to be secreted by the bacterium's T3SS.
- II. Generate a *Ct* genomic library to enable genome-wide screening for virulence proteins.
- III. Identify *Ct* virulence proteins involved in the disruption of host membrane trafficking using an established pathogen effector protein screening in yeast (PEPSY) screen.
- IV. Characterise the functionality of *Ct* virulence proteins identified through PEPSY screening.
- V. Identify the host protein(s) that interact with *Ct* effector proteins by mass spectroscopy.

Thus, the aims of this thesis were to identify *Ct* T3SS effector proteins that disrupt intracellular membrane trafficking and subsequently enable the pathogen to avoid destruction by the phagolysosome and then determine the host protein(s) that interact with these *Ct* T3SS effector proteins of interest.

Chapter 2: Materials and Methods

2.1. Antibiotics

Ampicillin stocks (Sigma) were prepared to 100mg/ml in sterile distilled H₂O, frozen for long-term storage and used at 100µg/ml. Hygromycin B was purchased as a 50mg/ml stock (Roche), stored at 4°C and used at 200µg/ml. Doxycycline stocks were prepared to 1mg/ml in sterile distilled H₂O, frozen for long-term storage and used at 1µg/ml. Cycloheximide was purchased as a 1mg/ml stock (Oxoid), stored at 4°C and used at 1µg/ml. Gentamicin was purchased as 10mg/ml stock (Gibco), stored at 4°C and used at 20µg/ml.

2.2. Microbiological culture and media

Unless otherwise stated, all bacterial media were purchased from either Oxoid or Formedium and all yeast media were purchased from Formedium.

All autoclaving was performed in a Prestige Medical Classic benchtop autoclave at 126°C and 1.4 bar for 22 min.

2.2.1. Bacterial media and culture

Lysogeny broth (LB) was prepared by dissolving 10g/L tryptone, 5g/L yeast extract and 5g/L NaCl in dH₂O followed by autoclaving. For LB agar, 15g/L agar was added prior to autoclaving.

Super optimal broth with catabolite repression (SOC) media was prepared by dissolving 20g/L tryptone, 5g/L yeast extract and 0.5g/L NaCl in dH₂O and adding KCl and MgCl₂ to a final concentration of 2.5mM and 10mM respectively and a final volume of 1 litre in dH₂O. Media was autoclaved followed by the addition of sterile-filtered glucose to a final concentration of 200mM.

2YT media was prepared by dissolving 16g/L tryptone, 10g/L yeast extract and 5g/L NaCl in dH₂O followed by autoclaving.

Unless otherwise stated, all bacterial cultures were grown in LB with appropriate antibiotics where necessary at 37°C with shaking at 250rpm.

2.2.2. Yeast media and culture

The yeast strains used in this study are outlined in Table 2.1.

Strain	Genotype	Source
SEY6210	<i>MATα leu2-3,112 ura3-52 his3-Δ200 trp1-Δ901 lys2-801 suc2-Δ9</i>	Robinson et al. (1988)
SEY6211	<i>MATα leu2-3,112 ura3-52 his3-Δ200 trp1-Δ901 ade2-101 suc2-Δ9</i>	Robinson et al. (1988)
BHY10	SEY6210 <i>leu2-3,112::pBHY11(CPY-Inv LEU2)</i>	Horazdovsky et al. (1994)
BHY11	SEY6210 <i>leu2-3,112::pBHY11(CPY-Inv LEU2)</i>	Horazdovsky et al. (1994)
BHY12	<i>MATα/MATα leu2-3,112::pBHY11(CPY-Inv LEU2/leu2-3,112::pBHY11(CPY-Inv LEU2) his3-Δ200/his3-Δ200 ura3-52/ura3-52 trp1-Δ901/trp1-Δ901 suc2-Δ9/suc2-Δ9 ADE2/ade2-101 lys2-801/LYS2</i>	Horazdovsky et al. (1994)
BY4741	<i>MATα his3Δ1 leu2Δ0 met15Δ0 ura3Δ0</i>	Dharmacon

Table 2.1 The genotypes of the yeast strains used in this study.

All yeast media were prepared according to the manufacturers' instructions.

Yeast extract peptone (YEP) media was prepared by dissolving 30g YEP (Formedium; cat #CCM0402) in 1 litre dH₂O and autoclaved. For YEP agar, 50g YEP agar (Formedium; cat #CCM0302) was dissolved in 1 litre dH₂O and autoclaved. Following autoclaving, a final concentration of 2% (v/v) sterile-filtered fructose was added as a carbon source.

Synthetic complete (SC) media was prepared by dissolving 6.9g yeast nitrogen base without amino acids and 1.926g synthetic complete mixture uracil dropout (-ura) in 1 litre dH₂O and autoclaved. For SC-ura agar, 15g agar was added per litre. Following autoclaving, a final concentration of 2% (v/v) sterile-filtered fructose was added as a carbon source.

Unless otherwise stated, all yeast were grown in non-selective (YEP fructose) media or selective (SC-ura) media in liquid cultures or on agar plates at 30°C. All liquid yeast cultures were incubated with shaking at 250rpm.

2.3. *Chlamydia trachomatis* culture

2.3.1. Ct propagation in McCoy cells

Ct serovar E (E/Bour) was propagated in McCoy cells. Adherent McCoy cells were cultured in tissue culture media (Dulbecco's modified eagle medium (DMEM; Gibco), 10% (v/v) foetal bovine serum (FBS; Invitrogen)) in 6-well tissue culture polystyrene plates (Corning). McCoy cells were inoculated with *Ct* that had been previously harvested from *Ct*-infected McCoy cells and suspended in infection media (DMEM (Gibco), 10% (v/v) FBS (Invitrogen), 1µg/ml cycloheximide, 20µg/ml gentamycin (Gibco)). Plates were centrifuged for 45 min at 550 x *g*. Infected cells were incubated at 37°C, 5% CO₂ for 72 h and inclusions were visible 48 h post-inoculation using light microscopy.

2.3.2. Harvesting Ct EBs

Ct EBs were harvested from McCoy cell monolayers when >80% cells contained inclusions 48 h post-inoculation. Cells were scraped, pelleted at 2000 x *g* for 10 min and resuspended in either infection media (for reinfection) or phosphate buffered saline (PBS; for freezing). McCoy cells were ruptured by vortexing with glass beads (5 x 1mm diameter beads per 75cm² flask) for 10 min/ml cell suspension and pelleted at 170 x *g* for 5 minutes. The supernatant was used for the reinfection of further McCoy cell monolayers or frozen in an equal volume of 4-sucrose phosphate buffer (4SP; 0.4M sucrose, 16mM Na₂HPO₄, pH 7.1, 0.2µm sterile-filtered). Typically, one harvest from all wells of a 6-well plate yielded sufficient *Ct* to infect 4 x 6-well plates.

2.3.3. Density gradient purification of EBs

Purification of *Ct* EBs was performed according to Scidmore (2005) with the following modifications. Firstly, 6-well tissue culture polystyrene plates (Corning) were used instead of 150cm² flasks. Secondly, to obtain large quantities of EBs,

aliquots of harvested bacteria were stored at -80°C until ready for density gradient purification. Finally, due to difficulties in obtaining renografin for gradient purification, gastrografen was instead used as the density media. Coombes *et al* (2002) have previously demonstrated gastrografen as suitable for the isolation of chlamydial EBs.

Briefly, supernatants from harvested *Ct* EBs were pooled into UltraClear centrifuge tubes (Beckman), sonicated for 40 seconds at 20W to disrupt any remaining intact host cells and pelleted at $500 \times g$, 15 min, 4°C in a Sorvall Evolution centrifuge with SS34 rotor. The EB-enriched supernatant was then pelleted at $30,000 \times g$, 30 min, 4°C in a Beckman Optima L-100XP with a SW28 rotor. The resulting pellet was then resuspended in sterile sucrose/phosphate/glutamate buffer (SPG; 0.2M sucrose, 10mM Na_2HPO_4 , 2.6mM $\text{Na}_2\text{H}_2\text{PO}_4$, 5mM L-glutamic acid, pH 7.4) and further sonicated for 10 seconds at 32W to ensure complete resuspension. The sonicated suspension was then underlaid with 8ml 30% (v/v) gastrografen (Bayer) and centrifuged at $58,300 \times g$, 30 min, 4°C . The resulting pellet was resuspended in SPG buffer and underlaid with discontinuous gastrografen gradients (4ml 40% (v/v), 12ml 44% (v/v), and 8ml 54% (v/v) gastrografen). The gradient was centrifuged at $58,300 \times g$, 60 min, 4°C and EBs were collected at the 45/54% (v/v) gastrografen interface. EBs were diluted in SPG buffer, pelleted at $30,000 \times g$, 30 min, 4°C to remove residual gastrografen and final pellets were resuspended in 200 μl nuclei lysis solution (Wizard SV Genomic DNA Purification kit, Promega) and stored at -20°C .

2.4. DNA extraction

2.4.1. Plasmid DNA extraction from bacteria by Miniprep

Plasmids were extracted from 7.5ml overnight bacterial cultures by alkaline lysis using a Miniprep kit (Qiagen) according to the manufacturers' instructions. For low copy plasmids, such as pVT100-U, twice the recommended volume of buffers P1, P2 and P3 were used.

2.4.2. Plasmid DNA extraction from bacteria by Midiprep

Plasmids were extracted from 50ml overnight bacterial cultures by alkaline lysis using a Midiprep kit (Qiagen) according to the manufacturers' instructions. Twice the recommended volume of buffers P1, P2 and P3 were used for the purification of the low copy plasmid, pVT100-U. Additionally, 500µl TE was used to elute the purified plasmid in the final elution step.

2.4.3. Plasmid DNA extraction from yeast

Yeast were grown overnight in 10ml SC-ura fructose media at 30°C with shaking at 250rpm. Yeast were pelleted at 1600 x g for 5 min, washed in 500µl ddH₂O and resuspended in 200µl lysis buffer (2% (v/v) Triton X-100, 1% (w/v) SDS, 100mM NaCl, 10mM Tris, pH 8.0, 1mM EDTA). 200µl phenol:chloroform:isoamyl alcohol (25:24:1) and 0.3g acid-washed glass beads (Sigma) were added to each yeast sample and vortexed for 4 min. 200µl TE was added to each sample before the yeast were briefly vortexed and centrifuged at 16,000 x g for 5 min. The upper aqueous layer was transferred to a fresh microcentrifuge tube and mixed with 1ml pre-chilled (-20°C) 100% (v/v) ethanol. Samples were mixed gently by inverting the microcentrifuge tube and were then incubated at -20°C for 30 min to precipitate the DNA. Precipitated DNA was pelleted at 16,000 x g for 5 min at 4°C. The supernatant was discarded and 200µl 70% (v/v) ethanol was added to the pellet. Samples were vortexed briefly and centrifuged at 16,000 x g for 2 min at 4°C. The ethanol was discarded and the DNA pellet left to air-dry. DNA pellets were resuspended in 40µl sterile ddH₂O for transformation into XL1-Blue electroporation-competent cells.

2.4.4. Genomic DNA extraction from chlamydial elementary bodies

2.4.4.1. Commercial Promega kit

DNA was extracted from isolated *Ct* EBs using a Wizard SV Genomic DNA Purification kit according to the manufacturer's instructions. All centrifugation steps were performed at 16,000 $\times g$ for 1 min unless otherwise stated. Briefly, DNA was incubated for 1 h at 55°C in digestion solution (200 μ l nuclei lysis solution, 400 μ g proteinase K (Fisher Scientific), 0.1M EDTA pH 8.0, 20 μ g RNase A). 250 μ l lysis buffer was added to digested DNA, vortexed and transferred to a mini column. The DNA solution was centrifuged for 3 min and the column was washed four times with 650 μ l column wash solution. The column was centrifuged for 2 min to dry the binding matrix before transferring to a new 1.5ml tube. The column was incubated for 2 min with 250 μ l nuclease-free water and centrifuged to elute the DNA. Purified DNA was stored at -20°C.

2.4.4.2. Phenol-chloroform extraction

Isolated EBs had been previously resuspended in 200 μ l nuclei lysis solution (section 2.3.3). EBs were then mixed with Tris-EDTA buffer (TE; 10mM Tris, 0.1mM EDTA, pH8) containing 10% (w/v) sodium dodecyl sulphate (SDS) and 20mg/ml proteinase K. Solutions were vortexed and incubated at 37°C for 1 h. 5M NaCl was added and mixed thoroughly followed by the addition of 10% (v/v) cetyltrimethyl ammonium bromide (CTAB) in 0.7M NaCl and subsequent incubation at 65°C for 10 min. An equal volume of chloroform/isoamyl alcohol (24:1) was added, mixed and centrifuged at 16,000 $\times g$ for 5 min. The top aqueous phase was mixed with an equal volume of phenol:chloroform:isoamyl alcohol (25:24:1) and centrifuged at 16,000 $\times g$ for 5 min. *Ct* genomic DNA in the resulting supernatant was then precipitated by the addition of 0.6 volumes of isopropanol. Tubes were gently inverted until an aggregated DNA pellet was visible. The DNA pellet was twice submerged in 70% (v/v) ethanol and then dissolved in TE buffer.

2.5. DNA electrophoresis

0.8% (w/v) agarose gels were prepared by dissolving 0.6g agarose in 75ml Tris-acetate-EDTA (TAE; 40mM Tris, 1mM EDTA, pH 8.0, 0.35% (v/v) acetic acid) buffer and heating in a microwave for 2 min until agarose was completely dissolved. Ethidium bromide or SybrSafe (Invitrogen) was added to the dissolved agarose at a dilution of 1:10,000 and gently mixed. DNA was prepared in sample buffer (0.04% (w/v) xylene orange, 100nM EDTA, pH 8.0, 5% (v/v) glycerol), loaded onto the agarose gel and electrophoresed in TAE at 60V for approximately 1 h. DNA visualisation was performed using UV light (for ethidium bromide-stained DNA) or a blue light transilluminator (for SybrSafe-stained DNA) and images were obtained using a Syngene gel imaging system and either GeneSnap or GeneTools analysis software.

2.6. Purification of PCR products

Amplified PCR products were electrophoresed using agarose gels and stained using SybrSafe. DNA was visualised using a blue light transilluminator and excised using a sterile scalpel blade. DNA was purified from gel fragments using the silica membrane encompassed in the QIAquick Gel Extraction kit (Qiagen) according to the manufacturer's instructions.

2.7. Restriction enzyme digests

All restriction enzyme digests were performed in a total volume of 40µl unless otherwise stated. DNA was incubated with 1 x potassium glutamate buffer (KGB; 500nM β-mercaptoethanol, 100mM glutamic acid (monopotassium salt), 25mM Tris acetate pH7.6, 10mM magnesium acetate, 0.05mg/ml BSA) and 1µl (6U *Sau3A*I; 10U *Bam*HI; 10U *Dra*I) restriction enzyme for 45 min at 37°C. For more extensive digests, an additional 1µl restriction enzyme was added to the digest and incubated for a further 45 min. Digested DNA was analysed by gel electrophoresis and purified using a gel extraction kit.

2.8. Polymerase Chain Reaction (PCR)

All PCRs were performed in a Biorad DNA Engine Peltier Thermal Cycler.

2.8.1. Generation of PCR products for cloning

High fidelity PCR products were generated using *pfu* DNA polymerase. PCRs were performed in a total reaction volume of 50µl containing 5µl 10 x *pfu* polymerase buffer, 100µM dNTPs (for each of dATP, dTTP, dCTP and dGTP from a 10mM stock), 0.5µM primers (for each of forward and reverse primers from a 10µM stock), 2.5U *pfu* polymerase and approximately 10ng template DNA. The PCR programme consisted of template DNA denaturation at 95°C for 45 seconds, primer annealing at 50°C for 45 seconds, and extension at 72°C for 1 min per kb of product length. These steps were repeated for a total of 30 cycles followed by a final extension at 72°C for 10 min.

2.8.2. Colony PCR screen of transformed bacteria

All PCRs were performed in a total volume of 20µl containing 4µl 5 X green GoTaq Flexi buffer and a final concentration of 1.5mM MgCl₂, 200µM dNTPs (for each of dATP, dTTP, dCTP and dGTP from a 10mM stock), 0.5µM primers (for each of forward and reverse primers from a 10µM stock), 1U GoTaq G2 Flexi DNA polymerase. A master mix was prepared for 12 reactions, vortexed and aliquoted for individual reactions. Transformed *E.coli* colonies were picked using a P10 pipette tip, spotted onto a second agar plate and then the remainder of the colony was added to the PCR mixture. The PCR programme consisted of template DNA denaturation at 95°C for 1 min, primer binding at 50°C for 1 min, and extension at 74°C for 1 min per kb of product length. These steps were repeated for a total of 30 cycles.

2.9. Sequencing

Unless otherwise stated, all DNA samples were submitted to Source Bioscience for Sanger sequencing.

2.10. DNA cloning

2.10.1. In-Fusion homologous end recombination

In-Fusion cloning was performed according to the manufacturer's instructions (Clontech). All cloning reactions were performed in a total volume of 10 μ l containing 50-100ng purified PCR product, 50-100ng linearised vector and 2 μ l 5 X In-Fusion HD enzyme premix. Reactions were incubated for 15 min at 50°C and 2 μ l was used for subsequent bacterial transformation.

2.10.2. Ligation-based cloning

Sticky-end ligation was performed using T4 DNA ligase (Thermo Scientific) in a total reaction volume of 20 μ l. *Ct* insert DNA was mixed with linearised vector DNA in a 3:1 ratio respectively. Unless otherwise stated, a total of 0.1 μ g DNA was incubated with 2 μ l 10 X T4 DNA ligase buffer (Thermo Scientific) and 1U T4 DNA ligase. Unless otherwise stated, ligation reactions were incubated for 1 h at 22°C followed by the heat-inactivation of the T4 DNA ligase by incubation at 70°C for 5 min. 2 μ l ligation reaction was used for subsequent bacterial transformation.

2.10.3. Bacterial transformation

2.10.3.1. Transformation of chemically competent cells

2 μ l ligation mix was added to 50 μ l chemically competent *E.coli* (thawed on ice; NEB 10- β , New England Biolabs; Stellar, Clontech; BL21 Gold DE3, Agilent Technologies) and incubated on ice for 30 min. Cells were heat-shocked at 42°C for 30 seconds, placed on ice for 5 min, suspended in 950 μ l SOC media (pre-warmed to 37°C) and incubated at 37°C for 1 h with shaking at 250rpm. 5 μ l or 50 μ l cells were then spread on to selective LB ampicillin plates and incubated overnight at 37°C.

2.10.3.2. Transformation of electrocompetent cells

1 μ l DNA was added to 40 μ l electrocompetent cells (thawed on ice; XL1-Blue, Agilent Technologies), transferred to a chilled 1mm electroporation cuvette and

pulsed at 1700V at 200Ω. Cells were immediately resuspended in 960μl SOC media (pre-warmed to 37°C) and incubated for 1 h at 37°C with shaking at 250rpm. 5μl or 50μl cells were then spread on to selective LB ampicillin plates and incubated overnight at 37°C.

2.11. Generating detergent soluble lysates

2.11.1. NP-40 lysis buffer

HeLa cells were washed once in PBS and scraped into ice cold cell lysis buffer (150mM NaCl, 20mM Tris-HCl pH 8.0, 0.5% (v/v) NP-40, 2mM EDTA) containing EDTA-free protease inhibitors (Roche). The lysate was incubated on ice for 15 min and centrifuged at 16,000 x g for 10 min at 4°C. The detergent soluble supernatant was quantified by bicinchoninic acid (BCA) protein assay and stored at -20°C until further use. Detergent insoluble material was discarded.

2.11.2. HEPES lysis buffer

HeLa cells were washed once in PBS and scraped into ice cold cell lysis buffer (50mM HEPES, 5mM EDTA, 150mM NaCl, 1% (v/v) Triton X-100) supplemented with 0.5mM Tris (2-carboxyethyl) phosphine (TCEP), 10mM NEM and EDTA-free protease inhibitors. The lysate was incubated on ice for 15 min and centrifuged at 16,000 x g for 10 min at 4°C. The detergent soluble supernatant was quantified by BCA protein assay and stored at -20°C until further use. Detergent insoluble material was discarded.

2.11.3. Urea lysis buffer

HeLa cells were washed once in PBS and scraped into urea lysis buffer (20mM HEPES pH 8.0, 9M urea, 1mM sodium orthovanadate (activated), 2.5mM sodium pyrophosphate, 1mM β-glycerophosphate) supplemented with 0.5mM Tris (2-carboxyethyl) phosphine (TCEP) and 10mM NEM. The lysate was sonicated at 12 W output with 3 bursts of 30 sec each and cooled on ice for 30 sec between each burst. The lysate was centrifuged at 16, 000 x g for 15 min at room temperature and the detergent soluble supernatant was quantified by

BCA protein assay and stored at -20°C until further use. Detergent insoluble material was discarded.

2.12. BCA protein assay

Protein concentration of samples was estimated in a 96 well plate (Corning). A standard curve of 0-10µg protein was prepared using 1mg/ml bovine serum albumin (BSA) diluted in 0.1M NaOH. Dilutions of protein were prepared in dH₂O and 5µl protein samples were further diluted with 5µl 0.2M NaOH. BCA Working Reagent was prepared by diluting 4% (w/v) Cu₂SO₄ in BCA Reagent A (1:50). 200µl BCA Working Reagent was added to each well and incubated for approximately 20 min at 37°C. A₅₆₁ was measured on a Multiskan Go plate reader (Thermo Scientific).

2.13. SDS-PAGE

Discontinuous polyacrylamide gels were prepared with a resolving gel and stacking gel. Resolving gels were prepared with 30% (w/v) acrylamide (Protogel) at 10, 12 or 15% (w/v) with a final concentration of 0.05% (w/v) ammonium persulphate (APS), 0.0005% (v/v) tetramethylethylenediamine (TEMED), and resolving gel buffer (0.375M Tris-HCl, 0.1% (w/v) SDS, pH8.8). Stacking gels were prepared with a final concentration of 4% (w/v) acrylamide, 0.05% (w/v) APS, 0.001% (v/v) TEMED, and stacking gel buffer (0.125M Tris-HCl, 0.1% (w/v) SDS, pH6.8). Protein samples were prepared in Laemmli sample buffer (3x stock: 188mM Tris, pH 6.8, 6% (w/v) SDS, 30% (v/v) glycerol, 10% (v/v) β-mercaptoethanol, 0.03% (w/v) bromophenol blue), denatured at 95°C for 5 min and electrophoresed at 200V. A protein ladder (Precision Plus Kaleidoscope ladder, BioRad) was used for the estimation of protein molecular weight.

2.14. Western blotting

Proteins were transferred to nitrocellulose or PVDF membranes using the iBlot system (Invitrogen) according to the manufacturer's instructions. Transferred proteins were rinsed in dH₂O and visualised by brief incubation with Ponceau S

stain (0.2% (w/v) Ponceau S in 3% (w/v) trichloroacetic acid (TCA)). Background staining was removed by extensive rinsing with dH₂O. Membranes were blocked for 30 min with either 5% (w/v) semi-skimmed milk (Marvel) or 5% (w/v) BSA in either PBS or Tris-buffered saline (TBS; 150mM NaCl, 10mM Tris-HCl, pH 7.4) with 0.1% (v/v) Tween-20 (PBS-T or TBS-T). Membranes were then incubated with primary antibody diluted in 5% (w/v) semi-skimmed milk or 5% (w/v) BSA in either PBS-T or TBS-T for 1 h at room temperature or overnight at 4°C. Membranes were thrice washed with TBS-T for 5 min/wash and incubated with horseradish peroxidase (HRP)-conjugated secondary antibody diluted 1:8000 in 5% (w/v) semi-skimmed milk or 5% (w/v) BSA in TBS-T for 30 min at room temperature. Membranes were thrice washed in TBS-T for 5 min/wash, incubated in Amersham ECL western blotting detection reagent (GE Healthcare Life Sciences) and proteins were visualised on x-ray film using an Xograph film developer.

2.15. CPY-invertase secretion assay

2.15.1. Qualitative assessment of CPY-inv secretion

Transformed BHY10 or BHY12 yeast were streaked on SC-ura plates alongside a positive (BHY10 $\Delta vps10$) and negative (BHY10 + pVT100-U) yeast controls. An overlay solution containing 0.125M sucrose, 100mM sodium acetate buffer pH 5.5, 0.4mM N-ethylmaleimide (NEM; Sigma), 10 μ g/ml HRP (Type IV; Sigma) in PBS, 8U/ml glucose oxidase (Type X-S from *Aspergillus niger*; Sigma) in PBS and 0.6mg/ml O-dianisidine (Sigma) was mixed with melted agar at a final concentration of 0.6% (w/v) and poured over plates harbouring transformed yeast and controls. The overlay solution was left to solidify and the colour change was observed after 30 min.

2.15.2. Quantitative assessment of CPY-inv secretion

Yeast expressing Ct genes were grown overnight in SC-ura selective media. 1ml of yeast culture was pelleted at 3,300 x g for 1 min, washed once in ddH₂O and resuspended in 1ml ddH₂O. 25 μ l yeast was added to 775 μ l acetate buffer (0.1M sodium acetate, pH 4.9) (1:32 dilution) and 200 μ l of this mixture was

incubated on ice for later assaying of exogenous invertase activity (i.e. the secreted sample). Meanwhile, 40µl of the 1:32 yeast dilution was added to 360µl acetate buffer and then 10µl 20% (v/v) Triton X-100 was added. Yeast were vortexed and freeze-thawed for three cycles of snap-freezing in liquid nitrogen and thawing in a 30°C water bath. 200µl freeze-thawed yeast were incubated on ice for assaying total invertase activity. At regular timed intervals, 50µl sucrose (0.5M, sterile-filtered) was added to 200µl secreted yeast sample and 200µl total invertase activity sample using a positive displacement pipette. Yeast samples were incubated in a shaking 30°C water bath for precisely 30 min to enable any secreted CPY-inv to hydrolyse the exogenous sucrose. This hydrolysis reaction was terminated upon the addition of 0.3ml K₂HPO₄ (0.2M, pH 10.0) and heating the yeast at 95°C for precisely 3 min. Yeast were then placed on ice to cool before the addition of 2ml glucostat reagent (97.5mM K₂HPO₄ pH 7.0, 2U/ml glucose oxidase in PBS, 2.5µg/ml HRP in PBS, 0.1mM NEM, 150µg/ml O-dianisidine) at regular timed intervals. Upon addition of glucostat reagent, yeast were immediately incubated in a shaking 30°C water bath for precisely 30 min. The reaction was terminated upon the addition of 2ml 6M HCl.

1ml assayed yeast was transferred to a cuvette and the absorbance at 540nm was measured using an Ultrospec 2000 UV/Visible spectrophotometer (Pharma Biotech). The percentage of CPY-inv secretion was calculated as follows:

$$\% \text{ CPY secreted} = \frac{\text{Secreted sample } OD_{540}}{\text{Total sample } OD_{540} \times 10} \times 100$$

Yeast lacking the Vps10 receptor ($\Delta vps10$) were used as a positive control for CPY-inv secretion, whilst yeast harbouring an empty pVT100-U plasmid were used as a negative control.

2.16. Visualisation of yeast vacuoles

5ml overnight cultures of yeast were diluted to an OD₆₀₀ of 0.3 and further grown to an OD₆₀₀ of 0.8-1.6. Yeast were pelleted at 1600 x g for 1 min and resuspended at 20-40 OD₆₀₀/ml in SC-ura fructose. The yeast cell suspension

was then incubated with 40 μ M N-(3-triethylammoniumpropyl)-4-(6-)4-(diethylamino) phenyl) hexatrienyl) pyridium dibromide (FM4-64; Life Technologies) for 30 min in an ice bath covered in foil due to the light sensitivity of FM4-64. Yeast were pelleted 1600 x g for 2 min at 0°C. A chase was started by resuspending yeast cells in SC-ura fructose media (pre-warmed to 30°C) at 10-20 OD₆₀₀/ml. Yeast were incubated at 30°C for 10 or 60 min. The addition of 15mM NaN₃ terminated the chase after either 10 or 60 min incubation. Yeast were stored on ice until visualisation using fluorescence microscopy.

2.17. Mammalian cell culture

Flp-In HeLa cells were transfected using FuGene (Clontech). Briefly, 94 μ l Opti-Mem (Gibco) and 6 μ l Fugene was added to 1 μ g pOG44 and 1 μ g purified pcDNA5/FRT/T0 plasmid encoding ChlaDUB1 or ChlaDUB2, incubated for 20 min at room temperature and then added dropwise into one well of Flp-In HeLa cells in a 6-well plate (Corning) containing 2ml DMEM and incubated at 37°C overnight. Transfected Flp-In HeLas were then washed, trypsinised and transferred to a 15cm dish (Corning) for adherence. The following day, transfected cells were selected for upon addition of 0.2mg/ml hygromycin. Selection and growth of transfected Flp-In HeLas was performed over 12 days. Colonies of ChlaDUB1- or ChlaDUB2-transfected Flp-In HeLa cells were then seeded into wells of a 24-well plate and either transferred to liquid nitrogen for long-term storage or maintained in tissue culture media for experimental use.

Flp-In HeLa cells were cultured in DMEM supplemented with 10% (v/v) FBS (Life Technologies), 2mM L-glutamine (Life Technologies) and 50U/ml penicillin-streptomycin (Life Technologies) in a humidified 5% CO₂ atmosphere at 37°C. When antibiotic selection was required, media was supplemented with 0.2mg/ml hygromycin B (Roche).

2.18. Long-term cell storage

Flp-In HeLa cells were grown to approximately 70% confluency, trypsin digested and resuspended in 5ml DMEM supplemented with 10% (v/v) FBS, 2mM L-glutamine, 50U/ml penicillin-streptomycin and, if required, 0.2mg/ml

hygromycin B. Cells were pelleted by centrifugation at 100 x *g* for 5 min. Cells were incubated on ice for 10 min before aspiration of the supernatant. Cell pellets were then resuspended in freezing media (DMEM, 25% (v/v) FBS, 10% (v/v) dimethyl sulfoxide (DMSO)) and transferred to a cryovial. Cryovials were wrapped in several layers of blue paper roll and stored at -80°C overnight. The viability of cells was confirmed the following day and successful stocks were then transferred to liquid nitrogen for long-term storage.

2.19. Contaminant removal by dialysis

α -I κ B α antibody was dialysed using a Slide-A-Lyzer dialysis cassette with a 10kDa molecular weight cut-off and a capacity of 0.1-0.5ml (Thermo Fisher Scientific) to eliminate the sodium azide present in the solution.

The Slide-A-Lyzer cassette was attached to a buoy and immersed in 0.5 litre PBS for 1 min to hydrate the cassette. The cassette was removed and α -I κ B α antibody was carefully injected into the syringe ports using an 18G needle attached to a syringe. Air was withdrawn from the cassette by using the syringe in an alternative syringe port. The cassette was immersed in 0.5 litre PBS overnight. The α -I κ B α antibody was withdrawn from the cassette using an 18G needle attached to a syringe.

2.20. Antibody coupling

α -I κ B α was covalently coupled to AminoLink coupling resin using a Direct IP kit (Pierce). Resin was thrice washed in 0.5ml PBS followed by the covalent coupling of 1 μ g antibody per 1 μ l AminoLink resin upon the addition of 3 μ l 5M NaCNBH₄ per 200 μ l volume of mixture. The suspension was gently rotated at 4°C for 2 h. The beads were pelleted by centrifugation at 3,000 x *g* for 1 min and thrice washed with 0.5ml 1M Tris-HCl pH 8.0. Beads were then resuspended in 0.5ml 1M Tris-HCl pH 8.0 and 3 μ l 5M NaCNBH₄ per 200 μ l volume of the Tris-resin solution and gently rotated for 15 min. The resin was then thrice washed with PBS, washed six times with 1M NaCl and finally thrice washed again with PBS. An equal volume of lysis buffer (see section 2.11) was

added to create a 50% bead slurry. The resin was stored at 4°C until further use.

2.21. Immunoprecipitation

Flp-In HeLa cells expressing myc-tagged ChlaDUB1 or ChlaDUB2 were induced upon the addition of 1µg/ml doxycycline for 16-18 h. A detergent soluble lysate was generated (see section 2.11) and quantified by BCA assay (see section 2.12). Lysates were mixed with 20µl bead slurry (consisting of 50% anti-myc coupled resin and 50% sepharose resin; previously prepared by Dr Adam Rofe) and incubated at 4°C for 2 h with gentle rotation. The mixture was transferred to a spin-X centrifuge tube (Corning Costar) and centrifuged at 16,000 x g for 1 min. The supernatant was removed and the beads were washed five times with 0.5ml lysis buffer (see section 2.11). For elution, myc-tagged proteins were incubated with 40µl IgG elution buffer (Pierce) for 10 min and then centrifuged at 16,000 x g for 1 min. The eluate was neutralised with 1M Tris pH 8.0, mixed with sample buffer and proteins were resolved on a 10% SDS-PAGE gel (see section 2.13).

2.22. Deubiquitinase activity assay

Soluble cell lysates of ChlaDUB1- or ChlaDUB2-transfected Flp-In HeLa cells were prepared and quantified by BCA assay. All samples were normalised to the lowest sample concentration in assay buffer (50mM Tris pH 8.0, 0.05% (w/v) CHAPS, 10mM DTT). For purified DUB activity assays, lysates were immunoprecipitated (IP) using α-myc-coupled beads. Either 50µl lysate or 20µl IP eluate was incubated with 200nM IQF-diUb K63-1 (LifeSensors) in a total volume of 100µl in a 96-well black assay plate (Corning). A kinetic read of 5-carboxytetramethylrhodamine (TAMRA) fluorescence (excitation 544nm, emission 590nm) was performed every minute for 90 min on a FLUOstar Optima microplate reader (BMG Labtech).

2.23. Immunofluorescence

Cultured cells adhered to glass coverslips were washed once with PBS and fixed with 4% (w/v) formaldehyde in PBS for 20 min. Formaldehyde was aspirated and coverslips were incubated with 50mM NH₄Cl in PBS for 10 min. Coverslips were either stored in this solution for up to one week at 4°C or processed immediately. Following fixation, cells were permeabilised with 0.2% (w/v) BSA, 0.05% (v/v) saponin, in PBS for 10 min. All further washes and antibody dilutions were performed in BSA-PBS-saponin.

Coverslips were incubated at room temperature for 1 h with primary antibody diluted in BSA-PBS-saponin by inverting the coverslips onto antibody solution dispensed onto parafilm (20µl antibody for 13mm round coverslips, 70µl for 22mm square coverslips). Coverslips were then thrice washed in 3ml BSA-PBS-saponin for 5 min/wash before incubation with Alexa fluorophore-conjugated secondary antibody diluted 1:300 with BSA-PBS-saponin. Finally, coverslips were thrice washed with BSA-PBS-saponin supplemented with 4',6-diamidino-2-phenylindole (DAPI; final concentration of 1µg/ml) to enable the visualisation of DNA. Coverslips were briefly rinsed in distilled water, blotted to dry and mounted onto slides with MOVIOL 4-88 (Calbiochem) containing 2.5% (w/v) 1,4-diazobicyclo [2,2,2]-octane (DABCO).

2.24. Image acquisition

Slides were viewed on a Zeiss LSM 880, with Airyscan where necessary, or Zeiss LSM 710 upright microscope both using Zen software (Carl Zeiss). All images are either single slices or maximum-intensity Z projections as indicated. Post-acquisition image processing was performed using Fiji software (Schindelin et al., 2012).

2.25. EGFR recycling

Flp-In HeLa cells stably transfected with myc-ChlaDUB1 or myc-ChlaDUB2 in 24-well plates (for immunofluorescence) or 25cm² tissue culture flasks (for immunoblotting) were induced with the addition of 1µg/ml doxycycline for 16-18

h. Cells were washed once in warm PBS and serum-starved (DMEM, 2mM L-glutamine, 50U/ml penicillin-streptomycin) for 4 h at 37°C. Cells were incubated on ice in a cold room (4°C) for 10 min to halt endocytosis before being thrice washed with ice cold binding media (RPMI, 0.1% (w/v) BSA, 10mM HEPES, pH 7.4). Cells were incubated with ice cold binding media containing 40ng EGF on ice at 4°C for 1 h and then thrice washed in ice cold binding media. EGFR internalisation was stimulated by incubating cells at 37°C with binding media (pre-heated to 37°C) for 0, 10, 20, 30, 60 or 120 min. After the appropriate specified time, binding media was aspirated and cells were either washed in PBS and fixed with 4% (v/v) formaldehyde (for immunofluorescence) or lysed upon the addition of hot sample buffer (deficient in β -mercaptoethanol and bromophenol blue) and heated to 95°C for 30 min (for BCA quantification and subsequent immunoblotting).

2.26. Protein production

BL21 Gold DE3 competent *E.coli* were transformed with pETFP_21 plasmids encoding His-ChlaDUB1 or His-ChlaDUB2. Overnight cultures were grown to an OD₆₀₀ 0.6 in 500ml LB media supplemented with ampicillin. Protein expression was induced in overnight bacterial cultures by the addition of 0.2mM isopropyl β -D-1-thiogalactopyranoside (IPTG) for either 1 or 4 h. Bacteria were then harvested by centrifugation at 3,000 x g for 30 min and bacterial pellets were lysed using a French press. The resulting bacterial lysate was centrifuged at 20,000 x g for 30 min in a Beckman Optima L-100XP ultracentrifuge with an SS34 rotor. The supernatant was 0.45 μ m filtered to remove aggregates before immobilised metal ion chromatography (IMAC).

2.27. Immobilised metal ion chromatography

His-tagged proteins were isolated using HisTrap HP 5ml columns (GE Life Sciences). Columns were firstly washed with 25ml dH₂O and then equilibrated with 25ml binding buffer (20mM sodium phosphate, 0.5M NaCl, 20mM imidazole, pH 7.4) at a rate of 1ml/min. Bacterial lysates were passed through the column at a rate of 1ml/min. Columns were then washed with 50ml binding buffer at a rate of 1ml/min. His-ChlaDUB1 or His-ChlaDUB2 was eluted upon

the addition of elution buffer (20mM sodium phosphate, 0.5M NaCl, 500mM imidazole, pH 7.4) in a linear gradient. 1ml elution fractions were collected every min for 60 min. Fractions were stored at -20°C until further use. When required, specified fractions were pooled and concentrated using an ultra-15 centrifugal filter device (up to 15ml, 3kDa cut-off; Amicon) according to the manufacturer's instructions. Briefly, the pooled fractions were transferred to the filter device and centrifuged at 5000 x g for approximately 40 min until the concentrated solute had reached the desired volume. Concentrated solutes were stored at -20°C until further use.

2.28. Mass spectroscopy

Samples were prepared by Hayley Clissold prior to LC-MS/MS. LC-MS/MS was then performed by the University of York Proteomics laboratory.

2.28.1. Sample preparation

Flp-In HeLa cells were cultured in tissue culture media in 10 x 150 mm culture dishes to 80% confluency. Cells were stimulated with lipopolysaccharide (LPS; Sigma) at a final concentration of 100ng/ml for 2 h, washed twice in PBS and harvested in urea lysis buffer supplemented with a final concentration of 0.5mM TCEP and 10mM NEM (see section 2.11.3). Proteins were extracted from the lysate by sonication at 12 W output with 3 bursts of 30 sec each and cooled on ice for 30 sec between each burst. Extracted proteins were centrifuged at 16,000 x g for 15 min at room temperature and the supernatant was quantified by BCA protein assay. The protein solution was then incubated on ice for 2 h to block the active sites of endogenous DUBs. Dithiothreitol (DTT) was added to proteins at a final concentration of 20mM and followed by a further 2 h incubation on ice in order to quench excess NEM. The efficiency of host DUB inactivation was assessed by incubating protein solutions at 37°C overnight followed by western blot using anti-ubiquitin antibodies.

2.28.2. LC-MS/MS

Protein was provided to the Proteomics lab for reduction and alkylation of proteins, followed by trypsin digestion. Trypsin was reconstituted in 100mM tri-

ethyl-ammonium bicarbonate (TAB) and added to protein solutions for overnight trypsin digestion. Peptides were acidified by the addition of a final concentration of 1% (v/v) trifluoroacetic acid (TFA). The acidified peptide was centrifuged at 1,780 x g at room temperature for 15 min. The resulting supernatant was then applied to a Sep-Pak C₁₈ column (Waters Corporation) that had been pre-wetted with 5ml 100% acetonitrile and washed sequentially with 1ml, 3ml and 6ml 0.1% (v/v) TFA. The column was again washed sequentially with 1ml, 5ml and 6ml 0.1% (v/v) TFA and washed with 2ml wash buffer (0.1% (v/v) TFA, 5% (v/v) acetonitrile). Peptides were eluted with a sequential wash of 3 x 2ml alternative wash buffer (0.1% (v/v) TFA, 40% (v/v) acetonitrile). The eluate was stored at -80°C overnight and lyophilised. Resulting peptides were returned to Hayley Clissold for antibody enrichment of K-ε-GG-containing peptides (section 2.28.3). Immunoaffinity purified peptides were returned to the Proteomics lab for liquid chromatography tandem mass spectroscopy (LC-MS/MS). K-ε-GG-containing peptides were eluted from a 50cm PepMap column into an Orbitrap Fusion mass spectrometer. The total acquisition time was 3 h per sample. Resulting peak lists were analysed using PEAKS *de novo* sequencing and database searching software with peptide matches filtered to achieve a global false discovery rate of 1%.

2.28.3. Immunoaffinity purification

Immunoaffinity purification was performed according to the manufacturer's instructions. Briefly, lyophilised peptide was centrifuged at 2,000 x g for 5 min and resuspended in 1.4ml PTMScan IAP buffer (Cell Signalling Technologies). Solution was centrifuged for 5 min at 10,000 x g at 4°C for 5 min in a microcentrifuge and the supernatant was cooled on ice. Meanwhile, PTMScan ubiquitin remnant motif antibody-bead conjugate slurry (Cell Signalling Technologies) was centrifuged at 2,000 x g for 30 sec and buffer was then removed from the beads. Beads were washed four times with 1ml PBS and centrifuged between each wash at 2,000 x g. Finally, beads were resuspended in 40µl PBS. The peptide solution was transferred to bead slurry and rotated for 2 h at 4°C. The peptide/bead slurry was centrifuged at 2,000 x g for 30 sec and the supernatant was discarded. 1ml IAP buffer was sequentially added thrice to

beads, mixed and centrifuged at 2,000 x g for 30 sec and the supernatant was discarded. 1ml HPLC grade water was sequentially added thrice to the beads, mixed and centrifuged at 2,000 x g for 30 sec and the supernatant was discarded. For the elution of purified peptides, 55µl 0.15% (v/v) TFA was added to the peptide/bead slurry and incubated for 10 min at room temperature. The peptide/bead slurry was centrifuged at 2,000 x g for 30 sec and the supernatant was transferred to a fresh Eppendorf tube. 50µl 0.15% (v/v) TFA was added to the peptide/bead slurry and the slurry was centrifuged at 2,000 x g for 30 sec. the supernatant was transferred to the same Eppendorf tube as previously.

2.29. Antibodies

All primary and secondary antibodies used throughout this thesis are listed in Table 2.2 and Table 2.3 respectively.

Antibody specificity	Target species	Source	Clone	Dilution	
				WB	IF
EEA1	Hu, Mu	CST	C45B10	-	1:500
ciM6PR	Hu, Mu	Abcam	EPR6599	-	1:500
LAMP1	Hu	DSHB	H4A3	-	1:500
LC3	Hu, Mu	NanoTools	5F10	-	1:500
EGFR (C-terminus)	Hu, Mu	CST	D38B1	1:1000	1:500
EGFR (N-terminus)	Hu	ProteinTech	22542-1-AP	-	1:500
IκBα	Hu, Mu, Rb	CST	44D4	1:1000	-
Ubiquitin	Hu, Mu, Rb	CST	P4D1	1:1000	-
γ-tubulin	Hu	Sigma	GTU-88	1:1000	-
Myc	Myc epitope	DSHB	9E10	1:1000	1:1000
6 x His	6 x His epitope	Thermo Fisher	HIS.H8	1:1000	-
CPY	Yeast	Thermo Fisher	A6428	1:1000	-

Table 2.2 Primary antibodies used in this study. Hu = human, Mu = mouse, CST = Cell Signalling Technologies, DSHB = Developmental Studies Hybridoma Bank, WB = western blotting, IF = immunofluorescence.

Antibody specificity	Source	Cat no.	Dilution	
			WB	IF
AlexaFluor 488 goat anti-mouse IgG	Life Technologies	A11029	-	1:300
AlexaFluor 555 goat anti-mouse IgG	Life Technologies	A21424	-	1:300
AlexaFluor 488 goat anti-rabbit IgG	Life Technologies	A11034	-	1:300
AlexaFluor 555 goat anti-rabbit IgG	Life Technologies	A21429	-	1:300
HRP-conjugated rabbit anti-mouse IgG	Sigma	A9044	1:8000	-
HRP-conjugated goat anti-rabbit IgG	Sigma	A9169	1:8000	-

Table 2.3 Secondary antibodies used in this study. WB = western blotting, IF = immunofluorescence.

Chapter 3: Identification of *Ct* virulence proteins by *in silico* predictions

3.1. Introduction

3.1.1. The type III secretion system

Pathogens have evolved multifaceted and intricate mechanisms to manipulate intracellular host signalling networks in order to evade host defences and establish successful infections. For example, many Gram-negative bacteria with symbiotic or parasitic lifestyles express a type III secretion system (T3SS) that enables the translocation of effector proteins from the bacterial cytosol into host cells. Once inside the host cytoplasm, effectors can mimic host proteins and manipulate signalling pathways to promote bacterial survival and growth during infection. Thus, bacterial T3SS themselves are a target for developing novel antibiotics because of their essentiality in the pathogenesis of many Gram-negative bacteria and because bacteria can be rendered non-infective if their T3SS are unable to function or assemble correctly (McShan and De Guzman, 2015). A detailed understanding of the repertoire of secreted effectors for a particular pathogen, together with the host substrates they interact with, is key to developing a systems biology model of host-pathogen interactions. Ultimately, these host-pathogen interactions or specific intracellular host substrates may represent novel targets for developing clinical interventions for the prevention of disease or inhibition of disease progression.

Chlamydiae encode a relatively large repertoire of virulence proteins that accounts for approximately 10% of the chlamydial genome (Betts-Hampikian and Fields, 2010). These effectors can be delivered by specialised secretion systems to the bacterial surface (by a type V secretion system (T5SS)), the inclusion lumen (by a type II secretion system (T2SS)), or the host cytoplasm or inclusion membrane (by a T3SS) (Elwell et al., 2016).

The *Chlamydia trachomatis* (*Ct*) genome contains all genes required to form a fully functional T3SS. Interestingly, the *Chlamydiales* are the only non-

proteobacteria that harbour a T3SS (Troisfontaines and Cornelis, 2005). Furthermore, unlike other Gram-negative bacteria, such as *Yersinia*, *Salmonella* and *Shigella* whose genes are located in pathogenicity islands (Peters et al., 2007), the genes required to form *Ct* T3SS are found in several gene clusters dispersed throughout the chlamydial genome. The presence and location of effector genes, but not T3SS apparatus genes, differs between chlamydial species (Beeckman and Vanrompay, 2010).

The T3SS functions as a 'molecular syringe' for the delivery of bacterial effector proteins directly into the host cytoplasm and inclusion membrane (Hueck, 1998). The chlamydial T3SS is largely comprised of the exporter, basal body, secreton, needle and the translocon (Figure 3.1). The proteins that form these complexes have been designated as secretion and cellular translocation proteins (Sct). The functions of these T3SS components are outlined below.

Firstly, the exporter consists of several proteins located in the bacterial inner membrane that surrounds the basal body and mediates the active transport of effectors through the periplasmic space. The exporter proteins SctR, SctS, SctT, SctU, SctV and SctN are integral inner membrane proteins and SctN uses ATP to energise the export of proteins across the inner membrane (Aizawa, 2001, Beeckman and Vanrompay, 2010).

Secondly, the basal body of the T3SS is situated between the bacterial inner and outer membranes and is required for the anchoring of the needle complex. The basal body is comprised of SctD, SctJ, SctQ and SctL proteins, which collectively bridge the inter membrane space to enable the ultimate secretion of bacterial effectors.

The secreton is a group of proteins located within the outer membrane that facilitate the transport of effectors and translocon components across the outer membrane. SctC forms a fundamental channel required for T3S, while SctW (referred to as CopN in chlamydiae) is probably involved in the contact-dependent secretion of other chlamydial Cop proteins and thus might play a role in regulating T3SS activity (Cheng et al., 2001).

The needle is the hollow channel through which T3S effector proteins can travel for secretion across bacterial membranes and into the host cytoplasm. The needle is largely comprised of several SctF subunits that are concentrated in the outer membrane of chlamydial EBs. Additionally, SctP functions to control the length of the needle, but a chlamydial homolog for SctP is yet to be identified (Beeckman and Vanrompay, 2010).

Finally, the T3SS translocon is a pore formed on eukaryotic host membranes upon interaction with the T3SS. The chlamydial translocon is formed of CopB and CopD, both of which are secreted by the T3SS to perform their role in assisting the translocation of other T3S effectors into the host cell (Ho and Starnbach, 2005, Fields et al., 2005).

De novo synthesis of the chlamydial T3SS occurs mid-development cycle during the metabolic RB phase (Shaw et al., 2000). The chlamydial T3SS has been shown to retain functionality following the differentiation of RB into EB (Fields et al., 2003). Furthermore, secretion of T3S effectors begins rapidly upon contact of the infective, non-metabolic EB with the host cell (Clifton et al., 2004). Thus, given the biphasic developmental cycle of chlamydiae and the lack of metabolic activity by EBs, T3SS apparatus and T3S effectors required for the invasion of host epithelial cells are believed to be pre-packaged in order to rapidly invade cells and avoid host cell degradative signalling (Mueller et al., 2014).

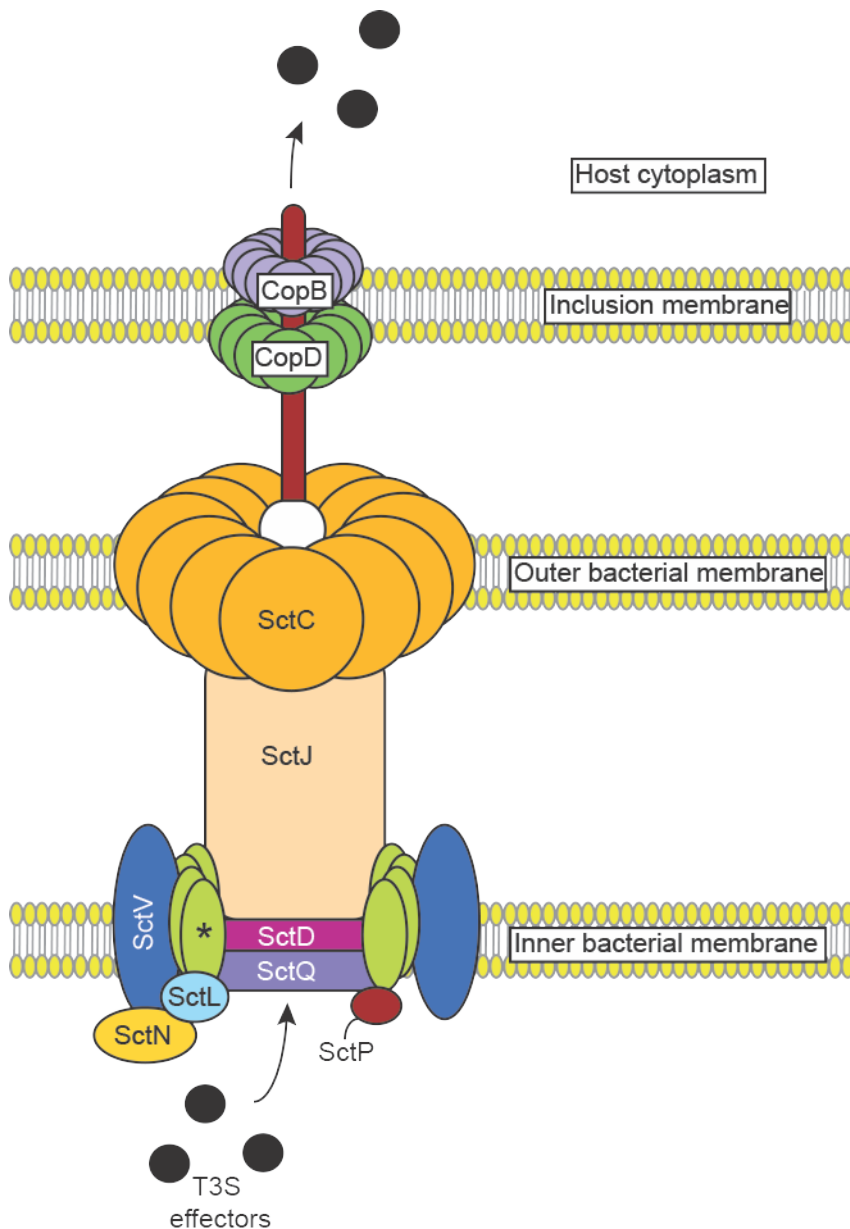


Figure 3.1 The chlamydial Type III Secretion System. The structure of the chlamydial T3SS following activation by contact of EB with an epithelial cell. * = SctR, SctS, SctT and SctU proteins. Adapted from a figure by (Beeckman and Vanrompay, 2010).

3.1.2. The targeting of effectors for secretion via a T3SS

Researchers have long been debating the existence of a conserved signal for targeting proteins for secretion via the T3SS. Initially, a secretion signal was believed to be a non-cleaved N-terminal sequence that was encrypted because there was no significant amino acid homology between T3S effectors (Beeckman and Vanrompay, 2010). However, the signal was soon believed to

be more conformational than sequence based given that radical changes in the amino acid sequence did not affect the ability of effectors to be secreted (Michiels and Cornelis, 1991). Furthermore, the signal might be fully or partially embedded within the 5' mRNA and thus T3S of effectors might be linked to translation (Anderson and Schneewind, 1997) or coupled with additional physical properties of the effector, such as amphipathicity (Lloyd et al., 2001). Moreover, Birtalan et al. (2002) demonstrated the presence of a chaperone-binding domain within the first 100 amino acids and downstream from a short, uncleaved N-terminal export signal that might target effectors for T3S. In addition, although no conserved sequence pattern could be determined, Subtil et al. (2005) have reported a T3S signal within the first 14 N-terminal amino acids of T3S effectors.

Although the understanding of a precise molecular signal that targets effector proteins for secretion by the T3SS remains unknown, several structural, bioinformatical and computational analyses suggest that the N-terminus of T3S effectors possess similar characteristics, such as flexibility and disorder in solution, amphipathicity and a bias for particular amino acids (Schechter et al., 2012). Several *in silico* prediction programs have been developed using the extensive experimental data available regarding putative T3S signals to predict effectors that are likely to be secreted by a T3SS (Arnold et al., 2009, Samudrala et al., 2009, Lower and Schneider, 2009).

3.1.3. Mechanism of secretion by the T3SS

The fundamental biological process of protein transport across membranes remains to be completely understood and the scientific community is still unravelling the complexities of the precise mechanism by which proteins are secreted into host cells by the T3SS.

The T3SS is believed to regulate its own assembly and then essentially pause in a primed state until it receives a relevant stimulus for resuming secretion (Notti, 2016). This regulation ensures the controlled secretion of substrates and is believed to play a role in the pathobiology of the T3SS (Notti, 2016).

Data from crystallographic and NMR studies indicate that bacterial T3S effectors are too large to fit through the T3SS needle complex (Loquet et al., 2012). Thus, in order for the secretion of T3S effectors to occur, it has been widely hypothesised that either the components of the needle complex would undergo conformational changes to allow for expansion of the channel (Fujii et al., 2012) or the effectors themselves are unfolded prior to or during secretion (Stebbins and Galan, 2001).

Chaperone proteins are thought to play a role in the secretion of substrates through the T3SS. The recognition of a substrate by its cognate chaperone protein is believed to retain the substrate in a partially unfolded state (Stebbins and Galan, 2001). This non-globular conformation is thought to prime the substrate for secretion through the narrow aperture.

The prevalent model of T3SS-dependent effector protein delivery into host cells describes a one-step mechanism by which effectors are translocated from the bacterial cytoplasm directly in the host cell cytosol. However, although this mechanism has long been accepted, evidence to support this process was only reported a few years ago (Radics et al., 2014). Radics et al. (2014) designed new T3SS substrates that could be trapped during their translocation through the *S. enterica* serovar Typhimurium injectisome and visualised by cryo-electron microscopy. By this method, the authors reported the detection of trapped substrates within the T3SS needle and the presence of a channel localised in the membrane-embedded base where substrate unfolding was likely to occur. Radics et al. proposed a model whereby substrates are secreted in an unfolded and polarised manner whereby the channel within the membrane-embedded base functions as a checkpoint to permit secretion to only unfolded proteins. They speculated that the refolding of substrates within the injectisome is potentially prevented by surface characteristics, which is typically the case for other molecular chambers such as chaperonins or the proteasome (Radics et al., 2014).

In 2014, Dohlich et al. reported further evidence of a T3S effector translocating through the needle channel. In this report, the authors generated a fusion

protein consisting of the T3S protein, IpaB, and the RNA 2'-O-ribose methyltransferase Rrm2 (referred to as Knot). The Knot domain prevents the unfolding of the fusion protein; thus, the fusion protein is too large to fit through the narrow needle channel. The authors demonstrated that the fusion protein was folded prior to secretion, but attenuated translocation into host cells. Furthermore, IpaB-Knot inhibited the subsequent secretion of T3S effectors by the hypersecretor *S. flexneri* $\Delta IpaD$. The authors hypothesised that the inhibition of IpaB-Knot unfolding causes the subsequent obstruction of the secretion channel and thus blocks the translocation of other effectors.

Although recent studies provide evidence into the widely accepted mechanism of T3S, Tejeda-Dominguez et al. (2017) reported an alternative mechanism of T3S whereby an extracytoplasmic bacterial T3S effector was translocated into the cytoplasm of host cells by binding to the outside of the T3SS and accessing the secretion system via pores. Together with previous studies, they demonstrated that the enteropathogenic *E. coli* (EPEC) protein, EspC, interacted with the EPEC T3SS translocon component, EspD, to control pore formation. These pores are believed to be involved in the translocation of EspC through the T3SS (Guignot et al., 2015, Tejeda-Dominguez et al., 2017). Tejeda-Dominguez et al. (2017) reported the steric hindrance of two components of the translocon pore, EspB and EspD, which prevented the translocation of EspC into the cytoplasm of epithelial cells.

These findings suggest that although the prevailing model of effector secretion by the T3SS occurs through a direct one-step process, some effectors may access the host cell cytoplasm by novel alternative means.

3.1.4. The use of bioinformatics as a tool to predict T3SS effectors

3.1.4.1. Opportunities offered by computational approaches

The use of computational and bioinformatical approaches is revolutionising biomedical research. The generation of *in silico* prediction programs have developed our understanding of a multitude of different research areas including post-translational modification sites (Plewczynski et al., 2005),

predicting secondary protein structures (Wang et al., 2016) and understanding the human immune system (Butler et al., 2016).

In silico prediction programs offer a promising platform for performing preliminary analyses and predictions that can direct *in vitro* and *in vivo* experimental studies. Previously, the identification of novel T3S effectors by experimental approaches has been challenging given the absence of a defined T3S signal peptide or motif. However, *in silico* approaches provide the opportunity to predict probable T3S effectors based on several factors including protein sequence, secondary and tertiary protein structure and amino acid composition.

3.1.4.2. EffectiveT3

EffectiveT3 is a computational prediction program developed by Arnold et al. (2009). Like many other prediction programs, EffectiveT3 was developed using a machine-learning approach whereby a computational algorithm is 'trained' on a selected set of experimentally validated T3S effectors (positive training dataset) and non-T3S effectors (negative training dataset). The algorithm is able to 'learn' patterns in the input protein sequences (e.g. G+C content, amino acid bias, structural regions, amino acid composition) that clearly discriminate between the positive and negative training datasets. Thus, when an unknown protein sequence is input into the algorithm, the program is able to determine whether the distinctive protein features resemble that of a T3S or non-T3S effector protein (Figure 3.2). Notably, Arnold et al. (2009) used a very large set of proteins from many different organisms in their training datasets compared to other prediction programs (Samudrala et al., 2009, McDermott et al., 2011).

Arnold et al. (2009) claim that EffectiveT3 is able to predict T3S effectors based on the length, position and composition of amino acids in a short N-terminal sequence of target proteins. Furthermore, a third of the proteins used for training and validation during the generation of EffectiveT3 were proteins from the *Chlamydia* taxa. Other protein sequences were derived from *Salmonella*, *Yersinia* and *Escherichia*. The use of chlamydial protein sequences in training and validation sets suggests that any potential discrepancies between effectors

from different organisms, notably chlamydiae as a non-proteobacterium, should in theory be mitigated.

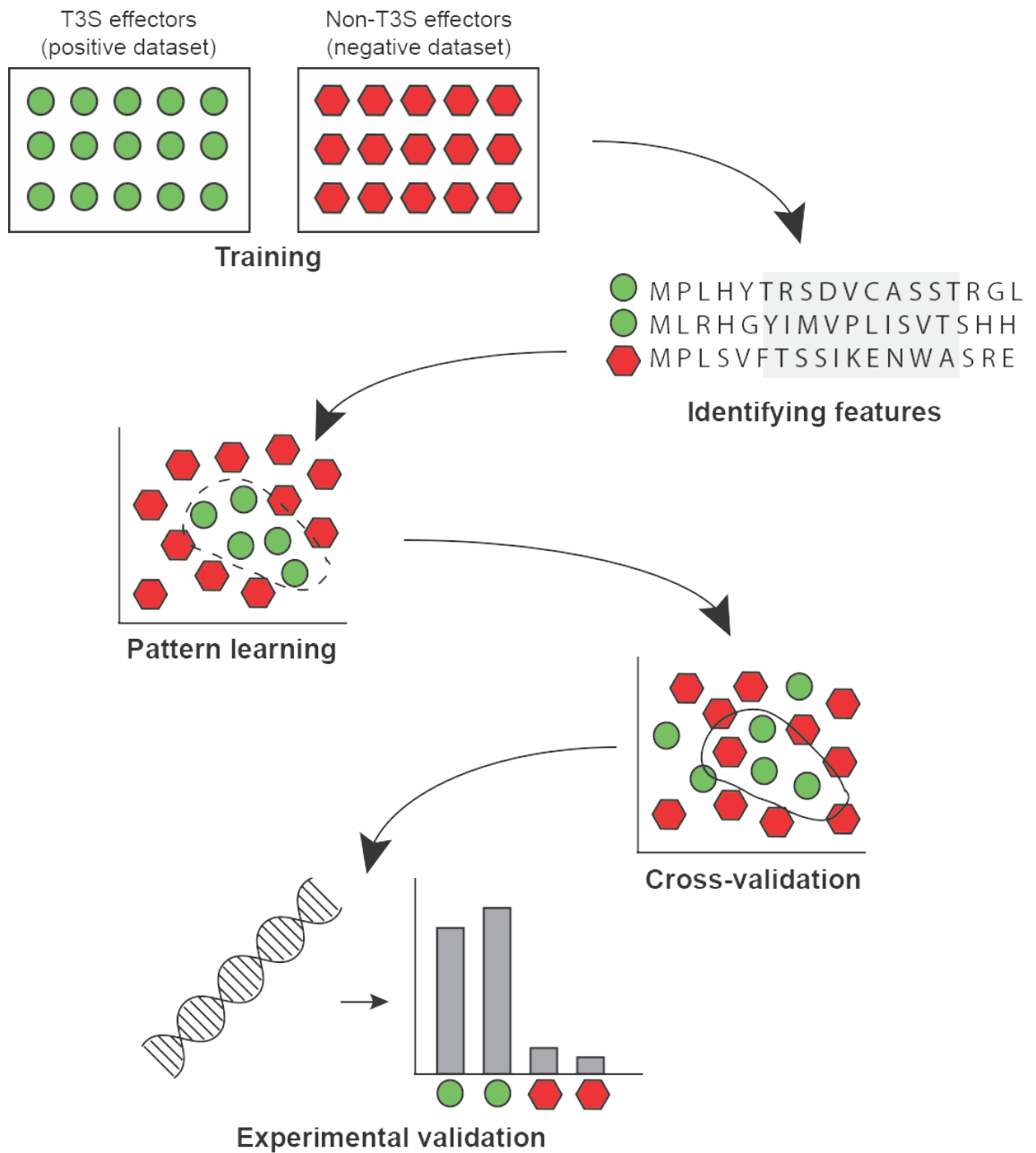


Figure 3.2 The generation of a machine-learning algorithm. Firstly, datasets of known T3S effectors and non-T3S effectors are selected and their protein features (e.g. sequence, amino acid conservation etc) are transformed into numerical representations. The machine-learning algorithm ‘learns’ how to discriminate between features of T3S and non-T3S effectors. Performance is then cross-validated using a set of known effectors that were not used in the training datasets. Finally, the algorithm can be used to predict unknown effectors and these predictions can be validated experimentally. Adapted from a figure by (McDermott et al., 2011).

3.1.5. Yeast as a tool to study bacterial pathogenicity

Bacterial pathogenicity and the molecular mechanisms underlying human disease are extensively studied in model organisms. The budding yeast, *S. cerevisiae*, was first successfully transformed with a plasmid that had been replicated in *E.coli* in 1978 (Hinnen et al., 1978) and has since become a leading model organism in a myriad of scientific research fields. *S. cerevisiae* is easy to culture in the laboratory, inexpensive to grow and maintain, not subjected to tight ethical restraints and is relatively simple to genetically manipulate. Yeast genes can be mutated or manipulated and exogenous proteins, such as bacterial effectors, can be easily expressed within a yeast model system using plasmid vectors or homologous recombination.

The *S. cerevisiae* genome has been fully sequenced (Goffeau et al., 1996) and its genes have been extensively characterised. Given the eukaryotic nature of yeast, various essential cellular processes, such as cell division cycle regulation (Dotan et al., 2001), intracellular protein transport (Dunphy et al., 1986), chromosomal segregation (Kitagawa and Hieter, 2001), mitogen-activated protein kinase (MAPK) signalling (Widmann et al., 1999) and membrane trafficking (Katzmann et al., 1999, Conibear, 2010) are conserved between yeast and humans. Thus, yeast is recognised as an ideal model organism to understand the basic mechanisms of complex cellular processes that can then inform and direct more extensive investigations in higher eukaryotes.

Effector proteins of bacteria that invade and infect higher eukaryotes have been extensively studied in yeast and hence provided a fundamental insight into the molecular interplay between microbe and host (Curak et al., 2009, Siggers and Lesser, 2008). The utilisation of yeast as a model organism for the study of bacterial pathogens relies upon the targeting of bacterial effectors to eukaryotic cellular processes that are conserved between yeast and humans (Siggers and Lesser, 2008). Yeast offers a valuable resource for studying bacterial effectors particularly for bacteria that are difficult to culture or genetically manipulate, such as *Ct*. Thus, the manipulation of eukaryotic cellular processes can be studied by expressing *de novo* bacterial effectors in yeast rather than within the

context of an infection. Expression of bacterial effectors typically results in a multitude of discernible yeast phenotypes, such as disrupted trafficking to the yeast vacuole (Shohdy et al., 2005, Raines et al., 2017), disruption of the actin cytoskeleton (Viboud and Bliska, 2005), altered morphology of vacuoles (Rofe et al., 2017, Sato et al., 2003) and growth defects in normal conditions (Lesser and Miller, 2001, Sisko et al., 2006) or upon exposure to stressors (Slagowski et al., 2008). The observation of such phenotypes can indicate which cellular processes or proteins might be affected by the expression of the bacterial effector and thus can guide further investigations in yeast or other, perhaps more physiologically relevant, models of disease.

3.1.6. Conservation of membrane trafficking in eukaryotes

There is a general consensus that the yeast vacuole is the equivalent of the mammalian lysosome. Several proteins and multi-protein complexes involved in vesicle trafficking to the lysosome, for example in vesicle formation, tethering, docking and fusion, are evolutionarily conserved in yeast and mammalian cells. Although lysosomes are also involved in metabolite and ion storage (Van Ho et al., 2002) and responding to various cell stresses (Kim and Klionsky, 2000, Hohmann, 2002), they are most commonly known for their degradative function. Thus, the ability to study vacuolar proteins and protein trafficking to the vacuole in yeast makes this organism an attractive model to examine effectors secreted by intracellular bacteria that are able to manipulate host trafficking pathways to avoid lysosomal degradation.

3.1.7. Yeast as a tool to study chlamydial virulence

Chlamydiae are obligate intracellular bacteria that, until recently, have been intractable to genetic manipulation. Given that research has been hampered by the inability to manipulate the chlamydial genome, a lot of research on chlamydial pathogenicity and virulence proteins has been performed by expression studies in yeast. Furthermore, given that Chlamydiaceae have been infecting and surviving intracellularly inside eukaryotic hosts for over 700 million years (Horn et al., 2004), the eukaryotic targets of *Ct* virulence proteins are

likely to be conserved among eukaryotes, thus implicating *S. cerevisiae* as an effective model organism to study *Ct* effectors (Sisko et al., 2006).

Huang et al. (2008) have previously screened five probable *Chlamydia pneumoniae* (*Cpn*) virulence genes in yeast to investigate their intracellular effects on eukaryotes. The expression of CopN, a likely T3S effector, was found to cause the accumulation of large budded yeast. Following closer investigation, the authors observed disrupted spindle apparatus and a specific G2/M cell cycle division block. They demonstrated that similar effects were identified when CopN was expressed in mammalian HeLa cells, thereby exemplifying the use of yeast as an investigative model organism. The ability of CopN to arrest the host cell cycle is likely to be advantageous for the intracellular survival of the bacterium as cellular resources can be redirected to the bacterial inclusion.

Furthermore, a comprehensive study of *Ct* effectors has been performed in yeast by Sisko et al. (2006). In their study, the authors use homologous recombination to express over 200 *Chlamydia*-specific proteins in *S. cerevisiae*. These recombinant yeast strains were then screened for their co-localisation with eukaryotic organelles and to identify chlamydial proteins involved in impairing yeast growth and cellular function. In total, 34 *Ct* effectors were shown to impact yeast growth and/or demonstrate a tropism towards a range of eukaryotic organelles, including the mitochondria, nucleus and cytoplasmic lipid droplets. Notably, following on from this screen, subsequent studies have demonstrated *Ct* interacting with lipid droplets during infection to aid intracellular survival (Kumar et al., 2006, Saka et al., 2015), thus demonstrating how basic screening procedures in yeast can provide useful insights into bacterial pathogenicity.

3.1.8. Pathogen effector protein screening in yeast (PEPSY)

In *S. cerevisiae*, the sorting of intracellular proteins is controlled by vacuole protein sorting (VPS) proteins that regulate the delivery of yeast hydrolases to the yeast vacuole (the equivalent of the mammalian lysosome) (Robinson et al., 1988). Disruption to normal membrane trafficking may result in the mislocalisation of vacuolar hydrolases.

In this study, we use an established pathogen effector protein screening in yeast (PEPSY) screening method that has previously been used to identify virulence proteins of *Legionella pneumoniae* (Shohdy et al., 2005) and *Salmonella* (Raines et al., 2017).

The PEPSY screen makes use of a *SUC2* knockout yeast strain, which expresses a hybrid protein generated from a fusion between invertase and the well-characterised yeast vacuolar hydrolase, CPY. Invertase is encoded by the *SUC2* gene and is normally present at the yeast cell surface where it is able to hydrolyse exogenous sucrose. However, due to the presence of the CPY vacuolar sorting signal within the hybrid protein, CPY-inv is delivered to the vacuole instead, thus the invertase is sequestered within the vacuole and is therefore unable to hydrolyse exogenous sucrose. However, if normal trafficking is perturbed, target vesicles normally destined for the vacuole are missorted, resulting in the secretion of CPY-inv from the cell, thus enabling the hydrolysis of exogenous sucrose by invertase.

To observe sucrose hydrolysis, an overlay solution is poured over the yeast colonies to be tested. This overlay solution, otherwise known as the glucostat reagent, is comprised of sucrose, glucose oxidase, horseradish peroxidase, O-dianisidine and NEM. The glucose oxidase in the glucostat reagent is able to oxidise the glucose produced during sucrose hydrolysis. The by-product of this reaction, hydrogen peroxide, acts as a substrate for horseradish peroxidase to oxidise the chromogen, O-dianisidine, resulting in the formation of a brown precipitate that can be measured qualitatively or quantitatively. Thus, yeast clones expressing *Ct* genes that disrupt intracellular membrane trafficking and cause CPY-inv to be secreted form a brown precipitate, otherwise referred to as a VPS⁻ phenotype.

3.1.9. Objectives

In this chapter, we describe the use of the *in silico* prediction program, EffectiveT3, to predict *Ct* proteins that are likely to be secreted by the bacterium's T3SS. The proteins predicted by this computational program were individually cloned into *Saccharomyces cerevisiae* and screened using

pathogen effector protein screening in yeast (PEPSY) to assess whether the putative *Ct* proteins disrupted intracellular membrane trafficking.

3.2. Results

3.2.1. Selection of EffectiveT3 as a tool to predict T3SS substrates

Effector proteins secreted by the chlamydial T3SS are likely to play a central role during infection. Several attempts have therefore been made to identify *Ct* proteins secreted via this mechanism to elucidate the underlying bacterial pathogenesis. The identification of *Ct* effectors secreted by the bacterium's T3SS is not a trivial task due to the absence of an easily recognisable T3S signal and because, until recently, *Ct* has been intractable to genetic manipulation.

Computational approaches have previously been used to predict proteins secreted by various secretion systems for a number of different bacteria (Martinez-Garcia et al., 2015, Trost et al., 2005, Sarris et al., 2010, Arnold et al., 2009). Therefore, we chose to use an *in silico* prediction program to predict *Ct* effector proteins that are secreted by the bacterium's T3SS. Given the probable role of T3S effectors in bacterial pathogenicity, together with the ability of chlamydiae to diverge away from the endolysosomal trafficking pathway, we reasoned that any effector proteins identified by computational approaches might play a role in disrupting normal intracellular membrane trafficking. Thus, *Ct* effectors involved in membrane trafficking disruption can be examined by pathogen effector protein screening in yeast (PEPSY).

There are several *in silico* programs available for predicting proteins specifically secreted by a T3SS, including EffectiveT3 (Arnold et al., 2009), Modlab (Lower and Schneider, 2009), SIEVE (Samudrala et al., 2009) and, more recently, pEffect (Goldberg et al., 2016).

The scope of our investigation required the screening of the entire *Ct* genome for T3SS effectors, thus Modlab was deemed an unsuitable prediction program for this purpose since it allows the submission of only 50 protein sequences with each run. On the other hand, SIEVE claims to predict T3SS substrates from an unlimited number of input sequences and EffectiveT3 is able to scan a

maximum of 10,000 input sequences at once: a value large enough to sufficiently scan the entire *Ct* E/Bour genome.

As reported, the creation of SIEVE and EffectiveT3 had involved the use of different experimental datasets for training and validating these machine-learning programs. A large set of experimentally characterised T3S effectors from the phylum *Chlamydiae* and the genera *Escherichia*, *Yersinia* and *Pseudomonas* that had been assembled from published studies had been used as a positive training dataset in the generation of EffectiveT3 (Arnold et al., 2009). On the other hand, the dataset used for training and validating in the creation of SIEVE contained proteins from only *Salmonella Typhimurium* and *Pseudomonas syringae* with the reasoning that these are both well-characterised bacteria particularly with regards to their T3S effectors (Samudrala et al., 2009).

We chose to use EffectiveT3 for the prediction of *Ct* T3S effectors on the basis of the speed at which predictions were outputted, the ability to submit the entire *Ct* genome for analysis, and because the training and validating dataset used in the generation of EffectiveT3 included organisms in the phylum *Chlamydiae*. Notably, however, McDermott *et al.* (2011) have previously reported that each of these *in silico* programs is able to predict T3S effectors with comparable accuracies.

3.2.2. Prediction of *Ct* T3S effectors using EffectiveT3

The entire *Ct* serovar E/Bour chromosomal genome was obtained from the National Centre for Biotechnology Information (NCBI) database in FASTA format (GenBank: HE601870.1) and entered into the *in silico* prediction program, EffectiveT3, as an input sequence. The minimal probability score of being T3S could have been set to either 0.95 or 0.9999. We reasoned that the use of either of these parameter scores would identify substrates with a strong probability of being secreted by the bacterium's T3SS. Over one hundred or 53 chlamydial proteins were identified to be likely T3S effectors when the minimal probability score was set to 0.95 or 0.9999 respectively. Thus, given that the

cloning of 53 substrates was a more manageable quantity within the given timescale of this project, we set the minimal probability parameter to be 0.9999.

At the time this prediction was performed, the only version of this *in silico* program available was EffectiveT3 Classification Module 1.0.1 (08/2009). Notably, however, the prediction software has since been updated and is now also available as EffectiveT3 Classification Module 2.0.2 (09/2015). This updated version of EffectiveT3 also examines the N-terminal peptide sequence for distinguishing between T3S and non-secreted proteins. However, the updated algorithm was developed through the iteration of over 500 verified secreted proteins in addition those used in the original training dataset. Furthermore, the user can now freely choose the minimal probability score parameter threshold.

EffectiveT3 identified 53 *Ct* proteins that were likely to be secreted by the bacterium's T3SS. The Basic Local Alignment Search Tool (BLAST) was used to determine the identity and functionality of these 53 predicted proteins (Table 3.1). Encouragingly, EffectiveT3 predicted the secretion of two well-characterised chlamydial T3S effectors, namely Tarp and CT694, which are represented in Table 3.1 as BOUR_00486 and BOUR_00742 respectively. The other predicted T3S effectors play a variety of different roles intracellularly. Most commonly, seven predicted effectors were inclusion membrane proteins (Incs) and 17 were uncharacterised proteins. However, predicted effectors were also found to play roles in DNA repair, methylation, deubiquitination, protein synthesis, glycosylation, sensory transduction and protein chaperoning.

Protein	Function	Protein	Function
BOUR_00006	Uncharacterised protein	BOUR_00420	Heat shock protein, GrpE
BOUR_00036	Putative permease	BOUR_00437	Chlamydial polymorphic outer membrane protein
BOUR_00050	Uncharacterised protein	BOUR_00439	Chlamydial polymorphic outer membrane protein
BOUR_00052	Uncharacterised protein	BOUR_00451	Metal-binding heat shock protein
BOUR_00084	Uncharacterised protein	BOUR_00469	Membrane protein
BOUR_00089	Glucanotransferase	BOUR_00471	Cysteine-rich outer membrane protein
BOUR_00090	Chaperone, SicP	BOUR_00486	TarP
BOUR_00107	Uncharacterised protein	BOUR_00493	tRNA synthase A
BOUR_00116	Oligoendopeptidase F	BOUR_00517	Uncharacterised protein
BOUR_00123	IncA	BOUR_00615	Secretion system effector C-like protein
BOUR_00137	Methylase	BOUR_00616	Secretion system effector C-like protein
BOUR_00151	Uncharacterised protein	BOUR_00662	CHLPN 76kD like-protein
BOUR_00154	Membrane protein	BOUR_00700	Uncharacterised protein
BOUR_00161	Nuclease NucT	BOUR_00742	Uncharacterised protein
BOUR_00163	Nuclease NucT	BOUR_00743	Uncharacterised protein
BOUR_00200	Inclusion membrane protein	BOUR_00760	Uncharacterised protein
BOUR_00204	Inclusion membrane protein	BOUR_00770	Cysteine desulfurase
BOUR_00240	IncA	BOUR_00786	Restriction endonuclease
BOUR_00244	Membrane protein	BOUR_00823	tRNA transferase
BOUR_00245	Inclusion membrane protein	BOUR_00872	IncA
BOUR_00272	Uncharacterised protein	BOUR_00910	Uncharacterised protein
BOUR_00310	DNA repair protein, RadA	BOUR_00911	Uncharacterised protein
BOUR_00365	DNA-binding ATP-dependent protease	BOUR_00916	Antibiotic transporter
BOUR_00380	Inclusion membrane protein	BOUR_00923	Uncharacterised protein
BOUR_00381	Membrane protein	BOUR_00926	Uncharacterised protein
BOUR_00389	Membrane protein	BOUR_00933	Deubiquitinase
BOUR_00417	Uncharacterised protein		

Table 3.1 *Ct* proteins predicted by EffectiveT3 to be T3S. The entire *Ct* genome was screened by the *in silico* prediction program, EffectiveT3, to identify proteins that were predicted to be secreted by the bacterium's T3SS with a probability of >0.9999.

Given the role of the *Ct* T3SS in translocating bacterial proteins into the host cytoplasm and membranes, we reasoned that the predicted *Ct* T3S effectors might be involved in bacterial virulence. Thus, some of these effectors might be virulence factors that play a role in preventing lysosomal degradation by hijacking intracellular membrane trafficking pathways. The capability of these effectors to disrupt intracellular membrane trafficking could be assessed by

cloning the *Ct* T3S effectors into a yeast model system and performing a PEPSY screen as described in section 3.1.8.

3.2.3. Isolation of *Ct* DNA

Ct serovar E (E/Bour) was propagated in adherent McCoy cells in 75cm² tissue culture flasks. At 3 days post-infection, *Ct* elementary bodies (EB) were harvested from *Ct*-infected McCoy cells and isolated by density gradient purification. *Ct* DNA was then extracted from the isolated EBs using the commercially available Wizard SV Genomic DNA Purification kit (Promega). DNA extraction was performed according to the manufacturer's instructions with the only modification of an extended digestion step of 6.5 h. By this method, we obtained 1.5µg genomic *Ct* DNA. This yield of genomic DNA was lower than expected, but sufficient for the gene amplification of each of the 53 predicted *Ct* T3S effectors by polymerase chain reaction (PCR).

3.2.4. Expression of predicted *Ct* T3S effectors in a yeast model system

3.2.4.1. The use of yeast as a model organism

Yeast is widely recognised as an effective model organism for determining individual gene functions and protein interactions and has been used extensively to greater understand human disease and biological processes in eukaryotes (Botstein and Fink, 1988, Botstein and Fink, 2011). In this study, we cloned predicted *Ct* T3S effectors into a yeast model system to assess any intracellular membrane trafficking defects induced upon their expression.

Each of the 53 predicted *Ct* T3S effectors were individually expressed in the yeast strain, BHY12. This URA⁻ diploid yeast strain encodes two copies of the carboxypeptidase Y (CPY) – invertase (*inv*) fusion gene that enables the assessment of CPY-*inv* secretion by an overlay assay described in section 3.1.8.

3.2.4.2. Linearisation of plasmid vector

1.5µg of the URA3+ 2µ expression vector, pVT100-U (Vernet et al., 1987) was linearised by the restriction enzyme, *Bam*HI (Figure 3.3).

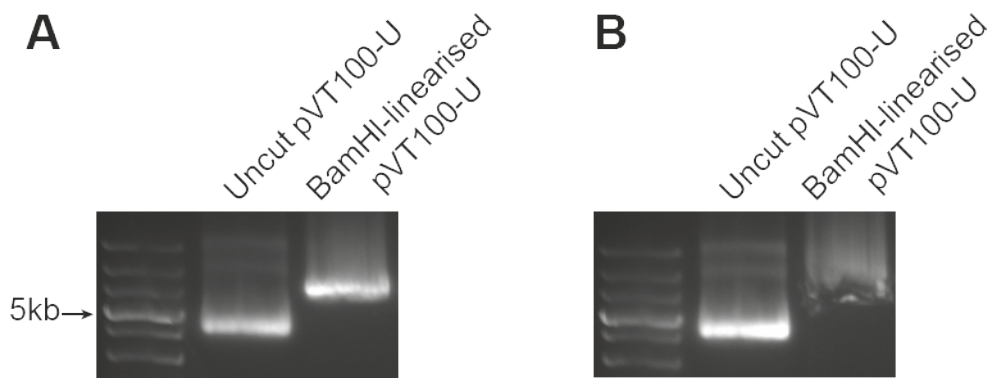


Figure 3.3 Linearisation of pVT100-U by BamHI. **A.** 1.5µg pVT100-U was digested with 20U *Bam*HI for 2 h at 37°C. **B.** Linearised pVT100-U was excised from the agarose gel using a sterile scalpel and purified by gel extraction.

3.2.4.3. Cloning *Ct* T3S effectors into yeast

For the cloning of each of the 53 predicted *Ct* T3S effectors into BHY12, specific primers were designed to enable gene amplification by PCR from genomic DNA previously isolated from *Ct* EBs. Amplified DNA products were electrophoresed on a 0.8% (w/v) agarose gel, excised according to their molecular weight and purified by gel extraction. Predicted *Ct* T3S effectors were then ligated into the BamHI-restriction site of linearised pVT100-U. This vector enables the expression of gene inserts under the control of the constitutive ADH3 promoter. Chemically competent *E.coli* were then transformed with pVT100-U encoding an individual predicted *Ct* T3S effector. Bacterial transformants were identified as ampicillin-resistant *E.coli* colonies and were subsequently tested for the presence of the respective chlamydial gene by a colony PCR screen. Bacterial colonies that were successfully transformed with the expression vector encoding a *Ct* T3S effector were grown overnight in LB media supplemented with ampicillin. The encoded plasmids were then isolated, purified and sequenced to confirm the successful cloning of *Ct* genes.

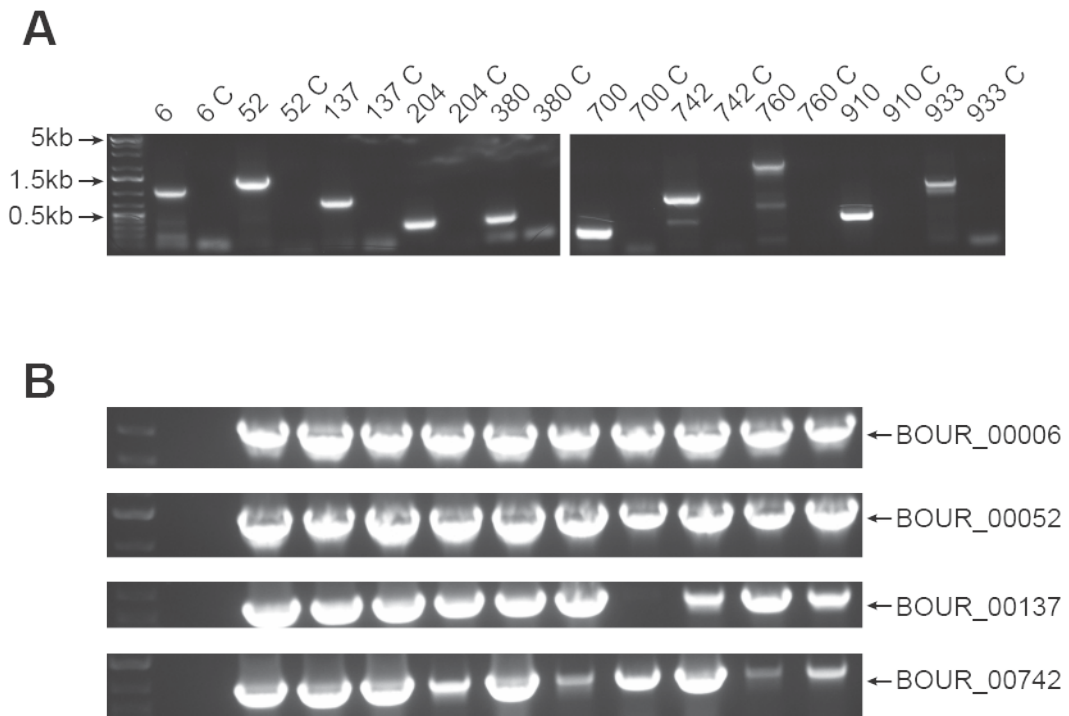


Figure 3.4 Cloning predicted *Ct* T3S effectors into pVT100-U. **A.** Specified genes (BOUR_00XXX) were amplified by PCR and electrophoresed on an agarose gel. C = no template DNA control. **B.** The multiple cloning site (MCS) of plasmids from ten *E. coli* colonies harbouring the specified genes were amplified by colony PCR and electrophoresed on an agarose gel. A representative selection of effectors is shown here.

All predicted *Ct* T3S effectors were successfully ligated into pVT100-U and transformed into *E. coli*. Sequencing traces also revealed that each full-length gene had been cloned successfully.

3.2.5. Assessment of intracellular membrane trafficking defects

BHY12 expressing individual predicted *Ct* T3S effectors were assayed for the presence of intracellular membrane trafficking defects using PEPSY screening. These yeast clones were cultured on selective media deficient in uracil (SC-ura) and supplemented with fructose as a carbon source. Yeast were then screened for a VPS⁻ phenotype using the overlay assay described previously (section 3.1.8). Following the addition of the glucostat reagent, putative *Ct* virulence factors involved in disrupting membrane trafficking were identified by yeast colonies that formed a brown precipitate. Most *Ct* T3S effectors did not display a VPS⁻ phenotype that would otherwise be indicative of perturbed intracellular

membrane trafficking. Notably, however, a VPS^- phenotype was observed for BHY12 expressing *BOUR_00381* or *BOUR_00916* (Figure 3.5).

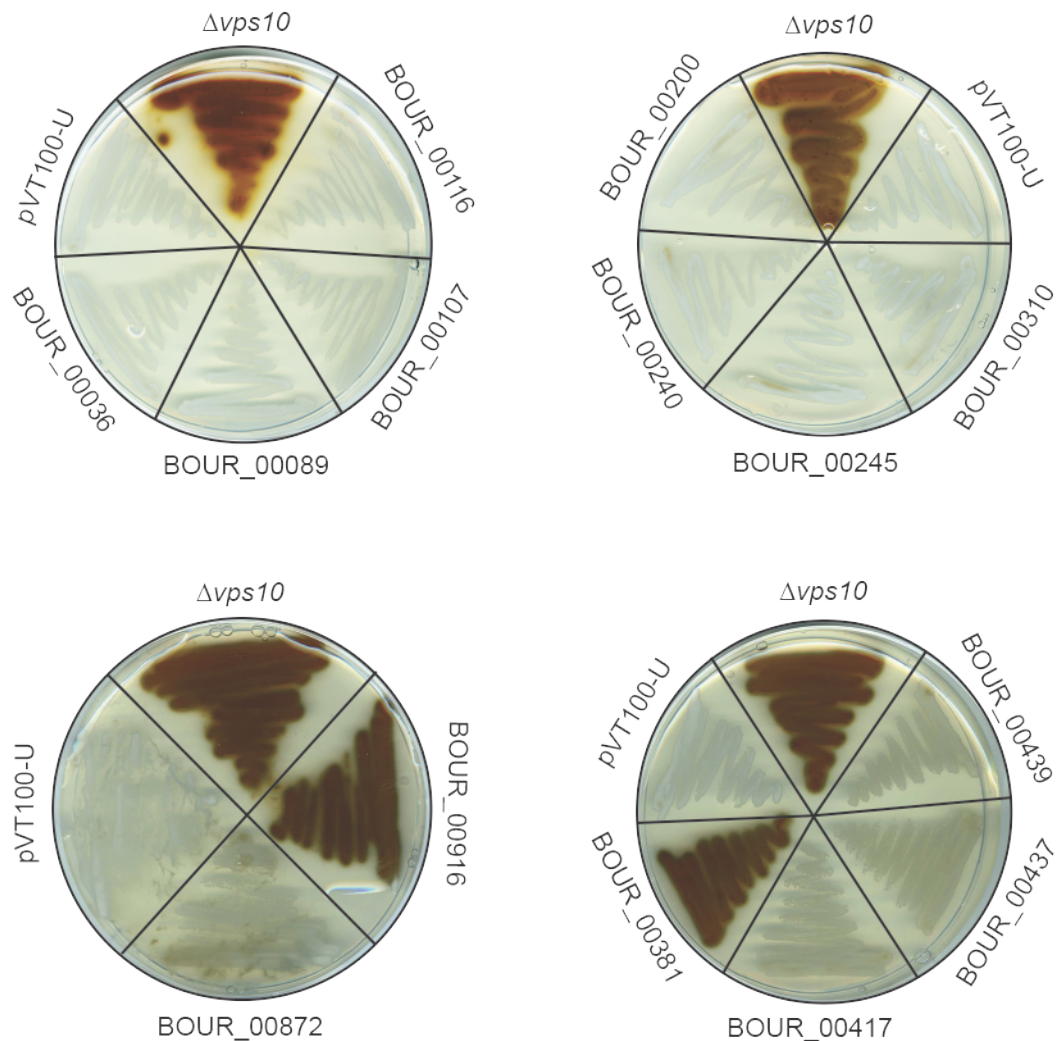


Figure 3.5 Assessing CPY-inv secretion in predicted *Ct* T3S effectors. A secretory assay was performed on all 53 predicted *Ct* T3S effectors. A representative selection of effectors is shown here. Production of a brown precipitate indicates CPY-inv secretion, thus disruption of normal membrane trafficking.

Thus, the yeast clones expressing *BOUR_00381* or *BOUR_00916* were picked, re-streaked and retested to confirm the VPS^- phenotype. Furthermore, we sought to assess whether the intracellular membrane trafficking disruption was plasmid-dependent and therefore an observation solely arising from the expression of the associated chlamydial gene.

Two different approaches were undertaken to test whether the VPS^- phenotype observed for these clones was plasmid-dependent. Firstly, plasmid minipreps were again used to transform more BHY12. Transformed BHY12 were then assayed for CPY-inv secretion with the assumption that CPY-inv missorting is plasmid-dependent if the VPS^- phenotype is again observed. Newly transformed BHY12 expressing either *BOUR_00381* or *BOUR_00916* were assayed for CPY-inv secretion. This time, however, a brown precipitate was not formed, thus suggesting that this is not a plasmid-dependent phenotype (Figure 3.6 A).

An alternative method for investigating whether CPY-inv secretion is plasmid-dependent is to cure yeast of their plasmid by growing the clones on media containing 5-fluoroorotic acid (5-FOA). In the presence of 5-FOA, yeast harbouring the URA3 gene (the selectable marker in pVT100-U) that encodes orotidine-5-monophosphate decarboxylase are able to convert 5-FOA into the toxic metabolite 5-fluorouracil (5-FU). 5-FU functions primarily as a thymidylate synthase inhibitor that disrupts thymidine synthesis and hence interferes with DNA replication. Subsequently, yeast clones expressing the URA3 gene are unable to grow on agar plates containing 5-FOA. However, given the toxicity of 5-FU for URA3⁺ yeast, there is a selective advantage for yeast to cure themselves of this plasmid. Thus, the growth of yeast colonies on agar plates containing 5-FOA is indicative of plasmid-cured yeast. These colonies can be picked, re-streaked onto fresh agar plates and tested for CPY-inv secretion. Given that these yeast colonies have been cured of their URA3⁺ plasmid (that also encodes *Ct* DNA), it can be hypothesised that CPY-inv should no longer be observed if the VPS^- phenotype is plasmid-dependent.

Plasmid-cured BHY12 expressing either *BOUR_00381* or *BOUR_00916* was assayed for CPY-inv secretion. A brown precipitate was still formed by both clones following plasmid curing, thus further indicating that the VPS^- phenotype originally observed was not plasmid-dependent (Figure 3.6 B).

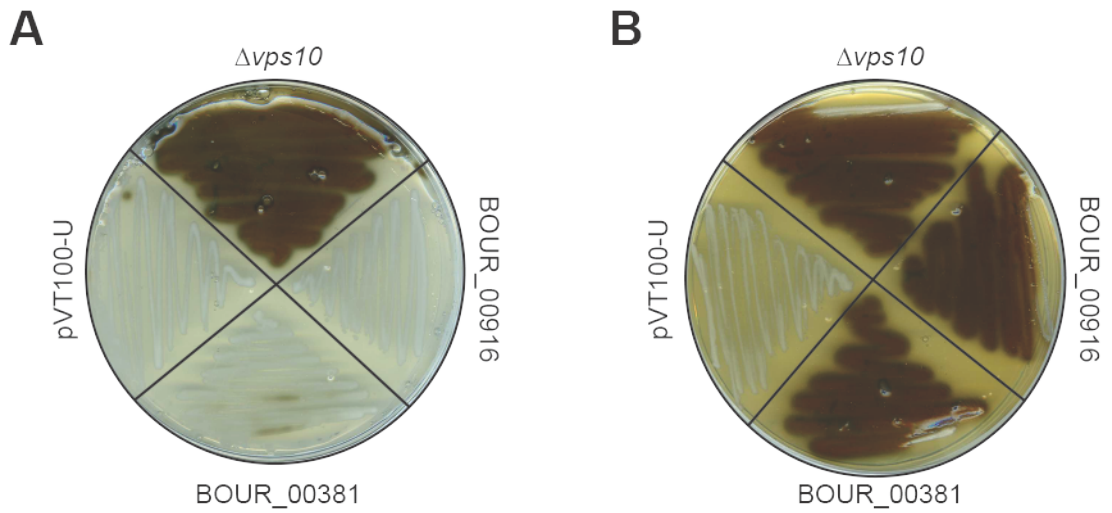


Figure 3.6 Assessing plasmid-dependent effects of chlamydial clones. A secretory assay was performed on newly transformed (**A**) or plasmid-cured (**B**) yeast clones.

3.3. Discussion

3.3.1. The use of *in silico* approaches to predict *Ct* T3S effectors

Like many other pathogens, the virulence of *Ct* relies upon the translocation of effector proteins via a T3SS to cytosolic and membrane targets within the infected host cell to aid bacterial invasion, colonisation, replication and intracellular survival.

T3S effectors do not contain an easily recognisable secretion signal and, until recently, *Ct* has long been intractable to genetic manipulation. Subsequently, the identification of *Ct* T3S effectors has not been a trivial task. Chlamydial researchers have identified T3S effectors by various means including (i) phenotypic analyses of *S. cerevisiae* expressing individual proteins (Sisko et al., 2006), (ii) using *Salmonella* (Ho and Starnbach, 2005), *Shigella* (Subtil et al., 2001) or *Yersinia* (Weber et al., 2015) as a heterologous expression system, or (iii) using computational approaches to predict T3S signals (Hovis et al., 2013, Arnold et al., 2009, Lower and Schneider, 2009, Samudrala et al., 2009).

Since we predicted *Ct* T3S effectors, da Cunha et al. (2014) have reported that several previously uncharacterised *Ct* proteins could be secreted into host cells by a heterologous *Yersinia enterocolitica* T3SS. This study also compared the experimental results with those obtained from *in silico* approaches whereby *Ct* proteins that were either secreted or not secreted experimentally via the *Y. enterocolitica* T3SS were also analysed by the *in silico* prediction programs EffectiveT3 (Arnold et al., 2009), SIEVE (Samudrala et al., 2009), Modlab (Lower and Schneider, 2009) and T3_MM (Wang et al., 2013). Here, a majority of the full-length *Ct* effectors that were shown experimentally to be not secreted by a T3SS were also predicted to be non-secreted by *in silico* approaches. This suggests a low rate of false positive results arising from each of these four *in silico* prediction programs.

Furthermore, ten of the eleven experimentally validated T3S proteins examined in this study had been predicted to be secreted by at least one of the *in silico* prediction programs above. However, when each *in silico* program was

assessed individually, they were only able to accurately predict T3S effectors in approx. 50% of instances. Thus, there is some correlation between experimental data and *in silico* predictions. However, each of these computational approaches generates different predictive outputs and hence by combining different *in silico* approaches and validating them experimentally, we could make more accurate predictions.

In our study, one *in silico* program was selected for the prediction of *Ct* T3S effectors. Although each of the prediction programs listed above are believed to predict T3S effectors with comparable accuracies (McDermott et al., 2011), the use of one *in silico* approach to independently predict T3S effectors may not have been the most effective means of identifying *Ct* effectors given the discrepancies between prediction programs and experimental validation. Thus, with hindsight, it may have been more beneficial to predict *Ct* T3S effectors using multiple *in silico* prediction programs and then collate the outputs for screening the effect of expressing those proteins in a yeast model system.

In this study, we performed parallel investigations to identify *Ct* T3S effectors. We carried out a targeted approach using computational methods to identify *Ct* T3S effectors that were then individually tested for their ability to disrupt intracellular membrane trafficking in a yeast model system. Meanwhile, as described later in Chapter 4, a *Ct* genomic library was generated and screened in a genome-wide search for *Ct* T3S effectors involved in disrupting intracellular membrane trafficking. We had hoped that any *Ct* T3S effectors identified during this targeted approach would also be identified in a genome-wide screen.

3.3.2. Analysis of predicted *Ct* T3S effectors

By using the *in silico* prediction program, EffectiveT3, we predicted that 53 *Ct* effectors had a strong probability (>0.9999) of being secreted by the bacterium's T3SS. A BLAST search was performed to determine the identity and functionality of these predicted effectors. Encouragingly, the two well-characterised *Ct* T3S effectors, Tarp and CT694, were identified using EffectiveT3. Of the other predicted proteins, 17 were uncharacterised and 7

were Incs. Other predicted proteins were found to play roles in methylation, DNA repair, deubiquitination, antibiotic transportation and protein translation.

Several predicted proteins were found to be Incs. For example, BOUR_00123, BOUR_00240 and BOUR_00872 share high sequence similarity with IncA, which has been reported to be involved in the homotypic fusion of chlamydial inclusions as well as the regulation of fusion with endocytic compartments (Hackstadt et al., 1999, Delevoeye et al., 2004, Paumet et al., 2009). We were not surprised by the prediction of Incs by EffectiveT3 given the general understanding that these proteins are inserted into the chlamydial inclusion membrane following their secretion by the bacterium's T3SS to enable crucial host-pathogen interactions (Fields and Hackstadt, 2003, Subtil et al., 2001, Hackstadt et al., 1999). *Ct* is believed to express 59 putative Incs and each of these harbours a characteristic bilobed hydrophobic domain of approximately 40-60 residues that enables the insertion of Incs into the inclusion membrane (Weber et al., 2015). Given the large number of previously predicted *Ct* Incs, the number of predicted Incs by EffectiveT3 appears to be relatively low by comparison. By definition, Incs are secreted by the chlamydial T3SS, thus we would have expected the *in silico* prediction program to report a larger number of Incs to be secreted.

As expected, the chlamydial protein, Tarp, was also predicted to be T3S. Tarp is one of the most well-characterised *Ct* effectors and has been shown to be translocated by the T3SS in the early stages of the chlamydial lifecycle. This protein recruits host actin to the site of chlamydial attachment to support the internalisation of the bacterium into host cells (Clifton et al., 2004). Given the role of Tarp in the early development of chlamydial infection, together with previous reports of its secretion by the T3SS, we would have expected this protein to be predicted by EffectiveT3.

Three predicted proteins (BOUR_00161, BOUR_00163 and BOUR_00786) function as nucleases. This was also a plausible output given that nucleases function to cleave nucleic acids and hence may prove advantageous for the intracellular bacterium upon entry into host cells. Other bacteria have also been

reported to secrete nucleases. For example, the bacterium, *Streptococcus pneumoniae*, secretes a nuclease, EndA, to aid the bacterium's escape from host inflammatory responses (Beiter et al., 2006) and, similarly, *Mycobacterium tuberculosis* secretes the extracellular nuclease, Rv0888, which is believed to act as a virulence factor during infection (Dang et al., 2016).

The predicted *Ct* T3S effector, BOUR_00310, is involved in DNA repair. This is a credible intracellular function that may prove advantageous for *Ct* by avoiding host immune responses. This functionality has been seen in other bacterial species, for example the evolutionarily conserved bacterial protein, Mfd, is able to prevent bacterial DNA damage that is induced by host reactive nitrogen species during an immune response (Guillemet et al., 2016).

One deubiquitinase (DUB), BOUR_00933, was identified by EffectiveT3 to be secreted by the chlamydial T3SS. This was also a conceivable output given that several other pathogenic bacteria, including *Salmonella typhimurium* (Rytönen et al., 2007), *Yersinia pestis* (Orth, 2002) and *E. coli* (Catic et al., 2007) also secrete DUBs to down-regulate host responses and to aid bacterial virulence. BOUR_00933 was later found to be an interesting chlamydial effector following a genome-wide PEPSY screen and will be revisited in Chapter 4.

Generally, the proteins predicted by EffectiveT3 to be T3S had rational and logical functionality in the context of chlamydial invasion and survival inside host cells.

3.3.3. Screening for T3S *Ct* virulence proteins

In this study, we sought to identify *Ct* T3S effectors that disrupted endosomal trafficking pathways. Each *Ct* effector predicted to be T3S by the *in silico* prediction program EffectiveT3 was individually cloned into yeast to enable PEPSY screening.

Firstly, we isolated EBs from McCoy cells infected with *Ct* serovar E (E/Bour) and extracted genomic DNA. The DNA yield obtained was much lower than anticipated, but was sufficient for the amplification of each of the predicted *Ct* T3S effectors for PEPSY screening. As described in Chapter 4, we later

optimised the *Ct* infections in order to extract greater quantities of *Ct* genomic DNA for library generation. All 53 predicted proteins were successfully cloned into pVT100-U and transformed into BHY12 yeast for PEPSY screening.

Yeast is a widely used model system that can be genetically manipulated with ease and is therefore commonly used to identify and characterise bacterial virulence proteins (Siggers and Lesser, 2008, Valdivia, 2004). Many bacterial effectors normally involved in mammalian infection retain their biological function in yeast (Valdivia, 2004). Previously, Lesser and Miller (2001) demonstrated that an array of bacterial effectors secreted by *Salmonella* or *Yersinia* localise to the same subcellular locations in yeast as they do in mammalian cells. They deduced that, provided the interacting partners of bacterial effectors remain conserved between yeast and higher eukaryotes, yeast could be used as a model system for studying bacterial virulence factors. Furthermore, despite the evolutionary divergence of yeast and mammals, bacterial proteins will still be targeted to the same subcellular compartments irrespective of whether they are synthesised *de novo* in yeast or translocated by specific bacterial secretion systems (Siggers and Lesser, 2008).

Using a yeast model system, we can screen for effectors that may interfere with the normal *vps* pathway (Campodonico et al., 2005, Shohdy et al., 2005). PEPSY screening has previously been used to identify virulence factors secreted by *Legionella* (Shohdy et al., 2005), *Yersinia* (Tabuchi et al., 2009) and *Salmonella* (Raines et al., 2017). All of these bacteria are Gram-negative and are able to survive intracellularly within pathogen-containing vacuoles (Isberg et al., 2009, Pujol et al., 2009, Steele-Mortimer, 2008). Furthermore, *Yersinia* and *Salmonella* also possess T3SS (Cornelis, 2002, Coburn et al., 2007), while *Legionella* possesses a T4SS (Qiu and Luo, 2013). Given that *Ct* is a Gram-negative bacterium that is able to survive intracellularly within the inclusion and uses a T3SS to translocate effector proteins into the host cytoplasm, we reasoned that a PEPSY screening method would also be suitable for identifying *Ct* virulence proteins *in vitro*.

Only two predicted *Ct* T3S effectors, BOUR_00381 and BOUR_00916, displayed a VPS⁻ phenotype when PEPSY screened for trafficking defects. However, when examined further, we established that the observed phenotype was not plasmid-dependent and thus could not be attributed to the chlamydial gene encoded in the expression plasmid. Instead, the VPS⁻ phenotype that was observed was likely due to a random mutation occurring in the yeast that coincidentally resulted in a trafficking defect.

Initially, given that all 53 *Ct* proteins tested had been predicted to be T3S, we had anticipated that at least some of these proteins would be translocated into the host cytoplasm with the role of perturbing normal endosomal trafficking to aid bacterial survival. We remained mindful that the predicted *Ct* T3S effectors may not play a role in disrupting intracellular membrane trafficking. However, given the relatively large number of proteins that we screened and the nature by which *Ct* is able to survive intracellularly, we had expected that at least one or few proteins was involved in manipulating this important trafficking pathway.

We anticipated that *Ct* effectors might not be detected by this PEPSY screening method for a number of reasons. Firstly, the methodology relies upon homology between yeast and mammals. If the host substrate is not evolutionarily conserved between higher and lower eukaryotes, the bacterial effector will not be able to manipulate trafficking effectively within a yeast host. For example, if substrates are involved in coordinating intercellular communication, regulating cell death or building innate or adaptive immunity in mammalian hosts, then yeast would not be an ideal model system to screen these chlamydial proteins (Valdivia, 2004). Moreover, some cellular functions, for example membrane fusion, may be highly conserved between eukaryotic organisms but individual components may be different enough for recognition to be hindered (Valdivia, 2004). Furthermore, in this study, chlamydial proteins are expressed at non-physiological levels and in non-physiological conditions in the absence of other factors that would otherwise be present during an infection. Thus, intracellular disruption may not be observed if the bacterial effector requires a chaperone or interactions with other *Ct* proteins, for example within a multi-protein complex. The eukaryotic host might also post-translationally modify bacterial effectors

following their secretion, thus if this modification does not occur within the yeast model, then the resulting defect that would otherwise be induced by the protein may not occur (Popa et al., 2016). Furthermore, if the post-translational modification does occur, the effector may still not retain its biological activity when expressed in yeast. The success of the PEPSY screen also depends on bacterial effectors being correctly folded into the 3-dimensional complex protein structures. Bacterial effector functionality may be seriously compromised if a yeast model system is unable to correctly fold the bacterial proteins.

Notably, the controls that were used in the PEPSY screens were BHY12 harbouring a $\Delta vps10$ knockout (positive control) or transformed with an empty pVT100-U vector (negative control). With hindsight, it would have been useful to include additional controls using yeast expressing bacterial effector proteins known to either induce or not induce a VPS^- phenotype. For example, the *Salmonella* protein SseJ and the *Legionella* proteins VipA and VipD have previously demonstrated a VPS^- phenotype when PEPSY screened (Raines et al., 2017, Shohdy et al., 2005) and could have been used as additional positive controls in this study.

We had assumed that *Ct* effectors were expressed in the yeast model system. However, this was not directly tested. Thus, with hindsight, it would have been beneficial to clone each of the predicted *Ct* T3S effectors with an epitope tag (e.g. myc tag) to enable us to confirm that effectors were expressed in yeast. Notably, however, this approach has been undertaken previously in the Pryor lab and indicated that BHY12 was able to successfully express the myc-tagged *Rhodococcus equi* virulence protein, VapA.

3.3.4. Study progression

This bioinformatics and targeted approach did not successfully identify *Ct* effector proteins that function to manipulate intracellular trafficking when expressed in a yeast model system. As discussed in Chapter 4, we next sought a genome-wide approach for identifying such effectors.

Chapter 4: Generation and screening of a *Chlamydia trachomatis* library to identify virulence proteins

4.1. Introduction

4.1.1. Objectives

In this chapter, we describe the larger-scale propagation of genital *Ct* serovar E/Bour in McCoy cells and the subsequent isolation of chlamydial EBs for the generation of a random *Ct* genomic library. We then screen the *Ct* library by pathogen effector protein screening in yeast (PEPSY) to identify *Ct* virulence proteins that disrupt intracellular membrane trafficking in *S. cerevisiae*. Yeast clones that demonstrated disrupted trafficking were further investigated to confirm plasmid-dependent trafficking disruption and were then subsequently characterised to identify the *Ct* gene(s) responsible for inducing the effect.

4.2. Results

4.2.1. Chlamydia trachomatis infections

Chlamydiae are obligate intracellular bacteria that are only able to propagate, replicate and survive intracellularly. Thus, for laboratory purposes, chlamydiae cannot be grown on conventional bacteriological medium. Culturing chlamydiae *in vitro* is not a trivial task. Most *Ct* strains, excluding the LGV serovars, are unable to readily infect tissue culture cells following lysis or extrusion from the host cell. Subsequently, additional chemical or mechanical assistance is required when culturing ocular and genital *Ct* strains *in vitro*. In theory, the culture of LGV serovars as a source of *Ct* DNA would have been less laborious, but instead we opted to culture the less hazardous genital serovar E as this serovar does not require the higher category 3 laboratory containment that is required for culturing LGV serovars.

Thus, *Ct* serovar E (E/Bour) was propagated in McCoy cells. Infections were performed on a reasonably large scale because we hoped to extract approximately 80-100µg *Ct* DNA for the generation of a genomic library. Although a genomic library requires only approximately 20-30µg DNA (Shohdy et al., 2005), we hoped to extract sufficient DNA to allow for experimental optimisation.

Infections were initially carried out in 75cm² flasks. We observed a low infection rate whereby only approximately 20% McCoy cells contained chlamydial inclusions. Upon closer inspection, we noticed that only McCoy cells positioned at the perimeter of the flask were infected and not those located centrally. Using Coomassie stain, we demonstrated that, when placed on a level surface, solutions within the flask naturally flow to the perimeter, thus resulting in smaller volumes settling in the centre of the flask. Assuming the flow of Coomassie stain is equivalent to that of the EB-containing media, this suggests that the EBs are more concentrated around the perimeter, thus have a greater possibility of infecting cells here than those positioned centrally. This supported the observation that infections predominantly occurred around the perimeter of the flask.

This perimeter bias was not observed for *Ct* infections carried out in 6-well plates; instead chlamydial inclusions were observed evenly dispersed throughout the entire surface area of the well. Thus, infection of McCoy cell monolayers with chlamydial EBs was carried out in 6-well plates to maximise *Ct* infection rates.

Further optimisation conditions were also examined to improve *Ct* infection rates. Scidmore has previously recommended the inoculation of McCoy cell monolayers with *Ct* EBs (Scidmore, 2005). However, given the initial low infection rates, we attempted to inoculate cells in suspension within a 50ml falcon tube prior to adherence to a 75cm² flask. This method of inoculation proved to be inefficient with very few inclusions identified 3 days post-inoculation.

Furthermore, the pre-treatment of McCoy cell monolayers with diethylaminoethyl dextran (DEAE-dextran; Sigma) has previously been reported to enhance the infectivity of non-LGV serovars of *Ct* (Scidmore, 2005). Thus, we attempted to optimise infection rates by pre-treating McCoy cells in 75cm² flasks with DEAE-dextran. DEAE-dextran has previously been reported to also enhance the uptake of vesicular stomatitis virus (VSV) (Bailey et al., 1984) and murine leukaemia virus (Ebbesen, 1973) and is believed to neutralise the cell surface charge and thereby allow for more efficient microbial attachment. Instead of spin-inoculating *Ct* onto the monolayer, McCoy cells were treated with 45µg/ml DEAE-dextran prior to inoculation with *Ct* EBs. Despite previous literature reporting the enhancement of infectivity using DEAE-dextran, the infection rate observed here was noticeably reduced compared with the spin-inoculation method previously used. Thus, DEAE-dextran was not used for further *Ct* infections.

4.2.2. Isolation of *Ct* DNA

EBs were harvested from *Ct*-infected McCoy cells and purified by density gradient purification. Typically, an isopycnic renografin density gradient is used to purify chlamydial EBs. However, due to difficulties obtaining renografin, we sourced gastrografen as an alternative gradient material. Gastrografen is

identical to urografin except for the addition of a flavouring agent and a wetting agent for medical use in radiological examinations. Gastrografin has been deemed suitable for the isolation of chlamydial EBs (Coombes and Mahony, 2002) while urografin has previously been used by Goodall *et al.* (2001) to isolate *Ct* EBs for genomic library construction. Thus, gastrografin was used here to isolate *Ct* EBs. For ease of purification, four separate gradients were performed.

Following isolation, the commercial Wizard SV Genomic DNA Purification kit (Promega) was used to extract the DNA from pellets of purified chlamydial EBs. DNA extraction was performed according to the manufacturer's instructions with the only modification of an extended digestion step of 6.5 hours. This method yielded 2.4µg DNA, thus predicting that a total of approximately 9.6µg DNA had been obtained collectively from all four gradients (Table 4.1). This was an unexpectedly low yield given the observed infection rates, thus we hypothesised that an alternative DNA extraction method may extract genetic material from the isolated EBs with greater efficiency than the commercial DNA purification kit.

Subsequently, a phenol-chloroform extraction method was used as an alternate method for extracting DNA from chlamydial EBs. Using this technique, a 4-fold greater yield of 8.83µg DNA was obtained, thus the phenol-chloroform extraction method was used to extract chromosomal DNA from the remaining two pellets of isolated EBs. These subsequent extractions yielded 4.34µg and 17.89µg DNA, hence a total of approximately 30µg DNA was assumed to have been attained from the density gradient purified EBs (Table 4.1).

Sample no.	DNA extraction method	Yield (μg)
1	Wizard SV Genomic Purification kit	2.40
2	Phenol-chloroform extraction	8.83
3	Phenol-chloroform extraction	4.34
4	Phenol-chloroform extraction	17.89

Table 4.1 *Ct* DNA extraction yields.

Before further experimentation, the four aliquots of purified chlamydial DNA were pooled. The concentration of this pool was measured to be 56.3 μg . This was an unexpectedly high value considering the concentrations of the individual isolates. We reasoned that this was likely due to either a lack of sufficient mixing when measuring the unpooled isolates or that the chromosomal DNA had not entirely dissolved in the TE buffer when Nanodrop measurements were initially taken.

4.2.3. Generation of a *Ct* genomic library

4.2.3.1. Digestion of *Ct* genomic DNA

The pooled DNA isolates were used to generate a *Ct* genomic library. *Ct* DNA was digested using the restriction enzyme, *Sau3AI*, to generate smaller DNA fragments that were suitable for cloning into the destination plasmid. The average size of a gene encoded by *Ct* chromosomal DNA is approximately 1.17kb (Thomson et al., 2008). Thus, *Ct* DNA fragments of 0.8-5kb in size were necessary to maximise the possibility of encoding full-length open reading frames (ORF) within the library.

Initial DNA digests were performed to determine the optimal concentration of *Sau3AI* required for generating DNA fragments within the desired size range. 0.87 μg *Ct* DNA isolated by density gradient purification was incubated with 0.0008-0.1U *Sau3AI* per 11 μl reaction for 1 hour at 37°C. The digested DNA was then electrophoresed on a 0.8% (w/v) agarose gel (Figure 4.1).

Figure 4.1 demonstrates that DNA fragments of size 0.8-5kb were generated upon incubation with 0.025U *Sau3AI*. Due to limited quantities of *Ct* DNA the concentration range of *Sau3AI* was not further optimised.

Following initial optimisation, the restriction enzyme digests were repeated using 15µg *Ct* DNA in order to scale up the reaction and subsequently generate sufficient quantities of fragmented DNA for library generation. Since a 17-fold increase in *Ct* DNA was digested, an equivalent 17-fold increase in *Sau3AI* concentration (0.429U) and reaction volume (188µl) was also used. As previously, the digest was performed for 1 h at 37°C and samples were then electrophoresed on a 0.8% (w/v) agarose gel.

DNA fragments of varying sizes were generated. A majority of DNA fragments were <0.3kb or >3kb in size. However, a noticeable amount of DNA was also visible within the 0.3-3kb range. The region corresponding to 0.8-5kb was excised from the gel and the DNA was purified across seven columns using a Gel Extraction kit (Qiagen). These seven purified DNA digests were pooled with a concentration of 13.6ng/µl.

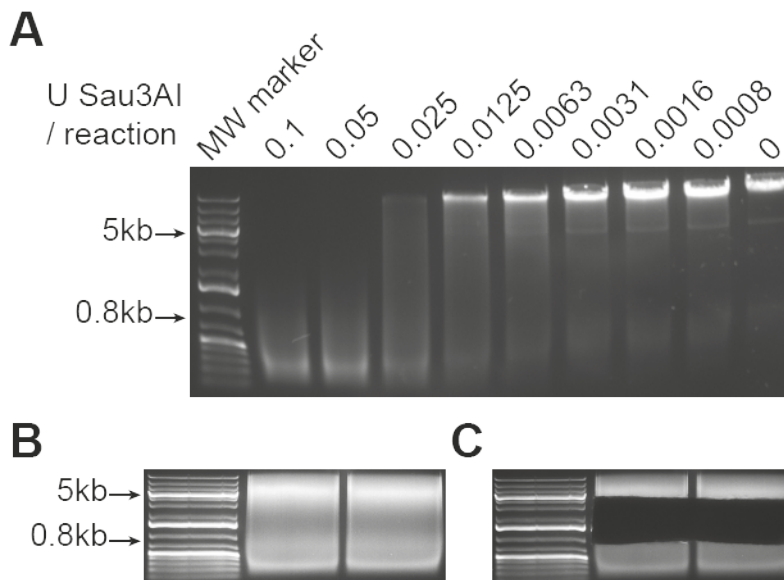


Figure 4.1 Digestion of *Ct* genomic DNA with *Sau3AI*. **A.** 0.87µg *Ct* DNA was digested with the indicated units of *Sau3AI* in an 11µl reaction for 1 h at 37°C and digests were electrophoresed on a 0.8% (w/v) agarose gel. **B.** 15µg *Ct* DNA was digested with 0.429U *Sau3AI*. **C.** Digested *Ct* DNA fragments of 0.8-5kb were excised from the agarose gel using a sterile scalpel and were purified by gel extraction.

4.2.3.2. Linearisation of plasmid vector

1.5µg of the URA3+ 2µ expression vector, pVT100-U (Vernet et al., 1987), was linearised by the restriction enzyme, *Bam*HI. *Bam*HI and *Sau*3AI generate complementary sticky ends that allow the *Ct* DNA fragments to be ligated into the plasmid vector.

Linearised pVT100-U was dephosphorylated using alkaline phosphatase to prevent the sticky ends from re-annealing.

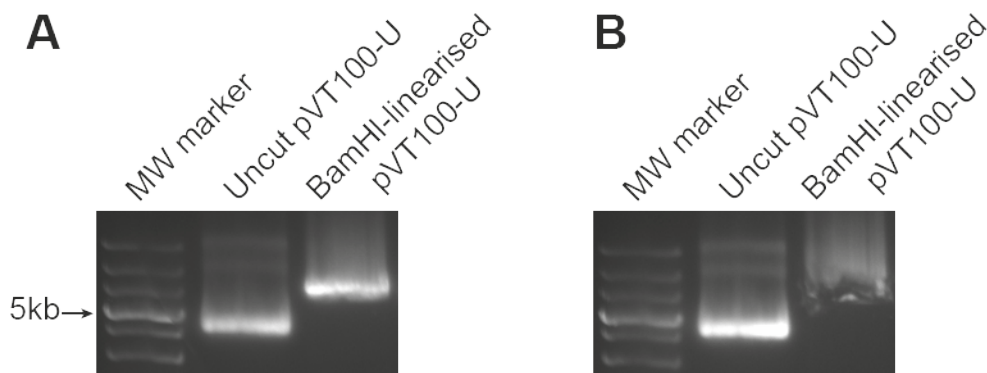


Figure 4.2 Linearisation of pVT100-U by *Bam*HI. **A.** 1.5µg pVT100-U was digested with 20U *Bam*HI for 2 h at 37°C. **B.** Linearised pVT100-U was excised from the agarose gel using a sterile scalpel and purified by gel extraction.

4.2.3.3. Plasmid ligation and the transformation of competent bacteria

Purified *Ct* DNA fragments of size 0.8-5kb were ligated into the dephosphorylated *Bam*HI-restriction site of pVT100-U. This vector enables the expression of gene inserts under the control of the constitutive ADH3 promoter.

Sticky-end ligation was performed using T4 DNA ligase. According to the manufacturer's instructions, the ratio of insert DNA and linear vector DNA should be 3:1 respectively and further optimisation may be achieved by varying the total amount of DNA (0.01-0.1µg), extending reaction time, inactivating the T4 ligase, or transforming competent cells with a 10-fold dilution of the ligation reaction. Thus, a series of ligation and transformation reactions were performed to determine the optimal conditions for yielding the maximum number of

transformed bacterial colonies evenly dispersed on an LB ampicillin plate (Table 4.2).

Reaction	Time (min)	Total DNA (μg)	Heat-inactivation of T4 ligase	Dilution of ligation reaction	No. colonies per ligation ($\times 10^3$)
1	10	0.01	✓	1:10	1
2	10	0.01	x	1:10	10
3	10	0.01	✓	Neat	2
4	10	0.01	x	Neat	7
5	10	0.10	✓	1:10	76
6	10	0.10	x	1:10	106
7	10	0.10	✓	Neat	51
8	10	0.10	x	Neat	66
9	60	0.01	✓	1:10	2
10	60	0.01	x	1:10	6
11	60	0.01	✓	Neat	3
12	60	0.01	x	Neat	9
13	60	0.10	✓	1:10	117
14	60	0.10	x	1:10	58
15	60	0.10	✓	Neat	155
16	60	0.10	x	Neat	105

Table 4.2 Optimisation of ligations and bacterial transformations.

In addition, a sample of competent NEB 10- β *E. coli* was transformed with empty vector to estimate the yield of background colonies. For this control, no colonies formed.

Based on Table 4.2, we deduced the optimal conditions for obtaining the maximum transformed bacterial colony count to be 0.10 μg total DNA, heat-inactivation of the T4 ligase after a 1 h incubation and using the neat ligation reaction to transform competent *E. coli* (Reaction 15).

4.2.3.4. Estimation of genome coverage

When generating the random gene library, we were mindful that bacteria harbouring plasmids containing short *Ct* DNA sequences would grow and divide at a quicker rate than those harbouring plasmids containing longer *Ct* DNA sequences. Thus, two approaches were taken to estimate the average size of *Ct* DNA inserts.

Firstly, plasmids from nine transformed bacterial colonies were amplified in a colony PCR and the amplification products were electrophoresed on a 0.8% (w/v) agarose gel (Figure 4.3 A). The DNA insert size was calculated for each bacterial colony with careful consideration towards an additional 300bp provided by the plasmid multiple cloning site (MCS) that is also amplified during PCR. By this method, the average *Ct* DNA insert was estimated to be 2.09kb.

Secondly, plasmids from nine bacterial colonies were purified by Miniprep and subjected to a *DraI* restriction enzyme digest. When empty pVT100-U vector is digested with *DraI*, DNA fragments of size 3809, 1381, 955, 692 and 2x18bp are generated. The size of the *Ct* DNA inserted into the plasmid can be estimated by analysing the electrophoretic shift pattern of fragments with the *Ct* DNA. The average insert size calculated from the *DraI* diagnostic digest was 1.24kb (Figure 4.3 B). Thus, collectively the average insert size from both colony PCR and *DraI* digest was calculated to be 1.69kb.

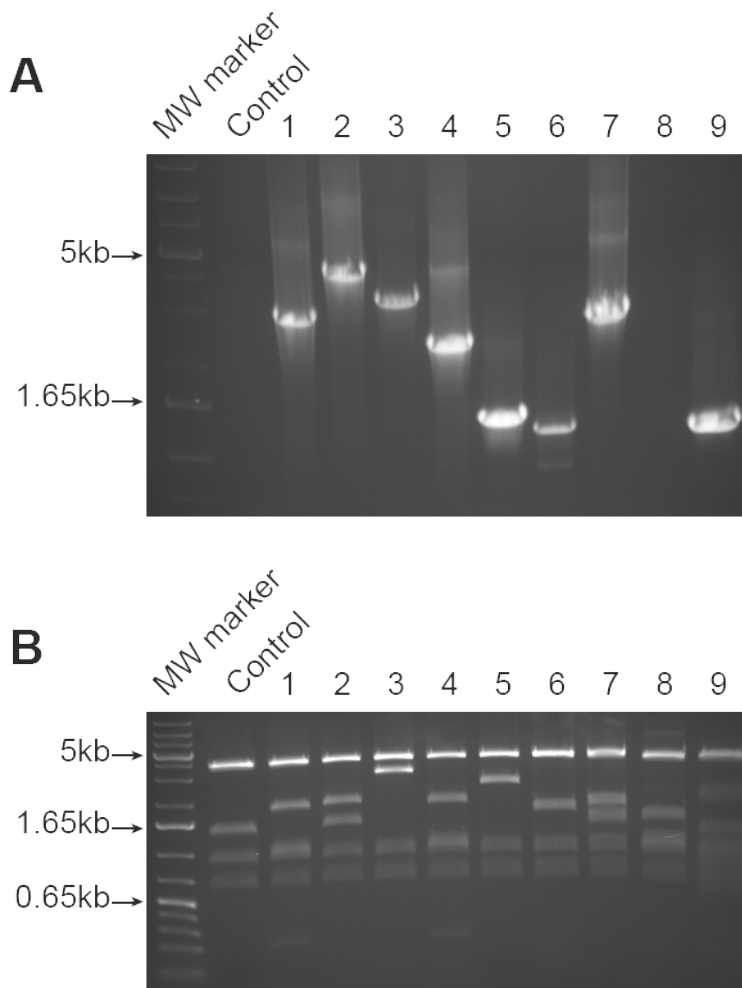


Figure 4.3 Estimation of *Ct* DNA insert size. A. The MCS of plasmids from nine *E. coli* colonies harbouring random *Ct* DNA fragments were amplified by colony PCR. **B.** Plasmids from nine *E. coli* colonies harbouring random *Ct* DNA fragments were purified and digested with *DraI*.

Not only does the estimation of the average *Ct* insert size potentially provide confidence in any library bias, but it also enables the determination of genome coverage within the library. When generating a random gene library it is necessary to estimate genome coverage in order to ensure that the whole genome is proportionately represented within the library. Libraries with a larger genome coverage present an increased likelihood of finding a particular gene.

Given that the size of the *Ct* genome is 1.03Mb and the average *Ct* DNA insert size was calculated to be 1.69kb, we can approximate that 610 transformed bacterial colonies would be required to cover the entire *Ct* genome once:

$$\frac{1030kb}{1.69kb} = 610 \text{ colonies}$$

Since the yield of transformed *E. coli* from a single ligation was approximately 1.55×10^5 , the random gene library represents an estimated 254-fold coverage of the genome, thus in theory each *Ct* gene should be represented 254 times in the library:

$$\frac{155,000}{610} = 254x \text{ coverage}$$

4.2.3.5. Scaling up the gene library

Given that the gene library provided sufficient coverage of the *Ct* genome, further bacterial transformations were performed on a larger scale in order to provide sufficient library sample for further experiments. Two ligation reactions were performed using 21fmol vector and 63fmol *Sau3AI*-digested *Ct* DNA followed by the transformation of competent NEB 10- β *E. coli* using the optimised conditions identified previously (Table 4.2). Transformed bacteria were plated across a total of twenty 245 x 245mm LB ampicillin plates and a yield of approximately 46,864 bacterial colonies was obtained across eighteen plates. Although fewer bacterial colonies were obtained (in comparison to the previous 155,000 colonies), the yield was still sufficient to obtain a satisfactory 76x coverage of the genomic library. Therefore, these colonies were scraped from the plates, pooled, and their plasmids extracted by Midiprep to give a total amount of 328 μ g DNA library (65.6ng/ μ l in 5ml volume).

4.2.4. *Ct* genomic library screen

4.2.4.1. Optimisation of yeast transformations

The amplified *Ct* genomic library was transformed into the URA⁻ haploid yeast strain, BHY10, and second into the URA⁻ diploid strain, BHY12, that encode one and two copies of the carboxypeptidase Y (CPY) – invertase (*inv*) fusion gene respectively. Both of these yeast strains enable the assessment of CPY-*inv* secretion by an overlay assay described in section 3.1.8.

Yeast transformations were optimised to determine the necessary amount of genomic library to use in the transformation procedure. Differing amounts of *Ct* genomic library (1.31, 2, 2.25 and 2.5µg) were tested for the transformation of 0.5ml BHY10 at an OD₆₀₀ of approximately 0.7. Yeast transformants were plated onto selective agar plates deficient in uracil and containing fructose as a source of carbon (SC-ura F). We concluded that the transformation of BHY10 with 2.5µg genomic library yielded the maximum number of transformed yeast colonies that were well distributed throughout the plate (Table 4.3). Thus, large-scale yeast transformations were performed to generate 50 plates of transformed yeast that were subsequently assayed for CPY-inv secretion.

Amount of DNA (µg)	Average colony count
1.31	40
2.00	11
2.25	130
2.50	211

Table 4.3 Optimisation of BHY10 yeast transformations. BHY10 was transformed with the specified amount of *Ct* genomic library, cultured on selective SC-ura media and the number of transformed colonies was counted.

4.2.4.2. Assessment of CPY-inv secretion

BHY10 transformed with the *Ct* genomic library were screened for putative T3S chlamydial virulence factors using the PEPSY screen described in section 3.1.8. Following the addition of the glucostat reagent, yeast colonies that formed a brown precipitate were picked, re-streaked and retested for their VPS⁻ phenotype. For identification purposes, each selected clone was assigned a Positively Secreting Colony (PSC) number (e.g. PSC1) and will henceforth be referred to their assigned identification name.

For a number of re-streaked PSCs, the resulting yeast population did not display a consistent VPS⁻ phenotype. Instead, a heterogenous population of both VPS⁺ and VPS⁻ phenotypes was observed. Thus, the re-streaking process was repeated until a homogenous population of yeast displaying a VPS⁻

phenotype was obtained in order to minimise the risk of selecting a colony that displayed a VPS⁻ phenotype due to a random mutation.

The secretion screen was performed four times; one of which was performed in the diploid yeast strain, BHY12, in an attempt to mitigate the high mutation rate observed in the secretion screens using BHY10. Each screen yielded varying numbers of PSCs but several of these were discarded during the re-streaking process due to their inability to maintain the secreting phenotype (Table 4.4).

For PSCs that successfully maintained their VPS⁻ phenotype, two different approaches were undertaken to test whether this phenotype was plasmid-dependent.

Firstly, plasmids were extracted from PSCs and used to transform yeast again to hopefully obtain the same phenotype. Here, plasmids were isolated by phenol:chloroform:isoamylalcohol (25:24:1) extraction and propagated in electrocompetent *E.coli*. Plasmids were isolated, purified and transformed into BHY12. Transformed BHY12 were then assayed for CPY-inv secretion with the assumption that CPY-inv missorting is plasmid-dependent if the VPS⁻ phenotype is again observed.

An alternative method for investigating whether CPY-inv secretion is plasmid-dependent is to cure yeast of their plasmid by growing the PSCs on media containing 5-fluoroorotic acid (5-FOA). In the presence of 5-FOA, yeast harbouring the URA3 gene (the selectable marker in pVT100-U), that encodes orotidine-5-monophosphate decarboxylase, are able to convert 5-FOA into the toxic metabolite 5-fluorouracil (5-FU). 5-FU functions primarily as a thymidylate synthase inhibitor that disrupts thymidine synthesis and hence interferes with DNA replication. Subsequently, yeast clones expressing the URA3 gene are unable to grow on agar plates containing 5-FOA. However, given the toxicity of 5-FU for URA3⁺ yeast, there is a selective advantage for yeast to cure themselves of this plasmid. Thus, the growth of yeast colonies on agar plates containing 5-FOA is indicative of plasmid-cured yeast. These colonies can be picked, re-streaked onto fresh agar plates and tested for CPY-inv secretion. Given that these yeast colonies have been cured of their URA3⁺ plasmid (that

also encodes *Ct* DNA), it can be hypothesised that CPY-inv should no longer be observed if the VPS⁻ phenotype is plasmid-dependent. For all PSCs identified by screening the haploid BHY10 yeast, CPY-inv secretion was still detected following the loss of the plasmid, thus suggesting that the VPS⁻ phenotype was not plasmid-dependent (Table 4.4).

As a result of inconsistencies with the overlay assay, we performed a quantitative assay of CPY-inv secretion when testing the PSCs identified from the fourth screen in BHY12. Principally, the quantitative assay performs in the same way as the qualitative overlay assay, but the assay is carried out in liquid cultures of yeast grown overnight.

Screen	Yeast strain	Colony count	Genome coverage	PSCs obtained	Putative effectors	Plasmid-dependent effectors
1	BHY10	2,000	3x	1	1	0
2	BHY10	47,100	77x	17	3	0
3	BHY10	44,200	72x	24	18	0
4	BHY12	26,300	43x	52	10	5

Table 4.4 Assessment of CPY-inv secretion in library-transformed BHY10 or BHY12.

PSCs were examined for plasmid-dependent CPY-inv secretion.

Of the ten PSCs from the fourth screen that maintained their VPS⁻ phenotypes, plasmid-dependent CPY-inv secretion was detected quantitatively in five PSCs (PSC48, PSC50, PSC54, PSC66 and PSC70) (Figure 4.4). Furthermore, PSC50, PSC66 and PSC72 also demonstrated plasmid-dependent CPY-inv secretion when examined by the re-transformation method (Figure 4.6, Figure 4.7 and Figure 4.9 respectively).

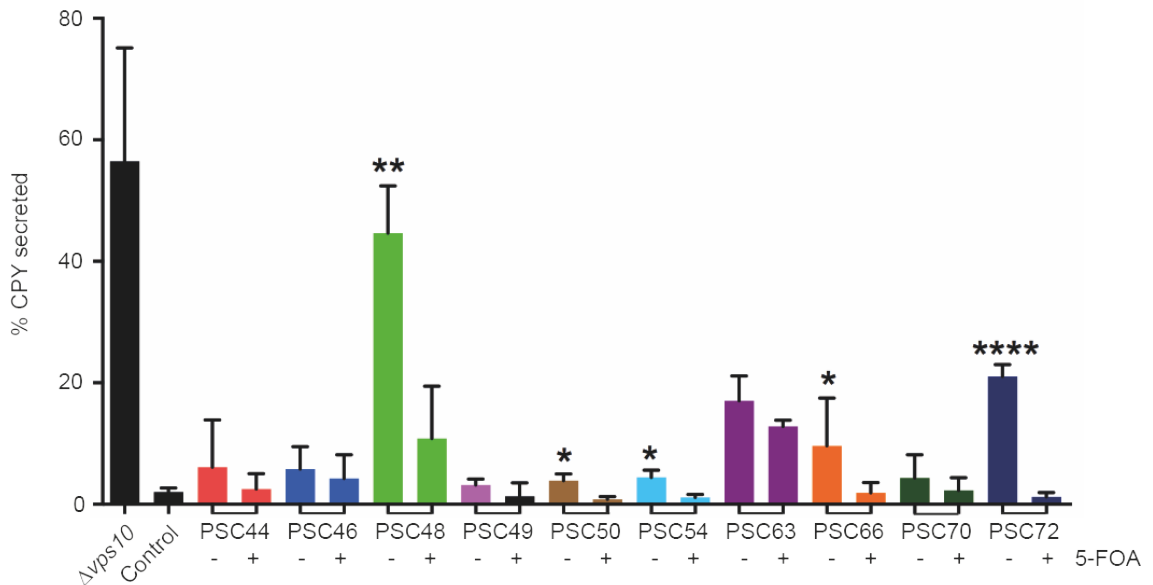


Figure 4.4 CPY-*inv* secretion by PSCs encoding putative *Ct* virulence proteins in the presence and absence of plasmid. A quantitative PEPSY screen was performed on BHY12 with $\Delta vps10$ (positive control) or transformed with pVT100-U (negative control) or all PSC clones that maintained their VPS^- phenotype when re-assayed in the presence or absence of the expression plasmid. Plasmid-cured clones are those + 5-FOA. Data are means + SD; n=2 (PSC44); n=3 (PSC48, 49, 50, 54, 63, 72), n=4 (PSC46, 70), n=7 (PSC66); *P<0.05, **P<0.01, ***P<0.001, ****P<0.0001.

4.2.5. Initial characterisation of PSCs

Each of the five candidates (PSC48, PSC50, PSC54, PSC66 and PSC72) that demonstrated plasmid-dependent CPY-*inv* secretion were sequenced and investigated further to determine the underlying cause of the intracellular trafficking defect observed in yeast. The analysis of each of these five clones is discussed below.

4.2.5.1. PSC48

The plasmid harboured by PSC48 was sequenced to reveal that the MCS encoded a short (83bp) DNA sequence spanning the ends of two genes; neither of which were fully encoded within the library insert. The two partially encoded genes were *BOUR_00272* and *BOUR_00273* (Figure 4.5 A). Interestingly, *BOUR_00272* was previously predicted to be a T3SS effector by the *in silico* prediction program EffectiveT3. However, when the single gene was cloned into

BHY12, no trafficking defect was observed when assayed for CPY-inv secretion (section 3.2.5).

PSC48 displayed a VPS⁻ phenotype when assayed for CPY-inv secretion (Figure 4.5 B). To investigate whether this observed phenotype was plasmid-dependent, PSC48 was cured of its expression plasmid and retested for CPY-inv secretion. In liquid culture, CPY-inv secretion was significantly greater in the plasmid-encoding clone compared to the plasmid-cured clone, thus suggesting that the observed trafficking defect is dependent on the plasmid (Figure 4.5 C). However, when BHY12 was transformed with the isolated plasmid from PSC48 and assayed for CPY-inv secretion, the VPS⁻ phenotype was no longer observed (Figure 4.5 D). This observation implies that the observed phenotype might have been a result of a random mutation.

Given the short *Ct* DNA insert in this clone and the inconsistencies observed when assessing plasmid-dependent CPY-inv secretion, PSC48 was discarded from further investigation.

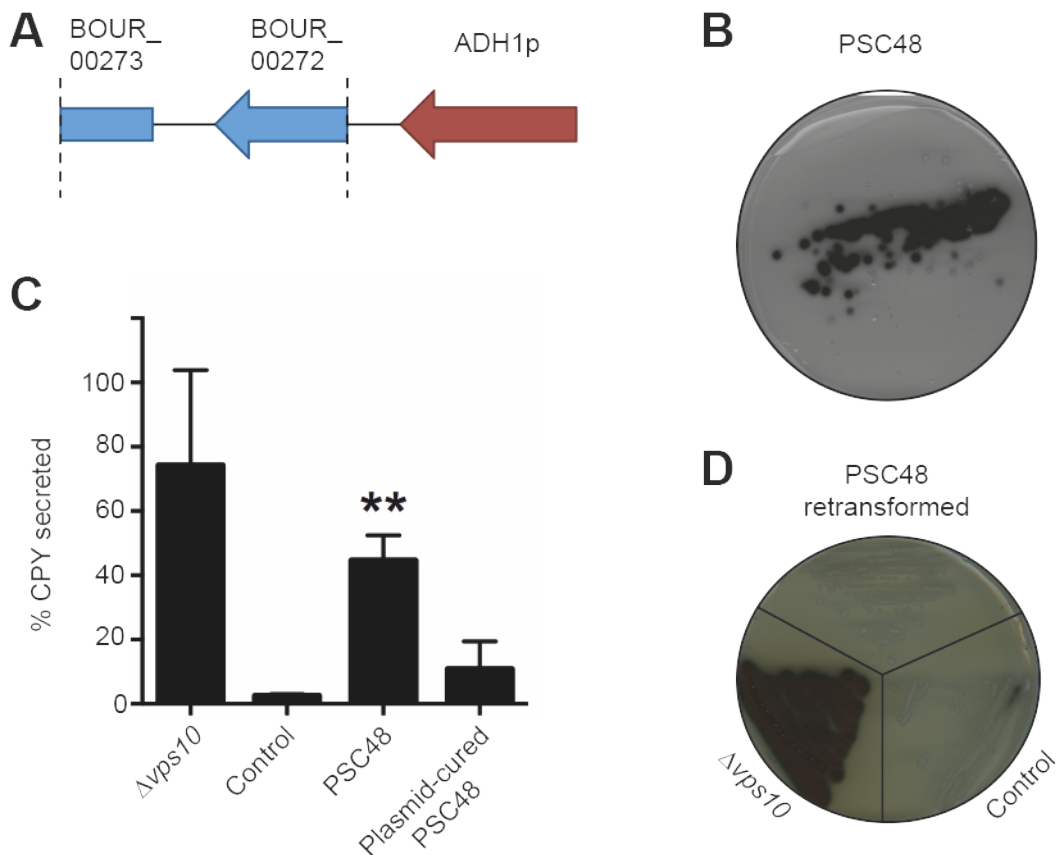


Figure 4.5 CPY-*inv* secretion by PSC48. **A.** PSC48 encodes two partial length genes, *BOUR_00272* and *BOUR_00273*. **B.** PSC48 was re-streaked onto fresh media and PEPY screened. **C.** A quantitative PEPY screen was performed on BHY12 with $\Delta vps10$ (positive control) or transformed with pVT100-U (negative control) or PSC48 in the presence or absence of the expression plasmid. Values for secreted and total invertase activity were measured and the percentage of secreted CPY-*inv* was calculated. Data are means + SD; n=3; **P<0.01. **D.** The plasmid encoded by PSC48 was isolated and transformed into BHY12. Retransformed BHY12 was screened for a *VPS*⁻ phenotype.

4.2.5.2. PSC50

The MCS of PSC50 was sequenced to reveal that this clone encodes one full-length gene (*BOUR_00932*) and two partial length genes (*BOUR_00931* and *BOUR_00933*) (Figure 4.6 A). A search using the Basic Local Alignment Search Tool (BLAST) was performed to determine the functionality of these genes. *BOUR_00931* encodes a glycogen branching protein, while both *BOUR_00932* and *BOUR_00933* encode deubiquitinases. Furthermore, a literature search

revealed that BOUR_00932 shared 99% identity (99.71% similarity) with the chlamydial deubiquitinase, ChlaDUB2, while BOUR_00933 shares 90% identity (97.49% similarity) with ChlaDUB1. Interestingly, BOUR_00933 was predicted to be T3S by the *in silico* prediction program, EffectiveT3, but did not produce a VPS⁻ phenotype when cloned into BHY12 (section 3.2.5).

ChlaDUB1 and ChlaDUB2 are proteases present in most Chlamydia species that possess deubiquitinating and deneddylating activity (Misaghi et al., 2006). Interactions with host targets and the precise functionality of ChlaDUB2 are currently unknown. However, Le Negrate et al. have demonstrated ChlaDUB1 binding to the NFκB inhibitory subunit IκBα thus impairing its ubiquitination and subsequent cytokine-induced degradation (Le Negrate et al., 2008b). This is understood to suppress the activation of the NFκB pathway that would otherwise be induced by pro-inflammatory stimuli.

The VPS⁻ phenotype was observed for PSC50 (Figure 4.6 B) and this phenotype was assessed for plasmid-dependence by firstly curing the yeast of the expression plasmid and assaying for CPY-inv secretion. In liquid culture, there was significantly greater CPY-inv secretion in plasmid-encoding PSC50 compared to the plasmid-cured clones (Figure 4.6 C). Secondly, the plasmid was extracted from PSC50, transformed into BHY12 and tested for CPY-inv secretion to confirm whether membrane trafficking was again perturbed. Re-transformed BHY12 displayed the VPS⁻ phenotype (Figure 4.6 D). Thus, both approaches for testing plasmid-dependence concluded that the observed VPS⁻ phenotype was dependent on plasmid expression and hence PSC50 encodes a *Ct* virulence factor that plays a role in disrupting intracellular membrane trafficking.

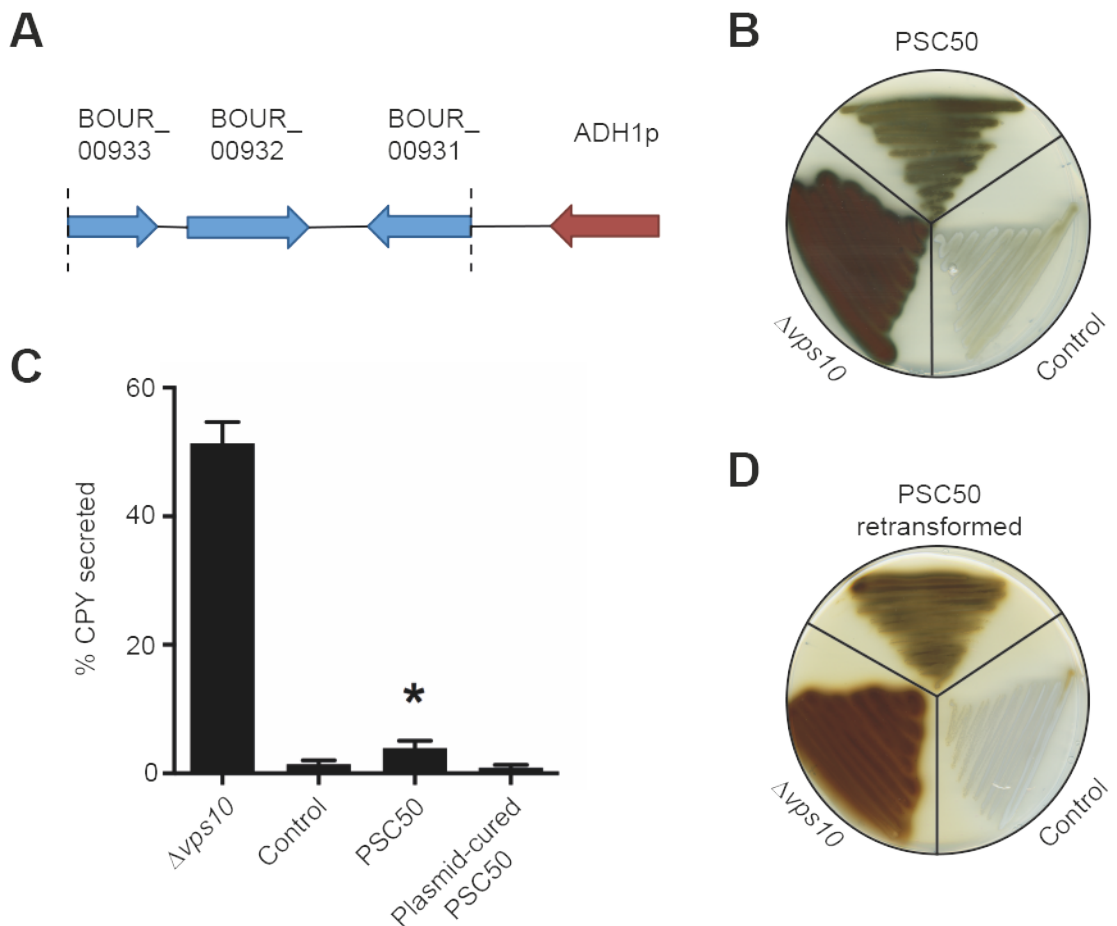


Figure 4.6 CPY-inv secretion by PSC50. **A.** PSC50 encodes one full-length gene, *BOUR_00932*, and two partial-length genes, *BOUR_00931* and *BOUR_00933*. **B.** PSC50 was re-streaked onto fresh media alongside BHY12 with $\Delta vps10$ (positive control) or BHY12 transformed with pVT100-U (negative control) and PEPSY screened. **C.** A quantitative PEPSY screen was performed on plasmid-encoding and plasmid-cured PSC50. Data are means + SD; n=3; *P<0.05. **D.** The plasmid harboured by PSC50 was isolated and transformed into BHY12. Retransformed BHY12 was screened for a VPS⁻ phenotype.

4.2.5.3. PSC66

The MCS of the plasmid harboured by PSC66 was isolated and sequenced to identify the encoded chlamydial genes. Remarkably, the sequencing data revealed that PSC66 encodes two partial length genes that are also encoded by PSC50 (*BOUR_00932* and *BOUR_00933*) (Figure 4.7 A). As mentioned above, both of these genes encode deubiquitinases. Notably, PSC66 does not encode the third gene encoded by PSC50 (*BOUR_00931*) suggesting that this glycogen

branching protein may not play a key role in the disruption of membrane trafficking in yeast.

PSC66 displayed a VPS⁻ phenotype when assayed for CPY-inv secretion (Figure 4.7 B). Plasmid-encoding and plasmid-cured PSC66 was examined for CPY-inv secretion and the plasmid-encoding clone was found to secrete a significantly greater amount of CPY-inv (Figure 4.7 C). Moreover, the expression plasmid harboured by PSC66 was isolated, transformed into BHY12 and tested to confirm whether the VPS⁻ phenotype was observed. This re-transformed BHY12 displayed the VPS⁻ phenotype indicative of a membrane trafficking defect (Figure 4.7 D). Together, these findings imply plasmid-dependent membrane trafficking disruption.

Our assumption that BOUR_00932 and/or BOUR_00933 may be *Ct* virulence factors involved in membrane trafficking disruption was reinforced given that both PSC50 and PSC66 encoded these genes. Notably, full-length *BOUR_00932* was only encoded by PSC50, but not PSC66, and *BOUR_00933* was not encoded as a full-length gene in neither PSC50 nor PSC66. However, these candidates were further investigated to identify which encoded genes were responsible for inducing the membrane trafficking defect (section 4.2.6.1).

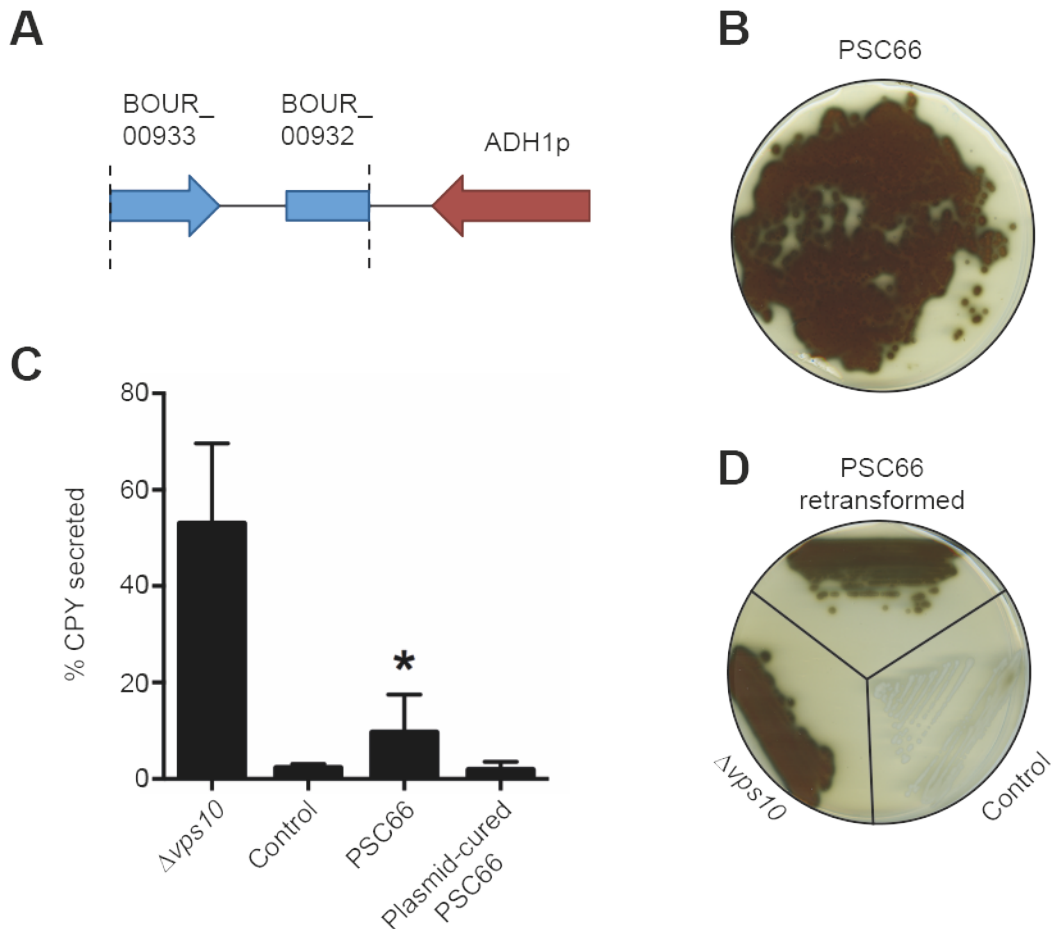


Figure 4.7 CPY-*inv* secretion by PSC66. **A.** PSC66 encodes two partial-length genes, *BOUR_00932* and *BOUR_00933*, both of which are also encoded by PSC50. **B.** PSC66 was re-streaked onto fresh media and PEPY screened. **C.** A quantitative PEPY screen was performed on plasmid-encoding and plasmid-cured PSC66. Data are means + SD; n=7; *P<0.05. **D.** The plasmid harboured by PSC66 was isolated and transformed into BHY12. Retransformed BHY12 was screened for a VPS⁻ phenotype.

4.2.5.4. PSC54

The plasmid encoded by PSC54 was isolated and sequenced. Sequencing revealed the MCS encoded three full-length genes (*BOUR_000926*, *BOUR_00927*, *BOUR_00928*) and two partial length genes (*BOUR_00925* and *BOUR_00929*) (Figure 4.8 A). A BLAST search was performed to identify the functionality of these genes and we found that *BOUR_00925* encodes a T3SS chaperone protein while *BOUR_00926* and *BOUR_00928* are currently documented as uncharacterised proteins. Furthermore, *BOUR_00927* encodes a tRNA and *BOUR_00929* encodes a site-specific tyrosine recombinase.

Interestingly, BOUR_00926 was predicted to be T3S by the *in silico* prediction program, EffectiveT3, but did not display a VPS⁻ phenotype when PEPSY screened (CROSS REF AT END).

PSC54 displayed a VPS⁻ phenotype when PEPSY screened as yeast colonies on agar media and in liquid culture (Figure 4.8 B and C respectively). The expression plasmid of PSC54 was isolated and retransformed into BHY12 to determine whether the membrane trafficking defect was plasmid-dependent. Plates of retransformed BHY12 maintained their VPS⁻ phenotype. Surprisingly, however, when retransformed yeast colonies were subsequently restreaked onto a fresh agar plate alongside $\Delta vps10$ and empty vector controls and retested for CPY-inv secretion, the VPS⁻ phenotype was no longer detected (Figure 4.8 D).

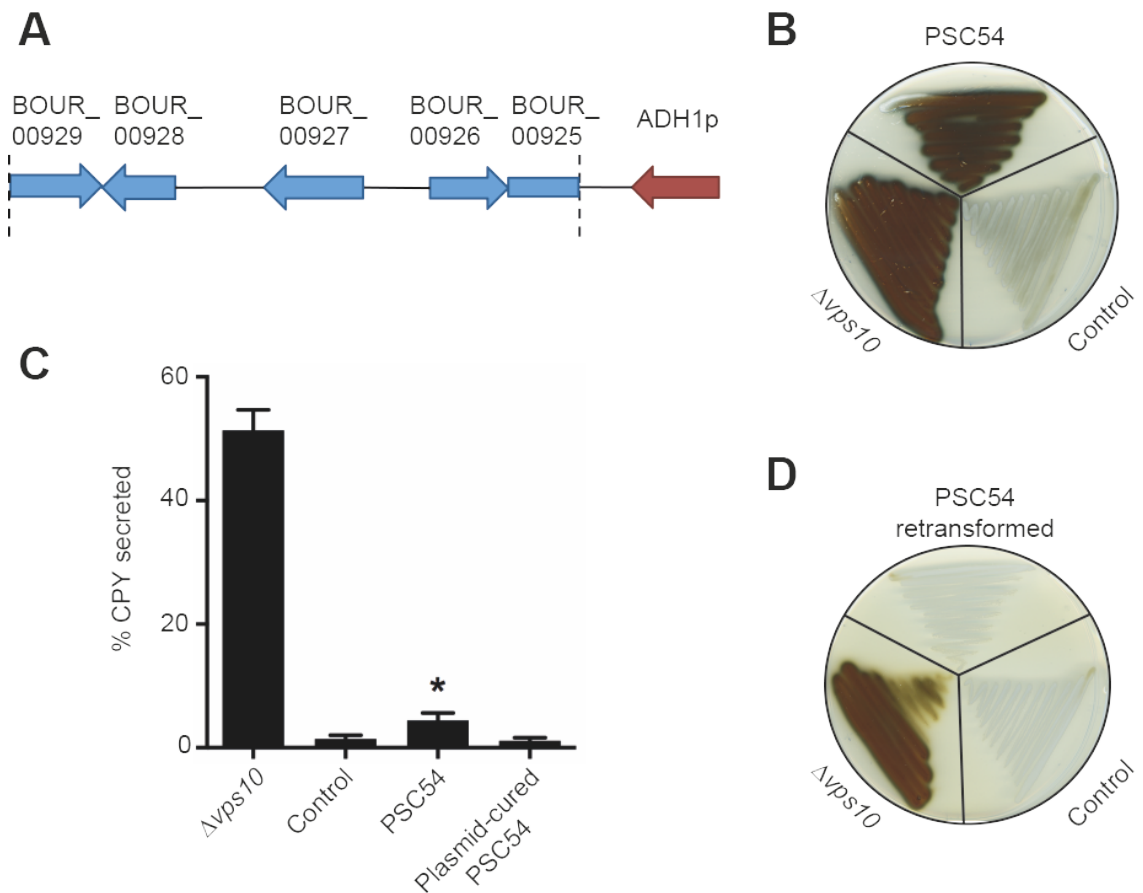


Figure 4.8 CPY-inv secretion by PSC54. **A.** PSC54 encodes five putative chlamydial virulence genes, *BOUR_00925-9*. **B.** PSC54 was re-streaked onto fresh media alongside BH12 harbouring $\Delta vps10$ (positive control) or transformed with pVT100-U (negative control) and PEPSY screened. **C.** A quantitative PEPSY screen was performed on plasmid-encoding and plasmid-cured PSC54. Data are means + SD; n=3; *P<0.05. **D.** The plasmid harboured by PSC54 was isolated and transformed into BH12. Retransformed BH12 was screened for a VPS⁻ phenotype.

4.2.5.5. PSC72

PSC72 consistently displayed a strong VPS⁻ phenotype when assayed for membrane trafficking defects (Figure 4.9 A). To examine whether this phenotype was plasmid-dependent, PSC72 was cured of the plasmid and assayed for CPY-inv secretion. Plasmid-encoding PSC72 consistently secreted significantly greater quantities of CPY-inv than the plasmid-cured strain when assayed both qualitatively and quantitatively (Figure 4.9 A & B). Furthermore,

when the plasmid encoded by PSC72 was isolated and transformed into wild-type BHY12, the VPS⁻ phenotype was again observed (Figure 4.9 C), thus suggesting that the trafficking defect is dependent upon plasmid expression.

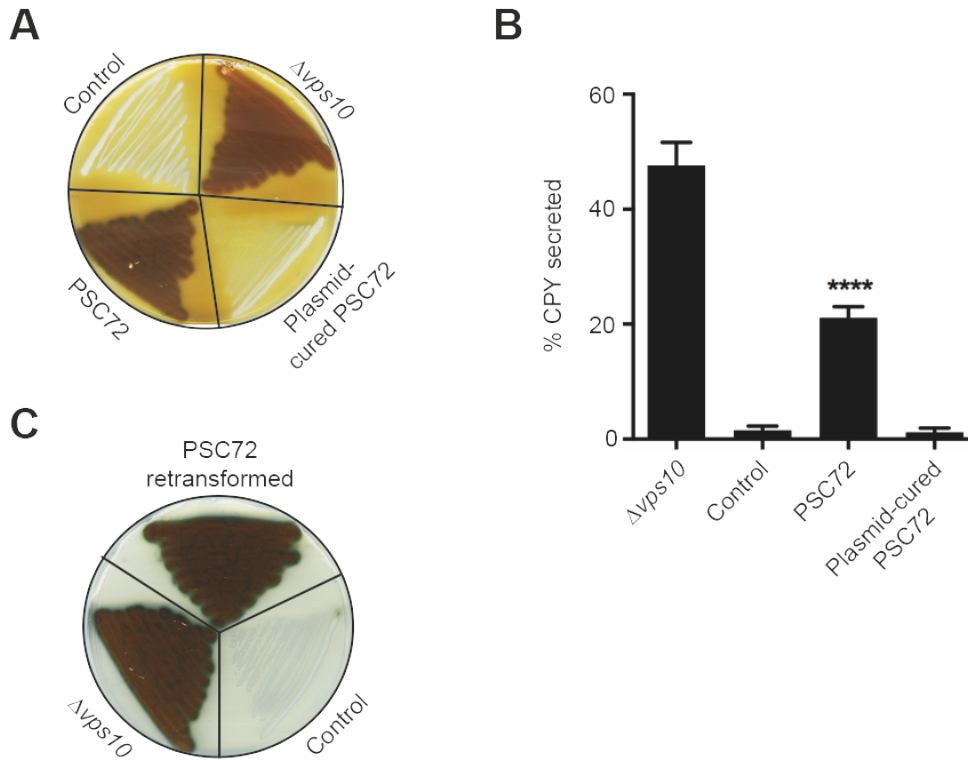


Figure 4.9 CPY-*inv* secretion in PSC72. **A.** Plasmid-encoding and plasmid-cured PSC72 was re-streaked onto fresh media alongside BHY12 harbouring $\Delta vps10$ (positive control) or transformed with pVT100-U (negative control) and PEPSY screened. **B.** A quantitative PEPSY screen was performed on plasmid-encoding and plasmid-cured PSC72. Data are means + SD; n=3; *P<0.05. **C.** The plasmid harboured by PSC72 was isolated and transformed into BHY12. Retransformed BHY12 was screened for a VPS⁻ phenotype.

Given that PSC72 likely encoded a putative *Ct* virulence factor of interest, the plasmid was isolated for sequencing. However, several attempts to sequence this plasmid by Sanger sequencing from three separate sequencing organisations (Source Bioscience, GATC, University of York Genomics Laboratory) failed to produce a sequencing trace.

To overcome these sequencing difficulties, several different primers that target alternative sites on the expression plasmid were designed and used in the sequencing reactions. For example, the restriction enzyme, *Pst*I, can linearise

pVT100-U at a site upstream from the *Bam*HI restriction site where the *Ct* DNA insert had been ligated. Thus, primers were designed around the *Pst*I restriction site and used for sequencing the *Ct* DNA insert. Unfortunately, sequencing reactions using these primers also failed to produce a sequencing trace.

Source Bioscience offers an additional service to include dGTP chemistry for sequencing reactions. This technology is particularly useful for resolving sequencing problems, such as G-C rich templates, hairpin structures, repetitive regions and troublesome sequences. Given the difficulties in sequencing the MCS of PSC72, we used dGTP chemistry in an attempt to overcome the difficulties previously encountered. However, again a sequencing trace was not successfully generated.

An alternative approach to sequencing was undertaken whereby the encoded plasmid was linearised in several separate restriction enzyme digests in order to isolate the *Ct* DNA insert for amplification by PCR and sequencing. Restriction enzyme digests were performed using *Dra*I, *Xho*I, *Pst*I, *Pvu*II and *Hind*III, but subsequent PCR failed to amplify the isolated DNA.

Furthermore, we previously observed that the restriction enzyme, *Not*I, is able to linearise the plasmid encoding PSC72 but not empty vector, implying that there is a *Not*I restriction site within the *Ct* DNA insert. Therefore, we linearised the PSC72 plasmid with *Not*I assuming that the linearization might unravel any secondary structural features that cause sequencing difficulties. However, again the sequencing reaction failed to produce a viable trace.

Moreover, a step-by-step sequencing approach was also undertaken whereby the plasmid was sequenced in stages until the troublesome sequence was reached and the sequencing reaction failed. We reasoned that as PSC72 was able to grow on SC-ura selective media, the plasmid must still harbour the *URA3* gene. Therefore, a primer targeting the *URA3* gene sequence was designed and used for sequencing a section of the plasmid. This sequencing reaction was successful, so using this sequence trace another primer was designed targeting the terminating region of the plasmid that had previously been sequenced. This approach was undertaken continuously until a

sequencing trace could no longer be generated. By this method, we determined that the sequencing reaction fails at approximately 350bp downstream of the *Bam*HI restriction site where *Ct* DNA was ligated.

Finally, with the help of Dr James Chong, we used MinIon technology (Oxford Nanopore) to sequence the DNA insert. This method uses nanopore sensing to measure ionic current when a single strand of DNA is passed through a nanopore. Individual bases can be identified according to their characteristic disruption in current as the DNA strand passes through the pore. Remarkably, PSC72 was successfully sequenced using this technology, but unfortunately the MCS insert contained the *S. cerevisiae* gene, *Aep2*. *Aep2p* is a yeast mitochondrial protein believed to be involved in the translation of the mitochondrial OLI1 mRNA. This unexpected sequencing result may be a result of contaminant yeast DNA that the plasmid encodes or a genetic recombination event may have occurred. Regardless, PSC72 was subsequently excluded from further investigation.

4.2.6. Investigation of the genes responsible for trafficking disruption

4.2.6.1. BOUR_00931-3 (PSC50)

The genes encoded by PSC50 were individually cloned into BHY12 as full-length genes in order to investigate which gene(s) is responsible for disrupting intracellular membrane trafficking in yeast and thus deduce putative secreted virulence factors for further investigation (Figure 4.10 A).

BOUR_00932 and *BOUR_00933* were successfully cloned into BHY12, but we faced difficulties when attempting to clone *BOUR_00931*. We were able to amplify *BOUR_00931* from *Ct* genomic DNA, ligate the gene into pVT100-U and transform this vector into competent *E.coli*. A colony PCR was performed to assess whether competent *E.coli* had been transformed with the *BOUR_00931*-encoding plasmid. However, no amplification of the gene occurred following PCR, thus implying that either ligation of *BOUR_00931* into plasmid vector or bacterial transformation had not been successful.

To mitigate experimental error, bacterial transformation was performed twice, but, again, amplification of *BOUR_00931* was not observed for any of the transformed bacterial colonies examined by colony PCR. Furthermore, two different primer pairs were used for gene amplification, but both failed to produce an amplification product. Thus, given the difficulties in cloning *BOUR_00931*, together with its absence in PSC66, this gene was discarded from further investigation.

BOUR_00932 and *BOUR_00933* were successfully cloned individually and as full-length genes into BHY12 and their effect on intracellular membrane trafficking disruption was assessed by a qualitative (Figure 4.10 B & C) and quantitative secretory assays (Figure 4.10 D). The assay was performed several times with differing results whereby the VPS⁻ phenotype was occasionally observed but this observation was not consistent. Thus, these contradictory outcomes placed doubt on whether membrane trafficking had been disrupted in BHY12.

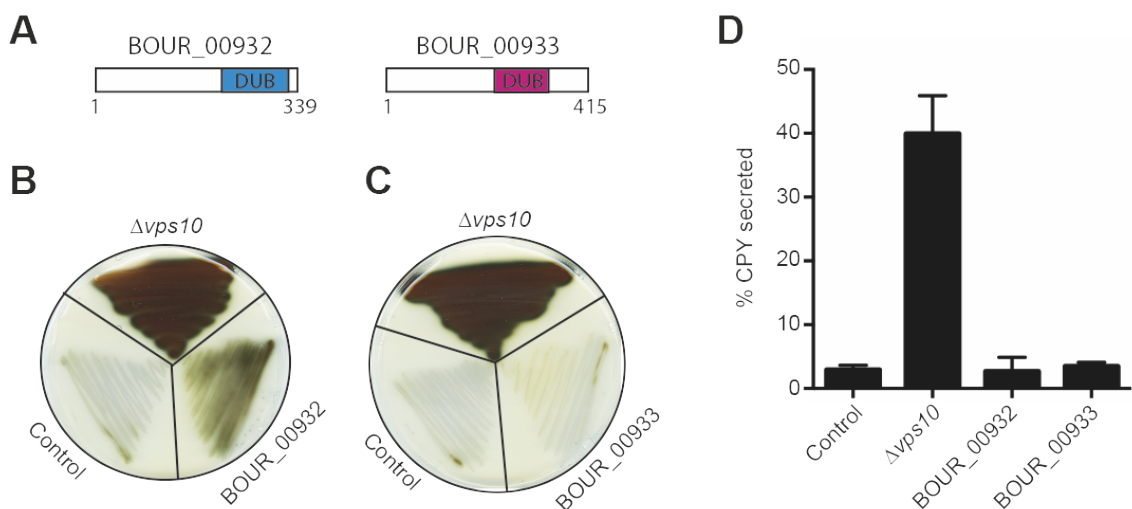


Figure 4.10 CPY-inv secretion by BHY12 encoding *BOUR_00932* or *BOUR_00933*. CPY-inv secretion of BHY12 encoding full-length *BOUR_00932* (339 aa) or *BOUR_00933* (415 aa) (A) was assessed by PEPY screening (B and C respectively). C. A quantitative PEPY screen was performed on BHY12 expressing full-length *BOUR_00932* or *BOUR_00933*. Data are means + SD; n=4. Aa = amino acids.

Despite the inconclusive secretory overlay assay results, we sought to assess whether the expression of both *BOUR_00932* and *BOUR_00933* was required

for membrane trafficking disruption in BHY12 given that both of these genes are encoded by PSC50 and PSC66. Thus, *BOUR_00932* and *BOUR_00933* were cloned into BHY12 as two consecutive full-length genes and the transformed yeast was assayed for CPY-inv secretion (Figure 4.11 A). The VPS⁻ phenotype was not observed when assayed qualitatively (Figure 4.11 B) or quantitatively (Figure 4.11 C).

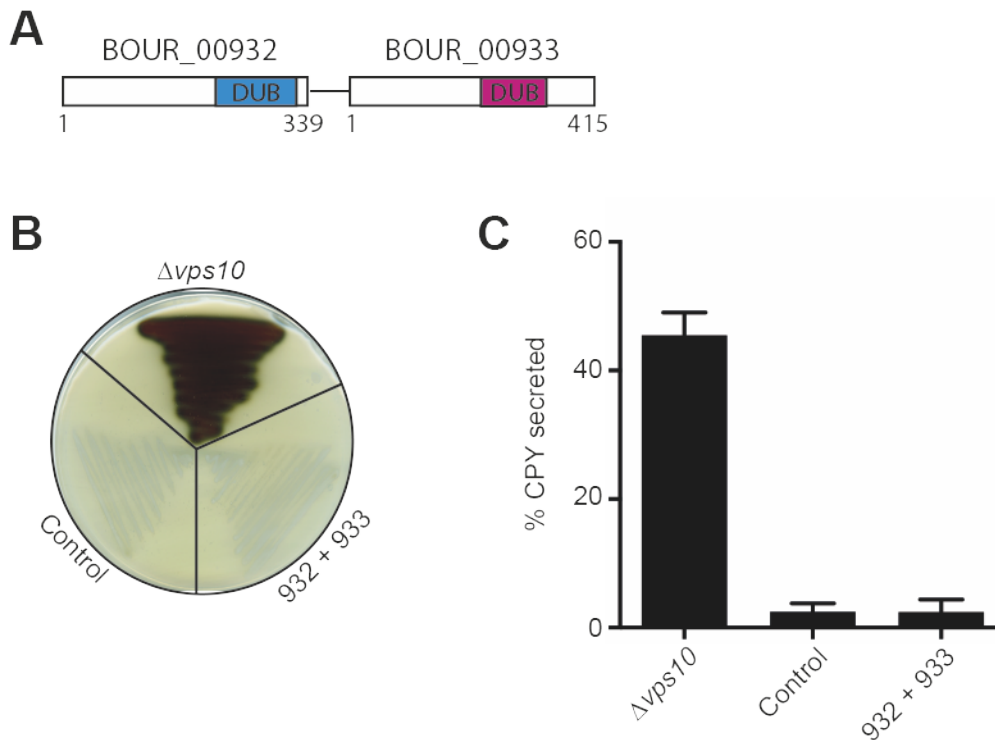


Figure 4.11 CPY-inv secretion by BHY12 encoding *BOUR_00932* and *BOUR_00933*. CPY-inv secretion of BHY12 encoding full-length *BOUR_00932* and *BOUR_00933* (A) was assessed by PEPYSY screening (B). A quantitative PEPYSY screen was performed on BHY12 expressing full-length *BOUR_00932* and *BOUR_00933* (C). Data are means + SD; n=3.

Following this, we reasoned that the upstream and downstream intragenic regions might be required for the promotion of gene expression. Therefore, *BOUR_00932* and *BOUR_00933* were individually cloned into BHY12 together with their respective upstream and downstream untranslated regions (UTR) regions (Figure 4.12 A). Cloning of *BOUR_00933* with its upstream and downstream UTR was unsuccessful, thus only the upstream UTR was cloned with the gene instead. When assayed for CPY-inv secretion, the VPS⁻

phenotype was not observed for either cloned gene regions tested (Figure 4.12 B and C).

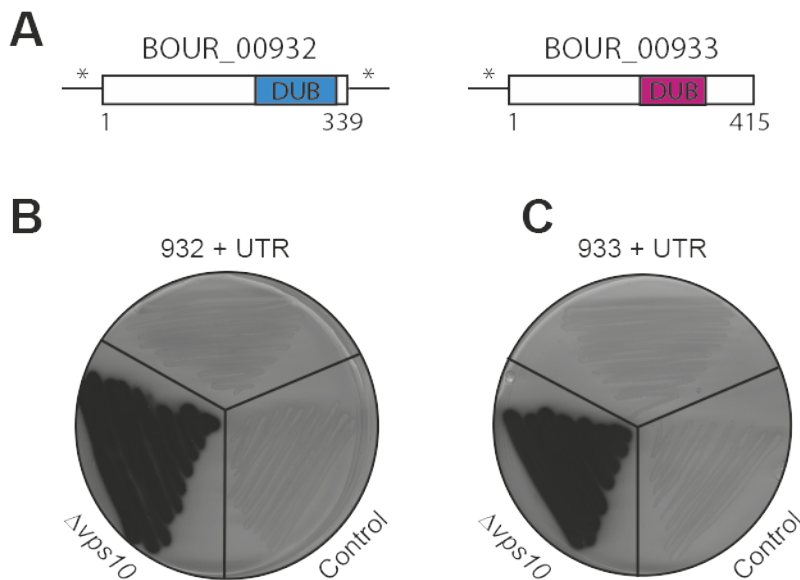


Figure 4.12 CPY-inv secretion by BHY12 encoding *BOUR_00932* or *BOUR_00933* with their intragenic regions. CPY-inv secretion of BHY12 encoding full-length *BOUR_00932* or *BOUR_00933* and their upstream and downstream or upstream UTR respectively (**A**) was assessed by PEPSY screening (**B** and **C** respectively). * = UTR.

Furthermore, given that *BOUR_00932* functions as a deubiquitinase enzyme, we sought to determine whether the catalytic deubiquitinase (DUB) domain of *BOUR_00932* alone was sufficient for disrupting intracellular membrane trafficking in BHY12. Interestingly, the *VPS*⁻ phenotype was observed in BHY12 transformed with full-length *BOUR_00932*, but not when the DUB domain was cloned in isolation (Figure 4.13 A).

Moreover, although *BOUR_00933* also functions as a deubiquitinase enzyme, the gene is not fully encoded by either PSC50 or PSC66. Approximately 15% of *BOUR_00933* is not encoded by either of these clones and this non-encoded region comprises approximately 20% of the catalytic DUB domain. Hence, the *BOUR_00933* gene fragment encoded by PSC50 and PSC66 was cloned into BHY12 to investigate whether this sequence alone was sufficient to disrupt intracellular membrane trafficking. Strikingly, when assayed for CPY-inv secretion, yeast transformed with the *BOUR_00933* gene fragment displayed

the VPS⁻ phenotype that is indicative of membrane trafficking disruption (Figure 4.13 B).

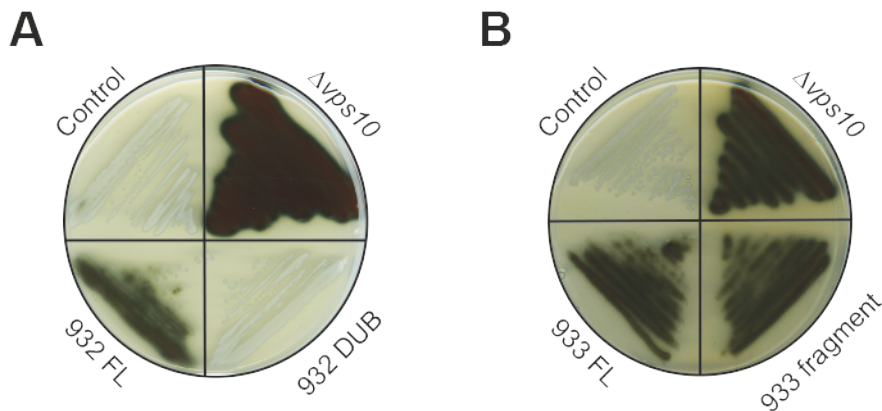


Figure 4.13 CPY-inv secretion by BHY12 encoding the catalytic DUB domain of BOUR_00932 or the PSC50-encoded gene fragment of BOUR_00933 fragment. A. CPY-inv secretion of BHY12 encoding full-length *BOUR_00932* or the catalytic DUB domain of *BOUR_00932* was assessed by PEPSY screening. **B.** CPY-inv secretion of BHY12 encoding full-length *BOUR_00933* or the 771bp fragment of *BOUR_00933* that was encoded by PSC50 was assessed by PEPSY screening. FL = Full Length.

4.2.6.2. BOUR_00925-9 (PSC54)

The five genes encoded by PSC54 were individually cloned into BHY12 to determine which gene(s) is responsible for disrupting intracellular membrane trafficking. Yeast encoding *BOUR_00925*, *BOUR_00926*, *BOUR_00927*, *BOUR_00928* or *BOUR_00929* were assayed for CPY-inv secretion, but none displayed a VPS⁻ phenotype (Figure 4.14).

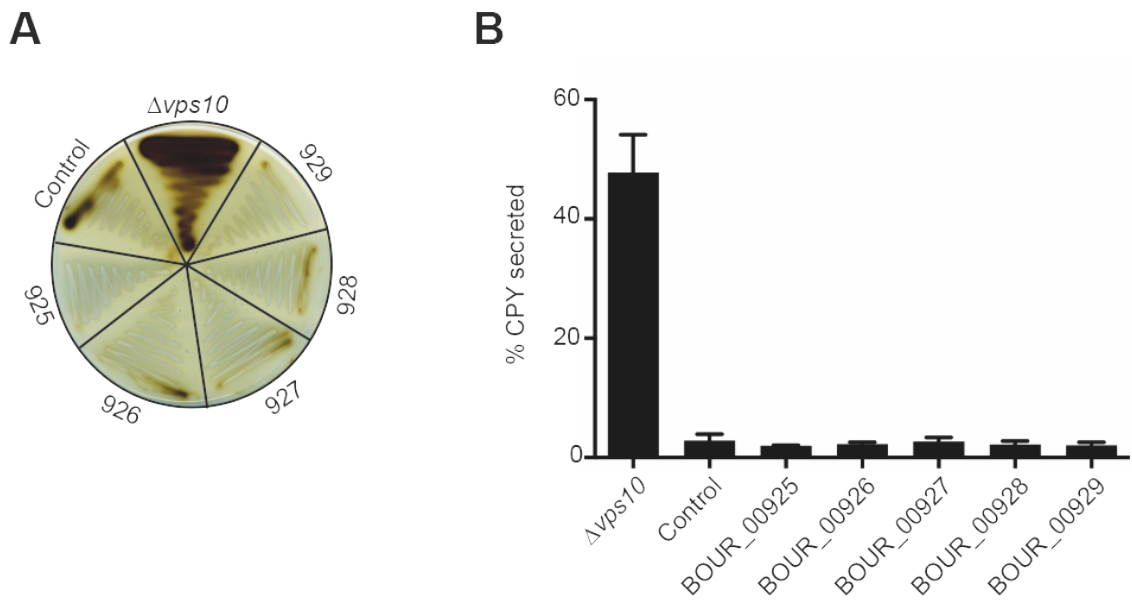


Figure 4.14 CPY-inv secretion by BHY12 encoding each of the individual full-length PSC54 genes. **A.** CPY-inv secretion of BHY12 encoding full-length PSC54 genes was assessed by PEPSY screening on agar media (**A**) or liquid culture (**B**). Data are means + SD; n=3.

We reasoned that some of the genes encoded by PSC54 might require the expression of consecutive genes to disrupt intracellular membrane trafficking. Thus, a series of different yeast clones were generated that encoded various combinations of the five consecutive genes encoded by PSC54. Transformed BHY12 were assayed for CPY-inv secretion, but none of the transformants displayed the VPS⁻ phenotype (Figure 4.15).

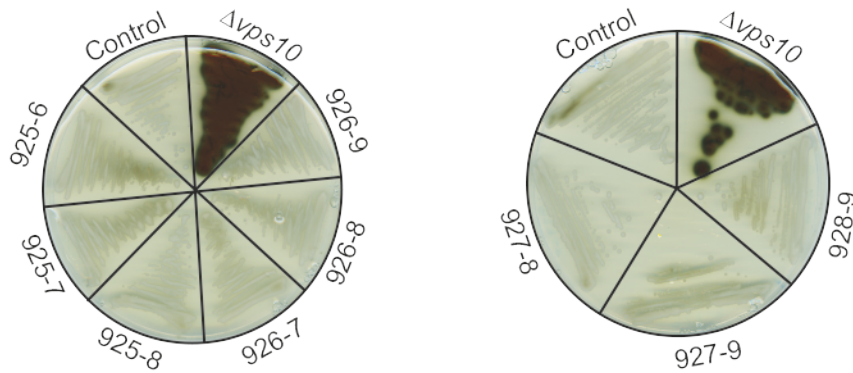
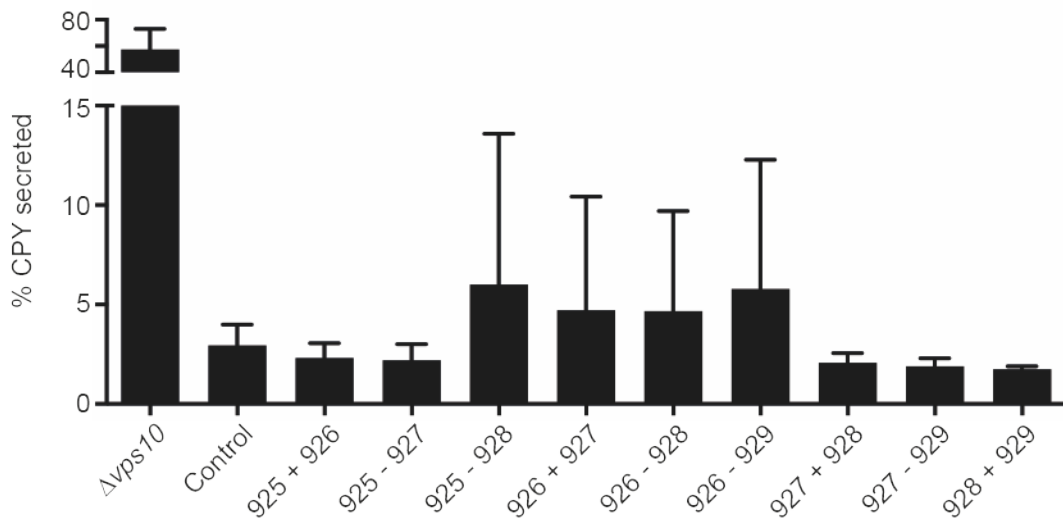
A**B**

Figure 4.15 CPY-inv secretion of BHY12 encoding gene combinations of PSC54 genes.

CPY-inv secretion of BHY12 encoding the specified gene combinations of PSC54 genes was assayed by PEPSY screening on agar media (A) or in liquid culture (B). Data are means + SD; n=3.

4.2.7. Visualisation of yeast vacuoles

The intracellular effects of PSC50 or PSC54 on yeast vacuolar membranes were visualised using the lipophilic styryl dye, N-(3-triethylammoniumpropyl)-4-(6)-4-(diethylamino) phenyl) hexatrienyl) pyridium dibromide (FM4-64). FM4-64 becomes incorporated into membranes and can be pulse-chased into the vacuolar membrane to observe vacuolar morphology.

A large collection of *S. cerevisiae* vacuolar protein sorting (*vps*) mutants that exhibit defects in the sorting and processing of several vacuolar hydrolases is available (Banta et al., 1988). These mutants have been assigned to multiple distinct classes (Class A-F) according to their effect on vacuolar morphology (Raymond et al., 1992). The characteristic vacuolar morphologies induced by the *vps* mutants are summarised in Table 4.5.

Class	Vacuolar morphology
A	Vacuoles are similar to those of WT cells
B	Fragmented vacuoles that are either clustered in one region of the cell or randomly dispersed throughout the cell
C	Lack of coherent vacuoles
D	Defects in vacuolar inheritance and acidification
E	Presence of a pre-vacuolar-like organelle
F	A large central vacuole surrounded by smaller vacuole-like compartments

Table 4.5 Vacuolar morphologies induced by *vps* mutants. *S. cerevisiae* *vps* mutants are assigned to distinct classes depending upon their effects on vacuoles.

To characterise the chlamydial clones, a selection of representative *vps* mutants from each of the six *vps* mutant classes was stained with FM4-64 and their vacuolar morphologies were compared to PSC50 and PSC54. The selected *vps* mutants were $\Delta vps38$, $\Delta vps17$, $\Delta vps16$, $\Delta vps9$, $\Delta vps36$ and $\Delta vps1$ and these are representative of classes A-F respectively. Given that these *vps* mutants have been generated in the yeast strain BY4741, we transformed wild-type BY4741 with pVT100-U (empty vector control) and the plasmids isolated from PSC50 or PSC54 to enable a fair comparison between controls and *vps* mutants.

As expected, each of the *vps* mutant yeast displayed their characteristic vacuolar morphologies (Figure 4.16). Visualisation of PSC50 and PSC54 vacuoles revealed that most vacuoles (>90%) appeared to be characteristic of either wild-type or a class A *vps* mutant. Occasionally, some vacuoles appeared

fragmented (Class B; 5%) or missing altogether (Class C; 3%), however the large majority studied were characteristic of wild-type vacuoles.

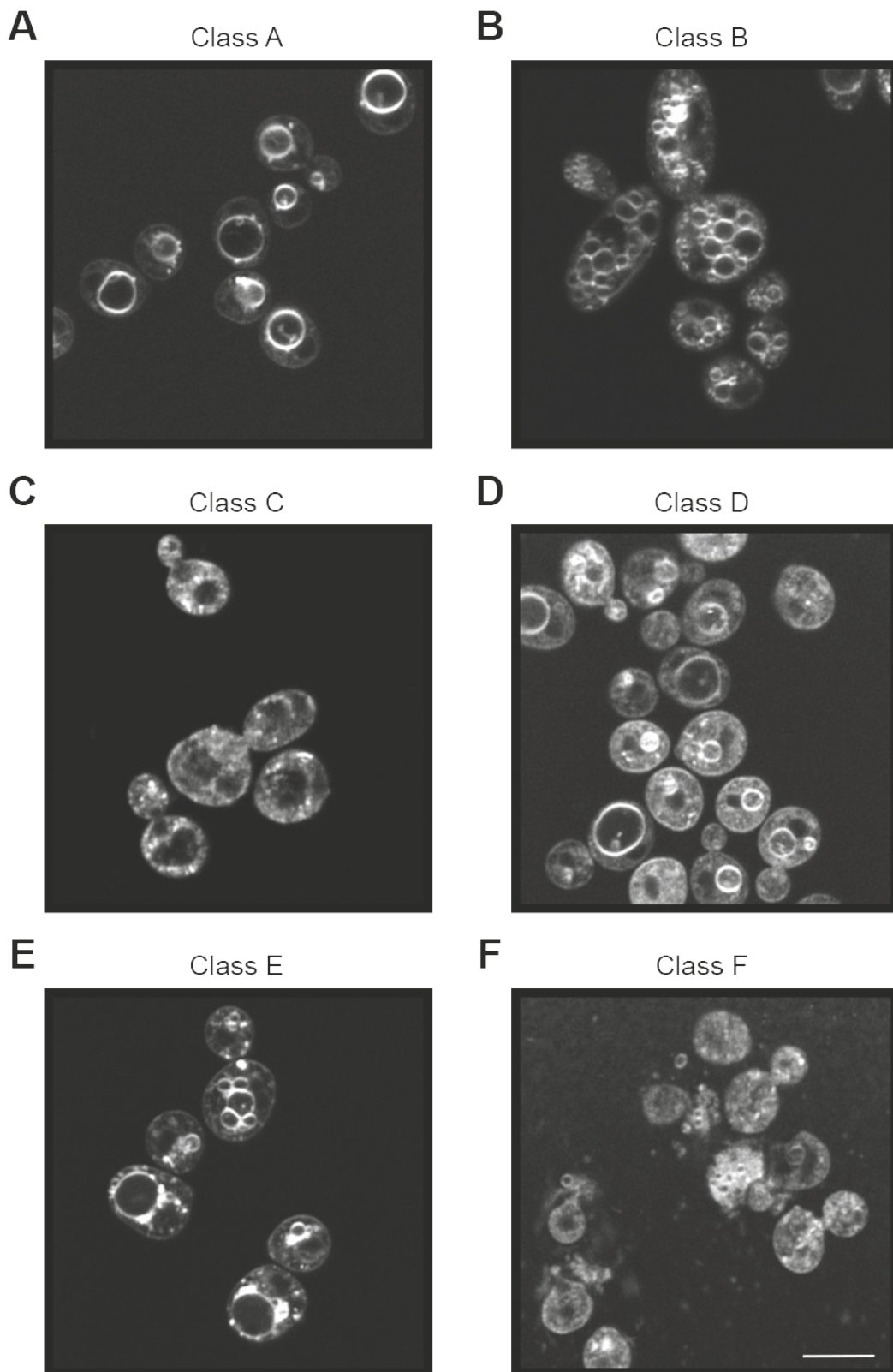


Figure 4.16 Vacuolar phenotypes induced by BY4741 *vps* mutants. Overnight cultures of BY4741 mutant classes A-F were labelled using 40 μ M FM4-64. Genetic knockouts of *vps38* (A), *vps16* (B), *vps16* (C), *vps9* (D), *vps36* (E) or *vps1* (F) represented classes A-F respectively. Cells were visualised by fluorescence microscopy. Scale bar = 5 μ m.

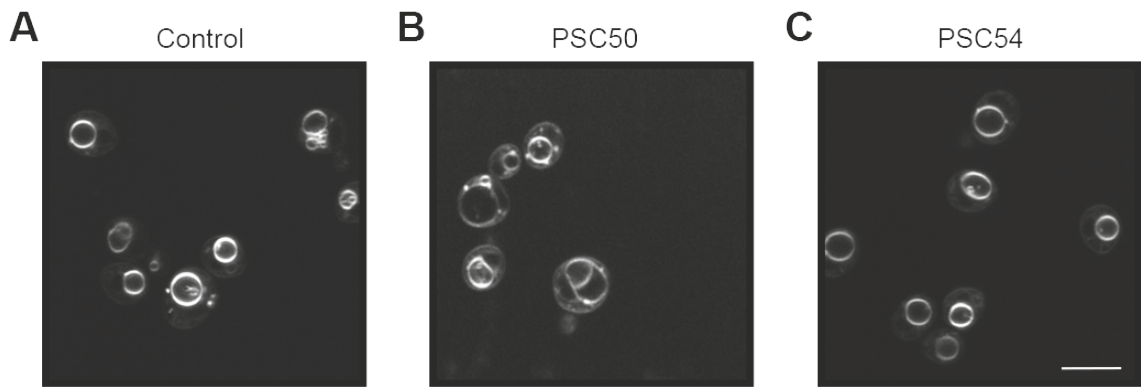


Figure 4.17 Vacuolar phenotypes induced by PSC50 or PSC54. BY4741 was transformed with empty vector (A), PSC50 (B) or PSC54 (C) and vacuoles were labelled with 40 μ M FM4-64. Cells were visualised using fluorescence microscopy. Scale bar = 5 μ m.

4.2.8. Examination of CPY precursors

CPY initially encompasses an amino terminal endoplasmic reticulum (ER) signal sequence that is cleaved upon entry into the ER, resulting in a 67kDa CPY precursor. Once this precursor is trafficked to the Golgi, modifications to the carbohydrate moieties increase the molecular weight to 69kDa. Eventually the proCPY protein is sorted away from soluble proteins destined for secretion and is instead delivered to the vacuole, where vacuolar endopeptidases process and cleave the precursor into the active 61kDa CPY form.

As CPY undergoes modification and processing steps that result in differing molecular weights throughout the maturation process, we sought to identify which CPY precursor was secreted by yeast transformed with *BOUR_00932* or *BOUR_00933* during the secretion assay. We reasoned that by immunoblotting for CPY we could determine which CPY precursor was secreted and thereby predict the intracellular trafficking step where membrane trafficking becomes perturbed.

Overnight cultures of control and *BOUR_00932*- or *BOUR_00933*-transformed BHY12 were pelleted and the supernatant was collected for immunoblotting to determine which CPY precursors were secreted. Additionally, a yeast cell lysate was generated using the pelleted yeast to examine which CPY precursor remained intracellularly.

Unsurprisingly, no mature vacuolar CPY was detected in the secreted sample for the $\Delta vps10$ BHY12 control and only relatively small amounts were detected intracellularly. Given that this positive control is defective in the expression of the CPY receptor, VPS10, the lack of mature vacuolar CPY is unsurprising given the inability of this yeast mutant to transport CPY to the vacuole.

Notably, BHY12 transformed with *BOUR_00933* demonstrated reduced vacuolar CPY in yeast lysates compared to the negative control, suggesting that there has been disruption to the normal trafficking of this enzyme (Figure 4.18). BHY12 expressing *BOUR_00932* did not appear to harbour or secrete noticeably different levels of CPY compared to the negative control (Figure 4.18).

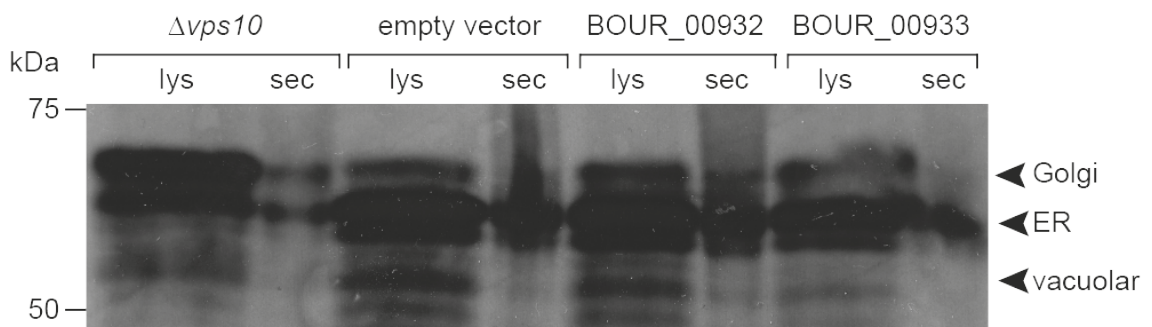


Figure 4.18 Assessment of CPY precursors in BHY12 expressing *BOUR_00932* or *BOUR_00933*. An overnight culture of BHY12 harbouring $\Delta vps10$ (positive control) or transformed with pVT100-U (negative control), *BOUR_00932* or *BOUR_00933* was prepared. For lysate samples, protein extracts were generated using TWIRL buffer. For secreted samples, overnight cultures were pelleted and the supernatant collected for SDS-PAGE gel electrophoresis. Precursor and mature CPY were analysed by immunoblot using anti-CPY antibody. Lys = lysate. Sec = secreted.

4.3. Discussion

4.3.1. Generation of a *Ct* genomic library

Ct genomic libraries have previously been generated to further understand the infection process, but these libraries have been generated using DNA extracted from EBs of the *Ct* LGV strain, L2. Thus, to my knowledge, at the time of our study, this is the first reported generation of a *Ct* E/Bour genomic library.

Goodall *et al.* have previously generated a *Ct* serovar L2 genomic library for the identification of *Ct* antigens that are recognised by human CD4⁺ T lymphocytes (Goodall *et al.*, 2001). They propagated *Ct* in HeLa cells and EBs were purified by a urografin density gradient. The genomic library was prepared by digesting the isolated L2 DNA with *Sau3AI* and DNA fragments of 1-4kb were then isolated for ligation into a pTrcHisC vector and subsequent transformation into *E.coli*.

Furthermore, Tipples and McClarty (1995) have also reported the generation of a *Ct* L2 expression library in pUC19. *Ct* L2 was propagated in mouse L cells in a suspension culture and EBs were purified through a renografin density gradient. A library was prepared by partially digesting genomic DNA with *HindIII* and fragments of size 2-4kb were then excised for ligation into pUC19.

Thus, we reasoned that the generation and PEPSY screening of a *Ct* genomic library, albeit using an alternative serovar, would be a feasible and effective method by which to identify virulence factors.

4.3.2. Screening the *Ct* genomic library

Using the *Ct* library generated in this study, a total of 610 colonies needed to be screened in order to cover the entire *Ct* E/Bour genome once. The PEPSY screen was performed a total of four times. Initially, the library was expressed in the haploid yeast strain, BHY10, but we later transitioned to the diploid yeast strain, BHY12, in the fourth screen. We used BHY10 initially with the justification that any yeast clones secreting CPY-*inv* at low levels would be more easily identifiable in a haploid yeast strain. However, after the PEPSY

screen had been performed in BHY10 three times, it became evident that there was a high mutation rate because all of the PSCs initially identified were discarded as their VPS⁻ phenotypes were not deemed to be plasmid-dependent.

Given that none of the PSCs that were initially identified displayed a plasmid-dependent VPS⁻ phenotype, we transitioned to using the diploid BHY12 yeast strain in an attempt to mitigate the high mutation rate previously observed. Any mutations arising in BHY10 that result in the disruption of CPY-inv trafficking would, in theory, be observed phenotypically because complementation by another allele cannot occur. Thus, we reasoned that if any given mutation were recessive, an additional mutated allele would be required for the mutation to be observed phenotypically in the diploid yeast strain, BHY12. The use of this alternative yeast strain may, therefore, help to mitigate the high mutation rate we observed in BHY10.

Thus, in the final PEPSY screen the *Ct* genomic library was expressed in diploid BHY12 yeast. In this screen, approximately 26,300 yeast colonies were assayed for CPY-inv secretion. This equates to approximately 43x library coverage and thus an extensive screen of the *Ct* genome was performed.

A greater number of PSCs were identified when BHY12 was PEPSY screened. However, approximately only 10% of the initially identified PSCs were found to consistently produce a plasmid-dependent VPS⁻ phenotype. Moreover, although there had been substantial coverage of the *Ct* genome, the number of PSCs was still relatively low.

Ct effectors might not be detected by this PEPSY screening method for several reasons. In addition to those discussed earlier in Chapter 3, *Ct* effectors may have been toxic to yeast and thus inhibited initial yeast growth. For example, the two *Legionella* virulence proteins LidA and RaIF both function to modify the *Legionella*-containing vacuole during infection and are detrimental to growth when expressed in a yeast model system (Derre and Isberg, 2005, Campodonico et al., 2005). However, although the intracellular substrates of these proteins are conserved between yeast and mammals, neither of these

virulence proteins was identified by PEPSY screening presumably due to their toxicity in yeast (Shohdy et al., 2005, Siggers and Lesser, 2008). To overcome this issue, it would be interesting to express *Ct* effectors under the control of the inducible GAL1/GAL10 promoters in order to investigate whether the expression of particular *Ct* proteins is firstly toxic to yeast and secondly whether trafficking is disrupted.

Another issue that was encountered throughout the PEPSY screening process was the inconsistency in observing a VPS⁻ phenotype for a particular clone. Each PSC was re-streaked and re-assayed to confirm a VPS⁻ phenotype. However, a majority of PSCs were discarded at this stage because of their inability to maintain the secretion phenotype. Upon re-assaying, many clones portrayed a heterologous population whereby a consistent VPS⁻ phenotype was not observed across the sample. To overcome this, we picked and re-streaked VPS⁻ colonies for re-assaying. However, following several iterations of re-streaking and re-assaying, a heterologous population was still observed. We reasoned that, although yeast are able to extrude their plasmids, the yeast clones here should still encode the URA3⁺ expression plasmid because colonies were formed on media deficient in uracil. However, if the *Ct* protein(s) encoded within the MCS of the expression plasmid are detrimental, but not lethal, to the yeast, there would be selective advantage for the excision or mutation of the gene from the plasmid. This would enable the yeast to grow on media deficient in uracil but would also lead to a non-secretory phenotype when PEPSY screened. In addition to this, the pVT100-U plasmid used to generate the *Ct* genomic library is a 2 μ plasmid and thus can be maintained intracellularly at a high copy number. This characteristic is beneficial for the expression of bacterial proteins in yeast because any resulting phenotype or disruption can be more easily detected. However, in this study, different yeast cells could potentially harbour a varying number of plasmids and thus could account for the inconsistencies in the VPS⁻ phenotype we have observed.

Of the ten PSCs that maintained a VPS⁻ phenotype, only five demonstrated plasmid-dependent CPY-inv secretion when assayed quantitatively. Furthermore, only three of these (PSC50, PSC66 and PSC72) also portrayed

plasmid-dependency when plasmids were isolated and transformed back into BHY12. This led us to assume that a high mutation rate has occurred within some of the clones that were initially identified despite being expressed in a diploid yeast strain.

4.3.3. Characterisation of PSCs

Each of the five yeast clones that had demonstrated plasmid-dependent CPY-*inv* secretion when PEPSY screened both qualitatively and quantitatively were investigated further to determine the protein(s) responsible for interfering with intracellular membrane trafficking.

4.3.3.1. PSC48

PSC48 encoded a short (83bp) *Ct* DNA sequence that spanned two partial gene fragments of *BOUR_00272* and *BOUR_00273*. Interestingly, *BOUR_00272* is documented as an uncharacterised protein and had been predicted to be T3S by the *in silico* prediction program, EffectiveT3 (Table 3.1). However, when the full-length gene was cloned into BHY12, no trafficking defect was observed (section 3.2.5). Furthermore, when BHY12 was retransformed with the isolated plasmid from PSC48 and PEPSY screened, the VPS⁻ phenotype was no longer observed. This observation of non-plasmid-dependent secretion, together with the small *Ct* DNA insert size, led us to discard PSC48 from our study.

4.3.3.2. PSC50 and PSC66

PSC50 and PSC66 shared commonalities when sequenced. PSC50 encoded one full-length gene (*BOUR_00932*) and two partial length genes (*BOUR_00931* and *BOUR_00933*). Both *BOUR_00932* and *BOUR_00933* were also partially encoded by PSC66. *BOUR_00933* had been predicted to be T3S by the *in silico* prediction program, EffectiveT3, but had not displayed a VPS⁻ phenotype when individually cloned into BHY12 and PEPSY screened (section 3.2.5). Furthermore, *BOUR_00932* had not been predicted to be T3S in the original version of EffectiveT3, but is predicted to be T3S in the updated 2015 version of the software.

As *BOUR_00931* was not encoded by PSC66, together with the numerous difficulties in cloning the individual gene, we decided to discard this candidate from our study at this stage.

BOUR_00932 and *BOUR_00933* were individually cloned into BHY12 in order to establish which protein(s) was responsible for disrupting intracellular membrane trafficking, but clear conclusions could not be made. When full-length *BOUR_00932* was expressed, a brown precipitate was observed, but the plasmid-encoding yeast clone did not secrete a significantly greater amount of CPY-inv relative to the plasmid-cured clone when assayed quantitatively. This suggests that the membrane trafficking defect observed qualitatively might be minimal and thus below the detection threshold for quantitative PEPSY screening. Unexpectedly, when full-length *BOUR_00932* was expressed together with its upstream and downstream UTR or when the DUB domain of *BOUR_00932* was expressed in isolation, the VPS⁻ phenotype was no longer observed. These data suggest that the catalytic domain alone is not sufficient to disrupt membrane trafficking, thus additional features of the gene are required for its activity. Furthermore, there might be an upstream or downstream regulatory domain that controls the expression or activity of *BOUR_00932*. Alternatively, given the inconsistencies observed in PEPSY screening throughout this study, additional repeats of these assays may lead to a clearer distinction between secretory and non-secretory phenotypes.

When full-length *BOUR_00933* was expressed in BHY12, a VPS⁻ phenotype was inconsistently observed following PEPSY screening and notably, when this protein was PEPSY screened in Chapter 3 following EffectiveT3 prediction, the VPS⁻ phenotype was not observed. Similar to *BOUR_00932*, when *BOUR_00933*-encoding BHY12 was assayed in liquid culture, the plasmid-encoding clone did not secrete significantly greater quantities of CPY-inv relative to the plasmid-cured clone. Furthermore, when the full-length gene was expressed together with its upstream UTR, the secretory phenotype was no longer observed. However, when the 771bp fragment of *BOUR_00933* that is encoded by PSC50 and PSC66 was expressed in BHY12 and PEPSY screened, the VPS⁻ phenotype was observed.

It was difficult to establish any precise conclusions from the PEPSY screen given the inconsistencies in generating a VPS⁻ phenotype. We reasoned that since a VPS⁻ phenotype was observed for full-length *BOUR_00932* and occasionally for full-length *BOUR_00933*, there was likely to be some kind of disruption to intracellular membrane trafficking. However, due to the lack of repeatability from this experiment, this could not be confirmed conclusively. Therefore, we sought to investigate whether the protein levels of CPY precursors in these yeast clones varied from controls. We immunoblotted using anti-CPY antibody to detect the three different CPY precursors that vary in their molecular weight and identified reduced levels of vacuolar CPY in the lysate of BHY12 encoding *BOUR_00933*. Although this further implied that intracellular membrane trafficking had been disrupted in this yeast clone, we were mindful that, in the absence of a loading control, a conclusive interpretation of this data could not be made. In a similar way and to further characterise the trafficking defect in future experiments, we could assess not only CPY but also carboxypeptidase S (CPS) levels of yeast clones by immunoblotting. CPS is another vacuolar protein that is sorted into multivesicular bodies (MVB) before delivery to and final processing in the vacuole. Thus, if immunoblotting with anti-CPS demonstrates a variation in CPS precursor or mature CPS between BHY12 encoding *BOUR_00932* or *BOUR_00933* and control yeast, the precise intracellular localisation of their trafficking disruption is likely to be in a trafficking step shared by these two pathways.

We further investigated any disruption to membrane trafficking in PSC50. We made use of the lipophilic dye, FM4-64, to visualise yeast vacuolar membranes using fluorescence microscopy. A majority of PSC50 vacuoles were classified as either wild-type or Class A *vps* mutants, but notably, a minority of vacuoles were also fragmented or missing altogether in some yeast cells, thus suggesting the presence of Class B or C *vps* mutants respectively. A possible reason for this discrepancy, together with the inconsistencies observed in the PEPSY screen may be due to plasmid copy number. The pVT100-U expression plasmid used in this study is a 2 μ plasmid. These 2 μ plasmids have a high copy number, thus yeast are able to maintain 50-100 copies of the plasmid in yeast cells. This high copy number is convenient for the overproduction of pathogen

proteins in yeast (Siggers and Lesser, 2008), but could also potentially lead to varying results whereby different yeast cells harbour varying numbers of plasmids. This variation may lead to differing expression rates of the encoded chlamydial genes and thus result in changeable CPY-inv secretions. For example, the stronger secreting colonies within the heterologous population may harbour a greater quantity of plasmid, while the non- or low secreting colonies might harbour fewer plasmids. Furthermore, mutations or *Ct* gene extractions may occur in some plasmids and subsequently result in the observed heterologous plasmid population. This may also explain the variation observed in both vacuolar morphology and CPY-inv secretion.

An undergraduate student in our lab investigated whether similar variability in CPY-inv secretion was observed in yeast expressing *BOUR_00932* or *BOUR_00933* in plasmids that regulated their copy number. The chlamydial genes were expressed in CEN or 2 μ plasmids under the control of the strong constitutive GPD yeast promoter. Unlike 2 μ plasmids, CEN plasmids maintain a low plasmid copy number, typically retaining 1-3 plasmids per cell. The two chlamydial genes were expressed in both types of plasmid and assayed for CPY-inv secretion. A slow growth rate was observed for these clones likely due to the metabolic burden induced by the strong GPD promoter. However, when assayed for CPY-inv secretion, a VPS⁻ phenotype was observed in 2 μ clones, but not in CEN clones. This implied that a VPS⁻ phenotype might not be observed in clones harbouring fewer plasmids and hence might explain the discrepancies observed in vacuolar morphology and CPY-inv secretion.

4.3.3.3. PSC54

PSC54 encodes three full-length genes (*BOUR_00926*, *BOUR_00927* and *BOUR_00928*) and two partial length genes (*BOUR_00925* and *BOUR_00929*). Notably, *BOUR_00926* is classified as an uncharacterised protein and was predicted to be T3S by the *in silico* prediction program, EffectiveT3.

PSC54 displayed a VPS⁻ phenotype when assayed qualitatively and also secreted significantly greater levels of CPY-inv than the plasmid-cured clone. As before, the expression plasmid was isolated from PSC54 and used for the

transformation of more BHY12. When the initial transformants were assayed for CPY-inv secretion, a VPS⁻ phenotype was observed. However, when a colony was re-streaked onto fresh media, the VPS⁻ phenotype was no longer observed. This inconsistency correlates to those observed for other clones and might be explained by some of the issues mentioned in section 4.3.3.2.

The genes encoded by PSC54 were individually cloned into BHY12 and assayed for any trafficking defects. None of the genes tested displayed a VPS⁻ phenotype. Likewise, none of the different yeast clones of BHY12 encoding various combinations of the five consecutive genes displayed a VPS⁻ phenotype. These observations, together with the inconsistency in testing for plasmid-dependency, led us to discard PSC54 and its corresponding chlamydial genes from our investigation.

4.3.4. Study progression

For the reasons discussed above, we discarded PSC48, PSC54 and PSC72 from our investigation and focused on the intracellular disruption induced by the two genes encoded by PSC50 and PSC66: *BOUR_00932* and *BOUR_00933*.

BOUR_00932 and *BOUR_00933* encode the proteins ChlaDUB2 and ChlaDUB1 respectively and both have been previously demonstrated to possess deubiquitinase activity (Misaghi et al., 2006). Although a role of ChlaDUB2 in chlamydial pathogenicity is yet to be determined, ChlaDUB1 has been shown to impair the ubiquitination and subsequent degradation of the NFκB inhibitory subunit IκBα (Le Negrate et al., 2008b) as well as stabilising the apoptotic regulator, Mcl-1 (Fischer et al., 2017). Like ChlaDUB1, a number of other bacterial DUBs typically function to attenuate NFκB-related inflammatory responses by deubiquitinating and thus preventing the degradation of IκBα (Rahman and McFadden, 2011). Thus, ChlaDUB1, and potentially ChlaDUB2, are likely to play key roles during chlamydial infection. Although we doubted that the disruption to NFκB signalling or the stabilisation of Mcl-1 would impair CPY-inv trafficking, we were mindful that the chlamydial DUBs, like other bacterial DUBs, might have multiple substrates that induce different intracellular effects. Moreover, we determined that the expression of these DUBs within a

clinically relevant host would be more beneficial for identifying any intracellular defects induced by these enzymes. Thus, we sought to investigate whether these DUBs induced similar trafficking defects in mammalian cells.

Chapter 5: Analysis of ChlaDUB1 and ChlaDUB2

5.1. Introduction

5.1.1. Ubiquitin signalling

Ubiquitination is a reversible post-translational modification (PTM) that modulates the modified protein's fate, function or localisation. This PTM is an essential cellular regulatory process and is used in the regulation of several signalling pathways, such as cell division, secretion, DNA replication, DNA repair and protein degradation. Unlike other PTMs, such as phosphorylation, ubiquitination is remarkably tuneable and harbours several layers of complexity (Mevisen and Komander, 2017).

Ubiquitination is the conjugation of the 76 amino acid ubiquitin polypeptide by the sequential action of activating enzymes (E1s), conjugating enzymes (E2s) and ligase enzymes (E3s). In humans, there are two E1s, 35 E2s and hundreds of E3s responsible for ubiquitination (Chaugule and Walden, 2016). Briefly, the E1s activate the C-terminus of ubiquitin to form an E1-ubiquitin thioester intermediate in which the ubiquitin is conjugated to a cysteine residue at the active site of the E1. The ubiquitin is then transferred to the active site of an E2 enzyme via a transthioesterification reaction and results in the formation of an E2-ubiquitin thioester intermediate. The transfer of ubiquitin from 'charged' E2s onto target proteins is mediated by E3s. E3s catalyse the formation of an isopeptide linkage between the C-terminus of ubiquitin and a primary amino group on the target protein. E3s vary significantly in size and subunit composition and thus use different mechanisms for the catalysis of isopeptide bond formation (Lorenz et al., 2013). The unique properties of the numerous E3s enables the ligases to operate in distinct cellular contexts, respond to different cellular signals and process a variety of protein substrates (Zheng and Shabek, 2017). Historically, E3s have been grouped into two classes: the really interesting new gene (RING)-type E3s and the homologous to the E6AP carboxyl terminus (HECT)-type E3s. The RING E3s are characterised by their RING or U-box fold catalytic domain, which mediates the direct transfer of

ubiquitin from an E2 to a substrate (Deshaies and Joazeiro, 2009). Alternatively, the HECT E3s do not directly transfer ubiquitin from the E2 to the substrate, but instead form a thioester-linked intermediate with ubiquitin before its transfer to the substrate (Zheng and Shabek, 2017). Furthermore, more recently, an emerging class of E3s has been defined as the RING-HECT hybrids that are characterised by the presence of 2 RING fingers, RING1 and RING2, with a central zinc-binding domain positioned between them (Wenzel et al., 2011). The cross-talk between E2s and E3s at the latter stages of ubiquitination determines the nature and target of the modification. Given the diversity of E2s and the large repertoire of E3s available, there are a substantial number of possible combinations that could arise from this interaction. This is reflected by the multitude of different ubiquitin signals present across numerous substrates that ensures the specificity of substrate selection (Chaugule and Walden, 2016).

Polyubiquitin chains are also formed via the concerted efforts of E1, E2 and E3 enzymes. Ubiquitin has 8 ubiquitination sites: seven lysine residues (K6, K11, K27, K29, K33, K48 and K63) and an N-terminal amine (Met1). All of these sites can participate in polyubiquitin chain formation. Furthermore, ubiquitinated polymers can contain several ubiquitin linkage types in mixed ubiquitin chains, or one ubiquitin moiety can be modified on multiple sites to form branched ubiquitin chains (Mevisen and Komander, 2017). These layers of complexity highlight the intricate nature of ubiquitin as a PTM and reinforce the requirement for molecular regulation (Popovic et al., 2014).

The isopeptide linkage type of polyubiquitin chains determines the subsequent fate of the protein. For example, K48- and K11-linked polyubiquitin chains typically target the substrate for proteasomal degradation, while K63-linked polyubiquitin chains usually act as a scaffold to assemble signalling complexes to regulated various cellular processes such as protein kinase activation or DNA repair pathways (Komander, 2010).

Given the intricacies of the ubiquitin system, any dysfunction in the ubiquitin system or ubiquitin signalling can lead to a myriad of disease states including

cancer and neurodegeneration disorders (Zheng et al., 2016). Thus, ubiquitination is carefully modulated and deubiquitinase (DUB) enzymes play a vital role in maintaining ubiquitin homeostasis.

5.1.2. Deubiquitinases

5.1.2.1. DUB families

DUBs are responsible for the removal of ubiquitin signals. There are approximately 100 DUBs in humans (Clague et al., 2013) and these are classified into six distinct DUB families. The six DUB families are comprised of the zinc-dependent JAB1/MPN/MOV34 metalloproteases (JAMMs) and five families of cysteine proteases: ubiquitin-specific proteases (USPs), the ovarian tumour proteases (OTUs), the ubiquitin C-terminal hydrolases (UCHs), the Josephin family and the more recently identified motif-interacting with ubiquitin (MIU)-containing novel DUB family (MINDYs). Around half of the DUBs expressed in humans are USPs (Mevissen and Komander, 2017). This study focuses on ChlaDUB1 and ChlaDUB2, both of which belong to the USP DUB family. Thus, unless otherwise stated, the use of the word 'DUB' hereafter refers to DUBs belonging to the USP family.

5.1.2.2. Layers of DUB complexity

The mechanisms behind DUB activity and specificity are still not fully understood. DUBs possess several layers of complexity that enable them to accurately select and approach their target, distinguish ubiquitin moieties from other ubiquitin-like modifiers (e.g. SUMO and Nedd8) and determine where to cleave the ubiquitin chain (Mevissen and Komander, 2017). Furthermore, DUBs commonly harbour isopeptide linkage preferences, thus the enzyme needs to distinguish between the numerous linkage types.

DUBs can modulate ubiquitin signalling by several different means. For example, DUBs can either bind to its target protein substrate or it can bind directly to the ubiquitin signal. Furthermore, DUBs can function in isolation or as part of a macromolecular complex that recruits substrates for deubiquitination, such as the proteasome (Mevissen and Komander, 2017). Moreover, DUBs can

cleave ubiquitin with endo- or exo-cleavage activity. Endo-cleavage involves the DUB cleaving ubiquitin from the substrate to release an unanchored polyubiquitin chain that requires further processing to regenerate monoubiquitin. Alternatively, exo-cleavage involves the sequential cleavage of ubiquitin from a polyubiquitin chain to directly produce monoubiquitin. The way by which a DUB recognises polyubiquitin determines whether the DUB is capable of endo- or exo-cleavage. For example, a DUB must be able to accommodate a distally extended chain if it is to perform endo-cleavage. The DUB, USP21, demonstrates both endo- and exo-activity (Ye et al., 2011).

DUB activity and specificity depends upon the ability of the enzyme to recognise ubiquitin and polyubiquitin chains. All DUBs have at least one ubiquitin-binding site, S1, which guides the ubiquitin C-terminus and the isopeptide bond into the active site where hydrolysis can occur. DUBs that demonstrate a ubiquitin linkage preference typically harbour an additional S1' site to accommodate the neighbouring ubiquitin moiety. In the absence of an S1' site, DUBs are non-specific towards ubiquitin linkages. DUBs can also possess additional ubiquitin binding sites (e.g. S2, S2', S3, S3') that provide increased interactions with the polyubiquitin and might contribute towards linkage specificity (Mevisen and Komander, 2017). Furthermore, substrate specificity can be enhanced by the binding of substrate or ubiquitin moieties to the catalytic domain.

5.1.2.3. Bacterial deubiquitinases

Several Gram-negative bacteria use T3SS to translocate effector proteins into host cells. The secreted effectors interfere with a variety of host trafficking and signalling pathways including cytoskeletal remodelling, endocytosis, secretory pathways, transcription, translation, cell division and immune responses (Rytönen and Holden, 2007). Given the importance of ubiquitination and deubiquitination in the regulation of host cellular processes, bacteria have evolved to interfere with these processes, for example by expressing deubiquitinases.

Yersinia translocates the DUB effector, YopJ, into host cells via a T3SS. The injection of YopJ suppresses host cell inflammatory responses and stimulates apoptosis in macrophages. YopJ interferes with mitogen-activated protein kinase (MAPK) kinases (MKK) and IKK β and thereby suppresses pro-inflammatory signalling and induces apoptosis (Monack et al., 1997, Orth et al., 1999, Palmer et al., 1998).

Similarly, the *Salmonella* DUB, AvrA, is a homolog of YopJ and functions to suppress pro-inflammatory host signalling pathways by deubiquitinating the inhibitory I κ B α subunit of the NF κ B signalling pathway. *Salmonella* also secretes another DUB, SseL, into host cells via the *Salmonella* pathogenicity island 2 (SPI-2) T3SS. The deubiquitinating activity of SseL is crucial for *Salmonella* virulence (Rytönen et al., 2007) as it has been shown to prevent the recruitment of the autophagy markers, p62 and LC3, thus leading to reduced autophagic flux during infection (Mesquita et al., 2012).

5.1.3. ChlaDUB1 and ChlaDUB2

The two chlamydial DUBs, ChlaDUB1 and ChlaDUB2, were first identified by Misaghi et al. (2006) following the use of activity-based probes to identify DUBs expressed during *Ct* infection in HeLa cells. ChlaDUB1 and ChlaDUB2 are expressed by *Ct*, but not *Cpn*, and their expression is first observed at 16 h post-infection (Misaghi et al., 2006). Although both ChlaDUB1 and ChlaDUB2 possess deubiquitinating and deneddylating activity, Misaghi et al. (2006) hypothesised that ChlaDUB1 might be expressed at lower levels than ChlaDUB2 during *Ct* infection.

Host substrates of ChlaDUB2 have not yet been identified, but ChlaDUB1 has been shown to bind the NF κ B inhibitory subunit, I κ B α and subsequently impair its ubiquitination and degradation (Le Negrate et al., 2008b). Thus, the action of ChlaDUB1 blocks the translocation of NF κ B into the host nucleus to activate the transcription of pro-inflammatory genes that could otherwise act to destroy the invading pathogen. More recently, ChlaDUB1 has also been shown to stabilise the apoptotic regulator, Mcl-1 (Fischer et al., 2017). Interestingly, Mcl-1 protein levels were increased and remained at high levels at 16 h post-infection and

this correlates to the time by which ChlaDUB1 is detected in infected cells (Fischer et al., 2017, Misaghi et al., 2006). A partial structure of ChlaDUB1 (amino acids 130-401) has also recently been reported (Pruneda et al., 2016).

5.1.4. Objectives

In this chapter, we first perform bioinformatic analysis of ChlaDUB1 and ChlaDUB2 and compare their protein sequences to other bacterial deubiquitinases. We then express ChlaDUB1 and ChlaDUB2 in HeLa cells to investigate their intracellular effects in a more clinically relevant model system. We assess the expression and deubiquitinating activity of ChlaDUB1 and ChlaDUB2 in HeLa cells and then go on to assess their effects on endosomal compartments, EGFR recycling and degradation, I κ B α protein levels and global ubiquitin levels. We also sought to identify interacting host substrates for each chlamydial DUB using mass spectroscopy.

5.2. Results

5.2.1. Bioinformatic analysis of ChlaDUB1 and ChlaDUB2

To gain an initial insight into the functionality of ChlaDUB1 and ChlaDUB2, we performed protein sequence alignments using the computational alignment programs, Serial Cloner and T-Coffee. Using these alignment tools, we aligned the full protein sequences of ChlaDUB1 and ChlaDUB2 against other bacterial enzymes that have previously been experimentally validated to demonstrate deubiquitinase activity. The bacterial deubiquitinases used for alignment comparisons were the *Yersinia* DUB, YopJ, and two *Salmonella* DUBs, SseL and AvrA. ChlaDUB1 and ChlaDUB2 were individually aligned to YopJ, SseL or AvrA by pairwise sequence alignment using Serial Cloner and, by this method, each pairwise sequence alignment demonstrated sequence similarity of 60-65%. This level of sequence similarity is typical of proteins sharing a common ancestor and thus these enzymes are likely to have a similar biological role.

A multiple sequence alignment of all of these DUBs was also performed using T-Coffee to determine the presence of any conserved sequence regions across the bacterial enzymes (Figure 5.1). Although the alignments demonstrated various regions of protein sequence similarity or identity, we were mindful that protein activity is highly linked to protein structure and so were cautious about inferring too much information with the observed level of similarity among these sequences.

We anticipated that the region of greatest sequence similarity and identity among bacterial DUBs would be the catalytic domain harbouring the active site residues. Commonly, enzymes possess a set of three coordinated amino acids in their active site known as a catalytic triad. The 3-dimensional protein structure ensures that the catalytic triad residues are brought together in a precise location to allow the crucial catalytic capability of the enzyme to occur. Catalytic triads are composed of an acid (aspartate or glutamate), base (most commonly histidine) and a nucleophile (most commonly serine or cysteine). Cysteine proteases typically harbour a catalytic triad composed of cysteine, histidine and aspartate residues (Cys-His-Asp).

To investigate whether there was greater sequence similarity among the catalytic domains of bacterial DUBs, we performed pairwise and multiple sequence alignments of ChlaDUB1 and ChlaDUB2 with the *Salmonella* DUB, SseL, and the *E.coli* DUB, ElaD. The active site residues for each of the DUBs studied are outlined in Table 5.1. Remarkably, ChlaDUB1 and ChlaDUB2, but not SseL and ElaD, harbour the catalytic Cys-His-Asp triad that is typical of cysteine proteases. Notably however, the importance of aspartate to enzyme catalysis varies as a result of the low pK_a of cysteine and hence several cysteine proteases, including SseL and ElaD, are effectively Cys-His dyads.

Deubiquitinase	Catalytic active site residues
ChlaDUB1	H288, D305 and C358
ChlaDUB2	H203, D220 and C282
SseL	H223 and C285
ElaD	H231 and C313

Table 5.1 The location of catalytic active site residues of bacterial DUBs. Active site residues of ChlaDUB1, ChlaDUB2, SseL and ElaD were identified using UniProt (IDs: CCP61134.1, CCP61133.1, Q8ZNG2.2 and Q47013.3 respectively).

Pairwise sequence alignments of the catalytic domains of chlamydial DUBs with that of SseL or ElaD demonstrated 65-75% sequence similarity, thus suggesting that ChlaDUB1 and ChlaDUB2 possess deubiquitinating capabilities. Moreover, multiple sequence alignments of the catalytic DUB domains of chlamydial DUBs with those of SseL and ElaD demonstrated a greater extent of protein similarity than that observed in the full-length sequence (Figure 5.2), thus further implying that ChlaDUB1 and ChlaDUB2 function as deubiquitinating enzymes.

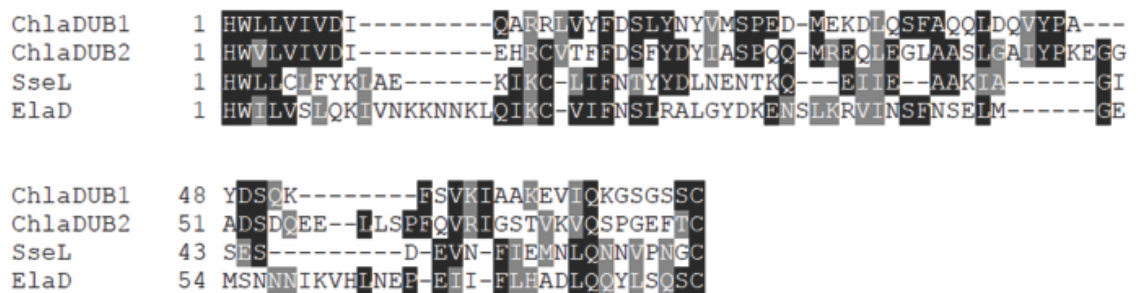


Figure 5.2 Protein alignment of the catalytic domain of bacterial DUBs. Active site residues of ChlaDUB1, ChlaDUB2, SseL and ElaD were determined using UniProt (IDs: CCP61134.1, CCP61133.1, Q8ZNG2.2 and Q47013.3 respectively) and aligned using T-Coffee. Darker shading is indicative of greater sequence similarity.

5.2.2. Expression of ChlaDUB1 and ChlaDUB2 in mammalian cells

Given the clinical relevance of *Chlamydia trachomatis* infection, the assessment of chlamydial DUB activity is most beneficial when DUBs are expressed in a mammalian host. Thus, two inducible HeLa cell lines that stably express either myc-tagged ChlaDUB1 (myc-ChlaDUB1) or myc-tagged ChlaDUB2 (myc-ChlaDUB2) were generated.

5.2.2.1. Cloning of myc-ChlaDUB1 and myc-ChlaDUB2

Myc-ChlaDUB1 or myc-ChlaDUB2 were amplified from previously isolated genomic *Ct* EB DNA by PCR using primers that incorporated a myc tag onto the N-terminus of the encoded genes. Amplified gene constructs were electrophoresed on a 0.8% (w/v) agarose gel, excised according to their molecular weight and purified by gel extraction. Myc-ChlaDUB1 or myc-

ChlaDUB2 was then ligated into the vector pcDNA5/FRT/T0 that uses the Tet promoter to control the expression of recombinant gene constructs. This pcDNA5/FRT/T0 vector also harbours a Flp Recombination Target (FRT) site, a hygromycin resistance gene lacking its promoter and the ATG initiation codon and can be used in the Flp-In transfection system.

In this study, we used a Flp-In HeLa cell line that was a gift from Professor M. Lowe from the University of Manchester. The Flp-In system introduces a FRT site into the HeLa cell genome to aid the integration of exogenous genes and requires the co-transfection of Flp-In HeLa cells with the pOG44 plasmid and pcDNA5/FRT/T0. Thus, upon co-transfection, the Flp recombinase mediates a homologous recombination event between the two FRT sites in the Flp-In HeLa cell line and pcDNA5/FRT/T0. This recombination event results in the insertion of the exogenous pcDNA5/FRT/T0 construct into the Flp-In HeLa genome at the FRT site and subsequently brings the SV40 promoter into proximity and in-frame with the hygromycin resistance gene. Thus, the resulting myc-ChlaDUB1- or myc-ChlaDUB2-transfected HeLa cells can be selected for using hygromycin resistance. The addition of tetracycline to cells induces the expression of myc-ChlaDUB1 or myc-ChlaDUB2. However, in this study we used doxycycline (Dox) as an alternative inducing agent as this agent demonstrates a similar mechanism of action, dose response and induction characteristics to tetracycline, but also has the benefit of a longer half-life of 48 h (compared to 24 h for tetracycline).

Myc-ChlaDUB1 (46kDa) and myc-ChlaDUB2 (38kDa) were successfully expressed in HeLa cells following doxycycline induction (Figure 5.3). However, to assess whether myc-ChlaDUB1 and myc-ChlaDUB2 were enzymatically active in HeLa cells, a DUB activity assay was performed.

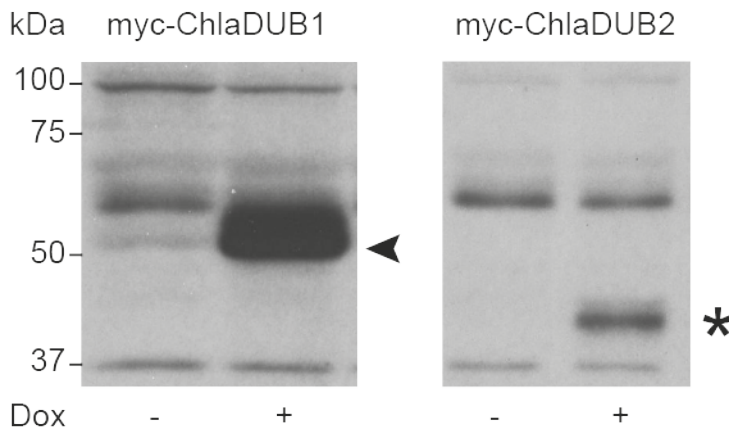


Figure 5.3 Expression of myc-ChlaDUB1 or myc-ChlaDUB2 in a HeLa cell line. Transfected HeLa cells were incubated with 1 μ g/ml doxycycline for 16-18 h to induce expression of myc-ChlaDUB1 or myc-ChlaDUB2. 20 μ g soluble cell lysate was electrophoresed on a 10% SDS-PAGE gel and immunoblotted using 9E10 anti-myc antibody. Arrowhead = ChlaDUB1. * = ChlaDUB2.

This DUB activity assay examines DUB activity by monitoring the cleavage of an internally quenched fluorescence resonance energy transfer (FRET) diubiquitin pair (IQF-diUb). This IQF-diUb pair consists of two ubiquitin molecules: one of which is attached to a fluorescence quencher and the other is attached to a 5-carboxytetramethylrhodamine (TAMRA) fluorescent reporter (excitation 540nm, emission 580nm). Cleavage of the IQF-diUb by a DUB causes separation of the fluorescence quencher and reporter, thereby resulting in an increase in fluorescence signal that can be measured quantitatively using a fluorescence plate reader.

An initial DUB activity assay was performed to assess whether greater DUB activity was detected in HeLa cells expressing myc-ChlaDUB1 or myc-ChlaDUB2 relative to the underlying DUB activity in wild-type (WT) control cells. Soluble cell lysates of doxycycline-induced or uninduced WT cells or cells expressing myc-ChlaDUB1 or myc-ChlaDUB2 were generated and incubated with the K63-linked IQF-diUb substrate. The ubiquitin-specific protease (USP), USP2, was used as a positive control due to its reported ability to cleave polyubiquitin chains via their K48 and K63 linkages (Komander et al., 2009). Fluorescence intensity measurements were recorded every minute over a 90 min period. DUB activity was detected in all test samples. Cells expressing myc-

ChlaDUB1 demonstrated greater levels of DUB activity than WT or uninduced myc-ChlaDUB1-expressing cells, thereby suggesting that the expression of myc-ChlaDUB1 may increase the net DUB activity of cell lysates in the presence of native HeLa DUBs (Figure 5.4). Meanwhile, cells expressing myc-ChlaDUB2 did not demonstrate noticeably greater levels of DUB activity than WT cells, suggesting that myc-ChlaDUB2 has low-level DUB activity or has an alternative linkage or substrate preference (Figure 5.4).

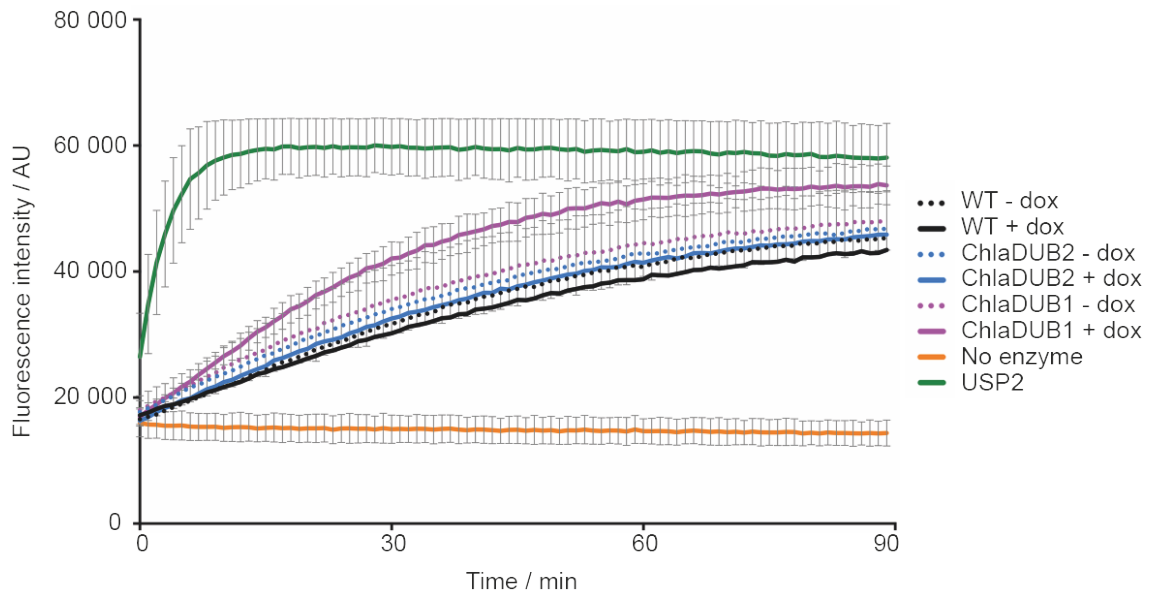


Figure 5.4 Enhanced DUB activity detected in HeLa lysates expressing ChlaDUB1. 1 μ g/ml doxycycline was added to HeLa cells to induce expression of myc-ChlaDUB1 or myc-ChlaDUB2. Soluble cell lysates were normalised and incubated with IQF-K63-diUb and the fluorescence intensities were recorded as a function of time. For clarity, error bars are shown for ChlaDUB1 \pm dox, USP2 and no enzyme control. Data are means \pm SD; n=3. Dox = doxycycline.

To confirm whether the increased DUB activity observed in the lysates was exclusively due to the chlamydial DUBs and not merely the native HeLa DUBs, myc-ChlaDUB1 or myc-ChlaDUB2 were immunoprecipitated (IP) using α -myc-coupled beads. Immunoprecipitation of myc-ChlaDUB1 or myc-ChlaDUB2 from HeLa lysates was first optimised to determine the optimal amount of lysate to use in the pull-down that would maximise DUB yield and minimise excess DUB in the flow-through. The optimal conditions were determined as the amount of protein whereby subsequent increases in protein from the IP eluate no longer have an effect on the binding of protein to beads. Visually, this corresponds to

the point at which the immunoblotted protein bands from the IP eluate remain at a constant size as protein amount increases. The optimised conditions for ChlaDUB1 and ChlaDUB2 pull-down were 400µg lysate/20µl beads and 1500µg lysate/20µl beads respectively (Figure 5.5 A and Figure 5.5 B respectively).

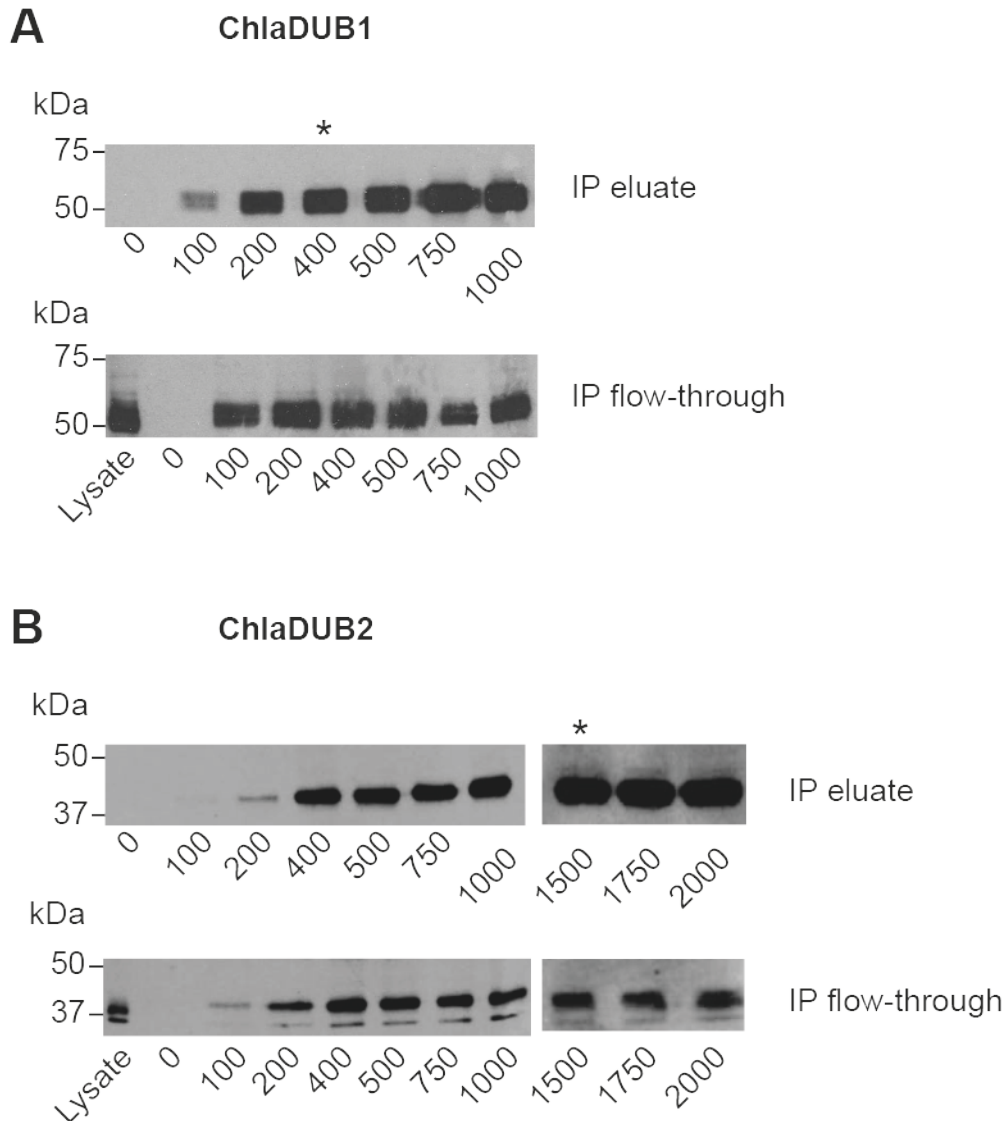


Figure 5.5 Optimisation of conditions required for immunoprecipitating myc-ChlaDUB1 or myc-ChlaDUB2. 1µg/ml doxycycline was added to HeLa cells to induce expression of myc-ChlaDUB1 or myc-ChlaDUB2. Soluble cell lysates of myc-ChlaDUB1 (**A**) or myc-ChlaDUB2 (**B**) were quantified and the specified amounts of protein (µg) were immunoprecipitated using anti-myc coupled resin. Eluates (upper panels) and first flow-through samples (lower panels) were electrophoresed on a 15% SDS-PAGE gel and immunoblotted with 9E10 anti-myc antibody. * = optimised condition.

Following optimisation, eluates from myc-ChlaDUB1 and myc-ChlaDUB2 immunoprecipitations were incubated with the K63-linked IQF-diUb substrate to assess specific DUB activity. Again, fluorescence intensity measurements were recorded every minute over a 90 min period. As before, isolated ChlaDUB1, but not ChlaDUB2, demonstrated K63-linked DUB activity (Figure 5.6).

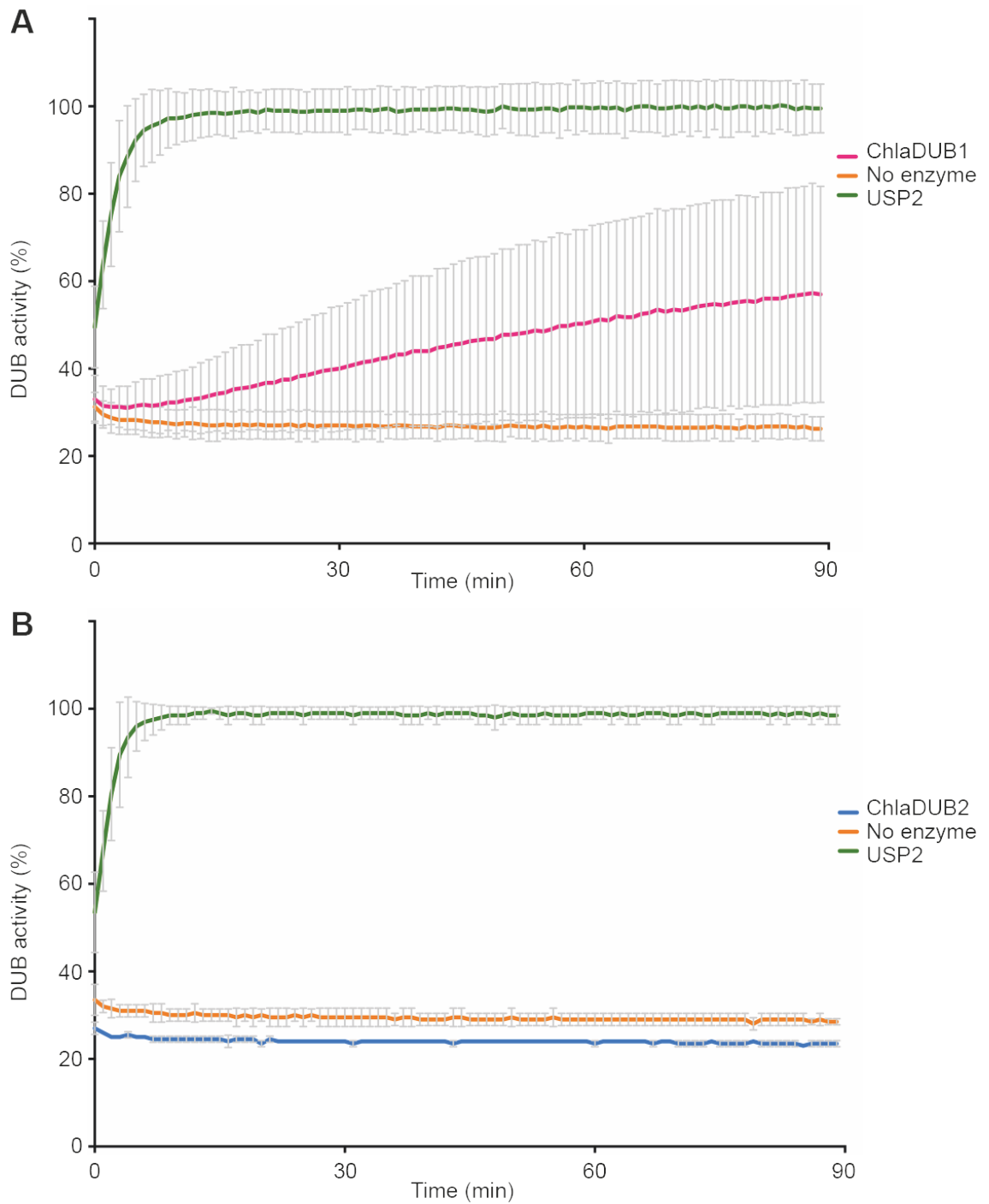


Figure 5.6 K63-linked deubiquitinase activity of ChlaDUB1 or ChlaDUB2. 20 μ l eluates of immunoprecipitated myc-ChlaDUB1 (**A**) or myc-ChlaDUB2 (**B**) were incubated with IQF-K63-diUb and the fluorescence intensities were recorded as a function of time. DUB activity is expressed as % of saturated USP2 control. Data are means \pm SD; n = 3.

Given that purified ChlaDUB2 did not demonstrate K63-linked DUB activity, we hypothesised that ChlaDUB2 may demonstrate linkage specificity towards an alternative lysine residue of ubiquitin. Thus, the activity assay was repeated using a K48-linked IQF-diUb substrate in an attempt to observe whether ChlaDUB2 harboured an alternative DUB linkage specificity. Furthermore, the K48-linked IQF-diUb substrate is commercially available from LifeSensors in six different forms whereby the IQF-diUb substrate has been prepared through site specific labelling at different positions (K48-1, -2, -3, -4, -5 or -6) on the lysine residue of ubiquitin. This allows for the optimisation of determining linkage specificities for a particular DUB. The activity assay was performed using the six different K48-linked IQF-diUb substrates incubated with myc-ChlaDUB2. Additionally, K48-1 was also used to examine K48-linked DUB activity of purified myc-ChlaDUB1. K48-linked DUB activity was not observed for either DUB tested (Figure 5.7).

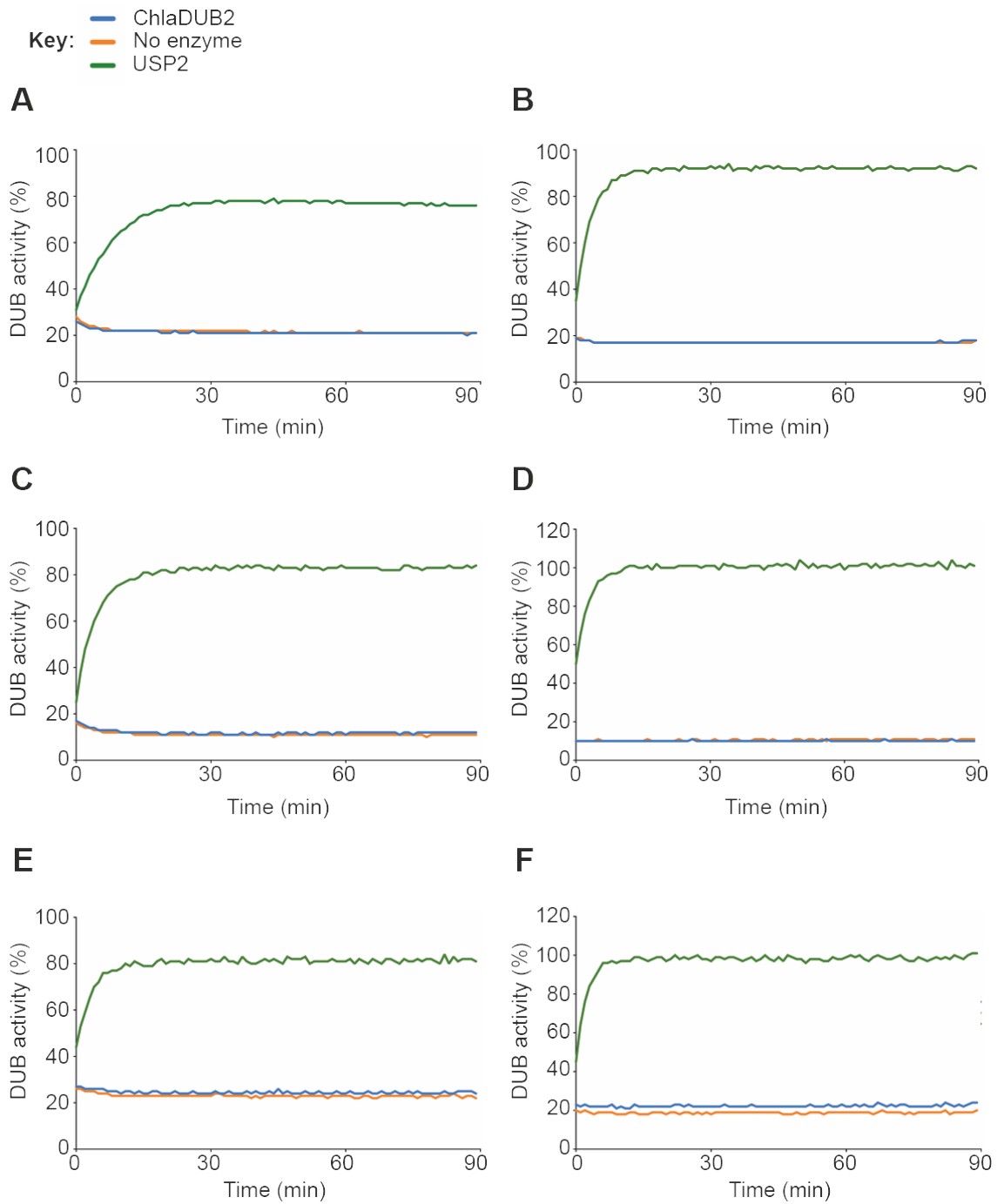


Figure 5.7 K48-linked deubiquitinase activity of ChlaDUB2. 20 μ l eluates of immunoprecipitated myc-ChlaDUB2 were incubated with IQF-K48-1 (**A**), K48-2 (**B**), K48-3 (**C**), K48-4 (**D**), K48-5 (**E**) or K48-6 (**F**) diUb and the fluorescence intensities were recorded as a function of time. DUB activity is expressed as % of saturated USP2 control.

5.2.3. Effect of ChlaDUB1 or ChlaDUB2 on intracellular compartments

Given that ChlaDUB1 demonstrated K63-linked DUB activity, we sought to investigate whether ChlaDUB1 induced any intracellular defects in mammalian cells. Moreover, although enzymatic activity of ChlaDUB2 had not been detected for either K63- or K48-linked IQF-diUb substrates, we decided to also investigate the presence of any intracellular defects in mammalian cells given that Misaghi *et al.* (2006) have previously suggested that ChlaDUB2 may only be lowly expressed during infection and thus enzymatic activity may be minimal.

Generally the internalisation of bacteria by phagocytosis results in the trafficking of bacteria through the phagosomal pathway and ultimately delivery to the lysosome for destruction by lysosomal acid hydrolases. *Ct* occupies an intracellular niche (the inclusion) upon entry into host cells to avoid fusion with endocytic machinery, thus we hypothesised that endocytic compartments may be manipulated upon the expression of chlamydial virulence factors.

To test whether early endosomal, late endosomal or lysosomal function was perturbed by chlamydial DUBs, we expressed myc-ChlaDUB1 or myc-ChlaDUB2 under a doxycycline-inducible promoter for 16-18 h in HeLa cells and examined the morphology and localisation of endocytic compartments by confocal microscopy. The antibody markers EEA1, ciMPR and LAMP1 were used to immunolabel early endosomes, late endosomes and lysosomes respectively. However, no distinguishable difference was observed for these endocytic compartments between control cells and cells expressing myc-ChlaDUB1 or myc-ChlaDUB2 by immunofluorescence (Figure 5.8 - Figure 5.9).

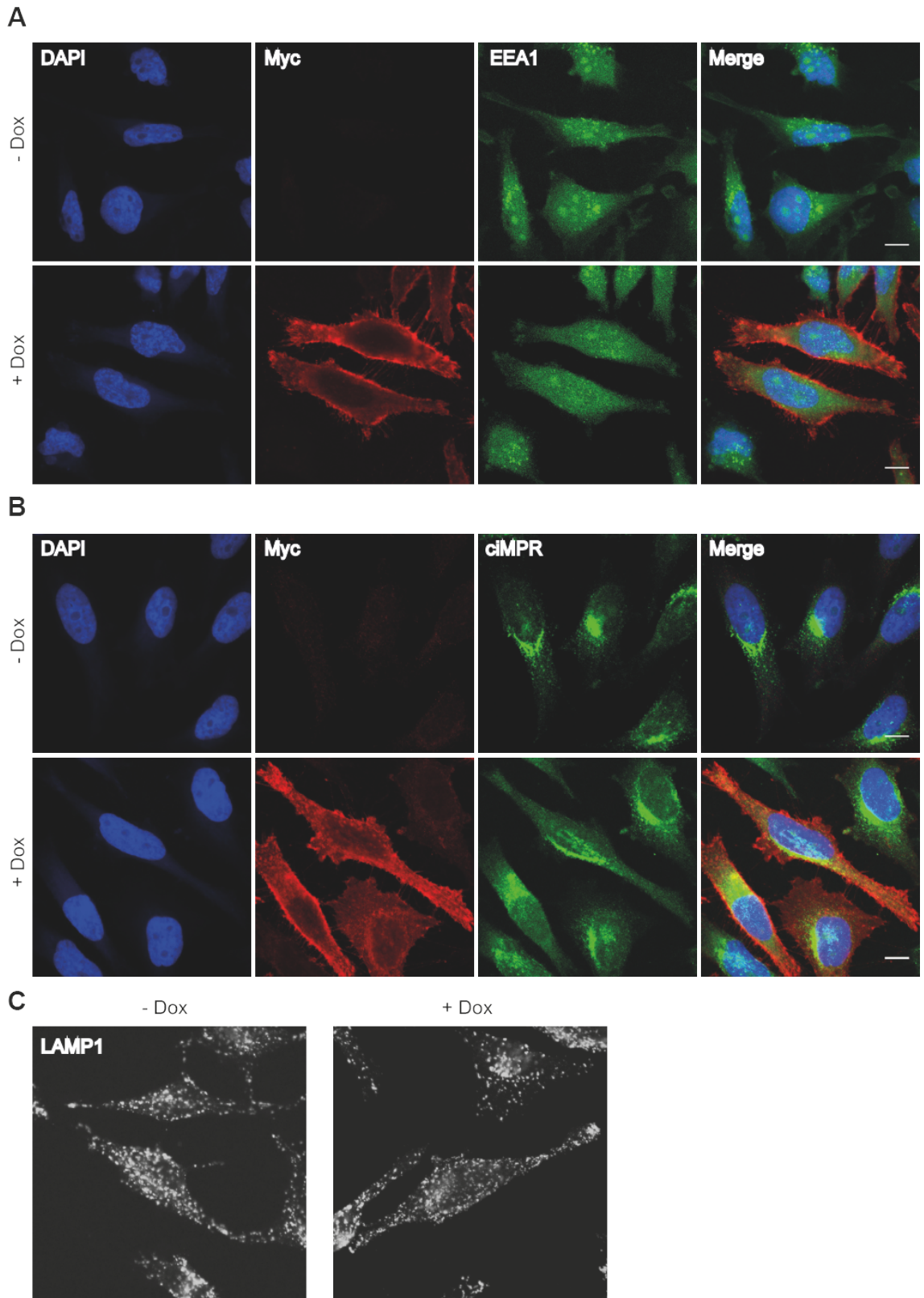


Figure 5.8 The effect of ChlaDUB1 expression on endocytic compartments. 1µg/ml doxycycline was added to HeLa cells to induce expression of myc-ChlaDUB1. Cells were fixed and labelled with myc and EEA1 (A), myc and ciMPR (B) or LAMP1 (C) antibodies followed by fluorescently labelled secondary antibodies. Scale bars = 10µm.

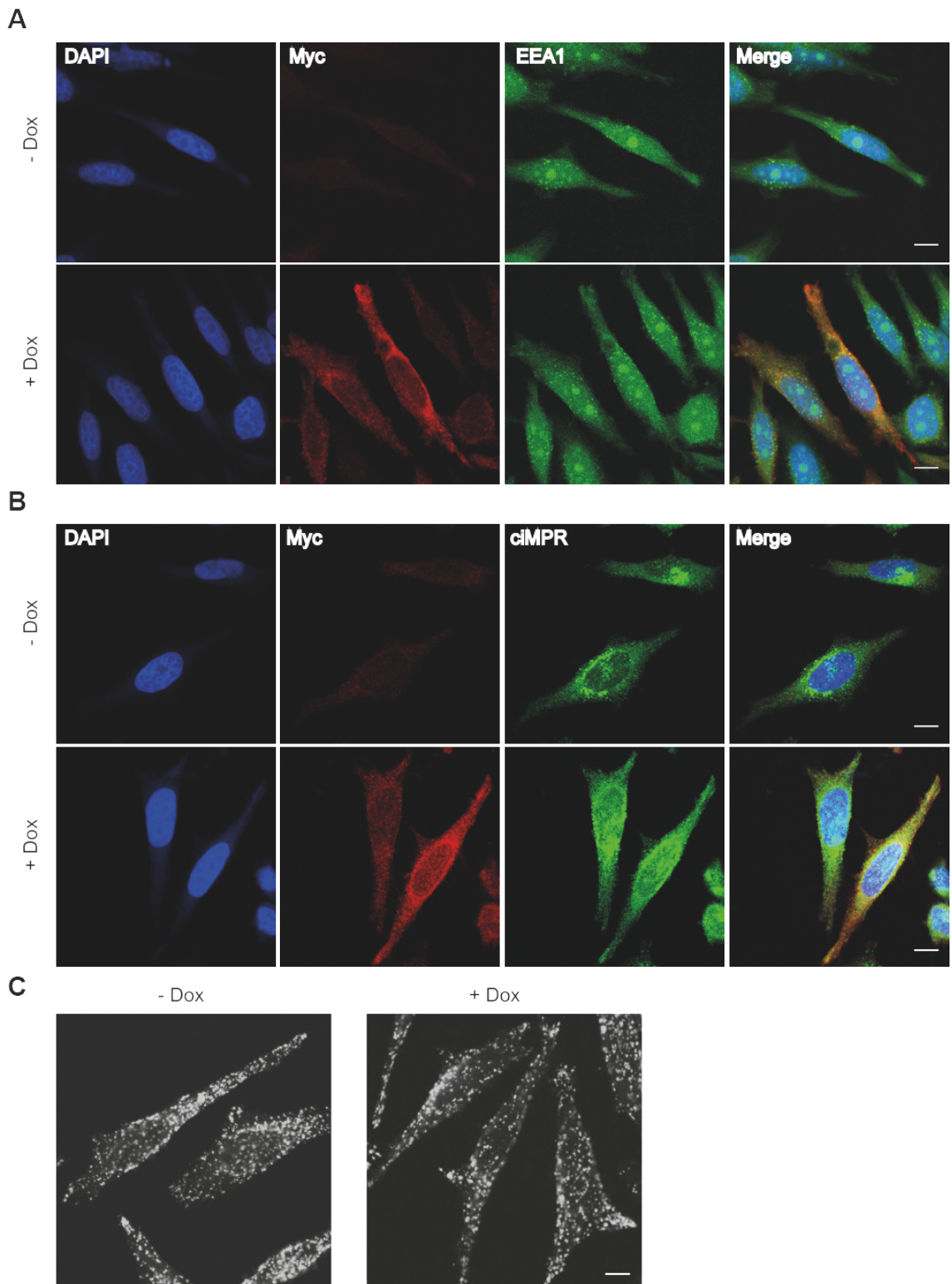


Figure 5.9 The effect of ChlaDUB2 expression on endocytic compartments. 1µg/ml doxycycline was added to HeLa cells to induce expression of myc-ChlaDUB2. Cells were fixed and labelled with myc and EEA1 (A), myc and ciMPR (B) or LAMP1 (C) antibodies followed by fluorescently labelled secondary antibodies. Scale bars = 10µm.

Deubiquitination has previously been shown to regulate autophagy and DUBs, such as USP22 (Liang et al., 2014) and UCH-L1 (Pukass and Richter-Landsberg, 2015) have been shown to be involved. Although the chlamydial inclusion does not fuse with autophagosomes, Al-Younes *et al.* (2004) have previously reported that autophagic markers become redistributed to the inclusion during infection. Therefore, we hypothesised that autophagosomes may be disrupted upon the expression of chlamydial ChlaDUB1 or ChlaDUB2. To test this hypothesis, HeLa cells expressing myc-ChlaDUB1 or myc-ChlaDUB2 were immunolabelled with the autophagosomal marker, LC3. However, the morphology and localisation of autophagosomes did not differ between control cells and cells expressing ChlaDUB1 or ChlaDUB2 (Figure 5.10).

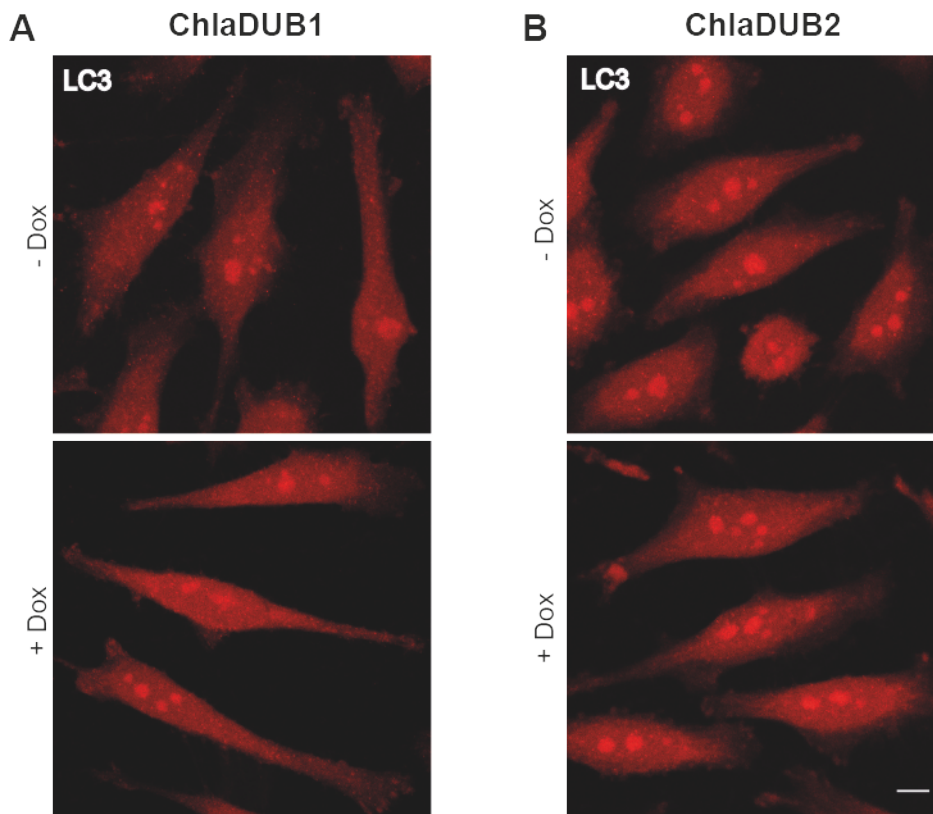


Figure 5.10 The effect of ChlaDUB1 or ChlaDUB2 expression on autophagosomes. 1 μ g/ml doxycycline was added to HeLa cells to induce expression of myc-ChlaDUB1 (A) or myc-ChlaDUB2 (B). Cells were fixed and labelled with LC3 antibody followed by fluorescently labelled secondary antibody. Scale bars = 10 μ m.

The internalisation of bacteria into cells typically induces cytoskeletal remodelling. Therefore, we assessed the effect of ChlaDUB1 and ChlaDUB2 on the actin cytoskeleton by confocal microscopy to investigate whether the actin cytoskeletal structure was disturbed upon chlamydial DUB expression. HeLa cells expressing myc-ChlaDUB1 or myc-ChlaDUB2 were stained with phalloidin, but the actin structure appeared indistinguishable from control cells (Figure 5.11).

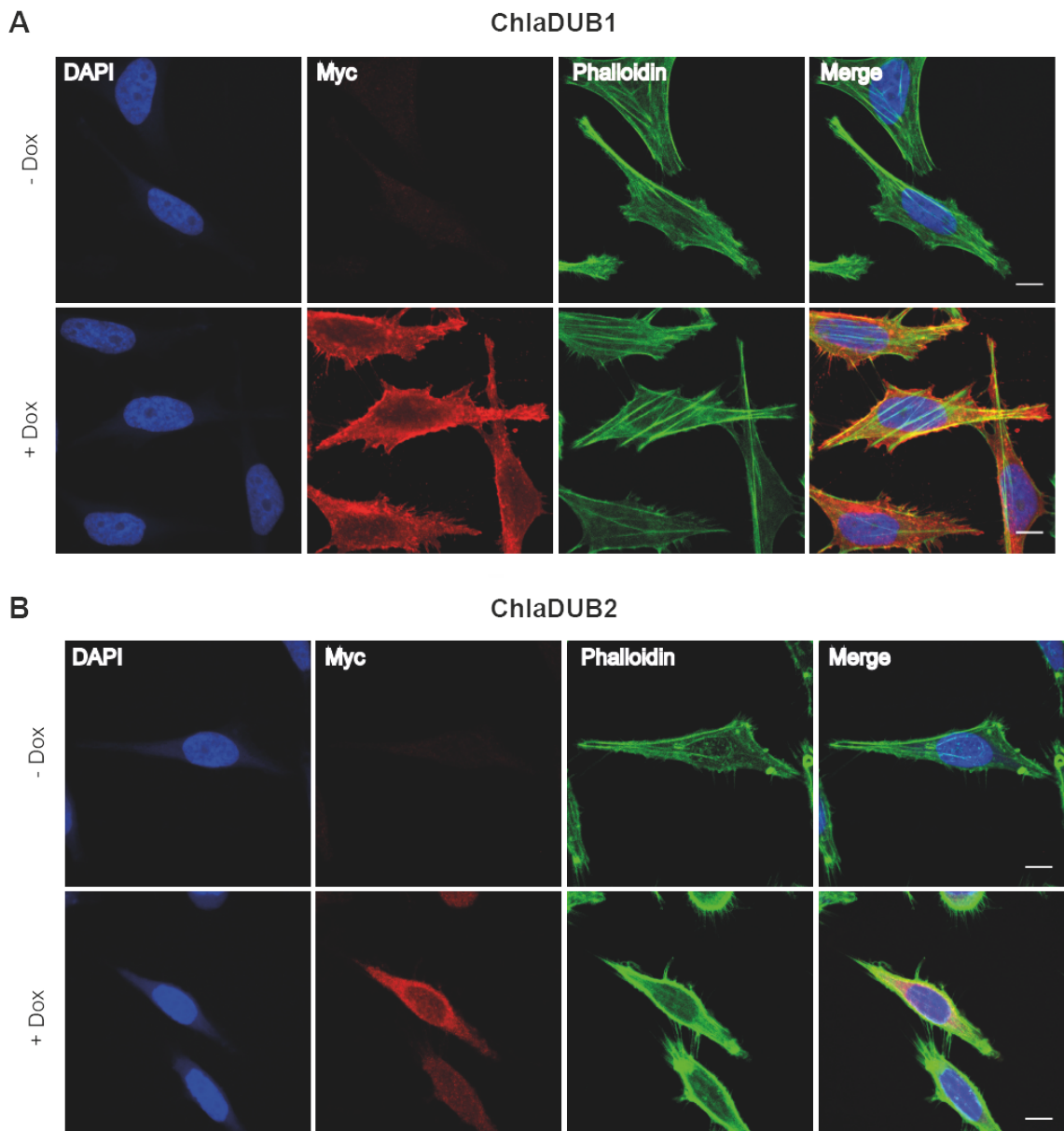


Figure 5.11 The effect of ChlaDUB1 or ChlaDUB2 expression on actin. 1 μ g/ml doxycycline was added to HeLa cells to induce expression of myc-ChlaDUB1 (**A**) myc-ChlaDUB2 (**B**). Cells were fixed and stained with phalloidin. Scale bars = 10 μ m.

5.2.4. Effect of ChlaDUB1 and ChlaDUB2 on global ubiquitin levels

ChlaDUB1 has previously been reported to suppress NF κ B activation through the inhibition of ubiquitination and subsequent degradation of I κ B α (Le Negrate et al., 2008b) and, more recently, has also been reported to stabilise the apoptotic regulator, Mcl-1 (Fischer et al., 2017).

Given that two distinct ChlaDUB1 substrates have been reported, we sought to investigate whether ChlaDUB1 demonstrated broad specificity for multiple intracellular host targets. Thus, we generated soluble cell lysates of HeLa cells expressing ChlaDUB1 or ChlaDUB2 in both uninduced and doxycycline-induced conditions. Immunoblots using anti-ubiquitin antibody were generated in order to compare the global ubiquitinated protein levels between samples.

In addition, HeLa cells expressing ChlaDUB1 or ChlaDUB2 were incubated with 10 μ M MG132 for 4 h prior to generating soluble cell lysates. MG132 is a specific and potent proteasome inhibitor that provokes an accumulation of ubiquitin-conjugated proteins in mammalian cells. Thus, given that proteasomal activity is inhibited in these samples, we reasoned that lysates incubated with MG132 would have a considerably greater amount of ubiquitinated proteins and thus the effect of global deubiquitination by ChlaDUB1 or ChlaDUB2 may be more easily visualised.

There was no substantial difference in the level of global ubiquitination upon the expression of ChlaDUB1 or ChlaDUB2 in HeLa cells (Figure 5.12). Notably, however, global ubiquitination arguably appeared slightly reduced in cells expressing ChlaDUB1 in the absence of MG132 when compared to the uninduced control (Figure 5.12 middle panel, column 1 and 2). Given that this difference was questionable, we deduced that neither ChlaDUB1 nor ChlaDUB2 demonstrate broad substrate specificity for a large number of ubiquitinated proteins in HeLa cells. Instead, we reasoned that both DUBs might demonstrate specific deubiquitinase activity towards a handful of ubiquitinated substrates. With this assumption, specific deubiquitinase activity towards few substrates would not necessarily be visible on a global ubiquitin blot given the vast array of ubiquitinated proteins in cell lysates.

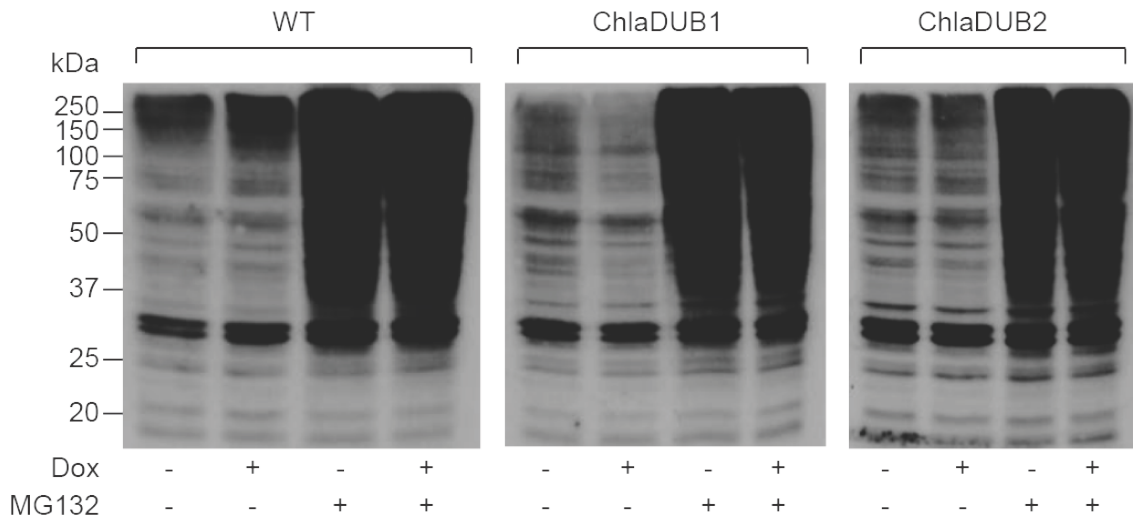


Figure 5.12 The effect of ChlaDUB1 or ChlaDUB2 on global ubiquitin levels. 1µg/ml doxycycline was added to HeLa cells to induce expression of ChlaDUB1 or ChlaDUB2. As specified, cells were incubated with 10µM MG132 for 4 h. Soluble cell lysates were generated, normalised and electrophoresed on a 10% SDS-PAGE gel. Blots were transferred to nitrocellulose, heated at 95°C for 30 min and immunoblotted with anti-ubiquitin antibody.

5.2.5. Identification of substrates for ChlaDUB1 and ChlaDUB2

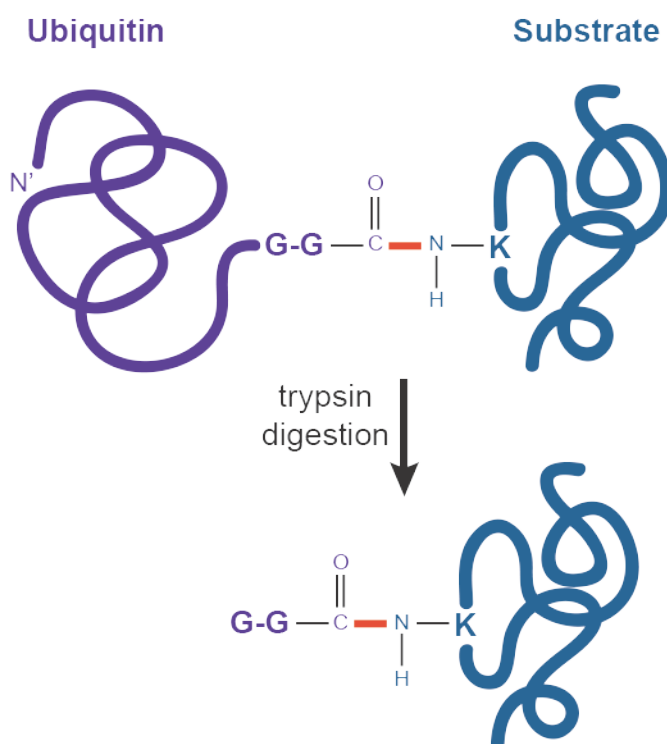
Due to the inconclusive deduction of substrate specificity of ChlaDUB1, we sought to use an alternative means of identifying host interacting partners. A mass spectroscopy proteomics approach was employed to investigate whether ChlaDUB1 had more host substrates in addition to IκBα and Mcl-1. Moreover, as no substrates have yet been reported for ChlaDUB2, we also sought to determine host interacting partners for this chlamydial DUB. We reasoned that this proteomics approach had the potential to identify one or several substrates for these enzymes.

5.2.5.1. Optimisation of mass spectroscopy experiments

For the identification of host substrates for ChlaDUB1 and ChlaDUB2, we based our mass spectroscopy approach on a previous report published by Nakayasu et al. (2015). Here, the authors describe a method to inhibit host cellular DUBs, treat cell lysates with endogenous recombinant DUB and then perform quantitative proteomic analysis to identify interacting partners. Using this approach, they successfully identified both known and two previously

unrecognised host substrates for the *Salmonella* DUB, SseL, that were then subsequently validated by enzymatic and binding assays.

Substrates for the *Salmonella* DUB, SseL, were recognised based on the identification of a di-glycine (K- ϵ -GG) motif; otherwise referred to as the residual ubiquitination signature remnant on ubiquitinated protein substrates following trypsin digestion (Figure 5.13). Peptides harbouring this K- ϵ -GG motif were immunoaffinity purified and analysed by mass spectroscopy. DUBs act to remove ubiquitin from their substrates, thus DUB substrates therefore would not harbour a K- ϵ -GG motif following trypsin digestion. Thus, assuming that DUB substrates are present in the lysates, one would expect to identify fewer peptides harbouring a K- ϵ -GG motif in lysates incubated with recombinant DUB than in control lysates. By this method, SseL substrates were identified as peptides harbouring a K- ϵ -GG motif following trypsin digestion in control lysates, but not in lysates incubated with SseL.



Mass shift of 114.1 Da on the lysine residue of the signature peptide

Figure 5.13 The formation of the signature ubiquitin K-ε-GG motif remnant following trypsin digestion. A residual di-glycine motif is remnant on ubiquitinated proteins following trypsin digestion.

We sought to identify substrates for ChlaDUB1 and ChlaDUB2 using a similar approach to Nakayasu et al. Initially we investigated the amount of peptides that harboured a K-ε-GG motif in WT lysates. Given that we would expect fewer peptides harbouring a K-ε-GG motif to be identified in lysates incubated with recombinant DUB, it was vital to first ensure that sufficient K-ε-GG-containing peptides were observed in control lysates.

Flp-In HeLa cells were cultured in 75cm² flasks to 90% confluency. We generated a soluble cell lysate using a 4-(2-hydroxyethyl)-1-piperazineethanesulfonic acid (HEPES) lysis buffer supplemented with Tris(2-carboxyethyl)phosphine (TCEP) and NEM. The presence of TCEP and NEM in the lysis buffer enables the inhibition of host cell DUB activity. While generating

lysates, we were unaware that the presence of Triton X-100 in the lysis buffer can be detrimental to mass spectroscopy. Triton X-100 is a polymer and thus ionises more readily than peptides and can hence lead to misleading mass spectroscopy data outputs. Following advice from the University of York Proteomics laboratory, we proceeded with a detergent removal procedure for the elimination of Triton X-100 from the prepared lysate. WT lysates were then trypsin digested and peptides were immunoaffinity purified for the K- ϵ -GG motif. Purified samples were then submitted to the University of York Proteomics laboratory for quantitative LC-MS/MS analysis. The dataset returned few proteins and none of these were ubiquitinated.

We anticipated that the detergent depletion procedure had removed ubiquitinated peptide as well as Triton X-100. Thus, we repeated the trial run with the only modification of lysing cells with a urea lysis buffer instead of a HEPES lysis buffer, hence omitting Triton X-100 from the prepared lysate. Again, 1mg WT cell lysates were submitted for quantitative LC-MS/MS.

Here, we compared samples pre- and post-K- ϵ -GG enrichment. In the pre-enriched sample, 117 peptides were identified as ubiquitinated from a total of 12,262 peptides (1%). In the post-enriched sample, 74 out of 1,280 peptides were identified as ubiquitinated (5.8%). This 6-fold enrichment was an improvement, but a total yield of 5.8% ubiquitinated peptides was still disappointing.

We sought to modify the protocol to optimise the yield of ubiquitinated peptides following LC-MS/MS in control lysates. We reasoned that the incubation of cells with the proteasome inhibitor, MG132, together with an increased amount of starting material together would increase the amount of ubiquitinated proteins in the sample. Furthermore, we chose to perform an additional reduction and alkylation step prior to trypsin digestion as well as purifying peptides using a Sep-Pak C₁₈ column and lyophilising the peptides without using a SpeedVac prior to immunoaffinity purification.

15mg WT cell lysate treated with MG132 was submitted for LC-MS/MS. The resulting dataset consisted of 1603 ubiquitinated peptides from 682 different

proteins, hence demonstrating a marked improvement against previous attempts. As expected, the proteins that these ubiquitinated peptides originated from have previously been reported to be post-translationally modified by ubiquitin. For example, the dataset identified ubiquitinated peptides from actin, pyruvate kinase, fatty acid synthase and RNA polymerase II, all of which can be post-translationally modified by ubiquitin (Terman and Kashina, 2013, Kim et al., 2015, Yu et al., 2013, Mitsui and Sharp, 1999). The raw dataset obtained from this final optimisation can be found in the accompanying material.

5.2.5.2. Expression of ChlaDUB1 or ChlaDUB2 in protein production vectors

The proteomics approach we employed for identifying host substrates requires the incubation of cell lysates with purified recombinant DUB. Thus, ChlaDUB1 and ChlaDUB2 were individually cloned into the protein production expression vector, pETFPP_21.

Specific primers were designed for the gene amplification of ChlaDUB1 or ChlaDUB2 by PCR from genomic DNA previously isolated from *Ct* EBs. Amplified genes were electrophoresed on a 0.8% (w/v) agarose gel, excised according to their molecular weight and purified by gel extraction (Figure 5.14 A and B). ChlaDUB1 or ChlaDUB2 were then ligated into the *Nde*I-restriction site of linearised pETFPP_21 (a gift from Jared Cartwright) that incorporates a C-terminal hexa-histidine (His) tag onto the cloned gene (His-ChlaDUB1 or His-ChlaDUB2 respectively). This vector enables the expression of gene constructs under the control of the T7 promoter and expression can be induced upon incubation with 0.2mM isopropyl β -D-1-thiogalactopyranoside (IPTG).

Chemically competent *E.coli* were transformed with pETFPP_21 encoding either His-ChlaDUB1 or His-ChlaDUB2. Bacterial transformants were identified as ampicillin-resistant *E.coli* colonies and were subsequently tested for the presence of the chlamydial gene construct by a colony PCR screen (Figure 5.14 C and D). Bacterial colonies that were successfully transformed with pETFPP_21 encoding His-ChlaDUB1 or His-ChlaDUB2 were then grown overnight in LB media supplemented with ampicillin. Plasmids were then

isolated, purified, sequenced to confirm successful cloning and then transformed into BL21 Gold DE3 *E.coli* for protein production.

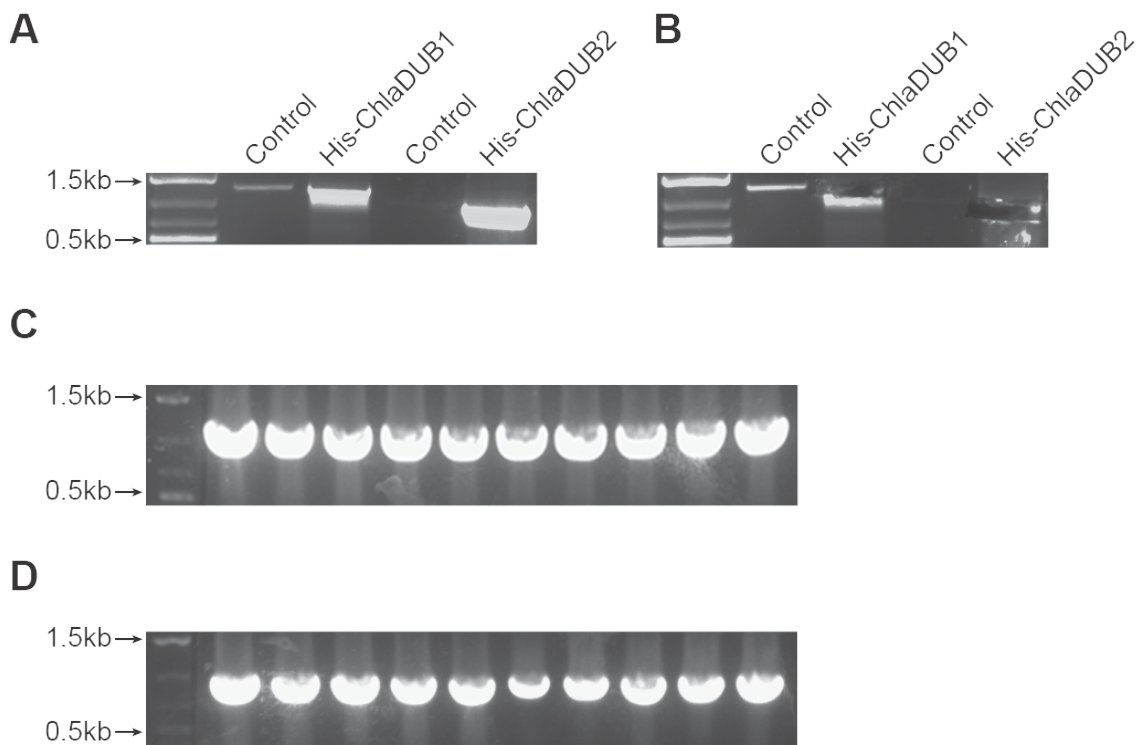


Figure 5.14 Cloning ChlaDUB1 or ChlaDUB2 into pETFPP_21. **A.** His-ChlaDUB1 or His-ChlaDUB2 was amplified from *Ct* genomic DNA by PCR and electrophoresed on an agarose gel. **B.** Amplified DNA was excised from the agarose gel and purified by gel extraction. **C, D.** The MCS of plasmids from ten *E.coli* colonies harbouring pETFPP_21 encoding His-ChlaDUB1 (**C**) or His-ChlaDUB2 (**D**) was amplified by colony PCR and electrophoresed on an agarose gel.

5.2.5.3. Protein production of ChlaDUB1 or ChlaDUB2

Initially, we assessed protein production of the His-ChlaDUB1 or His-ChlaDUB2 constructs in BL21 Gold DE3 cells following a 4 h induction with 0.2mM IPTG to assess the efficiency of protein production over this timeframe. Bacteria were harvested by centrifugation, resuspended in sample buffer and electrophoresed on a 10% SDS-PAGE gel. Protein bands of size 45kDa or 37kDa corresponding to His-ChlaDUB1 or His-ChlaDUB2 respectively were not clear from the gel (Figure 5.15 A), suggesting that these constructs had either been expressed at low levels or had been degraded following synthesis.

Faint protein bands of sizes less than 45kDa or 37kDa for His-ChlaDUB1 or His-ChlaDUB2 respectively were visible, thus suggesting that degradation of these constructs was plausible. To confirm whether the protein bands observed on the gel were degradation products of His-ChlaDUB1 or His-ChlaDUB2, we performed an immunoblot analysis using anti-His antibody on identical bacterial samples (Figure 5.15 B). Here, full-length constructs and degradation products were more easily identifiable. Full-length His-ChlaDUB1 was observed in the presence of the IPTG inducer together with degradation products of approximately 40kDa and 28kDa (Figure 5.15 B column 2). Expression of His-ChlaDUB2 is observed in uninduced conditions, although an additional degradation product of approximately 24kDa is observed in induced conditions (Figure 5.15 B column 4). The identification of these smaller degradation products further implies that the constructs have been degraded within this 4 h timeframe.

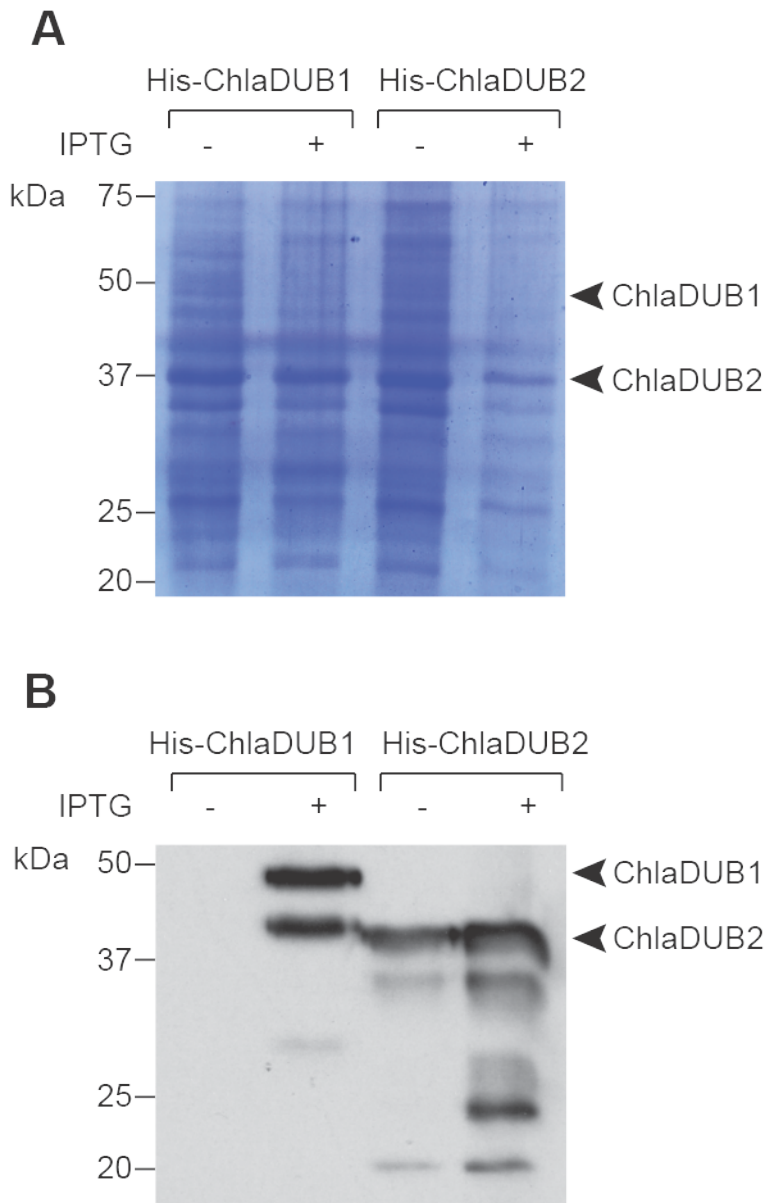


Figure 5.15 Bacterial expression of recombinant ChlaDUB1 or ChlaDUB2. 0.2mM IPTG was added to BL21 Gold DE3 bacteria for 4 h to induce expression of His-ChlaDUB1 or His-ChlaDUB2. Bacteria were pelleted, electrophoresed on a 10% SDS-PAGE gel and protein was either stained with Coomassie (**A**) or immunoblotted using anti-His antibody (**B**).

Although an extended IPTG induction period would, in theory, lead to the synthesis of more His-ChlaDUB1 or His-ChlaDUB2, we were mindful that constructs were being rapidly degraded. Thus, to perform larger-scale protein production, we reasoned that a reduced induction period of 1 h would be beneficial for bacterial production of these protein constructs.

The recombinant His-ChlaDUB1 or His-ChlaDUB2 constructs were purified by immobilised metal ion affinity chromatography (IMAC). HisTrap HP 5ml columns were used for purification and these columns are comprised of a matrix of immobilised Ni²⁺ ions that has a high affinity for binding His-tagged proteins in the *E.coli* lysate. Thus, when bacterial lysates were passed through the column, the exposed His-tags of His-ChlaDUB1 or His-ChlaDUB2 would form complexes with the Ni²⁺ ions. His-tagged constructs were eluted from the Ni²⁺ charged column using a linear imidazole gradient and 1ml fractions were collected every minute for 1 h.

To assess the purification of recombinant protein, 1µl from each fraction was spotted onto blotting paper and stained with Coomassie stain (Figure 5.16 A and B). Here, more protein was observed in fractions 6-14 and 9-12 for His-ChlaDUB1 and His-ChlaDUB2 respectively. Thus, we hypothesised that the His-tagged constructs had been eluted off within these fractions. To determine the size of these eluted proteins, we electrophoresed fractions 4-20 on an SDS-PAGE gel (Figure 5.16 C and D). Complementary to the Coomassie spot test, fractions 8-10 and fraction 10 for His-ChlaDUB1 and His-ChlaDUB2 respectively demonstrated the greatest amount of protein. However, protein bands corresponding to the chlamydial DUB constructs were not able to be confidently distinguished from other protein bands and, furthermore, degradation products could not be easily identified. Thus, fractions 6-12 and 8-14 of purified His-ChlaDUB1 and His-ChlaDUB2 respectively were immunoblotted using anti-His antibody to identify the presence of these chlamydial DUB constructs. Furthermore, we also immunoblotted samples obtained from the bacterial pellets and first flow-through from IMAC in order to confirm whether the constructs had been retained earlier in the methodology (Figure 5.16 E and F). His-ChlaDUB1, and seemingly His-ChlaDUB2, was observed in each of the fractions examined as well as in the pellet and IMAC flow-through. This suggests that the binding of His-tagged chlamydial DUB constructs to the Ni²⁺ column was not particularly efficient.

Initially, we had hypothesised that His-ChlaDUB1 and His-ChlaDUB2 were eluted in fractions 6-14 and 9-12 respectively on the basis that a greater

amount of protein had been eluted here. However, given that we had identified earlier on that neither protein was produced in particularly large quantities (Figure 5.16 C and D), we reasoned that the His-tagged chlamydial DUB constructs might have been eluted in later fractions and in smaller quantities. Thus, we immunoblotted fractions 12-28 for each construct using anti-His antibody to deduce whether the His-ChlaDUB1 or His-ChlaDUB2 was predominantly eluted at these higher imidazole concentrations (Figure 5.16 G and H). Full-length His-ChlaDUB1 was observed in fractions 12-20 as indicated by protein bands of size 45kDa (Figure 5.16 G). A smaller degradation product, approximately 37kDa in size, was also observed in these fractions alongside a product of approximately 26kDa in fractions 18-24. This complements our previous immunoblot (Figure 5.15 B). Full-length His-ChlaDUB2 was observed in all fractions tested here as indicated by protein bands of size 37kDa (Figure 5.16 H). Smaller degradation products of approximately 30kDa and 23kDa can also be seen in fractions 12-22 and 12-26 respectively. These protein bands also correlate to our earlier immunoblot (Figure 5.15 B).

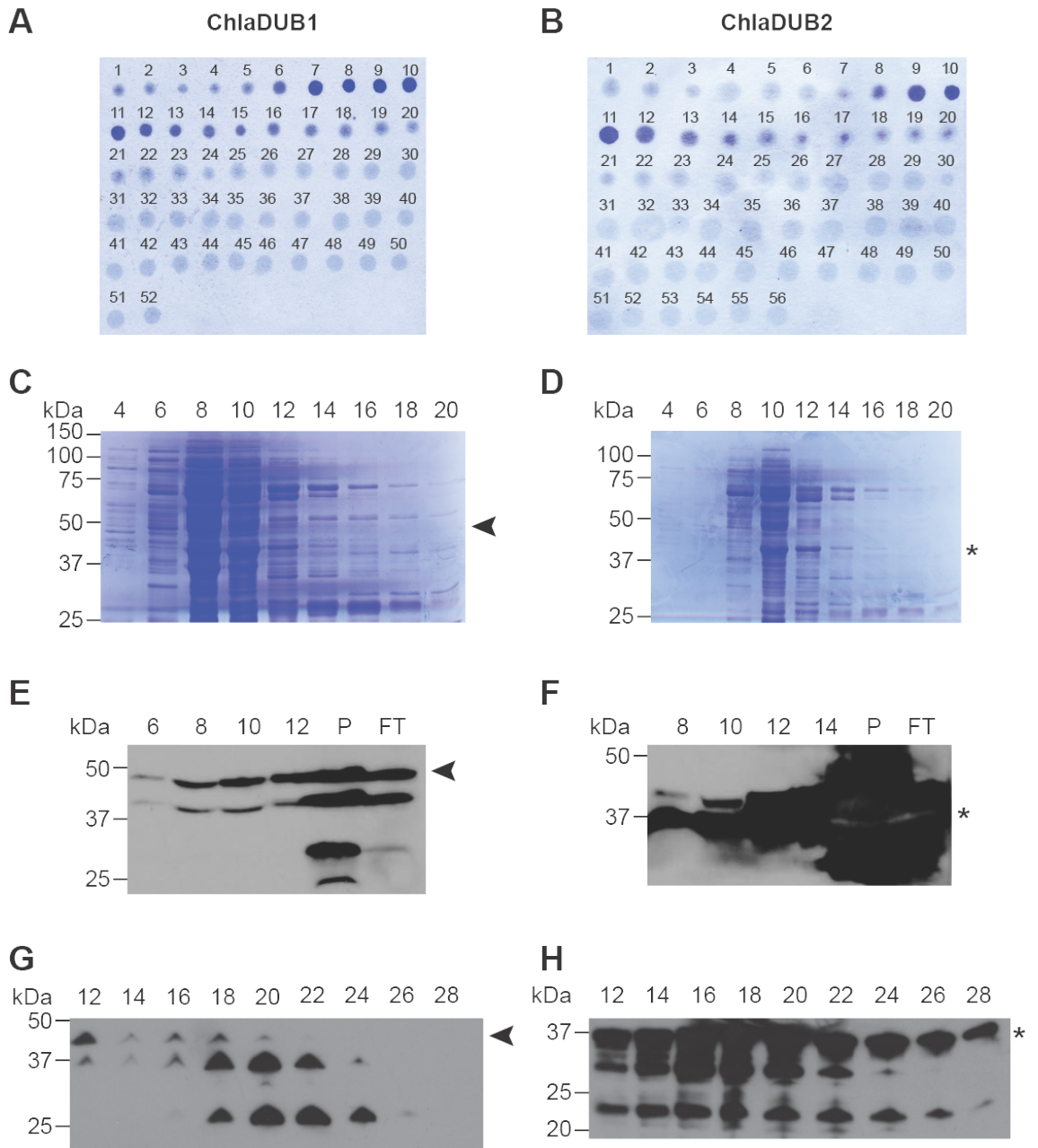


Figure 5.16 Purification of ChlaDUB1 or ChlaDUB2. His-ChlaDUB1 or His-ChlaDUB2 was purified from bacterial lysates by immobilised metal ion affinity chromatography. **A, B.** 1ml fractions were collected every min for 1 h. 1µl fraction was spotted onto blotting paper and stained with Coomassie. **C-H.** 20µl specified fractions were electrophoresed on a 10% SDS-PAGE gel and either stained with Coomassie (**C, D**) or immunoblotted using anti-His antibody (**E-H**). Left panels, His-ChlaDUB1; right panels, His-ChlaDUB2. Arrowhead = ChlaDUB1. * = ChlaDUB2.

Given the low level expression of His-ChlaDUB1 and His-ChlaDUB2, we pooled fractions 7-14 and 14-21 respectively and concentrated samples using an ultra-

15 centrifugal filter device (Amicon) with a 3kDa cut-off. Thus, any molecules less than 3kDa would be filtered out of this solution. We assessed whether His-ChlaDUB1 or His-ChlaDUB2 were still expressed post-concentration by Ponceau staining and immunoblotting. Ponceau staining of blots revealed that neither the His-ChlaDUB1 nor His-ChlaDUB2 samples are pure (Figure 5.17 A). As seen previously (Figure 5.16 C and D), several other protein bands of various sizes were also observed. A number of these were of a higher molecular weight than His-ChlaDUB1 or His-ChlaDUB2, thus these cannot be considered as DUB degradation products. Immunoblot analysis revealed that His-ChlaDUB1 is present in the sample together with a degradation product and another higher molecular weight protein that was also detected by the His antibody (Figure 5.17 B left panel). His-ChlaDUB2 was also detected by immunoblot alongside several degradation products and a number of higher molecular weight proteins (Figure 5.17 B right panel). This further indicates that the samples are not pure.

To investigate whether the His-ChlaDUB1 or His-ChlaDUB2 in the prepared samples were enzymatically active, we performed a K63-linked DUB activity assay. Samples were incubated with IQF-K63-linked diUb substrates and their fluorescence intensities were recorded every minute for 90 min. His-ChlaDUB1, but not His-ChlaDUB2, demonstrated DUB activity across the 90 min time course (Figure 5.17 C). Notably, however, ChlaDUB2 did not demonstrate neither K63- nor K48-linked DUB activity in previous experiments (Figure 5.6 B and Figure 5.7).

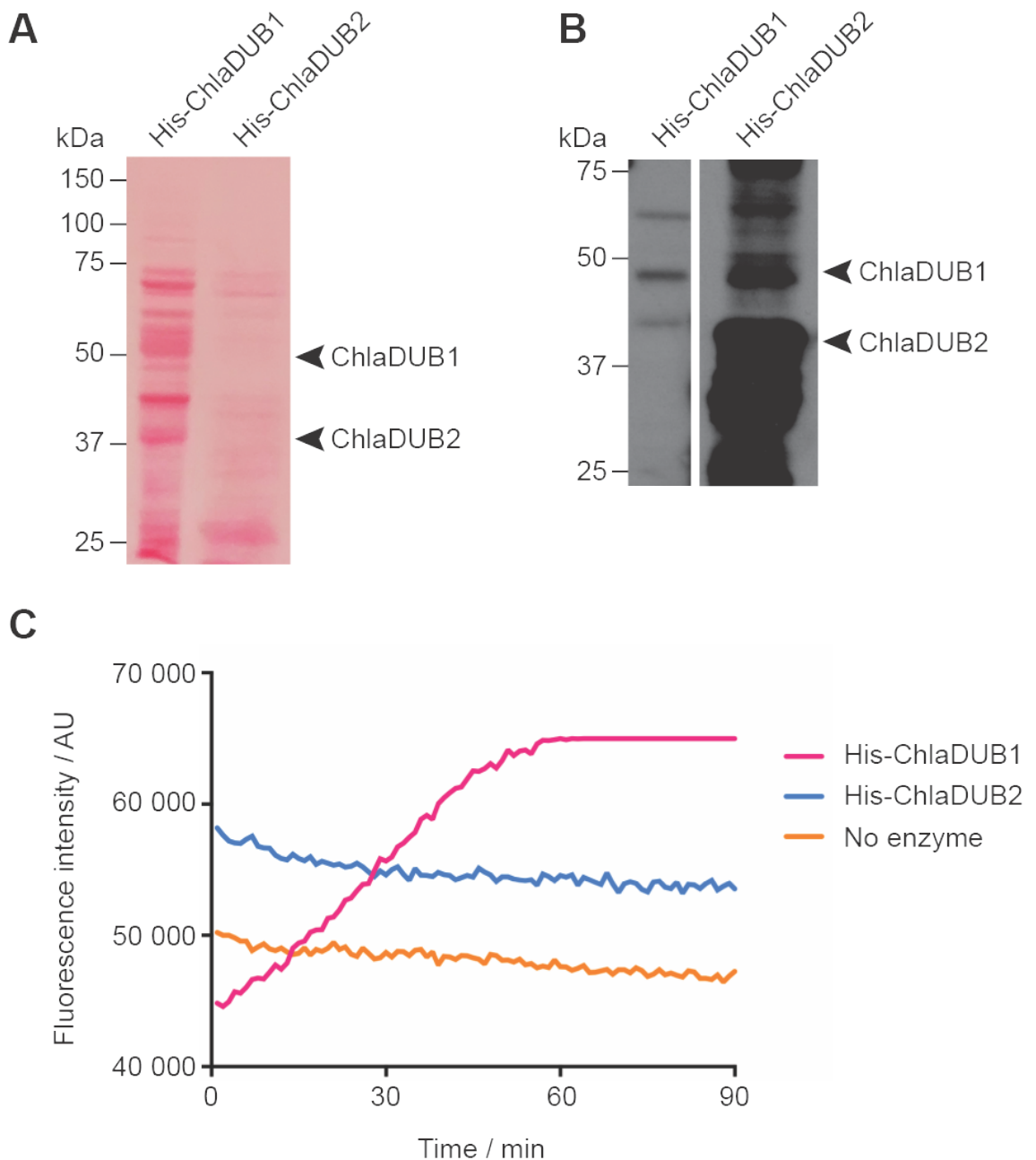


Figure 5.17 Expression and enzymatic activity of recombinant ChlaDUB1 and ChlaDUB2. IMAC fractions were pooled and concentrated. 20µg protein from pooled fractions was electrophoresed on a 15% SDS-PAGE gel and stained with Ponceau S stain (**A**) or immunoblotted using anti-His antibody (**B**). 50µg protein from pooled fractions was incubated with IQF-K63-diUb and the fluorescence intensities were recorded as a function of time (**C**).

Given that the purified chlamydial DUB preparations were also comprised of several other protein contaminants, we sought to repeat the bacterial production and purification of His-ChlaDUB1 and His-ChlaDUB2 from bacterial lysates in an attempt to generate purified recombinant DUB. Unfortunately, however, this

was not feasible within the time frame of this study. Ideally, with time permitting, we would have returned to the protein production stage to optimise the conditions required for producing stable full-length His-ChlaDUB1 or His-ChlaDUB2 in bacteria with the hope of minimising protein degradation. The IPTG induction period would also be further optimised to assess the time by which sufficient recombinant protein is produced with minimal degradation. Following these optimisations, we would have then repeated the IMAC purification to isolate His-ChlaDUB1 or His-ChlaDUB2 for use in mass spectroscopy (using previously optimised conditions) to identify interacting substrates.

5.3. Discussion

5.3.1. Bioinformatic analysis of ChlaDUB1 and ChlaDUB2

We initially performed bioinformatic analysis to investigate whether ChlaDUB1 and ChlaDUB2 were capable of deubiquitinating substrates as a result of their primary amino acid sequence. ChlaDUB1 has previously been reported to harbour such catalytic capabilities and substrates for this enzyme have previously been identified (Le Negrate et al., 2008b, Fischer et al., 2017). However, only one report has demonstrated the catalytic capability of ChlaDUB2 using reporter probes (Misaghi et al., 2006) and currently no substrates for this enzyme have yet been identified, thus placing doubt on the functionality of this enzyme during chlamydial infection.

The full protein sequence and catalytic domain alignments (both pairwise and multiple) revealed several regions of similarity between the chlamydial DUBs and other bacterial DUBs. This suggests that this selection of bacterial DUBs is likely to share a common ancestral protein and hence might perform a similar biological function. It is not uncommon for different bacterial proteins with similar catalytic capabilities to interact with similar or identical substrates in order to modulate host cell responses in a similar way to aid bacterial survival. For example, the inhibitory subunit of the NF κ B signalling pathway, I κ B α , is targeted by several different bacterial proteins during infection, including deubiquitinases secreted by *Yersinia* (Zhou et al., 2005, Mukherjee et al., 2006), *Salmonella* (Le Negrate et al., 2008a, Ye et al., 2007) and *Chlamydia* (Le Negrate et al., 2008b). Given that ChlaDUB1 and ChlaDUB2 share a similar level of sequence commonality to other bacterial DUBs, including those secreted by *Yersinia* and *Salmonella*, we anticipate that ChlaDUB2 is also likely to function in a similar way and that substrates will be identified upon further research.

Given that biological function is highly linked to protein structure and not simply the primary amino acid sequence, we were mindful not to infer too much from the sequence alignments because although the sequences shared some similar regions, few of these were highly identical. It would be beneficial to model the 3-dimensional structure of ChlaDUB1 and ChlaDUB2 and investigate how minor

changes to the primary amino acid sequence can alter the shape of the protein and affect the accessibility to the enzymes active site. This structural information would provide further insights into the functionality of chlamydial DUBs within the context of an infection. Unfortunately, the determination of protein structure was beyond the scope of this project, but we instead investigated the cellular effect of expressing ChlaDUB1 and ChlaDUB2 within a mammalian model system.

5.3.2. Expression of ChlaDUB1 and ChlaDUB2 in mammalian cells

We decided to transition our study of ChlaDUB1 and ChlaDUB2 from yeast to a mammalian model system. Although yeast provides a useful and effective model to study bacterial proteins, we reasoned that by studying the intracellular effect of these *Ct* DUBs in mammalian cells, we would achieve a more clinically relevant understanding of human infection and chlamydial pathogenesis.

We chose to investigate the intracellular effects of ChlaDUB1 or ChlaDUB2 expression in HeLa cells using a Flp-In transfection system. This transfection system is well established and widely used within the Pryor lab for the study of recombinant proteins of interest. HeLa cells were selected as the mammalian host cell of choice, because they have been used extensively in chlamydial research and for studying the intracellular effects of numerous bacterial effectors.

ChlaDUB1 and ChlaDUB2 were successfully expressed in Flp-In HeLa cells. Both DUBs were electrophoresed on an SDS-PAGE gel and immunoblotted using an α -myc antibody. However, the protein band for both DUBs was located at a slightly higher molecular weight than expected. We anticipated that myc-ChlaDUB1 and myc-ChlaDUB2 would be identified at 46kDa and 38kDa respectively following the incorporation of the 1.2kDa myc tag. However, the observed protein bands were approximately 50kDa and 40kDa respectively. There are several possible explanations for the discrepancy in molecular weight. For example, post-translational modification of the DUBs by host cell enzymes might have increased the mass of the proteins. Alternatively, the cell lysates might not have been fully denatured prior to electrophoresis or the

disulphide bonds within the DUBs were not fully reduced by the β -mercaptoethanol prior to electrophoresis. Given the clear distinction between uninduced and induced conditions, we were not concerned that the protein bands were representative of a different unexpected protein. Thus, we continued our investigation to test for enzymatic activity.

We sought to determine whether the chlamydial DUBs were enzymatically active when expressed in Flp-In HeLa cells and to do this we made use of the commercially available K63-linked IQF-diUb substrate. Previously, ChlaDUB1 has demonstrated K63-linked deubiquitinase activity, but no preference for other linkage types (Pruneda et al., 2016). On the other hand, although the linkage specificity of ChlaDUB2 has yet to be determined, the secretion of this enzyme has been demonstrated during the course of chlamydial infection (Claessen et al., 2013).

K63-linked deubiquitinase activity was detected in cell lysates expressing ChlaDUB1, but not ChlaDUB2. Our observation complements the work of Pruneda et al. (2016) who have previously demonstrated the linkage specificity of ChlaDUB1. We chose to immunoprecipitate myc-ChlaDUB1 or myc-ChlaDUB2 using α -myc-coupled beads to firstly confirm that the enhanced enzymatic activity observed in lysates expressing ChlaDUB1 was solely due to this bacterial DUB, and secondly, to test whether potentially low expression levels of ChlaDUB2 were responsible for the absence of enzymatic activity in this sample. Purified ChlaDUB1 isolates retained their catalytic ability to cleave the K63-linked diUb substrate. However, no enzymatic activity was demonstrated for ChlaDUB2 isolates.

Given the absence of deubiquitinase activity observed for ChlaDUB2, we reasoned that this DUB might possess a preference for an alternative ubiquitin linkage type. Thus, we performed an identical activity assay but instead used a K48-linked IQF-diUb substrate. Unlike K63-linked polyubiquitin chains that are usually involved in non-degradative signalling roles, K48-linked polyubiquitin chains are typically involved in targeting the respective ubiquitin-tagged protein for proteasomal degradation. Thus, an alternative linkage preference compared

to ChlaDUB1 would suggest a different role during chlamydial infection. However, no enzymatic activity was observed across the time course tested.

Although monoubiquitination and K48- or K63-linked polyubiquitin chains are the most abundant type of ubiquitin linkage (Mevissen and Komander, 2017), we remained mindful that ChlaDUB2 might demonstrate linkage preference towards K6-, K11-, K27-, K29- or K33-linked polyubiquitin chains. There are also numerous possible reasons that may explain the lack of enzymatic activity demonstrated here by ChlaDUB2. For example, ChlaDUB2 may require additional factors that induce DUB activity by forming a dimer or a multi-protein complex or perhaps modify the DUB via a post-translational modification. These additional factors might be absent or expressed in only small quantities in non-physiological conditions, but during a normal bacterial infection their expression could be triggered or upregulated following a host immune response. Given that several DUBs function within multi-protein complexes (Aufderheide et al., 2015, Echaliier et al., 2013, Lee et al., 2005), this is not an implausible theory. Furthermore, numerous DUBs have been shown to require PTMs, such as phosphorylation (Hutti et al., 2007, Hutti et al., 2009, Reiley et al., 2005), ubiquitination (Todi et al., 2009, Faggiano et al., 2015), SUMOylation (Kobayashi et al., 2015, Zhen et al., 2014) and oxidation (Lee et al., 2013, Kulathu et al., 2013) for functioning.

The enzymatic assay itself is also not representative of a physiological environment and thus is susceptible to flaws. The IQF-diUb substrates used in this assay are present in high concentrations and typically much higher than a DUB would encounter intracellularly. Given the saturation of substrate, there is the risk of non-specific DUB activity whereby enzymes cleave the substrate because of the saturation rather than linkage preference. Furthermore, the substrates used in this assay are cell-impermeable, thus can only be used in cell lysates. However, the lysis of cells typically dilutes the cytosol and can in turn lead to the dissociation of protein complexes and subsequently result in a loss of enzymatic activity (Claessen et al., 2013). Notably, however, although we should be aware of these flaws, assays of this kind have previously been used to determine linkage preference (Mevissen et al., 2016, Pruneda et al.,

2016). An alternative method that we could have used to assess linkage specificity of these chlamydial DUBs involves the incubation of DUBs with diubiquitin substrates of different linkage types for varying time intervals. To assess linkage specificity, samples can be resolved on a low percentage SDS-PAGE gel and silver stained to visualise diubiquitin and any monoubiquitin protein bands. The presence of monoubiquitin protein bands is indicative of deubiquitinating activity. This method has been previously used to determine DUB linkage preferences (Mevissen et al., 2013, Pruneda et al., 2016).

Although we were unable to demonstrate ChlaDUB2 enzymatic activity, we continued to investigate whether ChlaDUB2 induced any intracellular effects in mammalian cells because we were mindful that the DUB might harbour alternative linkage specificity or that its activity might have been below the detection threshold for this assay.

5.3.3. Effect of ChlaDUB1 or ChlaDUB2 on intracellular compartments

Chlamydiae are able to survive intracellularly by modifying the properties of the inclusion early during infection in order to traffic the inclusion to the peri-Golgi region and avoid fusion with lysosomes, meanwhile also promoting fusion with other compartments, such as nutrient-rich exocytic vesicles. Chlamydiae recruit different families of fusion regulators, such as Rab GTPases and their effectors, phosphoinositide lipid kinases and SNARE proteins in order to achieve the selective fusion of different endocytic compartments following uptake.

Bacterial virulence factors often disrupt the morphology or localisation of intracellular organelles. For example, the *Rhodococcus equi* virulence protein, VapA, has recently been shown to induce lysosomal swelling when expressed from within the lysosomal lumen (Rofe et al., 2017).

Given the ability of chlamydiae to selectively avoid interaction with lysosomes, we sought to assess whether ChlaDUB1 or ChlaDUB2 affected the morphology or localisation of endosomal compartments in Flp-In HeLa cells in order to hijack this trafficking pathway. We studied the effect of expressing ChlaDUB1 or ChlaDUB2 on early and late endosomes, lysosomes, autophagosomes and

actin filaments. Furthermore, notably, the myc staining of the chlamydial DUBs implied that both DUBs were distributed throughout the cytoplasm of the cell following expression under the doxycycline promoter. Previously, Le Negrate et al. (2008b) have reported the cytoplasmic localisation of ChlaDUB1 24 h post infection. However, contrary to this, Fischer et al. (2017) have recently shown ChlaDUB1 (referred to here as Cdu1) co-localising with the inclusion membrane protein, IncA. Although our finding corresponded to that of Le Negrate et al., we were mindful that we had expressed ChlaDUB1 as a recombinant protein, whereas Le Negrate et al. and Fischer et al. had studied the localisation of ChlaDUB1 during a chlamydial infection of HeLa cells. Thus, if any additional chlamydial factors are required for the targeting of ChlaDUB1 to its specific localisation, the localisation of ChlaDUB1 in our study may not reflect that during a chlamydial infection.

The markers EEA1, ciMPR and LAMP1 were used to stain early endosomes, late endosomes and lysosomes respectively. However, the appearance of these organelles in cells expressing myc-ChlaDUB1 or myc-ChlaDUB2 was indistinguishable from that seen in control cells. Notably, however, disruption to endosomal compartments may be dependent on the correct localisation of the DUBs within the cell. For example, previous work in the Pryor lab that examined the intracellular effect of expressing the *R. equi* virulence protein, VapA, in HeLa cells showed that lysosomes became swollen when VapA was expressed within the lumen of the lysosome, but not when expressed in the cytoplasm (Rofe et al., 2017). However, given that ChlaDUB1 is secreted by a T3SS and thus would be translocated in the host cell cytoplasm *in vivo*, together with its reported localisation to the cytoplasm during a chlamydial infection (Le Negrate et al., 2008b), we did not investigate the targeting of ChlaDUB1 to other intracellular compartments.

We also assessed whether ChlaDUB1 or ChlaDUB2 affected the morphology or localisation of autophagosomes. Previously, DUBs have been shown to regulate autophagy and bacterial expression of DUBs provides the opportunity for the bacterium to subvert or circumvent the host cell autophagic response. For example, the *Salmonella* DUB, SseL, functions to deubiquitinate

ubiquitinated structures to prevent them from being recognised by the autophagy receptor, p62, which would otherwise target them for autophagic degradation (Mesquita et al., 2012). In doing so, SseL DUB activity lowers the autophagic flux and favours bacterial survival. Although the chlamydial inclusion does not directly fuse with autophagosomes, autophagic markers are redistributed to the inclusion during chlamydial infection (Al-Younes et al., 2004). Thus, we chose to assess whether the morphology or localisation of autophagosomes was affected following the expression of chlamydial DUBs. However, cells expressing ChlaDUB1 or ChlaDUB2 were seemingly indistinguishable from control cells.

Furthermore, we also sought to test whether the chlamydial DUBs disrupted the structure of actin filaments throughout the cell. Like many other intracellular pathogens, *Ct* uses the host cytoskeleton for host cell invasion whereby virulence proteins induce actin polymerisation at bacterial attachment sites in order to promote bacterial entry (Carabeo et al., 2002, Rottner et al., 2005). In this study, we used phalloidin to stain actin filaments. Here, actin filaments in cells expressing myc-ChlaDUB1 or myc-ChlaDUB2 appeared indistinguishable from control cells. We reasoned that these DUBs alone did not therefore play a role in the reorganisation of the actin cytoskeleton during infection. However, these DUBs may contribute towards a multi-protein approach that leads to actin cytoskeletal manipulation that cannot be simulated in the model used in this study.

Although we did not explore other organelles within the scope of this study, it would be interesting to investigate the effect, if any, of expressing ChlaDUB1 or ChlaDUB2 on the Golgi and ER. Both of these organelles are involved in secretion and thus are widely targeted by bacteria for the establishment and maintenance of an intracellular replicative niche. Furthermore, chlamydiae have been shown to cause fragmentation of the Golgi (Heuer et al., 2009) and maintain close interactions with the ER during infection (Derre, 2015). Thus, given the exploitation of these organelles by the bacterium for inclusion divergence, nutrient acquisition and bacterial survival, it would be interesting to

investigate whether these organelles are affected by the recombinant expression of ChlaDUB1 or ChlaDUB2.

5.3.4. Effect of ChlaDUB1 and ChlaDUB2 on global ubiquitin levels

Mammalian and bacterial DUBs can demonstrate broad substrate specificities. For example, the *Salmonella* DUBs, SseL and AvrA, have both been shown to possess multiple substrates. ChlaDUB1 has also been reported to suppress NF κ B activation by preventing the degradation of I κ B α (Le Negrate et al., 2008b) and, more recently, Fischer et al. (2017) have demonstrated a role of ChlaDUB1 in the stabilisation of the apoptotic regulator, Mcl-1. Given that two distinct substrates have previously been identified for ChlaDUB1, we reasoned that ChlaDUB1 might also have additional currently unidentified substrates. In addition, although no substrates have yet been determined for ChlaDUB2, we anticipated that this DUB might also harbour broad substrate specificity.

To test whether ChlaDUB1 or ChlaDUB2 demonstrated broad substrate specificity, we performed a global ubiquitin immunoblot using an anti-ubiquitin antibody that detects ubiquitin, polyubiquitin and ubiquitinated proteins. However, we were mindful that if ChlaDUB1 or ChlaDUB2 had multiple, but only few, substrates, the overall effect of deubiquitinating activity might not be noticeable from the immunoblot.

Immunoblotting using the anti-ubiquitin antibody proved troublesome. Initially, immunoblots were difficult to interpret due to high background data and a poor ubiquitin signal. Typically, ubiquitinated proteins are observed as a 'smear' extending throughout a wide range of molecular weights. The smear, as opposed to a ladder, is a result of the heterogeneity of the modification, for example, linkage type, polyubiquitin, multi-monoubiquitin, or a combination of ubiquitination together with phosphorylation and sumoylation (Emmerich and Cohen, 2015). We performed standard optimisation steps, such as comparing the use of a nitrocellulose to PVDF membrane and blocking in PBS-T or TBS-T and BSA or milk, but to no avail. However, as suggested by Emmerich and Cohen (2015), we boiled the nitrocellulose membrane following protein transfer for 30 min and this significantly improved the signal strength of anti-ubiquitin

antibody and the quality of the blotting. This might have enhanced the ubiquitin signal, because ubiquitin is a small globular protein that is difficult to denature and thus, the ubiquitin epitopes required for antibody recognition might not be accessible. By incorporating a denaturing step into the immunoblotting procedure, the epitope required for antibody recognition might become more easily accessible (Emmerich and Cohen, 2015).

To assess the global ubiquitination levels of ChlaDUB1 or ChlaDUB2, we incorporated the additional denaturing step into our immunoblotting procedure. As anticipated, there was not a substantial difference in global ubiquitin levels between cells expressing ChlaDUB1 or ChlaDUB2 relative to controls. Arguably, however, there appeared to be slightly reduced levels of ubiquitinated proteins in cells expressing ChlaDUB1 compared to control cells in the absence of the proteasomal inhibitor, MG132. Given that we had initially predicted that any effect on global ubiquitination might be weak and difficult to detect, together with the two substrates that ChlaDUB1 has been reported to interact with, we reasoned that ChlaDUB1 might demonstrate specificity towards a handful of ubiquitinated substrates.

Although there was no identifiable distinction between cells expressing ChlaDUB2 and control cells, we remain positive that substrates for ChlaDUB2 will be identified by future research. ChlaDUB2 might harbour specificity towards fewer ubiquitinated substrates that were not detectable by this experiment. Furthermore, although ChlaDUB2 may preferentially deubiquitinate alternative linkage types, we were conscious that we were unable to demonstrate K48- or K63-linked DUB activity in earlier experiments; thus, it is reasonable to believe that ChlaDUB2 might be inactive in our sample.

5.3.5. Identification of substrates for ChlaDUB1 and ChlaDUB2

Seemingly, bacterial DUBs commonly function to attenuate NF κ B-related inflammatory responses by deubiquitinating and subsequently preventing the degradation of I κ B α (Le Negrate et al., 2008a, Ye et al., 2007, Kim et al., 2005, Zhou et al., 2005). However, bacterial DUBs have also been reported to manipulate other intracellular pathways. For example, the *Burkholderia*

pseudomallei DUB, TssM, has been shown to deubiquitinate I κ B α as well as TRAF-6 and TRAF-3 and hence disrupts the activation of not only the NF κ B pathway, but also the interferon stimulated response element (ISRE) pathway (Tan et al., 2010). Moreover, although the *Salmonella* DUB, SseL, prevents the degradation of I κ B α , it has also been shown to disrupt host lipid metabolism leading to the accumulation of lipid droplets in infected cells (Arena et al., 2011).

Given that we observed a slight reduction in global ubiquitin levels of cells expressing ChlaDUB1, together with the previous reporting of two different substrates for ChlaDUB1 (Le Negrate et al., 2008b, Fischer et al., 2017), we sought a broader approach to identify substrates for ChlaDUB1 and ChlaDUB2. We anticipated that these chlamydial DUBs might play multiple roles during infection and thus have a number of substrates particularly because *Ct* has a small genome and thus a limited number of genes required for virulence and intracellular survival.

5.3.5.1. Optimisation of mass spectroscopy experiments

A proteomics mass spectroscopy approach was an attractive option for investigating substrates given its ability to screen all proteins present in a cell lysate and identify those harbouring the unique K- ϵ -GG motif following trypsin digestion. This would ultimately enable us to discriminate between ubiquitinated substrates and non-ubiquitinated proteins and compare control and DUB samples to determine which proteins are likely substrates of ChlaDUB1 or ChlaDUB2.

We had based our proteomics approach on a report by Nakayasu *et al.* (2015) who previously identified both known and two previously unknown substrates for the *Salmonella* DUB, SseL. Given that SseL is a bacterial DUB and because *Ct* and *Salmonella* share similar intracellular lifestyles through their survival and replication within the inclusion or *Salmonella*-containing vacuole respectively, we reasoned that the approach undertaken by Nakayasu et al. would be relevant for the identification of ChlaDUB1 and ChlaDUB2 substrates.

We cooperated with the Proteomics laboratory within the Technology Facility at the University of York to optimise the conditions required for mass spectroscopy using WT Flp-In HeLa cells. Firstly, we replicated the methodology directly from Nakayasu et al. and lysed cells in a HEPES lysis buffer that contained Triton X-100. However, we became aware that the presence of this detergent in the lysis buffer could be detrimental to mass spectroscopy due to its polymeric nature that enables it to ionise more readily than peptides and hence result in misleading data outputs. Thus, we performed a detergent depletion protocol to mitigate any detrimental effects that the Triton X-100 may have on the samples. However, the ubiquitinated peptide's K- ϵ -GG motif contains an additional carboxyl terminal group and therefore, although they are peptides, they also harbour characteristics of a polymer, such as Triton X-100. Thus, by performing detergent depletion, there was a risk that ubiquitinated peptides would also be depleted from the sample. Given that few proteins and no ubiquitinated peptides were returned from the dataset, we anticipated that the presence of Triton X-100 in the lysis buffer and the subsequent depletion procedure had had a detrimental effect on our samples.

To improve yield, we modified our methodology by using a urea lysis buffer that was recommended for the preparation of cell lysates prior to the use of K- ϵ -GG immunoaffinity beads. This modification led to the identification of ubiquitinated peptides in the dataset returned from LC-MS/MS. However, the yield of ubiquitinated peptides was still relatively low and given that we anticipated fewer ubiquitinated peptides to be returned in DUB samples, we sought further optimisation.

To optimise further, we incubated cells with the proteasome inhibitor, MG132. We reasoned that this would prevent the degradation of ubiquitinated peptides and thus improve the yield of ubiquitinated peptides returned in our dataset. Although DUBs typically demonstrate linkage and/or substrate specificity, we note that the inhibition of the proteasome in this study deviates away from physiological conditions.

We also cultured cells on a larger scale to increase the amount of starting material, performed an additional reduction and alkylation step, purified peptides using a Sep-Pak C₁₈ column and lyophilised peptides without using a SpeedVac. These modifications led to a marked improvement in the yield of ubiquitinated peptides. Although we are unable to conclusively determine which final modification(s) resulted in this increased yield, we have now optimised this proteomics approach to identify ubiquitinated peptides in control cells.

5.3.5.2. Production of recombinant ChlaDUB1 and ChlaDUB2

E. coli were successfully transformed with His-ChlaDUB1 or His-ChlaDUB2 constructs. However, following a 4 h IPTG induction, neither of the protein constructs was strongly expressed. We had anticipated that a significant protein band would be visible at the appropriate molecular weight by Coomassie stain under induced conditions for both DUBs. However, there was no obvious protein band representing these constructs. Therefore, we generated an immunoblot using an anti-His antibody to determine whether the proteins had been expressed. Immunoblot analysis revealed that the proteins had been expressed albeit at a slightly higher molecular weight than expected. However, both His-ChlaDUB1 and His-ChlaDUB2 were visibly degraded with protein products at the full-length molecular weight as well as lower molecular weight bands. Furthermore, His-ChlaDUB2 was also expressed in uninduced conditions, suggesting that transcription has initiated in the absence of the IPTG inducer.

Given that His-ChlaDUB1 or His-ChlaDUB2 had not been abundantly expressed by these cells, the natural next step would be to prolong the incubation with IPTG, perhaps to an overnight induction. However, we anticipated that this might not prove beneficial because of the rapid degradation observed following a 4 h IPTG induction. Therefore, given that we required only a small amount of recombinant protein for proteomics, we chose to induce bacteria for 1 h in an attempt to mitigate the rapid degradation of these protein constructs.

Following a 1 h IPTG induction, bacteria were lysed and His-ChlaDUB1 or His-ChlaDUB2 constructs were purified by IMAC. A linear imidazole gradient was applied to elute the His-tagged constructs. Initially, we reasoned that His-ChlaDUB1 and His-ChlaDUB2 had been eluted in fractions 6-14 and 9-12 respectively given that these fractions demonstrated a greater amount of protein when Coomassie stained. When these fractions were immunoblotted, the DUB constructs were observed to be present. However, by previous experience in the Pryor lab, desired constructs would usually be eluted in later fractions than those observed here. Furthermore, given that a substantial protein band representing His-ChlaDUB1 or His-ChlaDUB2 was not initially observed when we tested for protein expression, we anticipated that perhaps the desired constructs had been eluted at later fractions, but were initially undetectable by traditional means because of their low level expression. Thus, we tested later fractions to test whether His-ChlaDUB1 or His-ChlaDUB2 had been eluted in greater quantities with an increased imidazole concentration. Unlike His-ChlaDUB1, His-ChlaDUB2 was observed in all later fractions tested (fractions 12-28) as a full-length protein, but also alongside degradation products.

Given that the chlamydial DUB constructs were present in these fractions, we pooled together fractions 7-14 and 14-21 for His-ChlaDUB1 and His-ChlaDUB2 respectively and concentrated the samples for further usage. Notably, the centrifugal filter devices used for the concentration of His-ChlaDUB1 and His-ChlaDUB2 had a 3kDa cut-off, thereby resulting in the depletion of components below this molecular weight. However, given that ChlaDUB1 and ChlaDUB2 are 45 and 37kDa respectively, it could have been more beneficial to use a higher molecular weight cut-off, although this might have removed chlamydial DUB degradation products too. The concentrated samples were tested to confirm the presence of His-ChlaDUB1 or His-ChlaDUB2. Both chlamydial DUB constructs were visible by Ponceau staining or immunoblotting. However, a substantial quantity of degradation products and contaminating proteins were also detected.

Although His-ChlaDUB1 demonstrated K63-linked DUB activity, we were cautious that a number of protein contaminants were present in the fractions and concentrated samples. Thus, by using these samples for mass spectroscopy experiments, we would be unable to conclusively determine whether any substrates identified by mass spectroscopy are solely substrates of ChlaDUB1 or ChlaDUB2 and not any of the contaminating proteins.

Subsequently, given the impurity of our His-ChlaDUB1 and His-ChlaDUB2 preparations and the limited time of this study, we were unable to identify substrates for ChlaDUB1 or ChlaDUB2 by mass spectroscopy within the timeframe. Notably, Misaghi et al. 2006 also experienced difficulties in expressing and purifying recombinant ChlaDUB1 and ChlaDUB2 in *E.coli* and other expression systems (Misaghi et al., 2006).

The use of a polyhistidine tag and IMAC offered numerous possibilities and several advantages for the purification of ChlaDUB1 and ChlaDUB2. For example, polyhistidine tags have a relatively small size and charge and thus their presence does not typically affect protein function. Furthermore, His-tagged proteins can be eluted from IMAC matrices under mild conditions thereby purifying proteins and retaining their biological activity. However, one major disadvantage of IMAC purification is the ease of non-specific binding of proteins to the IMAC column and this is particularly prevalent when the His-tagged protein is not expressed in high levels (Bornhorst and Falke, 2000). In our study, we observed low-level expression of His-ChlaDUB1 and His-ChlaDUB2 and high levels of protein contamination; hence we anticipate that an abundance of non-specific binding has affected this purification step. Histidine residues are relatively infrequent, particularly in bacterial hosts, thus we supposed that non-specific hydrophobic interactions might be responsible for the abundance of protein contaminants. If time had permitted, we would have investigated methods to reduce non-specific hydrophobic protein interactions with IMAC matrices, such as the addition of salt, glycerol or ethanol to bacterial lysates.

Alternatively, we could investigate the use of dual affinity tags for further purification of proteins. By this method, two or more affinity tags could be attached to the same protein, thus resulting in higher purity products than using each individual affinity domain alone. For example, His-tags can be coupled with the use of a GST affinity tag or a modified S-peptide of ribonuclease A (Panagiotidis and Silverstein, 1995, Kim and Raines, 1994).

5.3.6. Study progression

Within the time frame of this study, we were unable to identify host substrates of ChlaDUB1 or ChlaDUB2 substrates. However, we successfully optimised the conditions required for sample preparation and subsequent proteomics analysis in WT cells. Thus, time permitting, we would have repeated the protein production in order to yield purified His-ChlaDUB1 or His-ChlaDUB2 that could be subsequently fed to cells for mass spectroscopy analysis.

Despite the impure His-ChlaDUB1 sample preparation, we were able to demonstrate that the enzyme retains its biological activity following the incorporation of a polyhistidine tag and IMAC purification. Although DUB activity was not observed for His-ChlaDUB2, we anticipate that the absence of biological activity is similar to those explanations described in section 5.3.2.

Chapter 6: General discussion

This study explored the *Ct* virulence factor repertoire to identify proteins that manipulate intracellular membrane trafficking pathways that ultimately facilitates bacterial survival within infected cells. We applied targeted and random methodologies to identify these *Ct* virulence factors. We firstly performed a targeted screen whereby an *in silico* prediction program, EffectiveT3, was used to predict *Ct* proteins that were likely to be secreted by the bacterium's T3SS. These predicted proteins were then PEPSY screened to determine whether membrane trafficking had been disturbed. Secondly, we also generated and screened a *Ct* E/Bour genomic library in order to randomly screen the chlamydial genome for any virulence proteins involved in the disruption of intracellular membrane trafficking. In this study, we have identified two *Ct* virulence factors, ChlaDUB1 and ChlaDUB2, which demonstrate the ability to disrupt membrane trafficking. Both of these proteins have been previously defined as deubiquitinase enzymes and ChlaDUB1 has been shown to modulate the onset of host cell apoptosis and the NFκB inflammatory response (Misaghi et al., 2006, Le Negrate et al., 2008b, Fischer et al., 2017). In this study, we provide new insights into the putative role of ChlaDUB1 and ChlaDUB2 in the manipulation of intracellular membrane trafficking in host cells.

6.1.1. The host-pathogen interface

Ct is an obligate intracellular pathogen that modulates host signalling pathways and immune responses in an intricate and fine-tuned manner to facilitate bacterial survival and replication. It is widely understood that, upon internalisation, the chlamydial inclusion diverges away from the normal endolysosomal pathway that would otherwise lead to its destruction and instead migrates toward the MTOC while acquiring nutrients from redirected exocytic vesicles. Although developments in cell biology techniques, genetics, bacteriology and host biology have provided vital insights into the molecular mechanisms underpinning bacterial pathogenicity, the scientific community is still yet to fully elucidate the precise mechanisms by which *Ct* can manipulate

host trafficking responses to avoid lysosomal degradation. *Ct* harbours a small genome and approximately 10% of the chlamydial genome is believed to encode virulence factors (Betts-Hampikian and Fields, 2010). Researchers are continuing to unravel the complex and intricate mechanisms by which *Ct* uses virulence proteins to manipulate the host signalling pathways in order to enable the bacterium to survive intracellularly.

6.1.2. Identification of *Ct* virulence factors

In Chapter 3, we discuss a targeted approach to identifying T3S *Ct* effectors involved in disrupting membrane trafficking. We used an *in silico* prediction program, EffectiveT3, to predict *Ct* proteins that were likely to be secreted by the bacterium's T3SS. Although *Ct* also harbours a T2SS and T5SS we chose to predict proteins that were secreted via the T3SS with the reasoning that any virulence proteins that manipulate host trafficking pathways would be more likely to function within the host cytoplasm or inclusion membranes rather than the bacterial surface or inclusion lumen. Each of the several *Ct* proteins identified by this approach were expressed in a yeast model system and were screened for their ability to disrupt intracellular membrane trafficking using an established PEPSY screening method. This PEPSY screening method has previously been used to identify *Legionella* (Shohdy et al., 2005) and *Salmonella* (Raines et al., 2017) virulence proteins. This study is the first reported example of PEPSY screening to identify *Ct* virulence proteins. Disappointingly, however, such a VPS⁻ phenotype was not observed for any of the clones tested.

In Chapter 4, we present the generation of a *Ct* E/Bour genomic library. To our knowledge, this is the first reported non-LGV genital serovar E/Bour genomic library. The *Ct* genomic library was screened for proteins involved in disrupting intracellular membrane trafficking in yeast by PEPSY screening and, by this method, we identified 5 clones (PSCs) that displayed a plasmid-dependent VPS⁻ phenotype. Upon further characterisation and analysis of these clones, we identified two chlamydial deubiquitinases, namely ChlaDUB1 and ChlaDUB2, which were both encoded by two different clones (PSC50 and PSC66).

Interestingly, ChlaDUB1 was originally identified as a likely T3S effector by the *in silico* prediction program, EffectiveT3, and ChlaDUB2 was also predicted to be T3S by the updated version of this software. Although ChlaDUB1 was not seen to induce a VPS⁻ phenotype in Chapter 3, the clone demonstrated trafficking disruption, albeit inconsistently, when later tested in Chapter 4.

6.1.3. The role of ChlaDUB1 and ChlaDUB2 during Ct infection

In Chapter 5, we discuss the effects of ChlaDUB1 and ChlaDUB2 expression in a mammalian host. We reasoned that the use of a mammalian cell line would enable us to deduce a clinically relevant understanding of the role of chlamydial DUBs in bacterial pathogenicity. We demonstrated that ChlaDUB1 and ChlaDUB2 were successfully expressed in HeLa cells and that ChlaDUB1 possessed K63-, but not K48-, linked deubiquitinase activity. Similarly, Pruneda et al. (2016) have also demonstrated the preference of ChlaDUB1 for K63-linked polyubiquitin chains compared to all other ubiquitin linkage types. Remarkably, however, upon the activation of NF κ B signalling, the inhibitory subunit, I κ B α , becomes ubiquitinated via K48-linked polyubiquitination, thus targeting the protein for proteasomal degradation (Krappmann and Scheidereit, 2005). Interestingly, Le Negrate et al. (2008b) have previously demonstrated the presence of polyubiquitinated I κ B α in control HEK293N cells, but levels of polyubiquitination are visibly reduced upon the expression of ChlaDUB1. The authors also demonstrate the co-immunoprecipitation of ChlaDUB1 and I κ B α to further imply the association between these proteins and hence a likely linkage preference of ChlaDUB1 towards K48-linked polyubiquitin chains; a conclusion that opposes those from our study and Pruneda et al. (2016). Notably, however, Pruneda et al. report in their supplementary data that when the linkage specificity of ChlaDUB1 is examined using a 10-fold greater concentration of ChlaDUB1 (25nM instead of 2.5nM), the enzyme also demonstrates K48-linked and moderate levels of K11-linked deubiquitinase activity. Collectively, these findings suggest that perhaps ChlaDUB1 might function in a concentration dependent manner, whereby broader linkage specificity is demonstrated when ChlaDUB1 is present in greater concentrations. Alternatively, this observation might be a drawback of the experimental procedure used to assess linkage

specificity, whereby a high concentration of DUB or substrate leads to non-specific deubiquitination that is not necessarily representative of physiological conditions. However, I κ B α is a relatively common host target of bacterial DUBs and its inhibition can provide huge benefits for the invading bacterium. Furthermore, ChlaDUB1 and ChlaDUB2 are both expressed by *Ct*, but not by *Chlamydia pneumoniae* (*Cpn*) and, interestingly, the NF κ B signalling pathway is blocked during *Ct*, but not *Cpn*, infections (Misaghi et al., 2006). Thus, collectively, we predict that ChlaDUB1 might demonstrate less specific linkage preference and subsequently targets I κ B α for degradation at high and localised enzyme concentrations, but targets K63-linked polyubiquitin chains at lower enzyme concentrations.

When ChlaDUB1 and ChlaDUB2 were expressed in mammalian cells, we did not observe any localisation or morphological defects in early or late endosomes, lysosomes or autophagosomes. However, although we did not observe any morphological changes upon chlamydial DUB expression, we cannot rule out the possibility of any functional changes or defects induced by these chlamydial DUBs as this was not directly tested in this study. Furthermore, although *Ct* activates host RAC1 which, in turn, recruits host actin regulators to induce actin remodelling for internalisation of EBs into host cells (Nans et al., 2014), ChlaDUB1 or ChlaDUB2 did not induce any defects in actin structure in mammalian cells in this study. This further suggests that both chlamydial DUBs are unlikely to be pre-packaged T3S effectors that are rapidly secreted upon entry into host cells, particularly if the DUBs function in isolation. This correlates with Misaghi et al. (2006) who detect expression of the chlamydial DUBs at 16 h post-infection.

Although we did not observe any effect of ChlaDUB1 or ChlaDUB2 expression on EGFR internalisation, recycling or degradation, we would not yet eliminate the potential of EGFR to be a substrate of these DUBs given that the levels of EGFR are tightly regulated and thus are prone to ubiquitin modification. Furthermore, EGFR signalling pathways can lead to a diverse range of intracellular effects and therefore these receptors pose as an attractive target for manipulation by chlamydial DUBs. We anticipate that the use of

cycloheximide to inhibit *de novo* EGFR synthesis might provide a more accurate assessment of *in situ* EGFR internalisation, recycling and degradation.

We should also not discount the prospect of the presence of bacterial pseudoDUBs. Pseudoenzymes are present in all major enzyme families and function as a catalytically deficient variant of an enzyme. The field of pseudoenzymes is rapidly emerging and is highlighting the importance of the regulatory functions of these enzymes in signalling pathways together with their roles in disease (Reiterer et al., 2014, Evers and Murphy, 2016). Furthermore, pseudoenzymes have also been reported in the protozoan *Trypanosoma brucei* (Phillips, 2015). PseudoDUBs are typically found in conjunction with an active DUB, whereby the pseudoDUB acts as a direct modulator to activate, enhance or inhibit DUB activity. Given the absence of catalytic activity observed for ChlaDUB2 in this study and by Misaghi et al. (2006), there remains the possibility that ChlaDUB1 and ChlaDUB2 could potentially function as an active DUB : pseudoDUB pair. However, this would require substantial future investigation including sequence comparisons to known pseudoDUBs as well as structural, biochemical, and cellular and organism-based analysis. Thus, such conclusions regarding the pseudoenzyme status of ChlaDUB2 can, by no means, be made at this stage.

6.1.4. Future directions

There are several ways in which the results from this study could be built upon to deepen our understanding of ChlaDUB1 and ChlaDUB2 in *Ct* pathogenesis. Fundamentally, given that we have optimised the experimental procedure required for identifying ubiquitinated peptides via the K- ϵ -GG motifs generated following trypsin digestion, the primary focus for future work should be the preparation of purified ChlaDUB1 and ChlaDUB2 that can be fed to HeLa cells and processed by mass spectroscopy to identify interacting host substrates.

Given the role of ChlaDUB1 and ChlaDUB2 in the manipulation of the host ubiquitin system, it is reasonable to predict that these chlamydial DUBs might modulate host intracellular processes that rely on regulation by ubiquitin, for example protein degradation, vesicular trafficking and apoptosis (Misaghi et al.,

2006). ChlaDUB1 has previously been implicated in host cell apoptosis modulation (Fischer et al., 2017), the inhibition of I κ B α degradation (Le Negrate et al., 2008b) and, in this study, potentially in membrane trafficking. Thus, future experimental avenues should focus on other cellular functions that are closely regulated by the ubiquitin system, such as the cell division cycle, DNA damage responses and tyrosine kinase receptor signalling.

Given that the effect of ChlaDUB1 and ChlaDUB2 expression on intracellular membrane trafficking disruption was initially observed in a yeast model system, future experiments could be performed in yeast. For example, interaction studies, such as yeast 2-hybrid, could be performed to determine interacting substrates. This could inform future experiments in mammalian cells by examining mammalian homologs of yeast substrates.

Furthermore, given that *Ct*, but not *Cpn*, harbours the genes encoding ChlaDUB1 and ChlaDUB2 (Misaghi et al., 2006), avenues for future research could also compare intracellular membrane trafficking between *Ct* and *Cpn* infections to further define the roles of ChlaDUB1 or ChlaDUB2. Although the expression of ChlaDUB1 and ChlaDUB2 are not the only difference between *Ct* and *Cpn* genomes, a comparison might contribute towards the identification of trafficking manipulation mechanisms.

Additionally, to expand upon our understanding of ChlaDUB1 and ChlaDUB2 in a clinically relevant system, these chlamydial DUBs should be examined in an *in vitro*, and eventually *in vivo*, system following chlamydial infection. A flaw with our experimental design in this study is that we have recombinantly expressed ChlaDUB1 and ChlaDUB2 in model systems. Therefore, the pathogenic functionality of these chlamydial DUBs might have been overlooked if they function as part of a multi-protein complex or require activation by other chlamydial factors that are present during chlamydial infection. To investigate whether the chlamydial DUBs function in a multi-protein complex, co-immunoprecipitation (co-IP) or pull-down assays could be used to isolate the chlamydial DUB together with any other *Ct* or host proteins that may interact with it.

Until relatively recently, chlamydiae have been intractable to genetic manipulation and thus standard genetic approaches to elucidating the functionality of *Ct* virulence factors that are frequently used in other research fields, such as genetic knockouts, have largely been prevented. However, recent developments in chlamydial genetics offer a promising outlook for the future of the genetic modification of this bacterium (Wang et al., 2011, Nguyen and Valdivia, 2012, Kari et al., 2011, Johnson and Fisher, 2013, Yeung et al., 2017). For example, Mueller et al. (2016) have recently reported a novel system that targets chlamydial genes for deletion or allelic exchange and were able to successfully delete two known T3SS effector genes (Bastidas and Valdivia, 2016). This offers a promising future with the potential to assess the effect on chlamydial infections upon the deletion of the genes encoding ChlaDUB1 or ChlaDUB2. These emerging genetic methods, together with on-going technological advances, should be explored to investigate the effect of ChlaDUB1 or ChlaDUB2 mutants on chlamydial pathogenicity.

6.1.5. Concluding remarks

The work presented in this thesis offers new insights into a potentially novel role of ChlaDUB1 and ChlaDUB2 in the disruption of host membrane trafficking. Both ChlaDUB1 and ChlaDUB2 were identified as likely T3S *Ct* effectors as well as being detected by PEPSY screening of a *Ct* genomic library. The presence of both genes in two distinct VPS⁻ PSC clones further supports their role in membrane trafficking. However, further experimental validation is required to confirm their virulence in mammalian cells.

This work builds upon our current understanding of chlamydial pathogenicity and further implies that, like other bacterial DUBs, chlamydial DUBs likely demonstrate broad specificity towards a variety of host substrates. This paves the way for future research to investigate the role of chlamydial DUBs in the manipulation of host membrane trafficking during infection.

Appendix

Oligomer sequences

Construct	Oligomer	
BOUR_00933 fragment	F	CTCGTCTAGAGGATCATGTATGAAGATATGGCTCGACGA
	R	GTCCAAAGCTGGATCTTAGAAAGGAGCTTTTGCTTCAGG
BOUR_00932 DUB domain	F	CTCGTCTAGAGGATCATGAGCTCTGGCCGAGTAGGAAAT
	R	GTCCAAAGCTGGATCCTAATCCGTAGTTGGCCAGCTCAA
Myc-ChlaDUB1 pcDNA5/FRT/T0	F	TACCGAGCTCGGATCGCCACCATGGAACAAAAACTCATCTCA GAAGAGGATCTGATGTTGTCTCCCACCAACTCAACT
	R	GGCGATCCGAGCTCGCAGATCCTCTTCTGAGATGAGTTTTTG TTCCATGGTGGCCAAGCTTAAGTTTAA
Myc-ChlaDUB2 pcDNA5/FRT/T0	F	TACCGAGCTCGGATCGCCACCATGGAACAAAAACTCATCTCA GAAGAGGATCTGATGGAACCAATTCATAATCCTCCC
	R	GGCGATCCGAGCTCGCAGATCCTCTTCTGAGATGAGTTTTTG TTCCATGGTGGCCAAGCTTAAGTTTAA
ChlaDUB1 pETFPP_21	F	GAAGGAGATATACATATGTTGTCTCCCACCAACTCAACT
	R	GAACAGAACCTCGAGGAAAGGAGCTTTTGCTTCAGGCCA
ChlaDUB2 pETFPP_21	F	GAAGGAGATATACATATGGAACCAATTCATAATCCTCCC
	R	GAACAGAACCTCGAGATCCGTAGTTGGCCAGCTCAAAGA
BOUR_00006 pVT100-U	F	CTCGTCTAGAGGATCATGACTCCAGTAACACCAGTCCCTC
	R	GTCCAAAGCTGGATCTTATTTACGAGAGGGTTTCTTCTTTTG
BOUR_00036 pVT100-U	F	CTCGTCTAGAGGATCATGATGTCCTCCCCTCATCCAATG
	R	GTCCAAAGCTGGATCTTAGTTTGCGTCGGATTCCGTGGT
BOUR_00050 pVT100-U	F	CTCGTCTAGAGGATCATGGGAACAGCCAGAATAGTATT

	R	GTCCAAAGCTGGATCCTAAAGTCGTGAAACTAGCATTTC
BOUR_00052 pVT100-U	F	CTCGTCTAGAGGATCATGAACAAAAATAATTAAGAA
	R	GTCCAAAGCTGGATCTTAATAACCAGCGCCCATATATGA
BOUR_00084 pVT100-U	F	CTCGTCTAGAGGATCATGTCAATTTCTGGAAGTGGTAATG
	R	GTCCAAAGCTGGATCTCATGAATCGCCTCCTGCATCCTCT
BOUR_00089 pVT100-U	F	CTCGTCTAGAGGATCATGCCGTCATTATCCCAATCCCGA
	R	GTCCAAAGCTGGATCCTAAAATAGAGCCTCAAGTAAAGA
BOUR_00090 pVT100-U	F	CTCGTCTAGAGGATCATGCAAATCAATTTGAACAACTC
	R	GTCCAAAGCTGGATCTTACAGGTGATACATACCTAGAGC
BOUR_00107 pVT100-U	F	CTCGTCTAGAGGATCATGTCATTTGGTATTGGTAGTGCT
	R	GTCCAAAGCTGGATCCTATCCTATAGCTGCGGAGAGAAC
BOUR_00116 pVT100-U	F	CTCGTCTAGAGGATCATGACCACTGCTACTACTTCACAA
	R	GTCCAAAGCTGGATCTTATAGCAAGCTAGCTAGTTCTTC
BOUR_00123 pVT100-U	F	CTCGTCTAGAGGATCATGACAACGCCTACTCTAATCGTG
	R	GTCCAAAGCTGGATCCTAGGAGCTTTTTGTAGAGGGTGA
BOUR_00137 pVT100-U	F	CTCGTCTAGAGGATCATGTCCAGAAAACCGGCTTCTAAC
	R	GTCCAAAGCTGGATCTCATTTTGATATTTTTAATGCTGA
BOUR_00151 pVT100-U	F	CTCGTCTAGAGGATCATGACAACACCAGATAATAACT
	R	GTCCAAAGCTGGATCTTAAGGAACAACAGGTAGCCGAAC
BOUR_00154 pVT100-U	F	CTCGTCTAGAGGATCATGGCGAATCCGTCTACACCCTCA
	R	GTCCAAAGCTGGATCTTATTCTTTCTTATCTGTCAGTCT
BOUR_00161 pVT100-U	F	CTCGTCTAGAGGATCATGCTTCCACATCAGCAGAACAGC

	R	GTCCAAAGCTGGATCCTATTTTCTCATACGGATAGCTTG
BOUR_00163 pVT100-U	F	CTCGTCTAGAGGATCATGAGTGTACAAGGCTCTTCTTCT
	R	GTCCAAAGCTGGATCTTAAACAGGAGAGCTATTTTTTAA
BOUR_00200 pVT100-U	F	CTCGTCTAGAGGATCATGCAATCGGTTGGACAAGAAGCT
	R	GTCCAAAGCTGGATCTTAAACAATCATTGGAAACTAAATC
BOUR_00204 pVT100-U	F	CTCGTCTAGAGGATCATGGCAACAACAGTTAATCCTAATTA
	R	GTCCAAAGCTGGATCTTAATCGCAAGAGATATGCAGAAG
BOUR_00240 pVT100-U	F	CTCGTCTAGAGGATCATGAGTACTACTATTAGCGGAGAC
	R	GTCCAAAGCTGGATCCTAAGAAGCTTGGTTAGCGTCTAT
BOUR_00244 pVT100-U	F	CTCGTCTAGAGGATCATGGTTCATTCTGTATAACAATTCA
	R	GTCCAAAGCTGGATCCTATTCTTGAGGTTTTGTTGGGCT
BOUR_00245 pVT100-U	F	CTCGTCTAGAGGATCATGACGTA CTCTATATCCGATATA
	R	GTCCAAAGCTGGATCTTAGCTTACATATAAAGTTTGAGG
BOUR_00272 pVT100-U	F	CTCGTCTAGAGGATCATGACAACGTGGACTTTGAATCAC
	R	GTCCAAAGCTGGATCCTAAGGCTCTAGCTGATCGGATTG
BOUR_00310 pVT100-U	F	CTCGTCTAGAGGATCATGACAACAAAATTAACACAG
	R	GTCCAAAGCTGGATCTCATTGTAGTAAGCGGACAGCATC
BOUR_00365 pVT100-U	F	CTCGTCTAGAGGATCATGAACTCGACGAATAATACAGAC
	R	GTCCAAAGCTGGATCTTAAACCCCAGGGAAAGCAATCTT
BOUR_00380 pVT100-U	F	CTCGTCTAGAGGATCATGCCTGTAGTACAGAAACCTTCA
	R	GTCCAAAGCTGGATCTTATTGTTGTTTCTTTGTTGTAATC
BOUR_00381 pVT100-U	F	CTCGTCTAGAGGATCATGGCTACACCGATTGCTGTACCG

	R	GTCCAAAGCTGGATCTTAGCAGTGCTCTTCGAGGCTTCT
BOUR_00389 pVT100-U	F	CTCGTCTAGAGGATCATGGTTTCTAGGGTTCCCGGAAGT
	R	GTCCAAAGCTGGATCTTACGATTCTACAAAAGAATCCCC
BOUR_00417 pVT100-U	F	CTCGTCTAGAGGATCATGTCTTCTATAACAAGGAACATCG
	R	GTCCAAAGCTGGATCCTATTGAAATCCTCTATCATCATC
BOUR_00420 pVT100-U	F	CTCGTCTAGAGGATCATGACAGAAACCCCAAATACCTCG
	R	GTCCAAAGCTGGATCTTATTCTTTTTCTTCGTTACCGTC
BOUR_00437 pVT100-U	F	CTCGTCTAGAGGATCATGAATCGAGTTATAGAAATCCAT
	R	GTCCAAAGCTGGATCTTAGAAGCCAACATAGCCTCCGCA
BOUR_00439 pVT100-U	F	CTCGTCTAGAGGATCATGAAATTTCTGTCAGCTACTGCT
	R	GTCCAAAGCTGGATCTTAGAATGTCATACGAGCACCGCA
BOUR_00451 pVT100-U	F	CTCGTCTAGAGGATCATGGATCGATCTTCTCCTCAAATT
	R	GTCCAAAGCTGGATCTTATACTGCAGGACGTAATAACGC
BOUR_00469 pVT100-U	F	CTCGTCTAGAGGATCATGAAAGTTGTTGTGAATCCTACT
	R	GTCCAAAGCTGGATCTTATTTTTCTTTTGTGACAAGAAA
BOUR_00471 pVT100-U	F	CTCGTCTAGAGGATCATGAGCACTGTACCCGTTGTTCAA
	R	GTCCAAAGCTGGATCTCATTGGGTCTGATCCACCAGACT
BOUR_00486 pVT100-U	F	CTCGTCTAGAGGATCATGACGAATTCTATATCAGGTTAT
	R	GTCCAAAGCTGGATCTTATCCTACGGTATCAATCAGTGC
BOUR_00493 pVT100-U	F	CTCGTCTAGAGGATCATGACAGAAAAAATTGTTTTACAA
	R	GTCCAAAGCTGGATCTTACTTCCCTTCGCTAGAGTTATT
BOUR_00517 pVT100-U	F	CTCGTCTAGAGGATCATGTCTGTTGTCCCACAGAGTCCT

	R	GTCCAAAGCTGGATCCTACGGGGTAGTAGCTAAATAGCG
BOUR_00615 pVT100-U	F	CTCGTCTAGAGGATCATGTCCCTTTCATCTTCTTCGTCT
	R	GTCCAAAGCTGGATCTTAAGCTGCGGCGGCTAAGGCGCC
BOUR_00616 pVT100-U	F	CTCGTCTAGAGGATCATGACAACAGGAGTACGTGGAGAT
	R	GTCCAAAGCTGGATCTTAGTTAAACATAGAGGCTGTCGT
BOUR_00662 pVT100-U	F	CTCGTCTAGAGGATCATGGAATCAGGACCAGAATCAGTT
	R	GTCCAAAGCTGGATCTTAAGAAAGATAACCAGAGAATAG
BOUR_00700 pVT100-U	F	CTCGTCTAGAGGATCATGGACACGCAATTCATAGCGAGTC
	R	GTCCAAAGCTGGATCTCAATCTCTGTATACCGAACGCATTTTC
BOUR_00742 pVT100-U	F	CTCGTCTAGAGGATCATGAGTATTCGACCTACTAATGGGA
	R	GTCCAAAGCTGGATCTTAGTCTAAGAAAACAGAAGAAGTTA
BOUR_00743 pVT100-U	F	CTCGTCTAGAGGATCATGGTGAGTAGCATAAGCCCTATA
	R	GTCCAAAGCTGGATCTTAGATATTCCCAACCGAAGAAGG
BOUR_00760 pVT100-U	F	CTCGTCTAGAGGATCATGTCAATACAACCTACATCCATTTTC
	R	GTCCAAAGCTGGATCTTATTTAAATCTACGGATCAACTTA
BOUR_00770 pVT100-U	F	CTCGTCTAGAGGATCATGGACGGGACAAAATTACAGAA
	R	GTCCAAAGCTGGATCTCATAAGGATTGAGTAACCAGTGG
BOUR_00786 pVT100-U	F	CTCGTCTAGAGGATCATGACCACTAACTCTACTCAAGAC
	R	GTCCAAAGCTGGATCTTATTCTTCTTGGGGAACGAATTC
BOUR_00823 pVT100-U	F	CTCGTCTAGAGGATCATGTCCTCATCATCCTCTTCGGGA
	R	GTCCAAAGCTGGATCTTACCCACAAAGAAAATAGTCTTG
BOUR_00872 pVT100-U	F	CTCGTCTAGAGGATCATGACTACTCTTCCCAATAATTGC

	R	GTCCAAAGCTGGATCTTGATACCATGTTTTCTTTTTCG
BOUR_00910 pVT100-U	F	CTCGTCTAGAGGATCATGTGGCATAAAGAACCAATGCATG
	R	GTCCAAAGCTGGATCTTAGATATTCGCGATCAAGCTAAC
BOUR_00911 pVT100-U	F	CTCGTCTAGAGGATCATGTCAGCACCAACCTCACAGGTA
	R	GTCCAAAGCTGGATCTTAAGACAGGGGTTTATTTAATTG
BOUR_00916 pVT100-U	F	CTCGTCTAGAGGATCATGACGATTTCCGGGATCCCTCAG
	R	GTCCAAAGCTGGATCTTATAGGAAAGTTTGTTGTAGGCC
BOUR_00923 pVT100-U	F	CTCGTCTAGAGGATCATGACGATAACAGTACCGCAAGAG
	R	GTCCAAAGCTGGATCCTATTGGTAGAGGCTGCGGACTGC
BOUR_00926 pVT100-U	F	CTCGTCTAGAGGATCATGGATACTCCACACCCCTTTCC
	R	GTCCAAAGCTGGATCTTAGGGACGCATGTTGTAGATAAA
BOUR_00933 pVT100-U	F	CTCGTCTAGAGGATCATGTTGTCTCCACCAACTCAACTTCA
	R	GTCCAAAGCTGGATCTTAGAAAGGAGCTTTTGCTTCAGG

Abbreviations

aa	Amino acid
Arf1	Adenosine diphosphate-ribosylation factor 1
ATP	Adenosine triphosphate
BCA	Bicinchoninic acid
BSA	Bovine serum albumin
CD	Cluster of differentiation
CORVET	Class C core vacuole/endosome tethering
Cpn	<i>Chlamydia pneumoniae</i>
Cps	<i>Chlamydia psittaci</i>
CPY	Carboxypeptidase Y
CPY-inv	Carboxypeptidase Y-invertase
Ct	<i>Chlamydia trachomatis</i>
DAPI	4'-6' diamidine-2-phenylindole
DNA	Deoxyribonucleic acid
ddH₂O	Double distilled H ₂ O
DMEM	Dulbecco's modified eagle medium
DMSO	Dimethyl sulphoxide
DUB	Deubiquitinase
E1	Ubiquitin activating enzyme
E2	Ubiquitin conjugating enzyme

E3	Ubiquitin ligase enzyme
EB	Elementary body
EDTA	Ethylenediaminetetraacetic acid
EE	Early endosome
EEA1	Early endosome antigen 1
EGF	Epidermal growth factor
EGFR	Epidermal growth factor receptor
ER	Endoplasmic reticulum
ERC	Endosomal recycling compartment
ESCRT	Endosomal sorting complex required for transport
g	Grams
GAP	GTPase activating protein
GDP	Guanosine diphosphate
GEF	Guanine nucleotide exchange factor
GTP	Guanosine triphosphate
h	Hour
HeLa	Henrietta Lacks' cancer cell line
HOPS	Homotypic fusion and vacuole protein sorting
HRP	Horseradish peroxidase
IF	Immunofluorescence
IκBα	Inhibitor of NF κ B alpha

IL	Interleukin
ILV	Intralumenal vesicle
Inc	Inclusion membrane protein
IPTG	Isopropyl β -D-1-thiogalactopyranoside
Kb	Kilobase pairs
kDa	Kilodaltons
LAMP	Lysosome associated membrane protein
LB	Liquid broth
LC-MS/MS	Liquid chromatography-tandem mass spectroscopy
LE	Late endosome
LGV	Lymphogranuloma venereum
LPS	Lipopolysaccharide
M	Molar
M6P	Mannose-6-phosphate
M6PR	Mannose-6-phosphate receptor
mg	Milligram
min	Minutes
ml	Millilitre
mM	Millimolar
MOMP	Major outer membrane protein
MTOC	Microtubule organising centre

NFκB	Nuclear factor kappa-light-chain-enhancer of activated B cells
ng	Nanogram
nM	Nanomolar
ns	Non-significant
OD	Optical density
PAMP	Pathogen associated molecular pattern
PBS	Phosphate buffered saline
PCR	Polymerase chain reaction
PEPSY	Pathogen effector screening in yeast
Pmp	Polymorphic membrane protein
PRR	Pattern recognition receptor
PSC	Positively secreting colony
PTM	Post-translational modification
RB	Reticulate body
RNA	Ribonucleic acid
SDS-PAGE	Sodium dodecyl sulphate polyacrylamide gel electrophoresis
SNARE	Soluble N-ethylmaleimide-sensitive factor attachment protein receptor
STI	Sexually transmitted infection
T3SS	Type III secretion system
TAE	Tris base, acetic acid and ethylenediaminetetraacetic acid
TBS	Tris buffered saline

TCA	Trichloroacetic acid
TEMED	Tetramethylethylenediamine
TLR	Toll-like receptor
µg	Microgram
µl	Microlitre
µm	Micrometre
µM	Micromolar
USP	Ubiquitin-specific protease
VPS	Vacuole protein sorting
WB	Western blotting

References

- AIZAWA, S. I. 2001. Bacterial flagella and type III secretion systems. *FEMS Microbiol Lett*, 202, 157-64.
- AJONUMA, L. C., FOK, K. L., HO, L. S., CHAN, P. K., CHOW, P. H., TSANG, L. L., WONG, C. H., CHEN, J., LI, S., ROWLANDS, D. K., CHUNG, Y. W. & CHAN, H. C. 2010. CFTR is required for cellular entry and internalization of *Chlamydia trachomatis*. *Cell Biol Int*, 34, 593-600.
- AL-YOUNES, H. M., BRINKMANN, V. & MEYER, T. F. 2004. Interaction of *Chlamydia trachomatis* serovar L2 with the host autophagic pathway. *Infect Immun*, 72, 4751-62.
- ANDERSON, D. M. & SCHNEEWIND, O. 1997. A mRNA signal for the type III secretion of Yop proteins by *Yersinia enterocolitica*. *Science*, 278, 1140-3.
- ARENA, E. T., AUWETER, S. D., ANTUNES, L. C., VOGL, A. W., HAN, J., GUTTMAN, J. A., CROXEN, M. A., MENENDEZ, A., COVEY, S. D., BORCHERS, C. H. & FINLAY, B. B. 2011. The deubiquitinase activity of the *Salmonella* pathogenicity island 2 effector, SseL, prevents accumulation of cellular lipid droplets. *Infect Immun*, 79, 4392-400.
- ARNOLD, R., BRANDMAIER, S., KLEINE, F., TISCHLER, P., HEINZ, E., BEHRENS, S., NIINIKOSKI, A., MEWES, H. W., HORN, M. & RATTEI, T. 2009. Sequence-based prediction of type III secreted proteins. *PLoS Pathog*, 5, e1000376.
- AUFDERHEIDE, A., BECK, F., STENGEL, F., HARTWIG, M., SCHWEITZER, A., PFEIFER, G., GOLDBERG, A. L., SAKATA, E., BAUMEISTER, W. & FORSTER, F. 2015. Structural characterization of the interaction of Ubp6 with the 26S proteasome. *Proc Natl Acad Sci U S A*, 112, 8626-31.
- BAILEY, C. A., MILLER, D. K. & LENARD, J. 1984. Effects of DEAE-dextran on infection and hemolysis by VSV. Evidence that nonspecific electrostatic interactions mediate effective binding of VSV to cells. *Virology*, 133, 111-8.
- BALDERHAAR, H. J. & UNGERMANN, C. 2013. CORVET and HOPS tethering complexes - coordinators of endosome and lysosome fusion. *J Cell Sci*, 126, 1307-16.
- BANTA, L. M., ROBINSON, J. S., KLIONSKY, D. J. & EMR, S. D. 1988. Organelle assembly in yeast: characterization of yeast mutants defective in vacuolar biogenesis and protein sorting. *J Cell Biol*, 107, 1369-83.

- BASTIDAS, R. J., ELWELL, C. A., ENGEL, J. N. & VALDIVIA, R. H. 2013. Chlamydial intracellular survival strategies. *Cold Spring Harb Perspect Med*, 3, a010256.
- BASTIDAS, R. J. & VALDIVIA, R. H. 2016. Emancipating Chlamydia: Advances in the Genetic Manipulation of a Recalcitrant Intracellular Pathogen. *Microbiol Mol Biol Rev*, 80, 411-27.
- BATRA, S., GUPTA, P., CHAUHAN, V., SINGH, A. & BHATNAGAR, R. 2001. Trp 346 and Leu 352 residues in protective antigen are required for the expression of anthrax lethal toxin activity. *Biochem Biophys Res Commun*, 281, 186-92.
- BEATTY, W. L. 2008. Late endocytic multivesicular bodies intersect the chlamydial inclusion in the absence of CD63. *Infect Immun*, 76, 2872-81.
- BECKER, E. & HEGEMANN, J. H. 2014. All subtypes of the Pmp adhesin family are implicated in chlamydial virulence and show species-specific function. *Microbiologyopen*, 3, 544-56.
- BEECKMAN, D. S. & VANROMPAY, D. C. 2010. Bacterial secretion systems with an emphasis on the chlamydial Type III secretion system. *Curr Issues Mol Biol*, 12, 17-41.
- BEITER, K., WARTHA, F., ALBIGER, B., NORMARK, S., ZYCHLINSKY, A. & HENRIQUES-NORMARK, B. 2006. An endonuclease allows *Streptococcus pneumoniae* to escape from neutrophil extracellular traps. *Curr Biol*, 16, 401-7.
- BETTS-HAMPIKIAN, H. J. & FIELDS, K. A. 2010. The Chlamydial Type III Secretion Mechanism: Revealing Cracks in a Tough Nut. *Front Microbiol*, 1, 114.
- BIRTALAN, S. C., PHILLIPS, R. M. & GHOSH, P. 2002. Three-dimensional secretion signals in chaperone-effector complexes of bacterial pathogens. *Mol Cell*, 9, 971-80.
- BLOCKER, A., GOUNON, P., LARQUET, E., NIEBUHR, K., CABIAUX, V., PARSOT, C. & SANSONETTI, P. 1999. The tripartite type III secretion of *Shigella flexneri* inserts IpaB and IpaC into host membranes. *J Cell Biol*, 147, 683-93.
- BOCKER, S., HEURICH, A., FRANKE, C., MONAJEMBASHI, S., SACHSE, K., SALUZ, H. P. & HANEL, F. 2014. Chlamydia psittaci inclusion membrane protein IncB associates with host protein Snapin. *Int J Med Microbiol*, 304, 542-53.
- BONCOMPAIN, G., MULLER, C., MEAS-YEDID, V., SCHMITT-KOPPLIN, P., LAZAROW, P. B. & SUBTIL, A. 2014. The intracellular bacteria Chlamydia hijack peroxisomes and utilize their enzymatic capacity to produce bacteria-specific phospholipids. *PLoS One*, 9, e86196.

- BORNHORST, J. A. & FALKE, J. J. 2000. Purification of proteins using polyhistidine affinity tags. *Methods Enzymol*, 326, 245-54.
- BOTSTEIN, D. & FINK, G. R. 1988. Yeast: an experimental organism for modern biology. *Science*, 240, 1439-43.
- BOTSTEIN, D. & FINK, G. R. 2011. Yeast: an experimental organism for 21st Century biology. *Genetics*, 189, 695-704.
- BRICKMAN, T. J., BARRY, C. E., 3RD & HACKSTADT, T. 1993. Molecular cloning and expression of hctB encoding a strain-variant chlamydial histone-like protein with DNA-binding activity. *J Bacteriol*, 175, 4274-81.
- BRIGHT, N. A., REAVES, B. J., MULLOCK, B. M. & LUZIO, J. P. 1997. Dense core lysosomes can fuse with late endosomes and are re-formed from the resultant hybrid organelles. *J Cell Sci*, 110 (Pt 17), 2027-40.
- BUTLER, J. A., COSGROVE, J., ALDEN, K., TIMMIS, J. & COLES, M. C. 2016. Model-Driven Experimentation: A New Approach to Understand Mechanisms of Tertiary Lymphoid Tissue Formation, Function, and Therapeutic Resolution. *Front Immunol*, 7, 658.
- CAMPODONICO, E. M., CHESNEL, L. & ROY, C. R. 2005. A yeast genetic system for the identification and characterization of substrate proteins transferred into host cells by the Legionella pneumophila Dot/Icm system. *Mol Microbiol*, 56, 918-33.
- CARABEO, R. A., GRIESHABER, S. S., FISCHER, E. & HACKSTADT, T. 2002. Chlamydia trachomatis induces remodeling of the actin cytoskeleton during attachment and entry into HeLa cells. *Infect Immun*, 70, 3793-803.
- CATIC, A., MISAGHI, S., KORBEL, G. A. & PLOEGH, H. L. 2007. ElaD, a Deubiquitinating protease expressed by E. coli. *PLoS One*, 2, e381.
- CHAUGULE, V. K. & WALDEN, H. 2016. Specificity and disease in the ubiquitin system. *Biochem Soc Trans*, 44, 212-27.
- CHENG, L. W., KAY, O. & SCHNEEWIND, O. 2001. Regulated secretion of YopN by the type III machinery of Yersinia enterocolitica. *J Bacteriol*, 183, 5293-301.
- CHERNOMORDIK, L. V. & KOZLOV, M. M. 2003. Protein-lipid interplay in fusion and fission of biological membranes. *Annu Rev Biochem*, 72, 175-207.
- CHRISTOFORIDIS, S., MCBRIDE, H. M., BURGOYNE, R. D. & ZERIAL, M. 1999. The Rab5 effector EEA1 is a core component of endosome docking. *Nature*, 397, 621-5.

- CLAESSEN, J. H. L., WITTE, M. D., YODER, N. C., ZHU, A. Y., SPOONER, E. & PLOEGH, H. L. 2013. Catch-and-release probes applied to semi-intact cells reveal ubiquitin-specific protease expression in Chlamydia trachomatis infection. *Chembiochem*, 14, 343-52.
- CLAGUE, M. J., BARSUKOV, I., COULSON, J. M., LIU, H., RIGDEN, D. J. & URBE, S. 2013. Deubiquitylases from genes to organism. *Physiol Rev*, 93, 1289-315.
- CLIFTON, D. R., FIELDS, K. A., GRIESHABER, S. S., DOOLEY, C. A., FISCHER, E. R., MEAD, D. J., CARABEO, R. A. & HACKSTADT, T. 2004. A chlamydial type III translocated protein is tyrosine-phosphorylated at the site of entry and associated with recruitment of actin. *Proc Natl Acad Sci U S A*, 101, 10166-71.
- COBURN, B., SEKIROV, I. & FINLAY, B. B. 2007. Type III secretion systems and disease. *Clin Microbiol Rev*, 20, 535-49.
- COCCHIARO, J. L., KUMAR, Y., FISCHER, E. R., HACKSTADT, T. & VALDIVIA, R. H. 2008. Cytoplasmic lipid droplets are translocated into the lumen of the Chlamydia trachomatis parasitophorous vacuole. *Proc Natl Acad Sci U S A*, 105, 9379-84.
- CONIBEAR, E. 2010. Converging views of endocytosis in yeast and mammals. *Curr Opin Cell Biol*, 22, 513-8.
- COOMBES, B. K. & MAHONY, J. B. 2002. Identification of MEK- and phosphoinositide 3-kinase-dependent signalling as essential events during Chlamydia pneumoniae invasion of HEp2 cells. *Cell Microbiol*. England.
- CORNELIS, G. R. 2002. Yersinia type III secretion: send in the effectors. *J Cell Biol*, 158, 401-8.
- CURAK, J., ROHDE, J. & STAGLJAR, I. 2009. Yeast as a tool to study bacterial effectors. *Curr Opin Microbiol*, 12, 18-23.
- DA CUNHA, M., MILHO, C., ALMEIDA, F., PAIS, S. V., BORGES, V., MAURICIO, R., BORREGO, M. J., GOMES, J. P. & MOTA, L. J. 2014. Identification of type III secretion substrates of Chlamydia trachomatis using Yersinia enterocolitica as a heterologous system. *BMC Microbiol*, 14, 40.
- DAMIANI, M. T., GAMBARTE TUDELA, J. & CAPMANY, A. 2014. Targeting eukaryotic Rab proteins: a smart strategy for chlamydial survival and replication. *Cell Microbiol*, 16, 1329-38.
- DANG, G., CAO, J., CUI, Y., SONG, N., CHEN, L., PANG, H. & LIU, S. 2016. Characterization of Rv0888, a Novel Extracellular Nuclease from Mycobacterium tuberculosis. *Sci Rep*, 6, 19033.

- DAUTRY-VARSAT, A., CIECHANOVER, A. & LODISH, H. F. 1983. pH and the recycling of transferrin during receptor-mediated endocytosis. *Proc Natl Acad Sci U S A*, 80, 2258-62.
- DELEVOYE, C., NILGES, M., DAUTRY-VARSAT, A. & SUBTIL, A. 2004. Conservation of the biochemical properties of IncA from *Chlamydia trachomatis* and *Chlamydia caviae*: oligomerization of IncA mediates interaction between facing membranes. *J Biol Chem*, 279, 46896-906.
- DERRE, I. 2015. Chlamydiae interaction with the endoplasmic reticulum: contact, function and consequences. *Cell Microbiol*, 17, 959-66.
- DERRE, I. & ISBERG, R. R. 2005. LidA, a translocated substrate of the *Legionella pneumophila* type IV secretion system, interferes with the early secretory pathway. *Infect Immun*, 73, 4370-80.
- DERRE, I., SWISS, R. & AGAISSE, H. 2011. The lipid transfer protein CERT interacts with the *Chlamydia* inclusion protein IncD and participates to ER-*Chlamydia* inclusion membrane contact sites. *PLoS Pathog*, 7, e1002092.
- DESHAIES, R. J. & JOAZEIRO, C. A. 2009. RING domain E3 ubiquitin ligases. *Annu Rev Biochem*, 78, 399-434.
- DOTAN, I., ZIV, E., DAFNI, N., BECKMAN, J. S., MCCANN, R. O., GLOVER, C. V. & CANAANI, D. 2001. Functional conservation between the human, nematode, and yeast CK2 cell cycle genes. *Biochem Biophys Res Commun*, 288, 603-9.
- DUNPHY, W. G., PFEFFER, S. R., CLARY, D. O., WATTENBERG, B. W., GLICK, B. S. & ROTHMAN, J. E. 1986. Yeast and mammals utilize similar cytosolic components to drive protein transport through the Golgi complex. *Proc Natl Acad Sci U S A*, 83, 1622-6.
- EBBESSEN, P. 1973. DEAE-dextran enhancement of in vivo infection with murine leukemia virus. *Arch Gesamte Virusforsch*, 40, 307-10.
- ECHALIER, A., PAN, Y., BIROL, M., TAVERNIER, N., PINTARD, L., HOH, F., EBEL, C., GALOPHE, N., CLARET, F. X. & DUMAS, C. 2013. Insights into the regulation of the human COP9 signalosome catalytic subunit, CSN5/Jab1. *Proc Natl Acad Sci U S A*, 110, 1273-8.
- ELWELL, C., MIRRASHIDI, K. & ENGEL, J. 2016. *Chlamydia* cell biology and pathogenesis. *Nat Rev Microbiol*, 14, 385-400.
- ELWELL, C. A., CEESAY, A., KIM, J. H., KALMAN, D. & ENGEL, J. N. 2008. RNA interference screen identifies Abl kinase and PDGFR signaling in *Chlamydia trachomatis* entry. *PLoS Pathog*, 4, e1000021.
- EMMERICH, C. H. & COHEN, P. 2015. Optimising methods for the preservation, capture and identification of ubiquitin chains and

ubiquitylated proteins by immunoblotting. *Biochem Biophys Res Commun*, 466, 1-14.

- ESKELINEN, E. L., TANAKA, Y. & SAFTIG, P. 2003. At the acidic edge: emerging functions for lysosomal membrane proteins. *Trends Cell Biol*, 13, 137-45.
- EYERS, P. A. & MURPHY, J. M. 2016. The evolving world of pseudoenzymes: proteins, prejudice and zombies. *BMC Biol*, 14, 98.
- FAGGIANO, S., MENON, R. P., KELLY, G. P., TODI, S. V., SCAGLIONE, K. M., KONAREV, P. V., SVERGUN, D. I., PAULSON, H. L. & PASTORE, A. 2015. Allosteric regulation of deubiquitylase activity through ubiquitination. *Front Mol Biosci*, 2, 2.
- FERREIRA, C. R. & GAHL, W. A. 2017. Lysosomal storage diseases. *Transl Sci Rare Dis*, 2, 1-71.
- FIELDS, K. A., FISCHER, E. R., MEAD, D. J. & HACKSTADT, T. 2005. Analysis of putative *Chlamydia trachomatis* chaperones Scc2 and Scc3 and their use in the identification of type III secretion substrates. *J Bacteriol*. United States.
- FIELDS, K. A. & HACKSTADT, T. 2003. THE CHLAMYDIAL INCLUSION: Escape from the Endocytic Pathway1. <http://dx.doi.org/10.1146/annurev.cellbio.18.012502.105845>.
- FIELDS, K. A., MEAD, D. J., DOOLEY, C. A. & HACKSTADT, T. 2003. *Chlamydia trachomatis* type III secretion: evidence for a functional apparatus during early-cycle development. *Mol Microbiol*, 48, 671-83.
- FISCHER, A., HARRISON, K. S., RAMIREZ, Y., AUER, D., CHOWDHURY, S. R., PRUSTY, B. K., SAUER, F., DIMOND, Z., KISKER, C., SCOTT HEFTY, P. & RUDEL, T. 2017. *Chlamydia trachomatis*-containing vacuole serves as deubiquitination platform to stabilize Mcl-1 and to interfere with host defense. *Elife*, 6.
- FLANNAGAN, R. S., JAUMOUILLE, V. & GRINSTEIN, S. 2012. The cell biology of phagocytosis. *Annu Rev Pathol*, 7, 61-98.
- FREEMAN, S. A. & GRINSTEIN, S. 2014. Phagocytosis: receptors, signal integration, and the cytoskeleton. *Immunol Rev*, 262, 193-215.
- FROLOV, V. A. & ZIMMERBERG, J. 2010. Cooperative elastic stresses, the hydrophobic effect, and lipid tilt in membrane remodeling. *FEBS Lett*, 584, 1824-9.
- FUJII, T., CHEUNG, M., BLANCO, A., KATO, T., BLOCKER, A. J. & NAMBA, K. 2012. Structure of a type III secretion needle at 7-A resolution provides insights into its assembly and signaling mechanisms. *Proc Natl Acad Sci U S A*, 109, 4461-6.

- FUKUDA, M. 1991. Lysosomal membrane glycoproteins. Structure, biosynthesis, and intracellular trafficking. *J Biol Chem*, 266, 21327-30.
- GOFFEAU, A., BARRELL, B. G., BUSSEY, H., DAVIS, R. W., DUJON, B., FELDMANN, H., GALIBERT, F., HOHEISEL, J. D., JACQ, C., JOHNSTON, M., LOUIS, E. J., MEWES, H. W., MURAKAMI, Y., PHILIPPSEN, P., TETTELIN, H. & OLIVER, S. G. 1996. Life with 6000 genes. *Science*, 274, 546, 563-7.
- GOLDBERG, T., ROST, B. & BROMBERG, Y. 2016. Computational prediction shines light on type III secretion origins. *Sci Rep*, 6, 34516.
- GOODALL, J. C., YEO, G., HUANG, M., RAGGIASCHI, R. & GASTON, J. S. 2001. Identification of Chlamydia trachomatis antigens recognized by human CD4+ T lymphocytes by screening an expression library. *Eur J Immunol*, 31, 1513-22.
- GORDON, S. 2016. Phagocytosis: An Immunobiologic Process. *Immunity*, 44, 463-475.
- GUIGNOT, J., SEGURA, A. & TRAN VAN NHIEU, G. 2015. The Serine Protease EspC from Enteropathogenic Escherichia coli Regulates Pore Formation and Cytotoxicity Mediated by the Type III Secretion System. *PLoS Pathog*, 11, e1005013.
- GUILLEMET, E., LEREEC, A., TRAN, S. L., ROYER, C., BARBOSA, I., SANSONETTI, P., LERECLUS, D. & RAMARAO, N. 2016. The bacterial DNA repair protein Mfd confers resistance to the host nitrogen immune response. *Sci Rep*, 6, 29349.
- HACKSTADT, T., BRICKMAN, T. J., BARRY, C. E., 3RD & SAGER, J. 1993. Diversity in the Chlamydia trachomatis histone homologue Hc2. *Gene*, 132, 137-41.
- HACKSTADT, T., SCIDMORE-CARLSON, M. A., SHAW, E. I. & FISCHER, E. R. 1999. The Chlamydia trachomatis IncA protein is required for homotypic vesicle fusion. *Cell Microbiol*, 1, 119-30.
- HAM, H., SREELATHA, A. & ORTH, K. 2011. Manipulation of host membranes by bacterial effectors. *Nat Rev Microbiol*, 9, 635-46.
- HEUER, D., REJMAN LIPINSKI, A., MACHUY, N., KARLAS, A., WEHRENS, A., SIEDLER, F., BRINKMANN, V. & MEYER, T. F. 2009. Chlamydia causes fragmentation of the Golgi compartment to ensure reproduction. *Nature*, 457, 731-5.
- HIGH, N., MOUNIER, J., PREVOST, M. C. & SANSONETTI, P. J. 1992. IpaB of Shigella flexneri causes entry into epithelial cells and escape from the phagocytic vacuole. *Embo j*, 11, 1991-9.

- HINNEN, A., HICKS, J. B. & FINK, G. R. 1978. Transformation of yeast. *Proc Natl Acad Sci U S A*, 75, 1929-33.
- HO, T. D. & STARNBACH, M. N. 2005. The Salmonella enterica serovar typhimurium-encoded type III secretion systems can translocate Chlamydia trachomatis proteins into the cytosol of host cells. *Infect Immun*, 73, 905-11.
- HOHMANN, S. 2002. Osmotic stress signaling and osmoadaptation in yeasts. *Microbiol Mol Biol Rev*, 66, 300-72.
- HOPKINS, C. R. 1983. Intracellular routing of transferrin and transferrin receptors in epidermoid carcinoma A431 cells. *Cell*, 35, 321-30.
- HORAZDOVSKY, B. F., BUSCH, G. R. & EMR, S. D. 1994. VPS21 encodes a rab5-like GTP binding protein that is required for the sorting of yeast vacuolar proteins. *Embo j*, 13, 1297-309.
- HORN, M., COLLINGRO, A., SCHMITZ-ESSER, S., BEIER, C. L., PURKHOLD, U., FARTMANN, B., BRANDT, P., NYAKATURA, G. J., DROEGE, M., FRISHMAN, D., RATTEI, T., MEWES, H. W. & WAGNER, M. 2004. Illuminating the evolutionary history of chlamydiae. *Science*, 304, 728-30.
- HOVIS, K. M., MOJICA, S., MCDERMOTT, J. E., PEDERSEN, L., SIMHI, C., RANK, R. G., MYERS, G. S., RAVEL, J., HSIA, R. C. & BAVOIL, P. M. 2013. Genus-optimized strategy for the identification of chlamydial type III secretion substrates. *Pathog Dis*, 69, 213-22.
- HOWER, S., WOLF, K. & FIELDS, K. A. 2009. Evidence that CT694 is a novel Chlamydia trachomatis T3S substrate capable of functioning during invasion or early cycle development. *Mol Microbiol*, 72, 1423-37.
- HU, Y. B., DAMMER, E. B., REN, R. J. & WANG, G. 2015. The endosomal-lysosomal system: from acidification and cargo sorting to neurodegeneration. *Transl Neurodegener*, 4, 18.
- HUANG, J., LESSER, C. F. & LORY, S. 2008. The essential role of the CopN protein in Chlamydia pneumoniae intracellular growth. *Nature*, 456, 112-5.
- HUECK, C. J. 1998. Type III protein secretion systems in bacterial pathogens of animals and plants. *Microbiol Mol Biol Rev*, 62, 379-433.
- HUOTARI, J. & HELENIUS, A. 2011. Endosome maturation. *Embo j*, 30, 3481-500.
- HUTTI, J. E., SHEN, R. R., ABBOTT, D. W., ZHOU, A. Y., SPROTT, K. M., ASARA, J. M., HAHN, W. C. & CANTLEY, L. C. 2009. Phosphorylation of the tumor suppressor CYLD by the breast cancer oncogene IKKepsilon promotes cell transformation. *Mol Cell*, 34, 461-72.

- HUTTI, J. E., TURK, B. E., ASARA, J. M., MA, A., CANTLEY, L. C. & ABBOTT, D. W. 2007. IkappaB kinase beta phosphorylates the K63 deubiquitinase A20 to cause feedback inhibition of the NF-kappaB pathway. *Mol Cell Biol*, 27, 7451-61.
- HYBISKE, K. & STEPHENS, R. S. 2007. Mechanisms of host cell exit by the intracellular bacterium Chlamydia. *Proc Natl Acad Sci U S A*, 104, 11430-5.
- ISBERG, R. R., O'CONNOR, T. J. & HEIDTMAN, M. 2009. The Legionella pneumophila replication vacuole: making a cosy niche inside host cells. *Nat Rev Microbiol*, 7, 13-24.
- JEWETT, T. J., MILLER, N. J., DOOLEY, C. A. & HACKSTADT, T. 2010. The conserved Tarp actin binding domain is important for chlamydial invasion. *PLoS Pathog*, 6, e1000997.
- JOHNSON, C. M. & FISHER, D. J. 2013. Site-specific, insertional inactivation of incA in Chlamydia trachomatis using a group II intron. *PLoS One*, 8, e83989.
- JOVIC, M., SHARMA, M., RAHAJENG, J. & CAPLAN, S. 2010. The early endosome: a busy sorting station for proteins at the crossroads. *Histol Histopathol*, 25, 99-112.
- JUTRAS, I., ABRAMI, L. & DAUTRY-VARSAT, A. 2003. Entry of the lymphogranuloma venereum strain of Chlamydia trachomatis into host cells involves cholesterol-rich membrane domains. *Infect Immun*, 71, 260-6.
- KARI, L., GOHEEN, M. M., RANDALL, L. B., TAYLOR, L. D., CARLSON, J. H., WHITMIRE, W. M., VIROK, D., RAJARAM, K., ENDRESZ, V., MCCLARTY, G., NELSON, D. E. & CALDWELL, H. D. 2011. Generation of targeted Chlamydia trachomatis null mutants. *Proc Natl Acad Sci U S A*, 108, 7189-93.
- KATZMANN, D. J., EPPING, E. A. & MOYE-ROWLEY, W. S. 1999. Mutational disruption of plasma membrane trafficking of Saccharomyces cerevisiae Yor1p, a homologue of mammalian multidrug resistance protein. *Mol Cell Biol*, 19, 2998-3009.
- KIM, D. W., LENZEN, G., PAGE, A. L., LEGRAIN, P., SANSONETTI, P. J. & PARSOT, C. 2005. The Shigella flexneri effector OspG interferes with innate immune responses by targeting ubiquitin-conjugating enzymes. *Proc Natl Acad Sci U S A*, 102, 14046-51.
- KIM, J. & KLIONSKY, D. J. 2000. Autophagy, cytoplasm-to-vacuole targeting pathway, and pexophagy in yeast and mammalian cells. *Annu Rev Biochem*, 69, 303-42.

- KIM, J. H., JIANG, S., ELWELL, C. A. & ENGEL, J. N. 2011. Chlamydia trachomatis co-opts the FGF2 signaling pathway to enhance infection. *PLoS Pathog*, 7, e1002285.
- KIM, J. S. & RAINES, R. T. 1994. Peptide tags for a dual affinity fusion system. *Anal Biochem*, 219, 165-6.
- KIM, S. R., KIM, J. O., LIM, K. H., YUN, J. H., HAN, I. & BAEK, K. H. 2015. Regulation of pyruvate kinase isozyme M2 is mediated by the ubiquitin-specific protease 20. *Int J Oncol*, 46, 2116-24.
- KITAGAWA, K. & HIETER, P. 2001. Evolutionary conservation between budding yeast and human kinetochores. *Nat Rev Mol Cell Biol*, 2, 678-87.
- KOBAYASHI, T., MASOUMI, K. C. & MASSOUMI, R. 2015. Deubiquitinating activity of CYLD is impaired by SUMOylation in neuroblastoma cells. *Oncogene*, 34, 2251-60.
- KOMANDER, D. 2010. Mechanism, specificity and structure of the deubiquitinases. *Subcell Biochem*, 54, 69-87.
- KOMANDER, D., REYES-TURCU, F., LICCHESI, J. D., ODENWAELDER, P., WILKINSON, K. D. & BARFORD, D. 2009. Molecular discrimination of structurally equivalent Lys 63-linked and linear polyubiquitin chains. *EMBO Rep*, 10, 466-73.
- KRAPPMANN, D. & SCHEIDEREIT, C. 2005. A pervasive role of ubiquitin conjugation in activation and termination of I κ B kinase pathways. *EMBO Rep*, 6, 321-6.
- KULATHU, Y., GARCIA, F. J., MEVISSSEN, T. E., BUSCH, M., ARNAUDO, N., CARROLL, K. S., BARFORD, D. & KOMANDER, D. 2013. Regulation of A20 and other OTU deubiquitinases by reversible oxidation. *Nat Commun*, 4, 1569.
- KUMAR, Y., COCCHIARO, J. & VALDIVIA, R. H. 2006. The obligate intracellular pathogen Chlamydia trachomatis targets host lipid droplets. *Curr Biol*, 16, 1646-51.
- LE NEGRATE, G., FAUSTIN, B., WELSH, K., LOEFFLER, M., KRAJEWSKA, M., HASEGAWA, P., MUKHERJEE, S., ORTH, K., KRAJEWSKI, S., GODZIK, A., GUINEY, D. G. & REED, J. C. 2008a. Salmonella secreted factor L deubiquitinase of Salmonella typhimurium inhibits NF- κ B, suppresses I κ B α ubiquitination and modulates innate immune responses. *J Immunol*, 180, 5045-56.
- LE NEGRATE, G., KRIEG, A., FAUSTIN, B., LOEFFLER, M., GODZIK, A., KRAJEWSKI, S. & REED, J. C. 2008b. ChlDub1 of Chlamydia trachomatis suppresses NF- κ B activation and inhibits I κ B α ubiquitination and degradation. *Cell Microbiol*, 10, 1879-92.

- LEE, J. G., BAEK, K., SOETANDYO, N. & YE, Y. 2013. Reversible inactivation of deubiquitinases by reactive oxygen species in vitro and in cells. *Nat Commun*, 4, 1568.
- LEE, K. K., FLORENS, L., SWANSON, S. K., WASHBURN, M. P. & WORKMAN, J. L. 2005. The deubiquitylation activity of Ubp8 is dependent upon Sgf11 and its association with the SAGA complex. *Mol Cell Biol*, 25, 1173-82.
- LESSER, C. F. & MILLER, S. I. 2001. Expression of microbial virulence proteins in *Saccharomyces cerevisiae* models mammalian infection. *Embo j*, 20, 1840-9.
- LIANG, J. X., NING, Z., GAO, W., LING, J., WANG, A. M., LUO, H. F., LIANG, Y., YAN, Q. & WANG, Z. Y. 2014. Ubiquitinspecific protease 22induced autophagy is correlated with poor prognosis of pancreatic cancer. *Oncol Rep*, 32, 2726-34.
- LLOYD, S. A., NORMAN, M., ROSQVIST, R. & WOLF-WATZ, H. 2001. Yersinia YopE is targeted for type III secretion by N-terminal, not mRNA, signals. *Mol Microbiol*, 39, 520-31.
- LOQUET, A., SGOURAKIS, N. G., GUPTA, R., GILLER, K., RIEDEL, D., GOOSMANN, C., GRIESINGER, C., KOLBE, M., BAKER, D., BECKER, S. & LANGE, A. 2012. Atomic model of the type III secretion system needle. *Nature*, 486, 276-9.
- LORENZ, S., CANTOR, A. J., RAPE, M. & KURIYAN, J. 2013. Macromolecular juggling by ubiquitylation enzymes. *BMC Biol*, 11, 65.
- LOWER, M. & SCHNEIDER, G. 2009. Prediction of type III secretion signals in genomes of gram-negative bacteria. *PLoS One*, 4, e5917.
- LUCAS, A. L., OUELLETTE, S. P., KABEISEMAN, E. J., CICHOS, K. H. & RUCKS, E. A. 2015. The trans-Golgi SNARE syntaxin 10 is required for optimal development of *Chlamydia trachomatis*. *Front Cell Infect Microbiol*, 5, 68.
- MALHOTRA, M., SOOD, S., MUKHERJEE, A., MURALIDHAR, S. & BALA, M. 2013. Genital *Chlamydia trachomatis*: an update. *Indian J Med Res*, 138, 303-16.
- MARTINEZ-GARCIA, P. M., RAMOS, C. & RODRIGUEZ-PALENZUELA, P. 2015. T346Hunter: a novel web-based tool for the prediction of type III, type IV and type VI secretion systems in bacterial genomes. *PLoS One*, 10, e0119317.
- MATSUMOTO, A., BESSHO, H., UEHIRA, K. & SUDA, T. 1991. Morphological studies of the association of mitochondria with chlamydial inclusions and the fusion of chlamydial inclusions. *J Electron Microsc (Tokyo)*, 40, 356-63.

- MAXFIELD, F. R. & MCGRAW, T. E. 2004. Endocytic recycling. *Nat Rev Mol Cell Biol*, 5, 121-32.
- MAXFIELD, F. R. & YAMASHIRO, D. J. 1987. Endosome acidification and the pathways of receptor-mediated endocytosis. *Adv Exp Med Biol*, 225, 189-98.
- MCDERMOTT, J. E., CORRIGAN, A., PETERSON, E., OEHMEN, C., NIEMANN, G., CAMBRONNE, E. D., SHARP, D., ADKINS, J. N., SAMUDRALA, R. & HEFFRON, F. 2011. Computational prediction of type III and IV secreted effectors in gram-negative bacteria. *Infect Immun*, 79, 23-32.
- MCSHAN, A. C. & DE GUZMAN, R. N. 2015. The bacterial type III secretion system as a target for developing new antibiotics. *Chem Biol Drug Des*, 85, 30-42.
- MEHLITZ, A. & RUDEL, T. 2013. Modulation of host signaling and cellular responses by Chlamydia. *Cell Commun Signal*, 11, 90.
- MELLMAN, I., FUCHS, R. & HELENIUS, A. 1986. Acidification of the endocytic and exocytic pathways. *Annu Rev Biochem*, 55, 663-700.
- MESQUITA, F. S., THOMAS, M., SACHSE, M., SANTOS, A. J., FIGUEIRA, R. & HOLDEN, D. W. 2012. The Salmonella deubiquitinase SseL inhibits selective autophagy of cytosolic aggregates. *PLoS Pathog*, 8, e1002743.
- MEVISSSEN, T. E., HOSPENTHAL, M. K., GEURINK, P. P., ELLIOTT, P. R., AKUTSU, M., ARNAUDO, N., EKKEBUS, R., KULATHU, Y., WAUER, T., EL OUALID, F., FREUND, S. M., OVAA, H. & KOMANDER, D. 2013. OTU deubiquitinases reveal mechanisms of linkage specificity and enable ubiquitin chain restriction analysis. *Cell*, 154, 169-84.
- MEVISSSEN, T. E. T. & KOMANDER, D. 2017. Mechanisms of Deubiquitinase Specificity and Regulation. *Annu Rev Biochem*, 86, 159-192.
- MEVISSSEN, T. E. T., KULATHU, Y., MULDER, M. P. C., GEURINK, P. P., MASLEN, S. L., GERSCH, M., ELLIOTT, P. R., BURKE, J. E., VAN TOL, B. D. M., AKUTSU, M., OUALID, F. E., KAWASAKI, M., FREUND, S. M. V., OVAA, H. & KOMANDER, D. 2016. Molecular basis of Lys11-polyubiquitin specificity in the deubiquitinase Cezanne. *Nature*, 538, 402-405.
- MICHIELS, T. & CORNELIS, G. R. 1991. Secretion of hybrid proteins by the Yersinia Yop export system. *J Bacteriol*, 173, 1677-85.
- MISAGHI, S., BALSARA, Z. R., CATIC, A., SPOONER, E., PLOEGH, H. L. & STARNBACH, M. N. 2006. Chlamydia trachomatis - derived deubiquitinating enzymes in mammalian cells during infection. *Molecular microbiology*, 61, 142-150.

- MITAL, J., LUTTER, E. I., BARGER, A. C., DOOLEY, C. A. & HACKSTADT, T. 2015. Chlamydia trachomatis inclusion membrane protein CT850 interacts with the dynein light chain DYNLT1 (Tctex1). *Biochem Biophys Res Commun*, 462, 165-70.
- MITSUI, A. & SHARP, P. A. 1999. Ubiquitination of RNA polymerase II large subunit signaled by phosphorylation of carboxyl-terminal domain. *Proc Natl Acad Sci U S A*, 96, 6054-9.
- MOLLEKEN, K., BECKER, E. & HEGEMANN, J. H. 2013. The Chlamydia pneumoniae invasin protein Pmp21 recruits the EGF receptor for host cell entry. *PLoS Pathog*, 9, e1003325.
- MONACK, D. M., MECASAS, J., GHORI, N. & FALKOW, S. 1997. Yersinia signals macrophages to undergo apoptosis and YopJ is necessary for this cell death. *Proc Natl Acad Sci U S A*, 94, 10385-90.
- MOORE, E. R., MEAD, D. J., DOOLEY, C. A., SAGER, J. & HACKSTADT, T. 2011. The trans-Golgi SNARE syntaxin 6 is recruited to the chlamydial inclusion membrane. *Microbiology*, 157, 830-8.
- MOORHEAD, A. M., JUNG, J. Y., SMIRNOV, A., KAUFER, S. & SCIDMORE, M. A. 2010. Multiple host proteins that function in phosphatidylinositol-4-phosphate metabolism are recruited to the chlamydial inclusion. *Infect Immun*, 78, 1990-2007.
- MUELLER, K. E., PLANO, G. V. & FIELDS, K. A. 2014. New frontiers in type III secretion biology: the Chlamydia perspective. *Infect Immun*, 82, 2-9.
- MUELLER, K. E., WOLF, K. & FIELDS, K. A. 2016. Gene Deletion by Fluorescence-Reported Allelic Exchange Mutagenesis in Chlamydia trachomatis. *MBio*, 7, e01817-15.
- MUKHERJEE, S., KEITANY, G., LI, Y., WANG, Y., BALL, H. L., GOLDSMITH, E. J. & ORTH, K. 2006. Yersinia YopJ acetylates and inhibits kinase activation by blocking phosphorylation. *Science*, 312, 1211-4.
- NAKAYASU, E. S., SYDOR, M. A., BROWN, R. N., SONTAG, R. L., SOBREIRA, T. J., SLYSZ, G. W., HUMPHRYS, D. R., SKARINA, T., ONOPRIENKO, O., DI LEO, R., DEATHERAGE KAISER, B. L., LI, J., ANSONG, C., CAMBRONNE, E. D., SMITH, R. D., SAVCHENKO, A. & ADKINS, J. N. 2015. Identification of Salmonella Typhimurium Deubiquitinase SseL Substrates by Immunoaffinity Enrichment and Quantitative Proteomic Analysis. *J Proteome Res*, 14, 4029-38.
- NANS, A., SAIBIL, H. R. & HAYWARD, R. D. 2014. Pathogen-host reorganization during Chlamydia invasion revealed by cryo-electron tomography. *Cell Microbiol*, 16, 1457-72.

- NGUYEN, B. D. & VALDIVIA, R. H. 2012. Virulence determinants in the obligate intracellular pathogen *Chlamydia trachomatis* revealed by forward genetic approaches. *Proc Natl Acad Sci U S A*, 109, 1263-8.
- NORDMANN, M., CABRERA, M., PERZ, A., BROCKER, C., OSTROWICZ, C., ENGELBRECHT-VANDRE, S. & UNGERMANN, C. 2010. The Mon1-Ccz1 complex is the GEF of the late endosomal Rab7 homolog Ypt7. *Curr Biol*, 20, 1654-9.
- NOTTI, R. S., CE 2016. The Structure and Function of Type III Secretion Systems. *Microbiol Spectr.*, 4.
- OGAWA, M., YOSHIMORI, T., SUZUKI, T., SAGARA, H., MIZUSHIMA, N. & SASAKAWA, C. 2005. Escape of intracellular *Shigella* from autophagy. *Science*, 307, 727-31.
- OMSLAND, A., SIXT, B. S., HORN, M. & HACKSTADT, T. 2014. Chlamydial metabolism revisited: interspecies metabolic variability and developmental stage-specific physiologic activities. *FEMS Microbiol Rev*, 38, 779-801.
- ORTH, K. 2002. Function of the *Yersinia* effector YopJ. *Curr Opin Microbiol*, 5, 38-43.
- ORTH, K., PALMER, L. E., BAO, Z. Q., STEWART, S., RUDOLPH, A. E., BLISKA, J. B. & DIXON, J. E. 1999. Inhibition of the mitogen-activated protein kinase kinase superfamily by a *Yersinia* effector. *Science*, 285, 1920-3.
- OUELLETTE, S. P., DORSEY, F. C., MOSHIACH, S., CLEVELAND, J. L. & CARABEO, R. A. 2011. *Chlamydia* species-dependent differences in the growth requirement for lysosomes. *PLoS One*, 6, e16783.
- PALMER, L. E., HOBBIE, S., GALAN, J. E. & BLISKA, J. B. 1998. YopJ of *Yersinia pseudotuberculosis* is required for the inhibition of macrophage TNF- α production and downregulation of the MAP kinases p38 and JNK. *Mol Microbiol*, 27, 953-65.
- PANAGIOTIDIS, C. A. & SILVERSTEIN, S. J. 1995. pALEX, a dual-tag prokaryotic expression vector for the purification of full-length proteins. *Gene*, 164, 45-7.
- PARKAR, N. S., AKPA, B. S., NITSCHKE, L. C., WEDGEWOOD, L. E., PLACE, A. T., SVERDLOV, M. S., CHAGA, O. & MINSHALL, R. D. 2009. Vesicle formation and endocytosis: function, machinery, mechanisms, and modeling. *Antioxid Redox Signal*, 11, 1301-12.
- PAUMET, F., WESOLOWSKI, J., GARCIA-DIAZ, A., DELEVOYE, C., AULNER, N., SHUMAN, H. A., SUBTIL, A. & ROTHMAN, J. E. 2009. Intracellular bacteria encode inhibitory SNARE-like proteins. *PLoS One*, 4, e7375.

- PETERS, J., WILSON, D. P., MYERS, G., TIMMS, P. & BAVOIL, P. M. 2007. Type III secretion a la Chlamydia. *Trends Microbiol.* England.
- PHILLIPS, M. 2015. Pseudoenzymes as Activators of Enzyme Function: The Prozyme Paradigm in Trypanosomatid Polyamine Metabolism. *FASEB J*, 29.
- PLEWCZYNSKI, D., TKACZ, A., WYRWICZ, L. S. & RYCHLEWSKI, L. 2005. AutoMotif server: prediction of single residue post-translational modifications in proteins. *Bioinformatics*, 21, 2525-7.
- POPA, C. M., TABUCHI, M. & VALLS, M. 2016. Modification of Bacterial Effector Proteins Inside Eukaryotic Host Cells. *Front Cell Infect Microbiol*, 6, 73.
- POPOVIC, D., VUCIC, D. & DIKIC, I. 2014. Ubiquitination in disease pathogenesis and treatment. *Nat Med*, 20, 1242-53.
- PRUNEDA, J. N., DURKIN, C. H., GEURINK, P. P., OVAA, H., SANTHANAM, B., HOLDEN, D. W. & KOMANDER, D. 2016. The Molecular Basis for Ubiquitin and Ubiquitin-like Specificities in Bacterial Effector Proteases. *Mol Cell*, 63, 261-276.
- PUBLIC HEALTH ENGLAND 2017. Sexually transmitted infections and chlamydia screening in England, 2016.
- PUJOL, C., KLEIN, K. A., ROMANOV, G. A., PALMER, L. E., CIROTA, C., ZHAO, Z. & BLISKA, J. B. 2009. Yersinia pestis can reside in autophagosomes and avoid xenophagy in murine macrophages by preventing vacuole acidification. *Infect Immun*, 77, 2251-61.
- PUKASS, K. & RICHTER-LANDSBERG, C. 2015. Inhibition of UCH-L1 in oligodendroglial cells results in microtubule stabilization and prevents alpha-synuclein aggregate formation by activating the autophagic pathway: implications for multiple system atrophy. *Front Cell Neurosci*, 9, 163.
- PUOLAKKAINEN, M., KUO, C. C. & CAMPBELL, L. A. 2005. Chlamydia pneumoniae uses the mannose 6-phosphate/insulin-like growth factor 2 receptor for infection of endothelial cells. *Infect Immun*, 73, 4620-5.
- QIU, J. & LUO, Z. Q. 2013. Effector translocation by the Legionella Dot/Icm type IV secretion system. *Curr Top Microbiol Immunol*, 376, 103-15.
- RADICS, J., KONIGSMAIER, L. & MARLOVITS, T. C. 2014. Structure of a pathogenic type 3 secretion system in action. *Nat Struct Mol Biol*, 21, 82-7.
- RAHMAN, M. M. & MCFADDEN, G. 2011. Modulation of NF-kappaB signalling by microbial pathogens. *Nat Rev Microbiol*, 9, 291-306.

- RAINES, S. A., HODGKINSON, M. R., DOWLE, A. A. & PRYOR, P. R. 2017. The Salmonella effector SseJ disrupts microtubule dynamics when ectopically expressed in normal rat kidney cells. *PLoS One*, 12, e0172588.
- RAYMOND, C. K., HOWALD-STEVENSON, I., VATER, C. A. & STEVENS, T. H. 1992. Morphological classification of the yeast vacuolar protein sorting mutants: evidence for a prevacuolar compartment in class E vps mutants. *Mol Biol Cell*, 3, 1389-402.
- REILEY, W., ZHANG, M., WU, X., GRANGER, E. & SUN, S. C. 2005. Regulation of the deubiquitinating enzyme CYLD by I κ B kinase gamma-dependent phosphorylation. *Mol Cell Biol*, 25, 3886-95.
- REITERER, V., EYERS, P. A. & FARHAN, H. 2014. Day of the dead: pseudokinases and pseudophosphatases in physiology and disease. *Trends Cell Biol*, 24, 489-505.
- REPNIK, U., CESEN, M. H. & TURK, B. 2013. The endolysosomal system in cell death and survival. *Cold Spring Harb Perspect Biol*, 5, a008755.
- ROBINSON, J. S., KLIONSKY, D. J., BANTA, L. M. & EMR, S. D. 1988. Protein sorting in *Saccharomyces cerevisiae*: isolation of mutants defective in the delivery and processing of multiple vacuolar hydrolases. *Mol Cell Biol*, 8, 4936-48.
- ROFE, A. P., DAVIS, L. J., WHITTINGHAM, J. L., LATIMER-BOWMAN, E. C., WILKINSON, A. J. & PRYOR, P. R. 2017. The *Rhodococcus equi* virulence protein VapA disrupts endolysosome function and stimulates lysosome biogenesis. *Microbiologyopen*, 6.
- RONZONE, E., WESOLOWSKI, J., BAULER, L. D., BHARDWAJ, A., HACKSTADT, T. & PAUMET, F. 2014. An alpha-helical core encodes the dual functions of the chlamydial protein IncA. *J Biol Chem*, 289, 33469-80.
- ROTTNER, K., STRADAL, T. E. & WEHLAND, J. 2005. Bacteria-host-cell interactions at the plasma membrane: stories on actin cytoskeleton subversion. *Dev Cell*, 9, 3-17.
- ROWLAND, T. J., SWEET, M. E., MESTRONI, L. & TAYLOR, M. R. 2016. Danon disease - dysregulation of autophagy in a multisystem disorder with cardiomyopathy. *J Cell Sci*, 129, 2135-43.
- RYTKONEN, A. & HOLDEN, D. W. 2007. Bacterial interference of ubiquitination and deubiquitination. *Cell Host Microbe*, 1, 13-22.
- RYTKONEN, A., POH, J., GARMENDIA, J., BOYLE, C., THOMPSON, A., LIU, M., FREEMONT, P., HINTON, J. C. & HOLDEN, D. W. 2007. SseL, a *Salmonella* deubiquitinase required for macrophage killing and virulence. *Proc Natl Acad Sci U S A*, 104, 3502-7.

- RZOMP, K. A., MOORHEAD, A. R. & SCIDMORE, M. A. 2006. The GTPase Rab4 interacts with Chlamydia trachomatis inclusion membrane protein CT229. *Infect Immun.* United States.
- SACHSE, M., URBE, S., OORSCHOT, V., STROUS, G. J. & KLUMPERMAN, J. 2002. Bilayered clathrin coats on endosomal vacuoles are involved in protein sorting toward lysosomes. *Mol Biol Cell*, 13, 1313-28.
- SAKA, H. A., THOMPSON, J. W., CHEN, Y. S., DUBOIS, L. G., HAAS, J. T., MOSELEY, A. & VALDIVIA, R. H. 2015. Chlamydia trachomatis Infection Leads to Defined Alterations to the Lipid Droplet Proteome in Epithelial Cells. *PLoS One*, 10, e0124630.
- SAKA, H. A., THOMPSON, J. W., CHEN, Y. S., KUMAR, Y., DUBOIS, L. G., MOSELEY, M. A. & VALDIVIA, R. H. 2011. Quantitative proteomics reveals metabolic and pathogenic properties of Chlamydia trachomatis developmental forms. *Mol Microbiol*, 82, 1185-203.
- SAMUDRALA, R., HEFFRON, F. & MCDERMOTT, J. E. 2009. Accurate prediction of secreted substrates and identification of a conserved putative secretion signal for type III secretion systems. *PLoS Pathog*, 5, e1000375.
- SARRIS, P. F., SKANDALIS, N., KOKKINIDIS, M. & PANOPOULOS, N. J. 2010. In silico analysis reveals multiple putative type VI secretion systems and effector proteins in Pseudomonas syringae pathovars. *Mol Plant Pathol*, 11, 795-804.
- SATO, H., FRANK, D. W., HILLARD, C. J., FEIX, J. B., PANKHANIYA, R. R., MORIYAMA, K., FINCK-BARBANCON, V., BUCHAKLIAN, A., LEI, M., LONG, R. M., WIENER-KRONISH, J. & SAWA, T. 2003. The mechanism of action of the Pseudomonas aeruginosa-encoded type III cytotoxin, ExoU. *Embo j*, 22, 2959-69.
- SCHECHTER, L. M., VALENTA, J. C., SCHNEIDER, D. J., COLLMER, A. & SAKK, E. 2012. Functional and computational analysis of amino acid patterns predictive of type III secretion system substrates in Pseudomonas syringae. *PLoS One*, 7, e36038.
- SCHINDELIN, J., ARGANDA-CARRERAS, I., FRISE, E., KAYNIG, V., LONGAIR, M., PIETZSCH, T., PREIBISCH, S., RUEDEN, C., SAALFELD, S., SCHMID, B., TINEVEZ, J. Y., WHITE, D. J., HARTENSTEIN, V., ELICEIRI, K., TOMANCAK, P. & CARDONA, A. 2012. Fiji: an open-source platform for biological-image analysis. *Nat Methods*, 9, 676-82.
- SCIDMORE, M. A. 2005. Cultivation and Laboratory Maintenance of Chlamydia trachomatis. *Curr Protoc Microbiol*, Chapter 11, Unit 11A.1.
- SCOTT, C. C., VACCA, F. & GRUENBERG, J. 2014. Endosome maturation, transport and functions. *Semin Cell Dev Biol*, 31, 2-10.

- SETTEMBRE, C., FRALDI, A., MEDINA, D. L. & BALLABIO, A. 2013. Signals from the lysosome: a control centre for cellular clearance and energy metabolism. *Nat Rev Mol Cell Biol*, 14, 283-96.
- SHAW, E. I., DOOLEY, C. A., FISCHER, E. R., SCIDMORE, M. A., FIELDS, K. A. & HACKSTADT, T. 2000. Three temporal classes of gene expression during the *Chlamydia trachomatis* developmental cycle. *Mol Microbiol*, 37, 913-25.
- SHOHDY, N., EFE, J. A., EMR, S. D. & SHUMAN, H. A. 2005. Pathogen effector protein screening in yeast identifies *Legionella* factors that interfere with membrane trafficking.
- SIGGERS, K. A. & LESSER, C. F. 2008. The Yeast *Saccharomyces cerevisiae*: a versatile model system for the identification and characterization of bacterial virulence proteins. *Cell Host Microbe*, 4, 8-15.
- SISKO, J. L., SPAETH, K., KUMAR, Y. & VALDIVIA, R. H. 2006. Multifunctional analysis of *Chlamydia*-specific genes in a yeast expression system. *Mol Microbiol*, 60, 51-66.
- SLAGOWSKI, N. L., KRAMER, R. W., MORRISON, M. F., LABAER, J. & LESSER, C. F. 2008. A functional genomic yeast screen to identify pathogenic bacterial proteins. *PLoS Pathog*, 4, e9.
- SNAVELY, E. A., KOKES, M., DUNN, J. D., SAKA, H. A., NGUYEN, B. D., BASTIDAS, R. J., MCCAFFERTY, D. G. & VALDIVIA, R. H. 2014. Reassessing the role of the secreted protease CPAF in *Chlamydia trachomatis* infection through genetic approaches. *Pathog Dis*, 71, 336-51.
- STEBBINS, C. E. & GALAN, J. E. 2001. Maintenance of an unfolded polypeptide by a cognate chaperone in bacterial type III secretion. *Nature*, 414, 77-81.
- STEELE-MORTIMER, O. 2008. The *Salmonella*-containing vacuole: moving with the times. *Curr Opin Microbiol*, 11, 38-45.
- STEPHENS, R. S., KALMAN, S., LAMMEL, C., FAN, J., MARATHE, R., ARAVIND, L., MITCHELL, W., OLINGER, L., TATUSOV, R. L. & ZHAO, Q. 1998. Genome sequence of an obligate intracellular pathogen of humans: *Chlamydia trachomatis*. *Science*, 282, 754-759.
- STUART, E. S., WEBLEY, W. C. & NORKIN, L. C. 2003. Lipid rafts, caveolae, caveolin-1, and entry by *Chlamydiae* into host cells. *Exp Cell Res*, 287, 67-78.
- SUBBARAYAL, P., KARUNAKARAN, K., WINKLER, A. C., ROTHER, M., GONZALEZ, E., MEYER, T. F. & RUDEL, T. 2015. EphrinA2 receptor (EphA2) is an invasion and intracellular signaling receptor for *Chlamydia trachomatis*. *PLoS Pathog*, 11, e1004846.

- SUBTIL, A., DELEVOYE, C., BALANA, M. E., TASTEVIN, L., PERRINET, S. & DAUTRY-VARSAT, A. 2005. A directed screen for chlamydial proteins secreted by a type III mechanism identifies a translocated protein and numerous other new candidates. *Mol Microbiol*, 56, 1636-47.
- SUBTIL, A., PARSOT, C. & DAUTRY-VARSAT, A. 2001. Secretion of predicted Inc proteins of *Chlamydia pneumoniae* by a heterologous type III machinery. *Mol Microbiol*, 39, 792-800.
- SWANSON, A. F. & KUO, C. C. 1994. Binding of the glycan of the major outer membrane protein of *Chlamydia trachomatis* to HeLa cells. *Infect Immun*, 62, 24-8.
- TABUCHI, M., KAWAI, Y., NISHIE-FUJITA, M., AKADA, R., IZUMI, T., YANATORI, I., MIYASHITA, N., OUCHI, K. & KISHI, F. 2009. Development of a novel functional high-throughput screening system for pathogen effectors in the yeast *Saccharomyces cerevisiae*. *Biosci Biotechnol Biochem*, 73, 2261-7.
- TAN, K. S., CHEN, Y., LIM, Y. C., TAN, G. Y., LIU, Y., LIM, Y. T., MACARY, P. & GAN, Y. H. 2010. Suppression of host innate immune response by *Burkholderia pseudomallei* through the virulence factor TssM. *J Immunol*, 184, 5160-71.
- TEJEDA-DOMINGUEZ, F., HUERTA-CANTILLO, J., CHAVEZ-DUENAS, L. & NAVARRO-GARCIA, F. 2017. A Novel Mechanism for Protein Delivery by the Type 3 Secretion System for Extracellularly Secreted Proteins. *MBio*, 8.
- TERMAN, J. R. & KASHINA, A. 2013. Post-translational modification and regulation of actin. *Curr Opin Cell Biol*, 25, 30-8.
- THOMSON, N. R., HOLDEN, M. T., CARDER, C., LENNARD, N., LOCKEY, S. J., MARSH, P., SKIPP, P., O'CONNOR, C. D., GOODHEAD, I., NORBERTZCAK, H., HARRIS, B., ORMOND, D., RANCE, R., QUAIL, M. A., PARKHILL, J., STEPHENS, R. S. & CLARKE, I. N. 2008. *Chlamydia trachomatis*: genome sequence analysis of lymphogranuloma venereum isolates. *Genome Res*, 18, 161-71.
- TIPPLES, G. & MCCLARTY, G. 1995. Cloning and expression of the *Chlamydia trachomatis* gene for CTP synthetase. *J Biol Chem*, 270, 7908-14.
- TODI, S. V., WINBORN, B. J., SCAGLIONE, K. M., BLOUNT, J. R., TRAVIS, S. M. & PAULSON, H. L. 2009. Ubiquitination directly enhances activity of the deubiquitinating enzyme ataxin-3. *Embo j*, 28, 372-82.
- TROISFONTAINES, P. & CORNELIS, G. R. 2005. Type III secretion: more systems than you think. *Physiology (Bethesda)*, 20, 326-39.
- TROST, M., WEHMHONER, D., KARST, U., DIETERICH, G., WEHLAND, J. & JANSCH, L. 2005. Comparative proteome analysis of secretory proteins

- from pathogenic and nonpathogenic *Listeria* species. *Proteomics*, 5, 1544-57.
- VALDIVIA, R. H. 2004. Modeling the function of bacterial virulence factors in *Saccharomyces cerevisiae*. *Eukaryot Cell*, 3, 827-34.
- VAN HO, A., WARD, D. M. & KAPLAN, J. 2002. Transition metal transport in yeast. *Annu Rev Microbiol*, 56, 237-61.
- VAN MEEL, E. & KLUMPERMAN, J. 2008. Imaging and imagination: understanding the endo-lysosomal system. *Histochem Cell Biol*, 129, 253-66.
- VERNET, T., DIGNARD, D. & THOMAS, D. Y. 1987. A family of yeast expression vectors containing the phage f1 intergenic region. *Gene*, 52, 225-33.
- VIBOUD, G. I. & BLISKA, J. B. 2005. *Yersinia* outer proteins: role in modulation of host cell signaling responses and pathogenesis. *Annu Rev Microbiol*, 59, 69-89.
- WANG, S., PENG, J., MA, J. & XU, J. 2016. Protein Secondary Structure Prediction Using Deep Convolutional Neural Fields. *Sci Rep*, 6, 18962.
- WANG, Y., KAHANE, S., CUTCLIFFE, L. T., SKILTON, R. J., LAMB DEN, P. R. & CLARKE, I. N. 2011. Development of a transformation system for *Chlamydia trachomatis*: restoration of glycogen biosynthesis by acquisition of a plasmid shuttle vector. *PLoS Pathog*, 7, e1002258.
- WANG, Y., SUN, M., BAO, H. & WHITE, A. P. 2013. T3_MM: a Markov model effectively classifies bacterial type III secretion signals. *PLoS One*, 8, e58173.
- WEBER, M. M., BAULER, L. D., LAM, J. & HACKSTADT, T. 2015. Expression and localization of predicted inclusion membrane proteins in *Chlamydia trachomatis*. *Infect Immun*, 83, 4710-8.
- WENZEL, D. M., LISSOUNOV, A., BRZOVIC, P. S. & KLEVIT, R. E. 2011. UBC7 reactivity profile reveals parkin and HHARI to be RING/HECT hybrids. *Nature*, 474, 105-8.
- WIDMANN, C., GIBSON, S., JARPE, M. B. & JOHNSON, G. L. 1999. Mitogen-activated protein kinase: conservation of a three-kinase module from yeast to human. *Physiol Rev*, 79, 143-80.
- YAMASHIRO, D. J., TYCKO, B., FLUSS, S. R. & MAXFIELD, F. R. 1984. Segregation of transferrin to a mildly acidic (pH 6.5) para-Golgi compartment in the recycling pathway. *Cell*, 37, 789-800.

- YE, Y., AKUTSU, M., REYES-TURCU, F., ENCHEV, R. I., WILKINSON, K. D. & KOMANDER, D. 2011. Polyubiquitin binding and cross-reactivity in the USP domain deubiquitinase USP21. *EMBO Rep*, 12, 350-7.
- YE, Z., PETROF, E. O., BOONE, D., CLAUD, E. C. & SUN, J. 2007. Salmonella effector AvrA regulation of colonic epithelial cell inflammation by deubiquitination. *Am J Pathol*, 171, 882-92.
- YEUNG, A. T. Y., HALE, C., LEE, A. H., GILL, E. E., BUSHELL, W., PARRY-SMITH, D., GOULDING, D., PICKARD, D., ROUMELIOTIS, T., CHOUDHARY, J., THOMSON, N., SKARNES, W. C., DOUGAN, G. & HANCOCK, R. E. W. 2017. Exploiting induced pluripotent stem cell-derived macrophages to unravel host factors influencing Chlamydia trachomatis pathogenesis. *Nat Commun*, 8, 15013.
- YU, J., DENG, R., ZHU, H. H., ZHANG, S. S., ZHU, C., MONTMINY, M., DAVIS, R. & FENG, G. S. 2013. Modulation of fatty acid synthase degradation by concerted action of p38 MAP kinase, E3 ligase COP1, and SH2-tyrosine phosphatase Shp2. *J Biol Chem*, 288, 3823-30.
- ZERIAL, M. & MCBRIDE, H. 2001. Rab proteins as membrane organizers. *Nat Rev Mol Cell Biol*, 2, 107-17.
- ZHEN, Y., KNOBEL, P. A., STRACKER, T. H. & REVERTER, D. 2014. Regulation of USP28 deubiquitinating activity by SUMO conjugation. *J Biol Chem*, 289, 34838-50.
- ZHENG, N. & SHABEK, N. 2017. Ubiquitin Ligases: Structure, Function, and Regulation. *Annu Rev Biochem*, 86, 129-157.
- ZHENG, Q., HUANG, T., ZHANG, L., ZHOU, Y., LUO, H., XU, H. & WANG, X. 2016. Dysregulation of Ubiquitin-Proteasome System in Neurodegenerative Diseases. *Front Aging Neurosci*, 8, 303.
- ZHOU, H., MONACK, D. M., KAYAGAKI, N., WERTZ, I., YIN, J., WOLF, B. & DIXIT, V. M. 2005. Yersinia virulence factor YopJ acts as a deubiquitinase to inhibit NF-kappa B activation. *J Exp Med*, 202, 1327-32.